Identifying Epigenetic Modifiers of Glioblastoma Multiforme Apoptosis Resistance

By

Ezgi ÖZYERLİ GÖKNAR

A Dissertation Submitted to the
Graduate School of Health Sciences
in Partial Fulfillment of the Requirements for
the Degree of

Doctor of Philosophy
In

Cellular and Molecular Medicine

16.07.2019

Identifying Epigenetic Modifiers of Glioblastoma Multiforme Apoptosis Resistance

Koc University

Graduate School of Health Sciences

This is to certify that I have examined this copy of a doctoral dissertation by

Ezgi ÖZYERLİ GÖKNAR

and have found that it is complete and satisfactory in all respects,

and that any and all revisions required by the final

examining committee have been made.

Committee Members:

Assoc. Prof. Tuğba BAĞCI-ÖNDER (Advisor)

Assoc. Prof. Tamer ÖNDER

Prof. Batu ERMAN

Prof. Hakan Sedat ORER

Assoc Prof. Tolga EMRE

Date: 16.07.19

I would love to dedicate this thesis to my dear parents ***Songül & Selim Salih Özyerli*** *for their unconditional love and support during this long journey…*

ABSTRACT

Identifying Epigenetic Modifiers of Glioblastoma Multiforme Apoptosis Resistance
Ezgi ÖZYERLİ GÖKNAR
Doctor of Philosophy in Cellular and Molecular Medicine
July 16, 2019

Glioblastoma Multiforme (GBM) is the most common and aggressive primary brain tumor. Despite recent developments in surgery, chemo- and radiotherapy, the prognosis of GBM patients is extremely poor, highlighting an urgent need for novel treatment strategies. TNF-Related Apoptosis Inducing Ligand (TRAIL) is a potent anti-cancer agent that can induce apoptosis selectively in cancer cells by activating death receptor signaling. GBM cells frequently develop resistance to TRAIL, which renders clinical application of TRAIL therapeutics inefficient. Accumulating evidence suggest that death receptor pathway components can be regulated at a transcriptional level, especially through epigenetic silencing of pro-apoptotic mediators. Therefore, understanding the epigenetic mechanisms of apoptotic response is critical for better design of pro-apoptotic therapies for cancer. To this end, we undertook a chemical strategy to interrogate the roles of chromatin modifiers in GBM cell apoptosis. We identified Chaetocin, a fungal metabolite and an inhibitor of histone methyl transferase SUV39H1, as a novel TRAIL sensitizer. Combining low subtoxic doses of Chaetocin and TRAIL resulted in very potent and rapid apoptosis of GBM cells. Chaetocin also effectively sensitized GBM cells to further pro-apoptotic agents, such as FasL and BH3 mimetics. Chaetocin mediated apoptosis sensitization was achieved through Reactive Oxygen Species (ROS) generation and consequent DNA damage induction that involved *TP53* activity. Chaetocin induced transcriptomic changes showed activation of antioxidant defense mechanisms and DNA damage response pathways. Heme Oxygenase 1 (*HMOX1*) was among the top upregulated genes, whose induction was ROS-dependent. Finally, Chaetocin and TRAIL combinatorial treatment revealed efficacy *in vivo*.

Taken together, our results provide a novel role for Chaetocin as an apoptosis priming agent. Discovery of epigenetic factors modulating tumor drug response and survival via high throughput, robust and affordable screens such as our chemical screen will ultimately lead to rapid development of effective therapies.

ÖZETÇE

Glioblastoma Multiforme ’de Apoptoz Direncini Regüle Eden Epigenetik Faktörlerin Belirlenmesi

Ezgi ÖZYERLİ GÖKNAR

Hücresel ve Moleküler Tıp, Doktora

16 Temmuz 2019

Glioblastoma Multiforme (GBM) en yaygın ve agresif primer beyin tümörüdür. Cerrahi, kemo- ve radyoterapi alalarındaki gelişmelere rağmen, GBM hastalarının prognozunun iyileştirilememesi, yeni tedavi stratejilerine acil ihtiyaç duyulduğunu açıkça vurgulamaktadır. TNF-ilişkili Apoptoz Indükleyen Ligand (TRAIL), sağlıklı hücrelere zarar vermeden, seçici olarak kanser hücrelerinde apoptozu indükleyebilen güçlü bir anti-kanser ajanıdır. Ancak GBM hücrelerinin sıklıkla TRAIL’e direnç geliştirmesi, TRAIL terapötiklerinin klinik uygulamasını verimsiz hale getirmektedir. TRAIL ve reseptörleri tarafından aktive edilen sinyal yolağının epigenetik modülasyonu literatürde belirgindir. Bu nedenle epigenetik mekanizmaların, tümör hücrelerinin TRAIL’e tepkisinin düzenlenmesinde etkili olduğu öngörülmektedir. Tümörün başlaması, ilerlemesi ve apoptotik tepkisinin düzenlenmesinde epigenetik mekanizmaların önemi konusundaki farkındalığımız, araştırmamızı GBM apoptoz direncini ve sağ kalımını düzenleyen epigenetik faktörlerin kimyasal tarama aracılığıyla saptamaya yöneltmemizi sağlamıştır. Bu amaçla, GBM hücrelerinde TRAIL’e yanıtı artırabilecek bileşikleri saptayabilmek adına epigenetik hedefli ilaç kütüphanesini kullanarak kimyasal bir tarama gerçekleştirdik. Taramamız sonucunda bir histon metil transferaz inhibitörü olan fungal metabolit Kaetosin, TRAIL duyarlılaştırıcısı olarak tanımlanmıştır. Düşük ve toksik olmayan dozlarda Kaetosin ve TRAIL'in birlikte kullanımının GBM hücrelerinde güçlü ve hızlı apoptoza yol açtığı gözlemlenmiştir. Kaetosin’in GBM hücrelerini, FasL ve BH3 mimetikleri gibi diğer proapoptotik ajanlara karşı da duyarlılaştırdığı saptanmıştır. Kaetosin’ in yarattığı apoptoz duyarlılığının, ROS üretimi ve bunun takip eden DNA hasarı indüksiyonu ve artan *TP53* aktivitesi aracılığıyla gerçekleştiği gözlemlenmiştir. Kaetosin kaynaklı transkriptomik değişiklikler, antioksidan savunma mekanizmalarının ve DNA hasar tepki sinyal yolaklarının indüklendiğini göstermiştir. Transkripsiyonu en üst düzeyde regüle edilen genlerden biri olan Heme Oksijenaz 1 (*HMOX1*)’in indüksiyonunun ROS üretimine bağımlı olduğu saptanmıştır. Son olarak, Kaetosin ve TRAIL kombinasyon tedavisinin in vivo sistemde de etkinliği saptanmıştır.

Birlikte ele alındığında, sonuçlarımız Kaetosin’e apoptoz primeri rolünü kazandırmaktadır. Tümör ilaç tepkisi ve sağ kalımını modüle eden epigenetik faktörlerin, bu çalışmada detaylı olarak sunulan kimyasal taramamız gibi yüksek verimli, sağlam ve uygun fiyatlı taramalar yoluyla tespit edilmesi, yeni ve etkili tedavilerin üretilmesine imkân sağlayacaktır.

ACKNOWLEDGEMENTS

First, I would love to thank my advisor, Dr. Tuğba Bağcı Önder for her contributions to my academic skills as we as providing me the opportunity to work in very nice, friendly and competitive scientific environment with my lab members. My sincere thanks go to Dr Tamer Önder, Dr. Batu Erman and Dr. Mehmet Gönen for their guidance and help for improvement of my thesis. I thank to Dr. Hiroaki Wakimoto (Massachusetts General Hospital, Boston, MA) for providing the primary GBM cells and Dr Udo Oppermann (University of Oxford) for providing the epigenetic drug library.

I would like to thank all my lab members for their support, help and guidance during last 5 years I spent in Koç University. It was a great team to work with pleasure. My special thanks go to contributors of this work deeply explained in my thesis; namely İlknur Sur Erdem, Fidan Şeker, Ahmet Cingöz, Alişan Kayabölen, Zeynep Kâhya Yeşil, Fırat Uyulur, Melike Gezen and Nazife Tolay. In addition, I thank to Nareg Pınarbaşı, Filiz Şenbabaoğlu, Birsu Kölemen, Ali Cenk Aksu, Özlem Yedier Bayram, Göktuğ Karabıyık, Ezgi Yağmur Kala, Seher Emreoğlu, Özen Leylek, Ayyub Ebrahimi and Tunç Morova for their friendship and support. I would like to thank each and every member of KUSOM for establishing potent, efficient and enjoyable scientific environment.

I would love to thank also to my undergraduate students especially Dilan Gökyer, Miray Çetin and Berk Toy for their assistance and motivation they provided.

Lastly and the most sincerely, I want to thank to my parents Songül Özyerli and Selim Salih Özyerli with all my heart for their patience during growing me up into who I am today, supporting and loving me deeply and unconditionally, encouraging me during hard times that I tend to give up and being perfect role models and the greatest parents to admire and envy. I would love to thank sincerely to my husband Bora Göknar for his support, love and patience as well as for walking hand in hand with me through all difficult paths.

Financial support was obtained from The Scientific and Technological Research Council of Turkey (TUBITAK) BIDEB Program (#2211e) (EO), Marie Curie FP7 Career Reintegration Grant (EC Grant # 618673) (TBO), People Programme (Marie Curie Actions) of the European Union's Seventh Framework Programme (FP7/2007-2013) under REA grant agreement no [609305]. (UO), Koç University Center for Translational Medicine (KUTTAM), and Cancer Research UK and the Oxford NIHR Biomedical Research Centre. The SGC (registered charity number 1097737) receives funds from AbbVie, Bayer Pharma AG, Boehringer Ingelheim, Canada Foundation for Innovation, Eshelman Institute for Innovation, Genome Canada, Innovative Medicines Initiative (EU/EFPIA) [ULTRA-DD grant no. 115766], Janssen, Merck KGaA Darmstadt Germany, MSD, Novartis Pharma AG, Ontario Ministry of Economic Development and Innovation, Pfizer, São Paulo Research Foundation-FAPESP, Takeda, and Wellcome [106169/ZZ14/Z].

TABLE OF CONTENTS

LIST OF TABLES

LIST OF FIGURES

NOMENCLATURE

2-HG	2-hydroxyglutarate
AAV	Adeno-associated virus
AML	Acute myeloid leukemia
APAF-1	Apoptotic protease-activating factor 1
ATCC	American Tissue Type Culture Collection
BAK	BCL-2 homologous antagonist/killer
BAM	Bowtie and alignment file
BAX	BCL-2-associated X protein
BBB	Blood brain barrier
BCL-2	B-cell CLL/lymphoma 2
BCL-XL	B-cell lymphoma-extra large
BH	BCL-2 homology
BID	BH3 interacting-domain death agonist
Cas	CRISPR-associated
Caspases	Cysteine-aspartic proteases
CI	Combination index values
COX	Cyclooxygenases
CRISPR	Clustered Regularly Interspaced Short Palindromic Repeats
Cyt C	Cytochrome C
DAPK	Death-associated protein kinase
DED	Death effector domain
DISC	Death inducing signaling complex
DNMT	DNA methyltransferases
Dox	Doxycycline
DR4/5	Death Receptor-4/5
DSB	Double strand breaks
EGFR	Epidermal growth factor receptor
ETC	Electron transport chain
FADD	Fas-Associated protein with Death Domain
FDA	Food and Drug Administration
FLIP	Flice-like inhibitory protein
Fluc	Firefly Luciferase
FMC	Fluc-mCherry
GBM	Glioblastoma Multiforme
G-CIMP	Glioma CpG island methylator phenotype
gRNA	Guide RNA
GSC	Glioma stem cells

GSEA	Gene Set Enrichment Analysis
GSH	Glutathione
HAT	Histone acetyl transferases
HDAC	Histone deacetylases
HDM	Histone demethylases
HDR	Homology-directed repair
HMOX1	Heme Oxygenase 1
HMT	Histone methyl transferases
HRK	Harakiri
HSP	Heat shock proteins
IAP	Inhibitor of apoptosis protein
IDH	Isocitrate dehydrogenase
INDEL	Insertions and/or deletions
LGG	Lower grade glioma
LOH	Loss of heterozygosity
LOX	Lipoxygenases
MGMT	O-6-methylguanine-DNA methyltransferase
miRNA	MicroRNA
MOMP	Mitochondrial outer membrane permeabilization
NAC	N-acetyl cysteine
NCS	Neural stem cells
NES	Normalized Enrichment Score
NF-κB	Nuclear Factor kappa B
NHEJ	Non-Homologous End Joining
NOD/SCID	Non-obese diabetic/severe combined immunodeficiency
NOS	Nitric oxide synthase
NOX	NADPH oxidases
PAM	Protospacer-associated motif
PCA	Principle Component Analysis
PCR	Polymerase chain reaction
PI3K	Phosphoinositide 3-kinase
PTEN	Phosphatase and tensin homolog
Puro	Puromycin
RNAseq	RNA sequencing
ROS	Reactive oxygen species
RRA	Robust rank aggregation
SAHA	Suberoylanilide hydroxamic acid
SAM	S-adenosyl-L-methionine
SOD	Superoxide dismutase

TCGA	The Cancer Genome Atlas
TCGA	Cancer Genome Atlas
TMZ	Temozolomide
TRAIL	TNF Related Apoptosis Inducing Ligand
Trx	Thioredoxin
TrxR	Thioredoxin reductase
TSA	Trichostatin A
TSS	Transcriptional start site
TUNEL	Terminal deoxynucleotidyl transferase dUTP nick end labeling
UPR	Unfolded protein response
VEGF	Vascular endothelial growth factor
WHO	World Health Organization
XIAP	X-linked inhibitor of apoptosis

Chapter 1

1. REVIEW OF LITERATURE

1.1 Glioma

Glioma was initially identified by Dr. Rudolf Virchow in 1863 and further investigated with the help of modern microscopic and medical tools in following centuries[1]. Gliomas are highly aggressive primary brain tumors and constitute 80% of CNS malignancies, which make them the most prevalent CNS tumors[1]. Primary brain tumor related deaths accounts for 2.3 % of cancer-associated life loss in Europe and North America[2].

Despite being the most prevalent type of primary brain tumors, annual incidence of gliomas are only 5 out of 100,000 individuals[3]. Such frequency is low in comparison to extra-neural organ tumors and is suggested to stem from protection of brain against genotoxic stress due to blood brain barrier (BBB) which prevents massive diffusion of mutagens with the help of ABC family transporters[4]. Also, post-mitotic state of most of the brain cells contribute to low tumor formation incidence due to low replicative errors.

In the literature, capacity of neural stem cells (NCS), glial precursor cells and oligodendrocyte precursor cells (OPCs) to initiate glioma has been demonstrated, which predicts the cell of origin of gliomas[5,6,7]. This prediction is further supported by the observation that gliomas share similar morphology and transcriptome with indicated types of cells of the CNS[8,9]. Gliomas are named according to their cell of origin, as astrocytoma (astrocyte originated), oligodendroglioma (oligodendrocyte based), oligoastrocytoma (carrying both astrocyte and oligodendrocyte cells' features), and finally as ependymoma (ependymal cell based).

On the basis of histological evaluations for mitotic behavior, necrosis, endothelial cell proliferation and presence of atypic cells, gliomas are subdivided into four different grades by WHO[10]. Grade I glioma such as pilocytic astrocytoma tumors have slow growth rates and low metastatic ability. Oligodendrogliomas and oligoastrocytomas are assigned to grade II and grade III gliomas, respectively. Astrocytomas are further categorized as

pilocytic (grade I), diffuse (grade II), anaplastic (grade III) and glioblastoma multiforme (grade IV)[11].

1.2 GBM, grade IV glioma

Glioblastoma multiforme (GBM) is grade IV tumor, the highest grade assigned by the WHO. GBM represents large proportion (45.6%) of malignant primary brain tumors and occurs with 3.1/100 000 incidence per year[12] . GBM related cases correspond to 4% of all tumor associated deaths[13].

GBM is characterized by very infiltrative and angiogenic tumor cells[10]. Presence of necrotic foci, high proliferation rate, invasiveness, and highly angiogenic features are hallmarks of GBM, which makes it one of the most lethal form of cancer[14]. Median survival with standard care for GBM patients is 14.6 months and only a small fraction of patients (5.5%) can live longer than 5 years after diagnosis, which make it the top scoring among the deadliest human tumors[15].

The term "multiforme" emphasizes the heterogenous character of this tumor owing to various distinct genetic alterations, expression profile, treatment response and pathology[16]. Most frequently altered pathways in GBM are RTK/RAS/PI3K, TP53 and RB signaling with mutagenesis rates of 88%, 87% and 78%, respectively in adult gliomas[17]. NF1 tumor suppressor gene, ERBB2 and IDH1 are other important genes mutated in GBM. Function altering mutations in tumor suppressor genes such as TP53 and *RB* enable tumor cells to escape from growth suppressor signals such as apoptotic signals. Manipulation of RTK/RAS/PI3K pathway such as epidermal growth factor receptor (EGFR) overexpression or activating mutation enable tumor cell to sustain proliferative signal even in the absence of environmental growth factors[18]. RTK dysregulation is frequently observed in glioma, e.g. overexpression of EGFR (60%–70%), PDGFRA (12%–15%), and MET (5%)[19]. EGFR amplifications frequently possess a deletion in extracellular ligand binding pocket which results in ligand independent firing and consequent STAT3 signaling[20]. In addition, 36% of GBMs harbor an inactive/lost PTEN gene and thus PI3K cannot be negatively regulated, which results in emergence of highly proliferative tumor cells resistant to apoptosis. IDH1 and IDH2 mutations are frequently observed in GBM. Mutations are mostly missense mutations resulting from an amino acid substitution of R132 residue within the substrate-binding site. IDH1/2 genes

code for NADP-dependent enzymes that catalyze the oxidative decarboxylation of isocitrate to α-KG and simultaneously produce NADPH from NADP+[10]. NADPH is an important cofactor for lipid and glucose metabolism and defense against oxidative stress[21,22]. Mutations in IDH1/2 genes results in aberrant enzymatic activity that reduces α-KG to 2-hydroxyglutarate (2-HG) in NADPH dependent manner. 2-HG owns almost identical orientation within the catalytic core of the Jumonji class of histone demethylases (JHDMs) and DNA hydroxylases[23], thus leads to complete inhibition of mentioned demethylates and consequent elevation in histone methylation. Besides histone methylation, mutant IDH1 also affects DNA methylation establishing hypermethylation phenotype called "glioma CpG island methylator phenotype (G-CIMP)". Hypermethylation is due to inhibition of TET dioxygenase, which normally catalyzes sequential oxidation of 5-methylcytosine, leading to DNA demethylation[24]. Such demethylation process is malfunctional in IDH mutant cells, therefore DNA is maintained in hypermethylated state[25]. IDH1 mutations in GBM were found to be associated with MGMT promoter methylation. IDH-1/2 mutations in GBM is associated with better outcome, whereas IDH wild type GBM have quite poor prognosis[26]. hTERT gene codes for telomerase reverse transcriptase prevents consequent DNA instability due to telomere shortening at the end of chromosomes and therefore provides immortality to cancer cells. TERT activating mutations in gene promoter is found 51% of GBM and associated with poor outcome in patients [27].

GBM is named as primary or secondary depending on tumors' initial existence in body. Primary GBM tumors constitute the majority of GBMs (85%) and arise de novo (from scratch), whereas secondary GBM are very rare and has evidence of less malignant precursor lesion such as low grade diffuse or anaplastic astrocytoma[28]. Primary GBMs tend to occur in elderly patients whereas secondary GBM is prevalent among patients younger than 45 years-old[1].

There are important genetic differences reported between primary and secondary GBMs such as gene copy number variations, diversity in chromosome structures, and genomic instability. EGFR gene amplification and mutation, loss of heterozygosity (LOH) of PTEN gene, overexpression of MDM2, deletion of P16 tumor suppressor are among hallmarks of primary GBM. Characteristics of secondary GBM consist of mutations in TP53 and RB tumor suppressor genes, overexpression of PDGFA/PDGFRα

and LOH of 1p/19q[29,3]. IDH1 mutation is more prevalent among secondary GBM tumors than primary GBM (60–80% and 3–7 %, respectively). Genetic and molecular pathogenesis of primary and secondary GBM is illustrated in **Figure 1.1**. Despite all above listed genetic differences, primary and secondary GBMs have similar morphology and treatment outcome[30].

The Cancer Genome Atlas (TCGA) investigated molecular genetics of various cancers through diverse genome analysis technologies. TGCA further divides GBM in four different subtypes; namely mesenchymal, proneural, neural and classical subtypes, based on mutation, genomic, and transcript alterations. The proneural subgroup has IDH1/2 and TP53 mutations as well as amplifications of PDGFRA, CDK6, CDK4 and MET genes. The classical subtype harbor EGFR amplification besides constitutively active mutant form and loss of PTEN gene. The mesenchymal subclass is characterized by NF1 mutations as well as TP53 and CDKN2A gene loss. Finally, the neural subtype harbors increased neural marker NEFL and more frequent ERBB2 mutation[9].

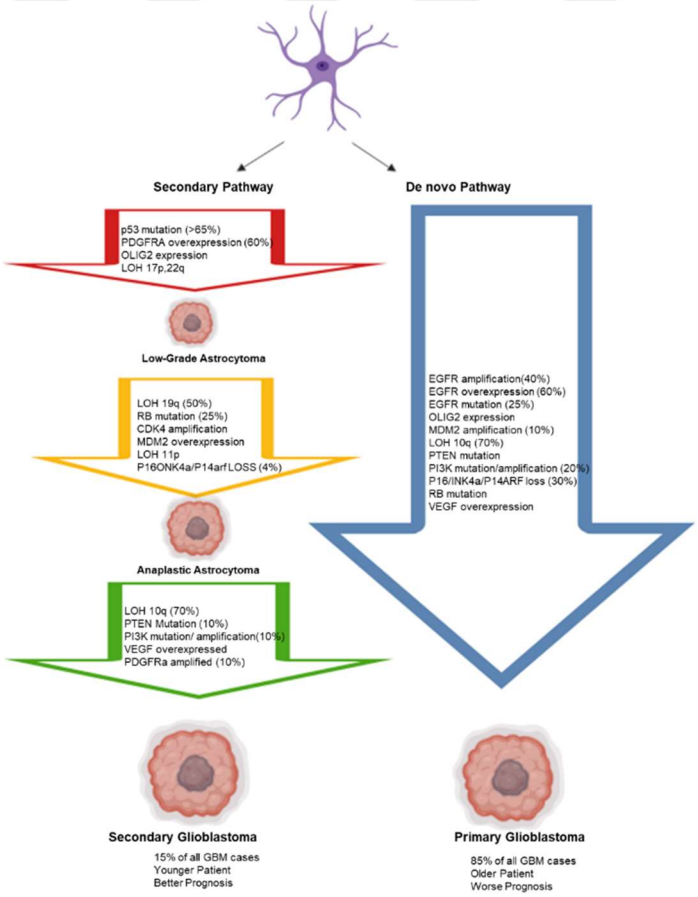

Figure 1.1 Genetic/ molecular pathogenesis of primary and secondary GBM (Adapted from Agnihotri et al., 2013b).

1.3 Conventional treatment strategies for GBM

Heterogeneity of GBM makes treatment challenging for patients. Surgery, chemotherapy and radiotherapy are conventional treatment regimes. Whenever possible, surgery aims the maximal resection of tumor tissue and is followed by external-beam radiation with concomitant systemic Temozolomide (TMZ) chemotherapy. Finally patients are administered with additional 6 cycles of TMZ[31].

TMZ is an alkylating agent prodrug, delivering a methyl group to purine bases of DNA (O6-guanine; N7-guanine and N3-adenine). The prodrug gets converted to active form within the cell at physiological pH. Small molecular weight of drug (194.15) is advantageous to cross BBB, which is one of the main obstacle in GBM treatment [32]. TMZ exerts toxicity on cancer cells through delivering a methyl group to purine bases of DNA, forming O6-methylguanine which form mismatch with thymine (T) during the next DNA replication cycle. Mismatches are recognized by DNA repair machinery and eventually leads to cell death[33]. Other alkylating agents are carmustine[34], lomustine[35] and carboplatin[36].

Additional treatment options for GBM are immunotherapy and combinatorial treatment of angiogenesis inhibitors with chemotherapeutics. Angiogenesis is formation of new blood vessels though migration growth and differentiation of existing endothelial cells. Angiogenesis is one of the hallmarks of GBM and is driven by Vascular endothelial growth factor (*VEGF*) expression. Antiangiogenic therapies aim at starving tumor cells through deprivation of oxygen and nutrients through neutralization of VEGF by antibodies[37]. Combining anti-VEGF antibody Bevacizumab with chemotherapeutics might improve GBM patient outcome[38].

Finally the use of low-intensity alternating electric fields for GBM therapy has FDA approval (NovoTTF- 100A; Novocure) though the efficacy is modest[39].

1.4 GBM resistance to conventional treatments

Despite recent developments in era of surgery, chemotherapy and radiotherapy, poor prognosis of GBM patients is still evident with progression-free survival of 7–8 months, a median survival of 14–16 months and 5-year overall survival (OS) of 9.8%[18].

GBM tumors are highly infiltrative with very ill-defined tumor borders and are disseminated all over the brain through the migration routes determined by brain structure and extracellular matrix (ECM) components[1]. Also, tumors are mostly populated in very close proximity to vital anatomical structures. These properties make total surgical resection of GBM mostly impossible and are directly related to high recurrence rate (90 %) of GBM either at initial site or distant location in the brain[40].

GBM tumors also bear a necrotic core that constitute a region of hypoxia, a low oxygen concentration. Reduction of oxygen levels interfere with the efficacy of radiotherapy due to decreased production of active free radicals in the absence of oxygen source[41]. To overcome this problem, oxygen diffusion-enhancing compound such as transsodium crocetinate (TSC) could be utilized as radiosensitizers[42].

Major limitation in GBM chemotherapy is the presence of BBB. BBB is very selective semipermeable membrane that isolates brain from blood circulation by blocking the passage of molecules >500 Da into the brain. BBB forms along all brain capillaries and consists of tight junctions[43]. While oxygen and carbon dioxide can freely diffuse and nutrients are carried by specific transporters on the membrane; toxic materials are avoided and the homeostasis is maintained. In light of these information, the need for alternative drug-delivery strategies for more efficient therapy of GBM patients is evident.

The main player in the resistance of GBM cells to alkylating chemotherapy such as TMZ is the expression of DNA repair enzyme, MGMT, which is O6-methylguanine DNA methyltransferase[44]. MGMT repairs mutagenic DNA lesion of O6-methylguanine back to guanine, therefore counteracts the cytotoxicity of alkylating drugs and consequently avoids mismatch related errors during DNA replication and transcription[17]. These features make MGMT the strongest biomarker for clinical decision of alkylating chemotherapy.

Other obstacles in GBM therapy are; GBM immunosuppressive phenotype, presence of radio- and chemo-resistant glioma stem cells (GSC) and resistance mechanisms to apoptotic stimuli. GBM resistance to conventional therapies are summarized in **Figure 1.2**. Inadequacy of current treatment options to efficiently fight with GBM encourage researchers to seek for alternative treatment strategies. The primary

focus of these strategies is to induce cancer cell death in tightly controlled and programmed manner, leaving healthy cells intact and undamaged.

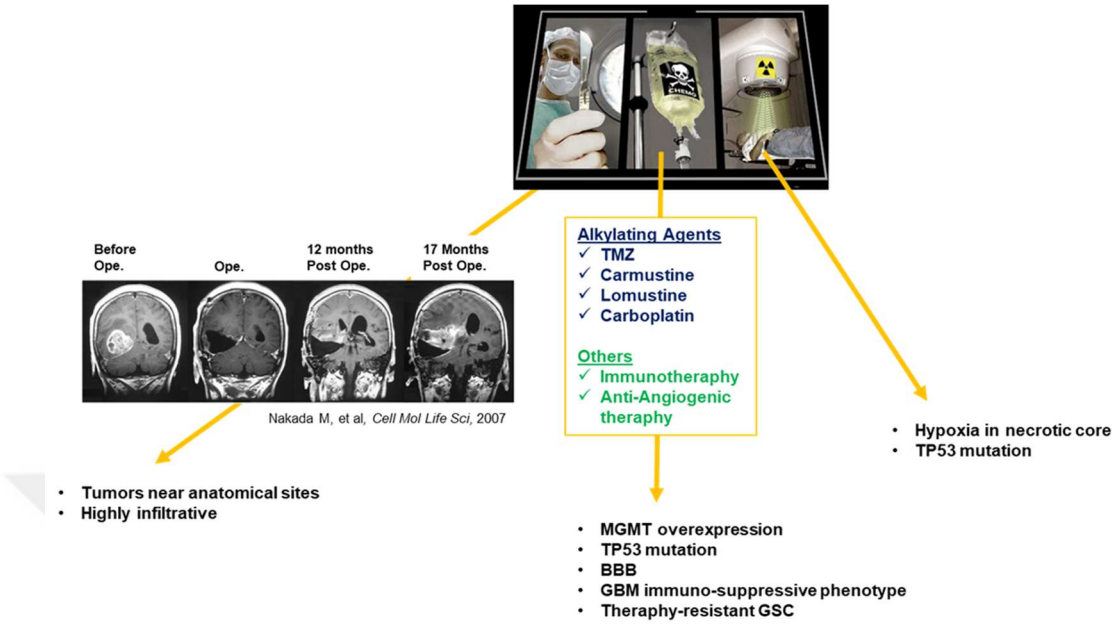

Figure 1.2 GBM resistance to conventional treatment strategies.

1.5 Apoptosis

Apoptosis is a form of programmed cell death observed in multicellular organisms[45] and it is a barrier to suppress cancer development and a way to maintain tissue homeostasis through elimination of disordered, infected or old cells. Cells make their decision on apoptosis based on their interpretation of environmental stimuli or self-assessment of cellular damage. Apoptotic cells are characterized by membrane blebbing, nuclear fragmentation, cell shrinkage, chromatin condensation, chromosomal DNA fragmentation, and global mRNA decay which consequently lead to formation of apoptotic bodies[46]. Apoptosis can be triggered in response to several stimuli such as chemicals and radiation[47] and is very tightly regulated under control of several signaling pathways. These pathways involve dozens of proteins, most significant of which are caspases (cysteine-aspartic proteases) responsible for proteolytic degradation of cellular components. Apoptotic caspases are subcategorized as initiator (caspase 2,8,9,10) and executioner (caspase 3,6,7). Active initiator caspase cleave and activate executioner caspases which degrade cellular components and cause apoptosis-related changes in cellular morphology[48].

Depending on the source of an apoptotic stimuli, either intrinsic or extrinsic pathway of apoptosis gets activated. Intrinsic pathway is triggered by intracellular signals in response to cellular genotoxic stress inducers, such as DNA damage, a defective cell cycle, lost ECM attachment, hypoxia and deprivation of cell survival factors. Such stimuli leads to mitochondrial outer membrane permeabilization (MOMP) that initiates mitochondrial release of pro-apoptotic factors such as cytochrome c, apoptosis-inducing factor (AIF), SMAC/DIABLO from the mitochondrial intermembrane space[49,50]. Released cytochrome *c* gets combined with apoptotic protease-activating factor 1 (APAF-1) to form large apoptosome complex[51] which triggers autoactivation of caspase 9 and consequent stimulation of effector caspases 3, 6 and/or 7. SMAC protein binds and blocks inhibitor of apoptosis proteins, IAPs (IAP-1, IAP-2, XIAP, NIAP, BRUCE, and SURVIVIN) therefore further promotes caspase-9 activation. Mitochondrial membrane permeability and consequent release of these factors are strictly regulated by pro- and anti-apoptotic BCL-2 family proteins[52,53]. Pro-apoptotic BCL-2 family members are subdivided in two categories based on the number of BH (BCL-2 homology) domains they contain (named as BH1, BH2, BH3 and BH4 domains). BCL-2-associated X protein (BAX) and BCL-2 homologous antagonist/killer (BAK) proteins possess several BH domains. However, proteins such as BID, BAD, BIM, BMF, PUMA and NOXA have only the BH3 domain. These BH3-only proteins are responsible for activation of BAX and/or BAK through initiating their oligomerization and insertion into outer mitochondrial membrane to form large pores allowing the permeabilization process[54]. On the other hand, anti-apoptotic BCL-2 family members such as B-cell CLL/lymphoma 2 (BCL-2), B-cell lymphoma-extra large (BCL-XL), MCL-1, A1 and BCL-W inhibit the BAX/BAK mediated pore formation on mitochondria through binding and retro-translocating BAX/BAK from mitochondria back into the cytosol[55]. That retro-translocation process is blocked by BH3-only protein binding and inactivation of anti-apoptotic BCL-2 family members, which emphasizes the importance of cellular balance of pro- and anti-apoptotic BCL-2 family protein expression for the control of apoptosis. Pro-apoptotic BCL-2 family protein expressions are tightly controlled by TP53 tumor suppressor gene, which partially explains the potency of DNA-damaging agents to induce intrinsic apoptosis[56]. On the other hand, extrinsic pathway is activated by extracellular signals transmitted to the cell with the help of pro-apoptotic ligands of TNF (tumor necrosis factor) family such as CD95L/FASL or TNF Related Apoptosis Inducing Ligand (TRAIL/Apo2L)[57] binding to their cell surface death receptors (CD95/ FAS and

DR4/DR5 respectively)[58]. Death domains at carboxyl terminus of ligand bound active receptors recruit FAS associated protein with death domain (FADD), which further recruits initiator caspases (caspase 8 or caspase 10) through death effector domain (DED) and consequently form death inducing signaling complex (DISC)[59]. Caspases are activated by autocleavage and further activate effector caspases 3, 6 and/or 7 to initiate apoptosis through degradation of cellular components[60]. Extrinsic apoptosis can be inhibited by decoy receptors which lacks the catalytic domain necessary for proper apoptosis induction[61] as well as by flice-like inhibitory protein (c-FLIP)[62]. c-FLIP protein has homologous sequence with caspase 8, thus can compete for binding to FADD and consequently form a distinct signaling complexes that activates NFκB, PI3K and MAPK pathways[63]. These pathways play important role in cell survival and proliferation.

The cross-talk exists between extrinsic and intrinsic apoptotic pathways and is mediated through protein "BID" which transmits signal from extrinsic to intrinsic pathway upon its' cleavage by initiator caspase 8[64]. Cleaved and truncated BID, now-called "tBID" oligomerizes BAK or BAX into mitochondrial pores, changes mitochondrial membrane polarization and causes release of cytochrome c and SMAC[65,66].

Cells are categorized as type I or II based on the type of apoptotic machinery they utilize. Type I cells rely solely on extrinsic apoptosis pathway without the involvement of mitochondrial signaling since the amount of active caspase 8 produced by DISC is adequate to directly activate the effector caspases and promote apoptosis [67]. Whereas in type II cells, both extrinsic and intrinsic pathways are utilized with the help of the cross-talk protein BID, which amplifies effector caspase activation for apoptosis induction[68]. Most cells are type II, whereas some cell types such as mesenchymal cells can be type I.

Apoptosis signaling pathway, its mediator and inhibitor components are schematized in **Figure 1.3**.

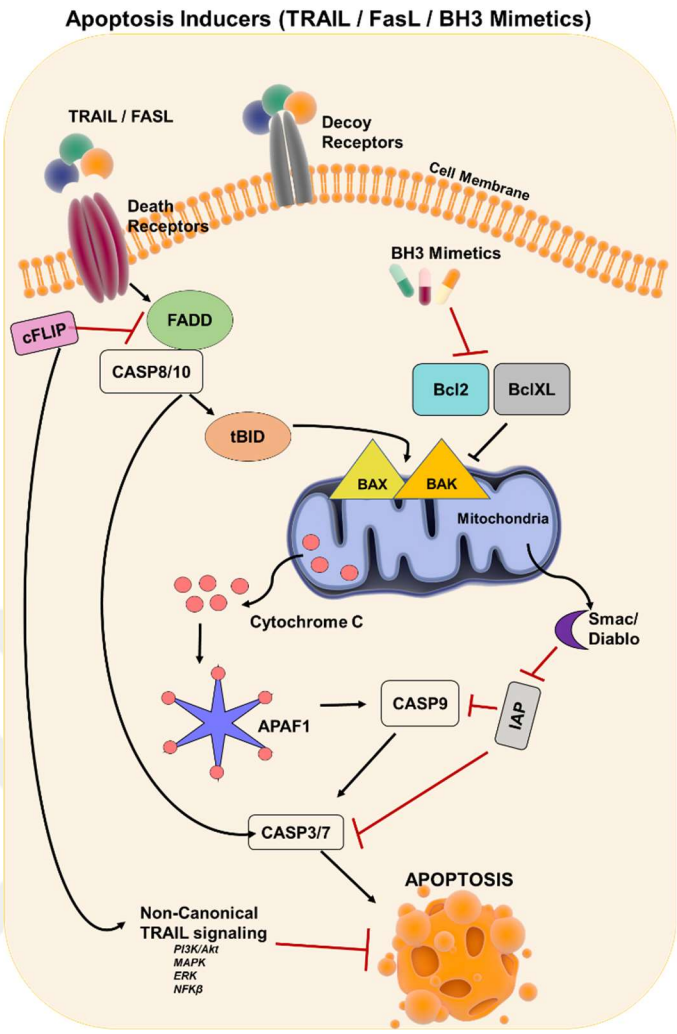

Figure 1.3 Schematic representation of extrinsic and intrinsic apoptosis and their regulators.

1.5.1 Apoptosis inducer "TRAIL" as an alternative treatment option for cancer

Manipulation of key players of apoptotic cascade and induction of extrinsic apoptosis via death receptors are important topics in cancer field. One of the most popular extracellular death-inducing ligand is TRAIL, and TRAIL mediated apoptosis in cancer cell is widely studied since the first characterization of ligand in the 1990s by Wiley et al.[57]. So far, TRAIL became one of the most promising death ligands for several cancer types[69].

TRAIL gene is located in chromosome 3 at position 3q26, and codes for the cytokine that can be expressed both as cell surface protein or a cleaved soluble form. It is produced by several cell types; predominantly spleen, lung and prostate as well as

immune cells[70]. TRAIL binds to death receptors DR4/TRAIL-R1 and DR5/TRAIL-R2 to transmit the apoptotic signals, as well as to the decoy receptors DcR1/TRAIL-R3, DcR2/TRAIL-R4 and soluble receptor osteoprotegerin (OPG) which cannot transmit any downstream signal (**Figure 1.4**). Decoy receptors have an intact ligand binding domain, lack death domain that is necessary for proper apoptosis induction[61]. *DR5* has the highest affinity to TRAIL among all receptors.

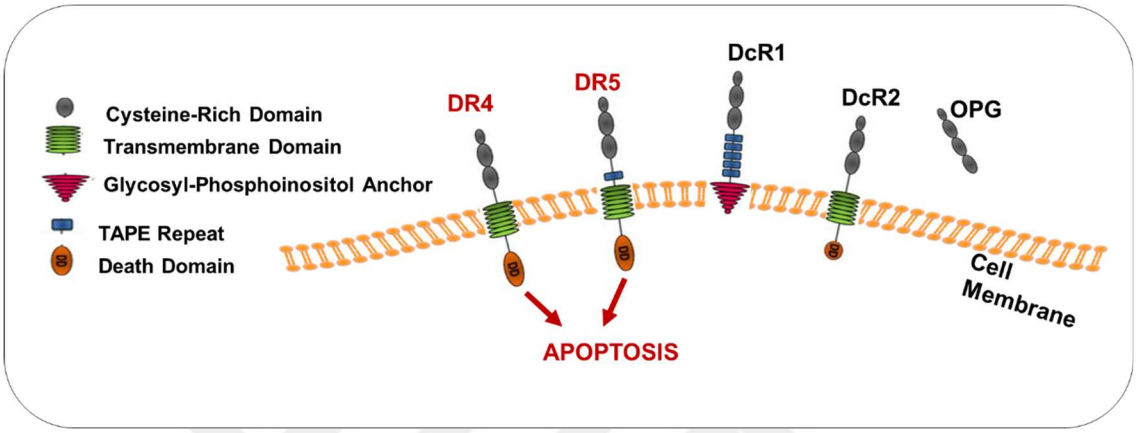

Figure 1.4 Types of death receptors bound by *TRAIL*.

Apoptosis induction by TRAIL is selective for cancer cells, leaving the healthy cells aside[71]. Such cancer specificity of TRAIL could be attributed to high decoy receptor expression in normal cells, which competes for ligand binding and also form a signal deficient heterocomplex with potent death receptors[72].

Expression of TRAIL receptors are evident in human primary glioma samples[73]. Also, key signaling molecules of apoptotic pathway are expressed in GBM cells, which makes them suitable for TRAIL based therapy. DR5 is the predominant receptor for TRAIL mediated apoptosis of human glioma cells[74] and its expression is correlated with better survival of glioma patients[75].

1.6 Hallmark of cancer: Evading apoptosis

Apoptosis tightly regulates tumor formation as well as response of tumor cells to currently available treatment strategies such as chemotherapy, irradiation, suicide gene

therapy or immunotherapy. However, most of the cancer cells possess an intrinsic resistance to apoptosis and find alternative strategies to evade cell death[76].

Changes in the balance of pro- and anti-apoptotic signal mediators as well as mutations in key genes of apoptotic signaling pathway are possible explanations of this resistance phenomenon. Balance of pro- and anti-apoptotic signal mediators are regulated both transcriptionally (e.g. DNA hyper/hypomethylation) and post-translationally (e.g. phosphorylation). Activity of caspases are reduced in cancer cells through phosphorylation in addition to inactivation/ degradation of pro-apoptotic BID, BIM, PUMA, BAD, NOXA, BAX, APAF-1 proteins by phosphorylation at distinct residues[76]. Overexpression of anti-apoptotic proteins such as IAPs, BCL-2, BCL-XL and AKT or enhancement of their activity by phosphorylation in cancer cells contribute to apoptotic resistance[76,77]. Overexpression of cFLIP prevents clustering of FADD and caspase 8 to form DISC complex and consequently results in activation of non-canonical TRAIL pathway. Non-canonical TRAIL pathway supports survival and proliferation of cells through activation of several signaling pathways, such as PI3K/AKT, MAPK, P38, ERK, TAK1, PKC, SRC, IkB/NF-kB, RIP1. NF-kB can induce high expression of anti-apoptotic genes cFLIP, BCL-XL, MCL-1 and cIAP and thus further contribute to apoptosis resistance[78]. Similarly, loss of pro-apoptotic BAX, BAK, caspase 8 results in reduced sensitivity to apoptosis. Mutations, altered glycosylation, mis-regulated endocytosis and reduced expression of death receptors as well as overexpression of decoy receptors may also confer apoptosis resistance. As an example, *DR5* mutations are widely encountered in head and neck, breast and lung cancer and decoy receptor expression was elevated in TRAIL resistant human osteoblast[70].

TRAIL resistance of tumor cells could be eliminated with combinatorial treatment strategies. Previously established sensitizing strategies are explained below:

BCL-2 and BCL-XL inhibitors, such as ABT-263, IAP inhibitors, MCL-1 inhibitors and SMAC mimetics can sensitize tumor cells to TRAIL mediated apoptosis[79,70].

Downregulation of NFκB, PI3K/AKT/MTOR or JAK/STAT pathway elements also contribute to TRAIL sensitization. Upon NFκB inhibition, IAPs and anti-apoptotic BCL-2 family members gets downregulated. Rapamycin is an MTOR inhibitor and

known to sensitize cancer cells to TRAIL induced apoptosis[58]. PI3K inhibitor Ly294002 also render glioma cells more susceptible to TRAIL mediated apoptosis[80].

Silencing of cFLIP sensitize cells to apoptosis[81]. Some chemotherapeutic drugs such as camptothecin, celecoxib and cisplatin break TRAIL resistance of cancer cells by downregulating *c-FLI* [82].

Irradiation can upregulate TRAIL receptor expression thus render cancer cells prone to extrinsic apoptosis[83]. JNK signaling also enhances TRAIL mediated apoptosis via upregulating DR5 expression[84].

Proteasome inhibitors such as PS-341[85], MG132[86], Bortezomib[87], NPI-0052[88] sensitizer cancer cells to death receptor mediated apoptosis through positive regulation of DR5 receptors. Proteasome inhibitors mediated TRAIL sensitization also depends on unfolded protein response (UPR) and ER stress due to misfolded protein build up. ER stress facilitates ROS release, which triggers several downstream pathways and causes DNA damage and consequent TP53 activation. Active TP53 leads either direct upregulation of DR5 and thus enhance extrinsic apoptosis pathway, or it can activate pro-apoptotic proteins like PUMA, NOXA and BAX and consequently enhance intrinsic apoptosis. TP53 is negatively regulated by MDM2 protein, thus MDM2 antagonists may play critical role in TRAIL sensitization of tumor cells[89,90].

Heat shock proteins (Hsp) are chaperones responsible for proper protein folding and prevent unfolded protein aggregation under cellular stress[91]. They are critical for stabilization and proper functioning, transportation of apoptosis related proteins[92]. Hsp inhibitors (e.g. Hsp90 inhibitor 17-AAG) are shown to synergize with TRAIL to induce apoptosis in glioma as well as prostate cancer cells[93],[94].

Mechanism of apoptosis evasion in cancer cells is summarized in **Figure 1.5**.

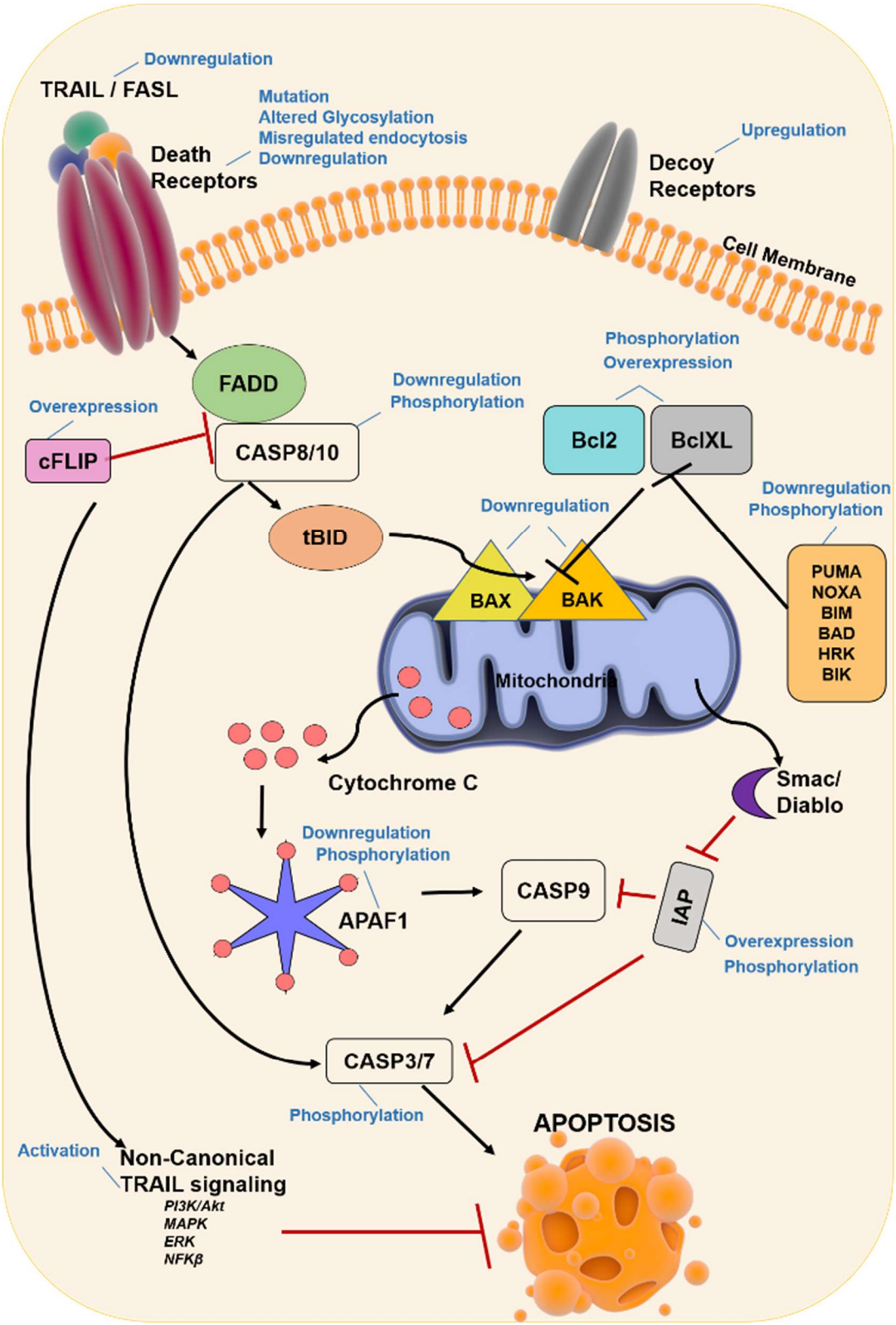

Figure 1.5 Mechanism of apoptosis evasion in cancer cells.

1.7 Epigenetic mechanisms of cancer apoptosis evasion

Epigenetics is heritable modifications of histones and DNA that modulate gene expression without altering the genetic code[95]. DNA methylation, histone modifications and chromatin remodeling are major epigenetic alterations that have broad effect on cell phenotype.

Mammalian cells pack their long DNA (around 2 meters long) into ordered structures called chromatin which is composed of nucleosomes. Nucleosomes consist of 146 bp DNA wrapped around octamers of DNA packaging proteins called Histones. Octamers consist of 2 copies of each four type of core histones (H2A, H2B, H3, and H4). Linker histone H1 is responsible for further folding and condensation of nucleosome chains to higher ordered structures[96].

Histone proteins are prone to a variety of posttranslational modifications at N-terminal tails as well as on the globular core region, which either modulate their affinity for wrapped around DNA or form new binding sites for protein modules[97]. These modifications lead to euchromatin (relaxed, allow gene transcription) or heterochromatin (condensed, no gene can be transcribed) formation. Phosphorylation (serine and threonine), acetylation (lysine), methylation (lysine and arginine), ubiquitination (lysine), SUMOylation, carbonylation, ADP-ribosylation and citrulation are possible posttranslational modification of core histones that occur in a dynamic manner; and these marks are added/removed by unique chromatin remodeling proteins[98]. Subgroups of epigenetic modifier enzymes are summarized in **Figure 1.6**. Histone modifying enzymes that add these post translational marks are named "writers", enzymes that remove these modifications are called "erasers" and finally proteins that recognize these marks for further functional outcome are called "readers"[99]. DNA methyltransferases (DNMT), Histone methyl transferases (HMT) and Histone acetyl transferases (HAT) are the most commonly encountered writer proteins; whereas Histone demethylases (HDM) and deacetylases (HDAC) are common erasers. Histone methylation can be associated with both transcriptional repression (e.g. H3K27me3, H3K9me2 and H3K9me3, H4K20me3*)* and activation (e.g. H3K4me3) depending on the position of the methyl group and methylation level, whereas histone acetylation (e.g. H3K9ac, H4K5ac, H4K8ac, H4K12 and H4K16ac) always leads to euchromatin state. Posttranslational modifications are recognized and further processed by various domains of epigenetic readers (namely

Bromo, Chromo, PHD, Tudor, MBT, BRCT, and PWWP domains) to regulate cellular processes such as gene transcription, DNA repair, replication and chromosome condensation[100].

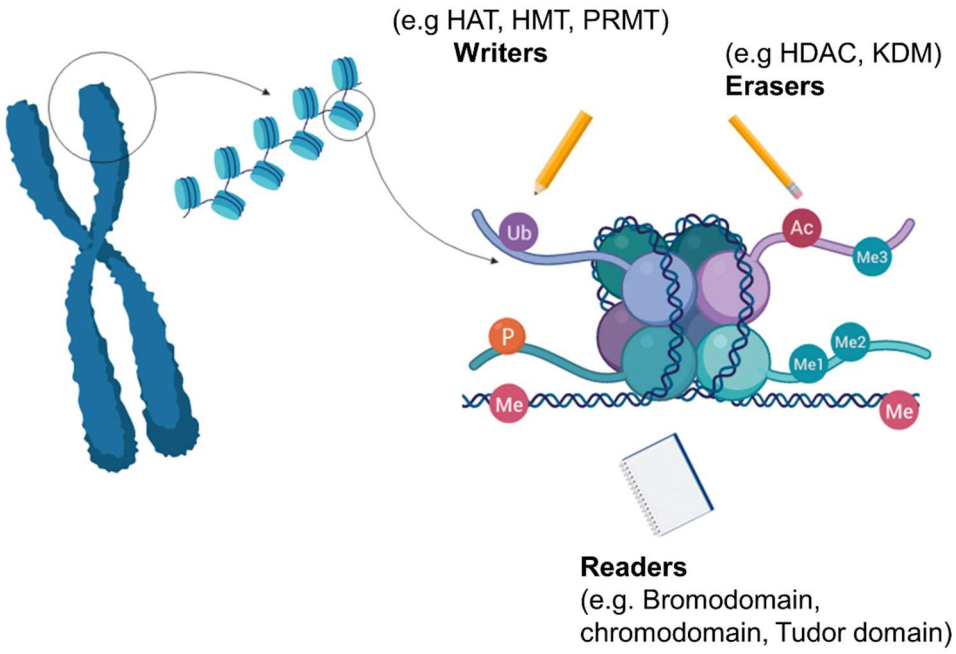

Figure 1.6 Subgroups of epigenetic modifier enzymes: Writers, erasers and readers.

Chromatin remodeling is another epigenetic alteration conducted by remodeling complexes called SWI2/SNF2 which physically modulate nucleosome through octamer sliding, DNA looping[101,102,103] and histone substitution[104] to induce transcription of various genes. Octamer sliding and DNA looping modulates transcriptome by changing the accessible surface area of the nucleosome. The replacement of H3 with its variant H3.3 by remodeling complexes results in the immediate activation of genes previously silenced by histone H3 lysine 9 methylation[105]. Similarly, replacement of the histone H2A with its variant H2A.Z is important for the regulation of a subset of genes' expression through changing the accessible surface area of the nucleosome[106].

Posttranslational modifications of histones modulate the capacity of genome to store and inherit genetic information and significantly differ among healthy versus tumor cells. Beside genetic abnormalities, epigenetic alterations also have major roles in initiation and progression of tumors as well as their therapy responses. Abnormal DNA

methylation and distinct histone modification patterns due to aberrant activity of epigenetic modifiers are highly encountered in tumor cells and have effect on drug response and tumor growth[107, 108]. Several epigenetic mechanisms are mis-regulated in cancer cells and could be categorized under two headlines, namely aberrant DNA methylations and aberrant histone modifications.

1.7.1 Evading apoptosis by aberrant DNA methylation

Regions in DNA where C nucleotide is followed by G nucleotide in 5' → 3' direction are called CpG sites. CpG nucleotide rich regions (300-3000 bp) in mammalian genomes are called CpG islands that concentrate in very close proximity to gene promoters[109]. Methyl residue is transferred from methyl donor SAM (S-adenosyl-L-methionine) to the 5′ carbon of cytosine in CpG sites by enzymes called DNMTs. DNMT1 functions as a 'maintenance' methyltransferase and responsible for copying DNA methylation during cell division, while DNMT3A and DNMT3B are *de novo* methyltransferases which do not require methylated template [110,111.] Methyl motif attracts specific methyl-DNA binding proteins (e.g. MECP2, MBD1, MBD2, MBD3, MBD4 and KAISO) and blocks the access of transcription factors (e.g. AP-2, c-MYC/ MYN, CREB, E2F and NF-κB) to CpG sites leading to transcriptional silencing[112]. Therefore, CpG island methylations at promoter sites should tightly be regulated.

CpG islands at tumor suppressor and pro-apoptotic gene promoters are mostly hypermethylated in cancer cells due to DNMT overexpression[113] or gene mutations (e.g. IDH1[114], SDH[115], TET2[116]), which lead to uncontrolled division and growth of cells [117]. Hypermethylation blocks the initiation and progression of both intrinsic and extrinsic apoptosis by modulating the expression of major players of cell death cascade. Promoter hypermethylation mediated silencing of Fas expression renders colonic epithelium cells resistant to apoptosis and contributes to neoplastic transformation into cutaneous T-cell lymphoma[118] and colon carcinoma[119]. Similarly DR4 and DR5 promoter methylation results in resistance to TRAIL mediated apoptosis in human neuroblastoma[120], melanoma[121] and ovarian cancer[122]. Caspase 8/10 silencing by promoter methylation disrupts the cycle of apoptosis in hepatocellular carcinoma[123], bladder cancer[124], small cell lung carcinoma[125], GBM[126], retinoblastoma and neuroblastoma[127]. In renal cell

carcinoma and chronic myeloid leukemia, silencing of BIM by promoter hypermethylation confer resistance to potent apoptosis induction[128]. APAF-1 silencing is evident in leukemia[129], melanoma[130], gastric[131], bladder and kidney cancer[132] and correlated with therapy resistance. In gastric and bladder cancer XAF1, inhibitor of anti-apoptotic XIAP, is downregulated by promoter hypermethylation and this is correlated with clinical outcome[133,134,135]. BCL-2 promoter is hypermethylated in prostate cancer[136]. Pro-apoptotic BAX, BAK and PUMA genes are also subject to promoter hypermethylation mediated silencing in multiple myeloma cells[137] and Burkitt lymphoma[138]. Pro-apoptotic BAD promoter is hypermethylated in myeloma[137]. BCL2L10 hypermethylation is observed in gastric cancer[139] and leukemia[140]. BIK is downregulated by hypermethylation in glioma[141], RCC[142], prostate cancer[143] and myeloma[144]. BNIP3 levels are modulated through methylation for gastric cancer[145], colorectal cancer[146], Leukemia[147] and HCC[148]. Pro-apoptotic Harakiri (HRK) hypermethylation is evident in colorectal, gastric[149], GBM[150], PCNSL[151] and Prostate cancer[152].

Other critical genes affected by hypermethylation are P16, a cell-cycle inhibitor, APC, a cell cycle regulator and DNA repair genes MGMT, BRCA1 and MLH1[153]. Silencing of MGMT gene by promoter hypermethylation predicts patient response to TMZ treatment and is associated with better prognosis[154]. Tumor suppressor DAPK (death-associated protein kinase) was previously shown to be silenced by promoter hypermethylation in colorectal cancer[155], lung cancers[156] and B-cell lymphoma[157], which render cancer cells less responsive to TNF-induced apoptosis. In various cancers HIC1 (hypermethylated in cancer 1) gene expression is silenced by DNA hypermethylation[158,159]. The loss of HIC1 results in inactivation of TP53, allowing cells to bypass apoptosis and survive DNA damage. TP53 gene itself is also subjected to hypermethylation in acute lymphoblastic leukemia patients[160]. RASSF1a tumor suppressor gene is also hypermethylated in several human tumors such as parathyroid tumors[161], nasopharyngeal carcinoma[162], non-small cell lung cancer[163] and hepatoblastoma[164]. In addition to gene silencing, CpG island methylation can also cause destabilizing genetic mutations and consequent tumorigenesis due to its's favorable conversion to thymine by hydrolysis of amine group. CpG sites are conducive to ~35% of all point mutations in the germline[165] and are important hotspots for acquired somatic

mutations leading to cancer[166,167]. In addition, cytosine methylations modulates the UV light absorption level of the nucleotide base, creating pyrimidine dimers[168].

Cancer-associated DNA hypomethylation in the human genome was discovered in 1983[169,170]; yet at the time the biological significance of such phenomenon was not clearly understood. Global genomic hypomethylation is evident in various types of human cancer, including prostate metastatic tumors[171]; B-cell chronic lymphocytic leukemia [172]; hepatocellular carcinomas[173]; and cervical cancer[174] as well as colorectal, gastric cancer and melanomas[108]. Heterochromatin repeats (e.g. satellite DNA, endogenous retrotransposons) are shown to be hypomethylated in various cancer types and such pattern could affect chromatin structure and genomic stability in addition to possible effect on transcription in other parts of the genome. Hypomethylation can lead to chromosome instability through translocations and deletions due to loosening of chromatin structure, reactivation of transposable elements and mitotic recombination[175]. Interspersed repeats (e.g. retrotransposon LINE-1) hypomethylation is observed in chronic lymphocytic leukemia[176], urinary bladder carcinomas[177], hepatocellular carcinomas[178], and prostate carcinomas[179]. Oncogene promoters and some gene regulatory sequences are mostly hypomethylated in cancer cells[180]. Cancer-associated hypomethylation occurs also in several tumor-initiator or proliferation-associated genes such as *pS2* gene[181], HOX11 proto-oncogene[182], c-MYC and c-N-RAS oncogenes[183,184].

1.7.2 Evading apoptosis by aberrant histone modifications

CpG island hypermethylation commonly observed in cancer cells is interrelated with histone marks such as elevated H3K9me and H3K27me3 levels, as well as H3 and H4 deacetylation and loss of H3K4me3[185,186,187.] Connection between DNA methylation and histone modifications is established with the help of methyl-DNA binding proteins such as MeCP2, MBD1, and Kaiso[188]. These proteins interact with methylated CpG islands and recruit histone deacetylases (HDACs, Sirtuins) and histone methyltransferase complexes to the site. Similarly, histone code can also further determine DNA methylation pattern by recruiting methyltransferase enzymes. For instance, histone

methyltransferase G9a recruits DNA methyltransferase, DNMT3A, and DNMT3b, to promoter site[189].

Aberrant histone modifications are hallmarks of cancer. Some of the histone marks related to tumorigenesis are reduced acetylation of H3 and H4 due to high HDAC or low HAT activity, decreased H3K4me3 mark and increased H3K9 and H3K27me3 modifications which can silence tumor suppressor genes or pro-apoptotic genes to facilitate uncontrolled growth and proliferation of cells. Deprivation of H4K16ac and H4K20me3 have been suggested to be prevalent hallmarks of cancer cells due to their contribution to chromosome instability[190]. Phosphorylation of histone H2A, H2B, H3 and H4, dephosphorylation of histone H1, and de-ubiquitylation of histone H2A have also been linked to the apoptotic process[191]. Cancer cells adopt epigenetic mechanisms, such as increasing H3K4me3 permissive mark to increase expression of drug resistance gene such as BRCA1, BRCA2 or MGMT75 and consequently avoid drug toxicity[192]. Hypoxic stress mediated epigenetic silencing of the DNA mismatch repair gene, MLH1 was observed accompanied by decreased H3K4 methylation at the promoter via demethylases[193]. Other apoptosis related genes repressed by epigenetic mechanism include $P16^{INK4a}$ [194], $P57^{Kip2}$ [195], GAS2, PIK3CG and $p21^{Waf}$ [196].

Several histone modifications are correlated with apoptotic chromatin alterations such as inter-nucleosomal DNA fragmentation, chromatin condensation and increased chromatin accessibility. Protein complexes governing cell death and survival decisions might be recruited by specific epigenetic histone marks. For instance H2A.X-Y142 phosphorylation inhibits MDC1 mediated binding of DNA repair factors (MRE11, RAD50, NBS1, 53BP1 and BRCA1) to H2A.X-S139ph (γ-H2A.X) sites, and rather facilitate recruitment of pro-apoptotic components (e.g. JNK1) and thus modulate cell fate after DNA damage induction[197,198]. The H2B-S14ph mark has been linked to chromatin condensation[199] and inter-nucleosomal DNA fragmentation[200] besides its contribution to the inhibition of survival pathways such as NF-κB[201]. Similarly, PKCδ mediated phosphorylation of H3T45 induces structural change within the nucleosome to augment DNA fragmentation during late apoptosis[202]. Harmony of wide variety of histone marks are critical determinant of cell fate.

Components of the apoptosis pathway are also subjected to regulation by aberrant histone modifications. DR4 gene expression is modulated by aberrant H3 and H4

acetylation patterns at promoter site in medulloblastoma patients[203]. Abnormal H3 and H4 acetylation patterns also modulate pro-apoptotic BAX protein levels[204]. H3K27me3 repressive mark modulates pro-apoptotic BIM levels in Burkitt's lymphoma[205]. HATs and HDACs contribute to tumorigenesis by modifying non-histone proteins like RB, E2F, TP53, KU70 and TFIIF[206]. Acetylation-dependent stabilization elevates E2F1-mediated apoptosis upon genotoxic stress[207]. Ku70 expression is induced upon DNA damage and plays critical role in apoptosis regulation. Ku70 normally interferes with BAX activation through blocking its translocation to mitochondrial membrane and inhibits apoptosis. Two important lysine residues of Ku70 (lysines 539 and 542) are acetylated by CBP and PCAF, which disrupts the Ku70–BAX interaction and thus facilitates apoptosis[208].

Besides epigenetic modifier enzymes, core epigenetic molecules such as histones might also contribute to tumorigenesis. Histone H2A.Z is an H2A variant which localizes especially in nucleosomes of the transcriptional start site (TSS) and reshape chromatin structure so that genes get activated through recruited transcription machinery. High level of histone variants H2A.Z is evident in several cancer types such as hepatocellular carcinoma and bladder cancer and contributes to proliferation and genomic instability[209]. H2A.Z knockdown results in the downregulation of BCL-2, and the upregulation of BAK, caspase-9, and both total and cleaved caspase-3 in in intrahepatic cholangiocarcinoma[210].

1.7.3 Evading apoptosis by epigenetic regulation of miRNAs

Aberrant DNA methylations and histone modifications also affect microRNA (miRNA) expression in cancer cells. miRNAs are small noncoding RNA endogenously expressed in the cells and are responsible for regulation of gene expression. They have broad effect on proliferation, differentiation and apoptosis[211]. Some miRNAs with critical gene targets are silenced by aberrant DNA and histone modifications in cancer cells. Some examples of these events are as follows:

miR15/16 miRNAs silences anti-apoptotic BCL-2 as well as Cyclin D1, MCL1 and Wnt3A at the post-transcriptional level[212, 213]. In several human malignancies, such as pituitary adenoma[214] and B-cell chronic lymphocytic leukemia[215], downregulation of miR-15-16 cluster is evident. miR15/16 cluster is epigenetically silenced by histone

deacetylation[215]. Indeed, MYC protein represses miR-15a/16-1 cluster expression through recruitment of HDAC3 in MCL[216].

miR-34 family targets Cyclin E2, Met, MycN, Notch1/2, Cdk4/6 as well as anti-apoptotic BCL-2 and is directly induced by TP53[217]. Mir-34 is repressed via hypermethylation in human gastric cancer, chronic lymphocytic leukemia, pancreatic, breast, colon and kidney cancer as well as Burkitt's lymphoma[218, 219.]

miR-29b targets DNMT3b[220] and MCL1, anti-apoptotic member of the BCL-2 family and is remarkably downregulated in lung[221], prostate[222], bladder[223] and ovarian cancer[224] as well as GBM[225]. miR-193a-3p , miR-512-5p, miR-153 and miR-133B also target MCL1 and are repressed via hypermethylation in AML[226], Gastric tumors[227], GBM[228] and lung cancer[229]. DNMT inhibitor 5-aza-2′-deoxycytidine and HDAC inhibitor 4-phenylbutyric acid restore the expression of the epigenetically silenced miR-512-5p in human gastric cancer cells[227].

miR-127 directly targets proto-oncogene Bcl6[230] and is hypermethylated in bladder, prostate, breast and lung cancer as well as lymphoma[231]. miR-106b and miR-93 impair TGFβ-induced apoptosis through inhibition of BIM expression in gastric cancer cells[232]. miR-106b and miR-93 are intronic miRNA whose transcription is modulated by the CpG island located in the promoter of the host gene MCM7. SAHA, an HDAC inhibitor, repressed their expression by repressing MCM7 in hepatocellular carcinoma cells[233].

There are several other cancer-associated miRNAs, whose expression modulation is not yet well understood from epigenetics aspect. For instance, miR-221 and miR-222 cluster targets several genes including PTEN, Timp3, $p27^{Kip1}$, $p57^{Kip2}$, Ddit4, FoxO3A[234] as well as pro-apoptotic PUMA[235] and caspase 3[236] and is upregulated in multiple solid tumors such as bladder cancer[237] and glioma[238]. miR-17-92 cluster and its paralog miR-106b-93-25 cluster target $p21^{Cip1}$ and pro-apoptotic BIM[239] and are known to be overexpressed in multiple solid tumors including lung and colon cancer, as well as lymphoma, medulloblastoma and multiple myeloma[240,241]. miR-135a inhibits JAK2 and results in consequent downregulation of anti-apoptotic BCL-XL[242,243]. miR-135a is downregulated in Classic Hodgkin lymphoma, AML[244] and ovarian cancer[245]. miR-491 also targets BCL-XL in colorectal cancer[246]. EGR2 is a tumor-suppressive transcription

factor which induces apoptosis through BNIP3L and *BAK* activation[247]. miR-150 targets EGR2 to promote gastric cancer progression[248]. Macrophage migration inhibitory factor (MIF) triggers apoptosis in gastric epithelial cells through repressing *TP53* phosphorylation and upregulating of BCL-2 expression[249]. miR-451 targets MIF and is downregulated in gastric cancer[250]. Epstein–Barr virus (EBV) is the first human virus discovered to express miRNA called miR-BART5[251] and is associated with gastric cancer[252]. miR-BART5 render gastric cancer cells resistant to apoptosis by targeting PUMA[253]. PTEN is a tumor suppressor which facilitates apoptosis through negatively regulating PI3K/Akt survival pathway[254]. PTEN is targeted by miR-21[255] and miR-21 expression is elevated in gastric cancer tissues. miR-375 also modulates the activity of PI3K/Akt pathway through direct targeting of PDK1 and downregulated in gastric cancer[256]. NF-κB signaling is also inhibitor of apoptosis[257] and is directly targeted by miR-9 which is downregulated in gastric cancer.

Epigenetic modification of core apoptotic machinery is summarized in **Table 1.1**. Modulation of other apoptosis regulatory pathways and genes is illustrated in **Table 1.2**.

Table 1.1 Epigenetic modification of core apoptotic machinery.

Pro/Anti-Apoptotic Genes	Epigenetic Modification	Outcome	Cancer Type
FAS	DNA Hypermethylation	Down-regulation	T-cell lymphoma[118], colon carcinoma[119]
DR4/DR5	DNA Hypermethylation	Down-regulation	Neuroblastoma[120], melanoma[121] and ovarian cancer[122]
	H3 and H4 deacetylation	Down-regulation	Medulloblastoma patients[203]
Caspase 8/10	DNA Hypermethylation	Down-regulation	Hepatocellular carcinoma[123], bladder cancer[124], small cell lung carcinoma[125], GBM[126], retinoblastoma and neuroblastoma[127]
BIM	DNA Hypermethylation	Down-regulation	Renal cell carcinoma and chronic myeloid leukemia[128]
	H3K27me3 repressive mark	Down-regulation	Burkitt's lymphoma[205]
APAF-1	DNA Hypermethylation	Down-regulation	Leukemia[129], melanoma[130], gastric[131], bladder and kidney cancer[132]
XAF1	DNA Hypermethylation	Down-regulation	Gastric and bladder cancer[133, 134, 135]
BCL-2	DNA Hypermethylation	Down-regulation	Prostate cancer[136]
	miR-15/16 silencing by histone deacetylation	Up-regulation	Pituitary adenoma[214] and B-cell chronic lymphocyte leukemia[215]
	miR-34 hypermethylation	Up-regulation	Gastric cancer, chronic lymphocytic leukemia, pancreatic, breast, colon and kidney cancer as well as Burkitt's lymphoma[218,219]
BAX	DNA Hypermethylation	Down-regulation	Multiple myeloma cells[137] and Burkitt lymphoma[138]
	H3 and H4 deacetylation	Down-regulation	Colon cancer cells[204]

BAK	DNA Hypermethylation	Down-regulation	Multiple myeloma cells[137] and Burkitt lymphoma[138]
PUMA	DNA Hypermethylation	Down-regulation	Multiple myeloma cells[137] and Burkitt lymphoma[138]
BAD	DNA Hypermethylation	Down-regulation	Multiple myeloma cells[137]
Bcl2L10	DNA Hypermethylation	Down-regulation	Gastric cancer[139] and leukemia[140]
BIK	DNA Hypermethylation	Down-regulation	Glioma[141], RCC[142], prostate cancer[143] and myeloma[144]
BNIP3	DNA Hypermethylation	Down-regulation	Gastric cancer[145], colorectal cancer[146], Leukemia[147], and HCC[148]
HRK	DNA Hypermethylation	Down-regulation	Colorectal, Gastric[149], GBM[150] , PCNSL[151] and Prostate cancer[152]
MCL1	miR-29b downregulation	Up-regulation	Lung[221], prostate[222], bladder[223] and ovarian cancers[224] as well as GBM[225]
	miR-193a-3p, miR-512-5p, miR-153 and miR-133B hypermethylation	Up-regulation	AML[226], Gastric tumors[227], GBM[228] and lung cancer[229]
Bcl6	miR-127 hypermethylation	Up-regulation	Bladder, prostate, breast and lung cancer as well as lymphoma[231]

Table 1.2 Epigenetic modification of apoptosis regulatory pathways and genes.

Other Apoptosis Related Genes	Epigenetic Modification	Outcome
DAPK	DNA Hypermethylation[155,156,157]	Down-regulation
HIC1	DNA Hypermethylation[158,159]	Down-regulation
P16	DNA Hypermethylation[153]	Down-regulation
APC	DNA Hypermethylation[153]	Down-regulation
TP53	DNA Hypermethylation[160]	Down-regulation
RASSF1	DNA Hypermethylation[161,162,163,164]	Down-regulation

MGMT	DNA Hypermethylation[153,154]	Down-regulation
	increasing H3K4me3[192]	Down-regulation
BRCA1	DNA Hypermethylation[153]	Down-regulation
	increasing H3K4me3[192]	Down-regulation
MLH1	DNA Hypermethylation[153]	Down-regulation
	Decreased H3K4 methylation[193]	
pS2	DNA Hypomethylation[181]	Up-regulation
HOX11	DNA Hypomethylation[182]	Up-regulation
c-MYC	DNA Hypomethylation[183,184]	Up-regulation
c-N-ras	DNA Hypomethylation[183,184]	Up-regulation
MRE11	H2A.X-Y142 phosphorylation[197,198]	Binding to γ-H2A.X sites was blocked
RAD50		
NBS1		
53BP1		
BRCA1		
NF-κB	H2B-S14ph[201]	Inhibited by reduced nuclear trafficking
E2F1	Protein Acetylation[207]	Half-life and DNA binding affinity increased
KU70	Protein Acetylation[208]	Interaction with *BAX* was disrupted

1.8 Reprogramming of the cancer epigenome by epi-drugs to reverse apoptosis evasion

Reversion of epigenetic modulations of DNA and histone by drug interventions can provide therapeutic advantage for various type of cancers. DNMT1 inhibitors result in gradual hypomethylation across cell divisions and lead to elevated expression of tumor suppressors. Azacitidine, its deoxy derivative decitabine, guadecitabine, and 4-thio-2-deoxycytidine are DNMT1 inhibitors designed for clinical use[258,259.] Azacitidine and decitabine are approved by US Food and Drug Administration (FDA) for treatment of myelodysplastic syndromes (MDS) and acute myeloid leukemia (AML) since they decrease malignant cell burden, improve blood cell count and survival of patients[260], [261]. Guadecitabine has longer effective half-life due to improved pharmacology and pharmacodynamic and has shown promise in early clinical trials[262]. 4-thio-2-deoxycytidine is orally bioavailable and is currently in a phase I trial in patients with advanced solid tumors[258]. Mutated forms of isocitrate dehydrogenase (IDH1 and IDH2) genes are known to be a major reason of aberrant DNA methylation in cancer. IDH1 and IDH2 inhibitors that are currently in clinical trials for low grade gliomas and AML include Ivosidenib (AG-120), Enasidenib (AG-221), AG-881, and IDH305[263].

HDAC inhibitors make up the largest group of epigenetic drugs and exert their activity through maintaining the expression of tumor suppressor genes. Vorinostat[264,265], Belinostat[266] and Romidepsin[267,268] are FDA-approved for treatment of cutaneous or peripheral T-cell lymphoma. Panobinostat is approved for treatment of drug-resistant multiple myeloma in combination with the proteasome inhibitor Bortezomib[269].

Histone acetylation readers, the bromodomain and extra-terminal (BET) proteins are also pharmacologically inhibited for cancer therapy. BRD4 inhibitor OTX015 mediates a rapid tumor regression with low toxicity[270]. Other BET inhibitors such as ABBV-075, BMS-986158, GSK2820151 are also in clinical trials for several malignancies.

The histone methyltransferase EZH2 generates H3K27me3 mark, which leads to transcriptional repression[271]. EZH2 inhibitors, such as Tazemetostat, CPI-1205, DS-3201, and GSK2816126 are in clinical trials. Inhibition of EZH2 blocks proliferation of drug resistant stem cell population and thereby prevents tumor growth[272]. Pinometostat, an

inhibitor for H3K79 methyltransferase DOT1L, recently completed phase I clinical trial in AML patients. Demethylase LSD1 gene has been shown to play an important role in cancer and is very highly expressed in several cancer cell lines[273,274,275]. LSD1 inhibitors tranylcypromine, GSK2879552 and INCB059872 are in clinical trials in patients with AML, MDS, and small cell lung cancer.

Tumor suppressive microRNA (miR-16) supplementation is currently under clinical trial on advanced non-small cell lung cancer, or mesothelioma patients (NCT02369198). In addition, DNMT inhibitor 5-aza-2'-deoxycytidine and HDAC inhibitor 4-phenylbutyric acid were shown to induce miR512-5p expression in human gastric cancer and trigger apoptosis by suppressing the MCL-1[227]. HDAC inhibitors suberoylanilide hydroxamic acid (SAHA) and Trichostatin A (TSA) decreases proliferation and increases apoptosis in colorectal cancer by downregulating miR-17-92 cluster expression and consequently elevating PTEN, BCL-2L11, and CDKN1A expression[276].

Epigenetic modulations can also be utilized to break drug resistance in several cancer types by combinatorial treatment approach. Several cell culture[277,278] and *in vivo* models[279, 280, 281] proved the efficacy of combinatorial treatment of DNMT and HDAC inhibitors for various cancer cells. Combined treatment of TSA with the DNMT inhibitor Decitabine resulted in reactivation of densely methylated tumor suppressor genes[277]. TSA, Belinostat and Vorinostat showed synergistic activity with conventional chemotherapeutic agents such as paclitaxel[282], gemcitabine[283], cisplatin[284], etoposide and doxorubicin[285]. Decitabine acts synergistically with paclitaxel[286,287] and cisplatin[281]. Non-small-cell lung cancer are sensitized to EGF tyrosine kinase inhibitors (TKIs) by HDAC inhibitor[288]. Bromodomain inhibitor JQ1 similarly sensitizes T cell acute lymphoblastic leukemia to γ-secretase inhibitor-mediated apoptosis[289]. HDAC inhibitors can also sensitize cancer cells to ionizing radiation by modulating cell cycle and growth-related gene expression. HDAC inhibitor sodium butyrate elevated the radiation sensitivity of human colon carcinoma cell lines[290]. TSA, Entinostat, Valproic acid, Tributyrin, Vorinostat, bicyclic depsipeptide and Hydroxamic acid analogues were shown to sensitize various cancer cell lines to towards ionizing radiation[291,292].

Epigenetic modulation of death receptor mediated pathway has been one successful approach for better apoptosis response of tumor cells. To this end, HDAC

inhibitors, such as MS275[293], SAHA[294], Valproic acid[295], Depsipeptide[296], SBHA[297], LAQ824[298] have been shown to augment TRAIL responses in various tumor types including prostate cancer, primary myeloid leukemia, melanoma, breast cancer, medulloblastoma, GBM and CLL. HDAC mediated sensitization involves upregulating the DR expression and pro-apoptotic gene activity (BID, BAD, Caspases, p21, BAK, BAX), and downregulating anti-apoptotic proteins (e.g. Cflar, BCL-2, BCL-XL, Xiap, Mcl1, Survivin, CyclinD1). HDACi such as MS275 elevates acetylation oh H3 and H4 at *DR4* promoter and causes increase in TRAIL receptor expression in medulloblastoma Daoy cells. Under combinatorial treatment with MS275, medulloblastoma cells are much more prone to TRAIL mediated cell death[203]. HDACs can also induce expression of pro-apoptotic genes such as caspases, BAX and BAK while blocking expression of anti-apoptotic genes like XIAP and CFLAR and consequently sensitize tumor cells to extrinsic and intrinsic apoptosis [107].

On the other hand, some epigenetic changes might contribute to apoptosis resistance due to gene expression silencing. Modulation of DNA methylation with the methyltransferase inhibitor 5-Aza-2′-deoxycytidine has been proven to be effective in modulating TRAIL response, by restoring caspase-8 expression[299, 300, 301]. Combination of Decitabine with Valproic acid significantly increases caspase-8 expression in SCLC and sensitizes tumor cells to TRAIL[302]. DNMT1 and DNMT3b silencing was shown to sensitize human hepatoma cells via up-regulation of DR5 and caspase-8[303]. Similarly, in Burkitt's lymphoma DNMT1 inhibitor Iso-3 synergized with TRAIL via reduction of survivin expression and induction of DR5 surface expression[304].

1.9 Epigenetic modifier Chaetocin

Chaetocin is a fungal metabolite produced by Chaetomium fungal species and has antimicrobial and cytostatic activity[305]. Chaetocin was found to be a specific inhibitor of the lysine-specific histone methyltransferase SU(VAR)3-9 at a narrow concentration range (IC_{50}= 0.6 μM) and acts as a competitive inhibitor for S-adenosyl methionine [306]. Suv39H1 methylates lysine 9 on histone H3 (me3) and recruits heterochromatin proteins like HP. It is also DNMT linked, thus facilitates methylation of DNA CpG islands and causes further heterochromatin formation. Chaetocin is known to induce cell cycle arrest

and apoptosis by regulating ROS-mediated ATM/YAP1 and ASK-1/JNK signaling pathways. It has been previously shown to be effective apoptosis inducer in glioma at micromolar concentrations[307].

Chaetocin also inhibits the oxidative stress mitigation enzyme thioredoxin reductase-1 (TrxR1 or TXNRD1)[308] and leads to generation of cellular oxidative stress. Oxidative stress is induced upon insufficiency of antioxidants to balance cellular production of ROS namely peroxides, superoxide, hydroxyl radicals. Apart from exogenous sources such as UV, pollutants, tobacco, drugs, xenobiotics; ROS is generated intracellularly by mitochondria, peroxisomes and endoplasmic reticulum[309] as well as by reaction of several oxidase and oxygenase enzymes such as NADPH oxidases (NOX)[310], xanthine oxidase, Cyclooxygenases (COX) and lipoxygenases (LOX)[311] and nitric oxide synthase (NOS)[312].

Mitochondrial ROS is generated as a consequence of electron leakage during electron transport chain (ETC). Leaky electrons couple by oxygen to form superoxide anion (O_2^-)[313]. Superoxide can also be formed by NADPH oxidase, xanthine oxidase, nitric oxide synthase which later is converted to hydrogen peroxide (H_2O_2) by superoxide dismutase (SOD). Hydrogen peroxide through Fenton reaction is converted to reactive hydroxyl radicals (OH) which cause severe cellular damage. Misfolded protein accumulation results in ER stress mediated ROS production. ROS is produced in peroxisomes during long-chain fatty acid metabolism[309]. Produced ROS is converted to nontoxic substances (H_2O and O_2) by glutathione (GSH) peroxidase, catalase, or thioredoxin (Trx) peroxidase. Glutathione peroxidases utilize glutathione (GSH) as the electron donor for detoxification of hydroxyl radical. The thioredoxin system consists of TrxR and Trx which detoxify H_2O_2 by providing electron to Trx peroxidase.

Generation and the detoxification process of cellular ROS is summarized in **Figure1.7**.

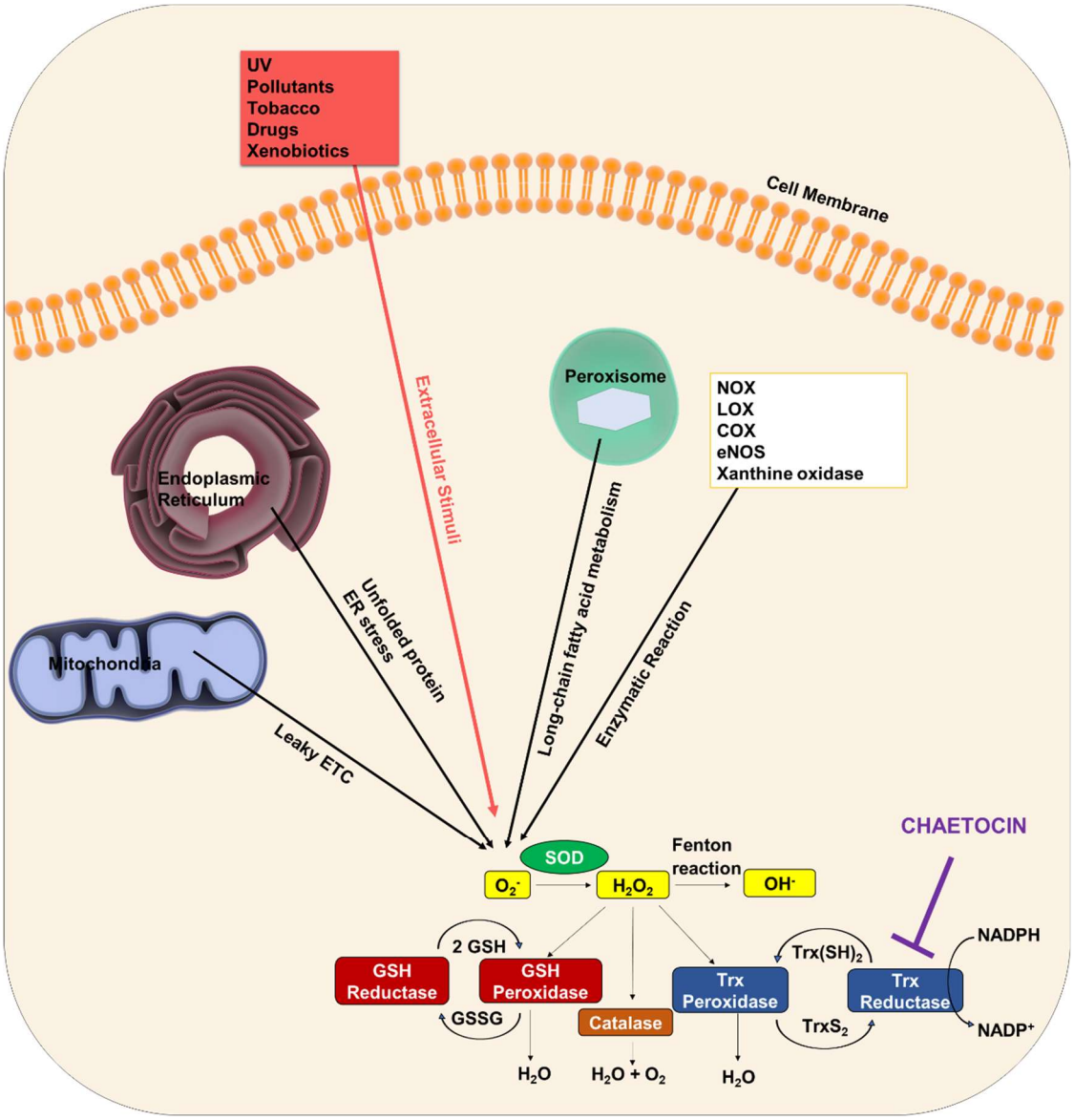

Figure 1.7 Generation and the detoxification process of cellular ROS.

Generated ROS disrupts cell homeostasis by various ways: 1) ROS directly attacks nucleic acids (DNA, RNA, mitochondrial DNA), causing mutations and genomic instability[314], 2) activates/inhibits proteins through oxidizing cysteine and tyrosine residues[315], 3) disturbs redox signaling[316], modifies critical kinase and phosphatases consequently regulating downstream signaling pathways (MAPK[317], PI3K[318], PKC[319]) transcription factors (APE1/Ref-1, HIF-1α, AP-1, NRF2, NF-κB, TP53, FOXO, STAT, and β-CATENIN)[320]. Regulating critical signaling pathways, ROS facilitates tumor growth, metastasis, vascularization and contribute to apoptosis resistance.

1.10 CRISPR/Cas9 genome editing of cancer cells

CRISPR (Clustered Regularly Interspaced Short Palindromic Repeats) and CRISPR-associated (Cas) genes are crucial components of bacterial and archaeal adaptive immunity against invading genetic materials, such as virus and plasmids. CRISPR loci include variable short repeat sequences (around 20 bps) derived through fragmentation and incorporation from previously encountered invasive DNAs. Transcription of this loci yields small RNAs (crRNA – CRISPR RNA). These small RNAs are utilized to guide effector endonuclease Cas9 to cleave invading DNA through sequence complementarity as illustrated in **Figure 1.8**[321].

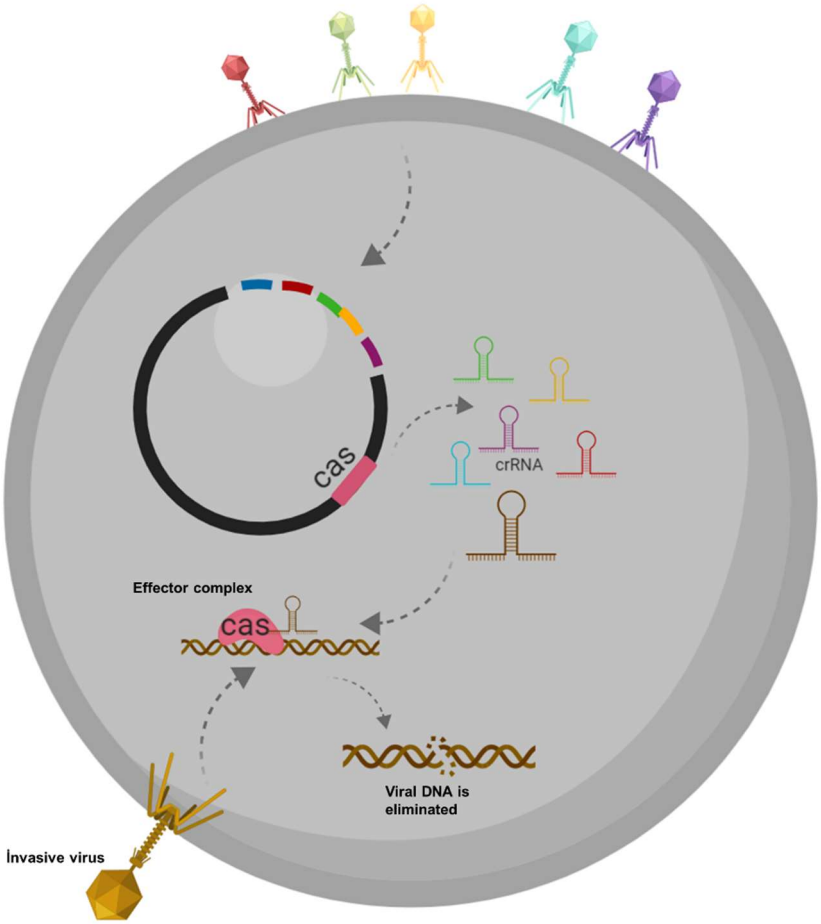

Figure 1.8 RNA guided CRISPR machinery as bacterial defense system (Adapted from Sontheimer EJ, 2010)

CRISPR/Cas9 system is widely used as genome editing tool by delivering synthetic guide RNA (gRNA) targeting 5′ exons of candidate gene into the cell. Cas9

endonuclease requires a short-conserved sequence, (2–5 nts) known as protospacer-associated motif (PAM), at 3′- of the gRNA complementary sequence for proper binding[322]. Upon binding, site-specific cleavage of DNA by Cas9 forms double strand breaks (DSB). DSBs can be repaired in the cell through two distinct mechanism: 1) Non-Homologous End Joining (NHEJ) pathway, which results in insertions and/or deletions (indels) within targeted gene that interfere with gene function. 2) homology-directed repair (HDR) pathway in presence of homologous donor template, which enables introduction of specific mutations as illustrated in **Figure 1.9**[323].

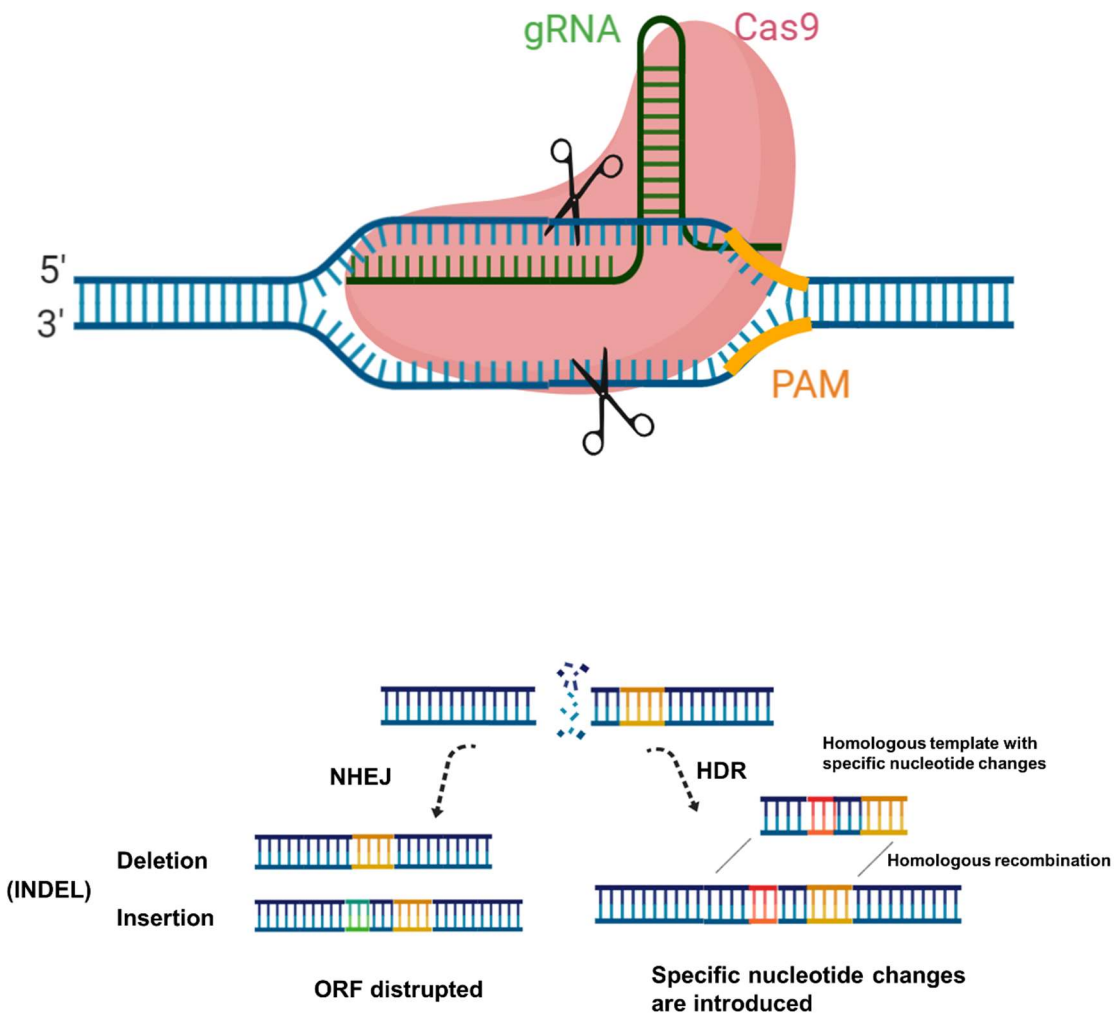

Figure 1.9 Mechanism of CRISPR/Cas9 technology.

CRISPR/Cas9 technology was shown to be more potent than previously published shRNA screens in terms of identifying novel essentiality genes which are critical targets

for cancer therapy[324, 325]. CRISPR is also used to investigate synthetic lethality in various cancer types[326] as well as to identify gene knockouts acting synergistically with drugs to induce cancer cell death. Modulators of TRAIL[327], ATR inhibitors[328] and Ras inhibitors[329] were previously investigated by pooled CRISPR screens for diverse cancer types. CRISPR technology also enables the interrogation of noncoding elements such as enhancer regions of malignancy-linked genes such as TP53 [330], CUL3, NF1[331]. CRISPR mediated genome editing is widely used for generation of 3D organoids to model and study cancer progression *in vitro* through knockout of tumor suppressor and oncogenes[332, 333, 334]. Besides *in vitro* applications, CRISPR/Cas9 mediated genome editing can be utilized *in vivo* through implantation of genome edited tumor cell[335] and *in vivo* injection of the plasmids encoding cas9 and gRNA against target genes[336] as well as adeno-associated virus (AAV) mediated delivery of gRNAs[337]. Encouraging results of *in vitro* CRISPR/Cas9 technology facilitated the clinical trials. First phase I clinical trial (NCT02793856) was held in 2016[338] for curing metastatic non-small cell lung cancer through delivery of PD-1 knockout of T-cells generated by CRISPR technology and followed by similar still-ongoing clinical studies[339].

Chapter 2

2. MATERIALS & METHODS

2.1 Cell culture

U87MG and U373 GBM cell lines were purchased from American Tissue Type Culture Collection (ATCC) and authenticated. U87MG-TR cells were TRAIL resistant derivatives of U87MG cells *(manuscript in prep)*. 293T cells were kind gift of Dr. Tamer Onder (Koç University, Turkey). Cells were grown in DMEM medium (Gibco, USA) supplemented with %10 fetal bovine serum (Gibco, USA) and %1 Pen/Strep (Gibco, USA) in humidified incubator at 37ºC with 5% CO2 level. Primary cell line GBM8 was obtained from Dr. Hiroaki Wakimoto (Massachusetts General Hospital, Boston, MA) and grown as neurospheres in cell culture flasks containing EF medium (Neurobasal medium supplemented with EGF, FGF, B-27, N2, Heparin, L-Glutamine, and Pen/Strep).

2.2 Reagents

TRAIL was commercially supplied (SuperKiller, Enzo Life Sciences, Farmingdale, NY, USA) or produced from 293T cells as described[340]. Caspase inhibitors (BD Pharmingen, San Diego, CA, USA) were: Z-VAD-FMK (general caspase inhibitor), Z-FA-FMK (negative control). BCL-2, BCL-XL inhibitors ABT-263 and WEHI-539 were purchased from Cayman Chemicals (Ann Arbor, MI, USA). FasL and N-acetyl-L-cysteine (NAC) were purchased from Sigma-Aldrich (MO, USA). NUTLIN-3a was purchased from MedChemExpress (NJ, USA). Doxycycline hyclate (Dox) was purchased from Sigma-Aldrich (Cat. No: D9891). D-luciferin was purchased from Biotium (CA, USA). Chaetocin was purchased from two sources (C9492-1mg, Sigma-Aldrich, MO, USA) and (S8068, Selleckchem, Houston, TX, USA). The epigenetic tool library was constructed as described[341]. Vectors used for the study is listed at **Table 2.1**.

Table 2.1 List of vectors used for the study.

Vectors	Cat. No
pUMVC	Addgene Plasmid #8449
pCMV-dR8.2 dvpr	Addgene Plasmid #8455
pCMV-VSV-G	Addgene Plasmid #8454
3544 pMIG *BCL-2*	Addgene Plasmid #8793
3541 pMIG BCL-XL	Addgene Plasmid #8790
pBABE GFP-puro	Addgene Plasmid #10668
MSCV	Addgene Plasmid #24828
Pico2-Fluc.mCherry	gift from Dr. Andrew Kung (Dana Farber Cancer Institute)
lentiCas9-Blast	Addgene Plasmid #52962
lentiCRISPR v2	Addgene Plasmid #52961
lentiGuide-Puro	Addgene Plasmid #52963
hAAVS1 1L TALEN	Addgene Plasmid #35431
hAAVS1 1R TALEN	Addgene Plasmid #35432
AAVS1 SA-2A-puro-pA donor	Addgene Plasmid #22075
PG13-luc (wt TP53 binding sites)	Addgene Plasmid #16442
pGL3-Basic	Promega
pENTR1A	Addgene plasmid # 17398
pLIX_402	Addgene plasmid # 41394

2.3 Cell viability, caspase activity and caspase inhibition assays

Cell viability was detected by ATP based Cell Titer-Glo (CTG) Luminescent Cell Viability Assay (Promega) according to the manufacturer's instructions using a plate reader (BioTek's Synergy H1, Winooski, VT, USA). 5.000 cells/well were seeded to 96-well plates (Corning Costar, clear bottom black side) as triplicates for each condition and treated with corresponding chemicals of interest for defined period. For all cell viability assays Chaetocin was applied simultaneously with extrinsic (TRAIL/FasL) and intrinsic (BH3 mimetics) apoptosis inducers. After treatment is completed, cell Titer Glo reagent is added on top of cells (4 µl CTG reagent in 40 µl DMEM for each well) and measurement made in plate reader at 560 nm wavelength after 2 minutes shaking period

followed by 8 minutes incubation of plate in dark. Viability data is normalized to control condition and T test performed to assess significance of viability changes among different treatment conditions. Epigenetic chemical screen was performed by Zeynep Kahya Yeşil. For caspase inhibition assay, Z-FA-FMK (Negative Control for Caspase Inhibitors) or Z-VAD-FMK (General Caspase Inhibitor) pretreatments were performed at 20 µM final concentration for 24h before following drug treatments. For caspase inhibition assay, cells were subjected to Chaetocin and caspase inhibitor treatment for 24h prior to *TRAIL* treatment. For caspase activity assays, cells were treated with Chaetocin (100 nm, 24h) followed by TRAIL (100 ng/ml for 3h). For measurement of caspase activity, cells were subjected to Chaetocin treatment for 24h followed by TRAIL treatment for 3h since caspase cleavage is evident at early stages of apoptosis. Caspase 3/7 activity was measured by Caspase-Glo® 3/7 (Promega) assays according to manufacturer's instructions. NAC was used as ROS scavenger. Cells were pretreated with NAC (10 µM) for 24h. Next day cells were treated with the drug of interest in presence of NAC and cell viability was measured.

2.4 Drug synergism calculation

We utilized CompuSyn software (Chou, 2010) based on Chou-Talalay model (Chou & Talalay, 1984) for synergy quantification. Dosage and the effect (decrease in cell viability) of both single drugs and the combination were given as an input to CompuSyn software which yields combination index values (CI) as an output. In Chou-Talalay model CI<1, =1, and >1 indicates synergistic, additive and antagonistic effect respectively.

2.5 Live cell imaging

All live-cell imaging experiments were carried out by Olympus Xcellence Pro inverted microscope (Center Valley, PA, USA) with a × 10 air objective in a chamber at 37°C, supplied with 5% CO_2. Cells were seeded as 150.000 cells/well to 6-well plates and treated with chemicals of interest simultaneously in combination. Time-lapse images were captured right after drug treatments with 5 or 6 min intervals. From each well, random positions were recorded to obtain image stacks and death/live cells in each image were counted using the ImageJ Software (NIH Image, Bethesda, MD, USA).

Quantifications were performed by counting 3 different image fields for each condition for selected time points. Live cell imaging experiments were performed with help of Fidan Şeker.

2.6 Quantitative RT-PCR

Cell pellets are collected after treatment with chemical of interests and subjected to RNA extraction by MN NucleoSpin RNA isolation kit. Concentrations of extracted RNA are measured by NanoDrop. cDNA was generated by M-MLV Reverse Transcriptase (Invitrogen). Detailed procedure is as follows: PCR reaction was set with equivalent amount of RNA for each sample (vary 200 ng to 1000 ng) by mixing RNA, 2.5 µl dNTP (2 mM ,Life Technologies), 1 µl random hexamer (50 µM) or 2,5 µl hexanucleotide mix and NF water up to 16.5 µl. 5 min incubation at 65°C was performed and then sample was mixed with 0.5 µl RNasin (Promega), 5 µl 5X First Strand Buffer (Invitrogen) and 2 µl DTT (0.1M, Invitrogen) , mixed and kept at RT for 10 min. Samples were supplemented with 1 µl of MMLV-RT enzyme (Invitrogen) and incubated at 37°C for 1 hour and for 15 min at 70°C. Final sample volume was arranged to 100 µl by dilution with nuclease free water. Quantitative RT-PCR was performed by Syber Green using primer pairs of genes of interest at LightCycler 480 Instrument II (Roche) following the procedure: 10 µl of LightCycler 480 SYBR Green I Master Mix (Roche) was mixed with 2 µl prepared cDNA, 2 µl of primer mix (2.5 mM), and 6 µl NF water. GAPDH was utilized as internal control since it is a housekeeping gene. Primers used for qPCR are listed in **Table 2.2**.

Table 2.2 List of utilized q-RT-PCR primers.

Gene		Sequence
CHK2	F	CTCGGGAGTCGGATGTTGAG
	R	GAGTTTGGCATCGTGCTGGT
CHK1	F	CGGTATAATAATCGTGAGCG
	R	TTCCAAGGGTTGAGGTATGT
TP53BP1	F	CCTCAGGCTCTGGTGACTTC
	R	TGACAGCACAGCCCAGTAAG
BRCA2	F	CAGTGGTATGTGGGAGTTTGT

	R	ATCCATGACTTGCAGCTTCTC
H2AX	F	ACTCAACTCGGCAATCCAAG
	R	GGGTT AGCTGCAGAATTCCA
DDB2	F	CTCCTCAATGGAGGGAACAA
	R	GTG ACCACCATTCGGCTACT
EXO1	F	CTTTCTCAGTGCTCTAGTAAGGACTCT
	R	TGGAGGTCTGGTCACTTTGA
MSH2	F	GGAGAGATTGAATTTAGTGGAAGC
	R	TCATTTCCTGAAACTTGGAGAA
MSH6	F	CATGCGGCGACTGTTCTAT
	R	CACACTTCAGCAGGGACGTA
KU70	F	GCTAGAAGACCTGTTGCGGAA
	R	TGTTGAGCTTCAGCTTTAACCTG
RAD51	F	CTTTGGCCCACAACCCATTTC
	R	ATGGCCTTTCCTTCACCTCCAC
BRCA1	F	CTGAAGACTGCTCAGGGCTATC
	R	AGGGTAGCTGTTAGAAGGCTGG
MSH3	F	CCATCATGGCTCAGATTGGC
	R	ATCATGAGTGCTCGTCCCTC
MLH1	F	CTACTTCCAGCAACCCCAGA
	R	AGAACCTCATGTCCCTGCTC
PMS1	F	ATGAGTGGAGCAGGGGAAAT
	R	CACTTGCTGACATGGGTTTCT
PMS2	F	ACTTCCGTGGATTCTGAGGG
	R	GTGTTTGGGGTTGCGAGATT
MGMT	F	CCCGTTTTCCAGCAAGAGTC
	R	GGATTGCCTCTCATTGCTCC
ATM	F	CATCGCATGTGATTAAAGCA
	R	TTCTGATAGGAATCAGGGC
ATR	F	CAATTGTGGAGGAGATTTCC
	R	CTTCTGAGAACTCTTGTATCTG
BIM	F	GCAATGGCTTCCATGAGGCAG
	R	TCCACACCAGGCGGACAATG

CASP8	F	ACACCAGGCAGGGCTCAAAT
	R	GCAGGTTCATGTCATCATCCAGTT
CASP7	F	CGGTCCTCGTTTGTACCGTC
	R	CGCCCATACCTGTCACTTTATCA
CASP3	F	CATGGAAGCGAATCAATGGACT
	R	CTGTACCAGACCGAGATGTCA
BAD	F	CCCAGAGTTTGAGCCGAGTG
	R	CCCATCCCTTCGTCGTCCT
BCL-2	F	CAGGGCGATGTTGTCCACC
	R	GGGGAGGATTGTGGCCTTC
BCL-XL	F	GGTCGCATTGTGGCCTTTTTC
	R	TGCTGCATTGTTCCCATAGAG
BIRC2 (CIAP1)	F	AGCACGATCTTGTCAGATTGG
	R	GGCGGGGAAAGTTGAATATGTA
BIRC3 (CIAP2)	F	CAGGGCTCCTGGGTAGAACT
	R	CTACTCCGTCCAGACTCATGC
FADD	F	GCTGGCTCGTCAGCTCAAA
	R	ACTGTTGCGTTCTCCTTCTCT
HRK	F	AGGTTGGTGAAAACCCTGTG
	R	GCATTGGGGTGTCTGTTTCT
Mcl1	F	TGCTTCGGAAACTGGACATCA
	R	TAGCCACAAAGGCACCAAAAG
NOXA	F	ACCAAGCCGGATTTGCGATT
	R	ACTTGCACTTGTTCCTCGTGG
PUMA	F	GACCTCAACGCACAGTACGAG
	R	AGGAGTCCCATGATGAGATTGT
DR4	F	ACCTTCAAGTTTGTCGTCGTC
	R	AACTCTCCCAAAGGGCTATGT
DR5	F	AAGACCCTTGTGCTCGTTGT
	R	AGGTGGACACAATCCCTCTG
BID	F	CCTACCCTAGAGACATGGAGAAG
	R	TTTCTGGCTAAGCTCCTCACG
HMOX1	F	AAGAGGCCAAGACTGCGTTCC

	R	GCAGAATCTTGCACTTTGTTGCTG
ARL14EPL	F	AATTGGACAGAAACAACTGCAACAA
	R	GATGAGCCTGCCACTTTTGTCA
MLC1	F	GTGCCATTTCCTGCTCGGGT
	R	GCACTTGGAAAGCAGGCCAC
CCDC64	F	CACGGGCTGTCCAGGAACTG
	R	ACAGCATCTTGATCTCGGCCTG
ANO8	F	CACCTCCCAGGAACGCCAGA
	R	TGGATGATCCCACGTGCTGC
ITGA11	F	GTGGCCAGGGTTCACGGA
	R	CGTCTCCCGTCTTCTGGTAGC
ITGA2	F	CTGCTGGTGTTAGCGCTCAGT
	R	GGGTGAACCAACCAGTAACCAGT
TENM2	F	ACCAGCATCTTGGAGTTACGAAATA
	R	GTCCCTGCCACAACTTCCGA
EFEMP1	F	AACTCTGCTAGCTCAAGATTCACA
	R	TGCTGTCTCACAGGATCCCA
IGFN1	F	ACTATGGCAGGAAAGCTCCG
	R	TCGCCTGTCAGCTTGTTGAT
TrxR1	F	ACG AAA GGC AAG AAC GGC GA
	R	TCTTTACCTCAGTACAGCGTGTG
MYT1	F	AGGGTCCCTCAATGGCTCGT
	R	CCTGACAAACTCCGGTGGGT
NQO1	F	AGGCTGGTTTGAGCGAGTGTT
	R	ATGCCACTCTGAATTGGCCAGAG
GCLM	F	GCAGACGGGGAACCTGCTGAA
	R	ACATCTGGAAACTCCCTGACCAAAT

2.7 Western blotting

Cells were treated with Chaetocin for 24 hr followed by 3hr TRAIL treatment to check caspase cleavage, BID truncation and PARP cleavage. Western blots involving

NAC-treated samples were performed on cells pretreated with NAC for 24 hr followed by Chaetocin and TRAIL simultaneous combinatorial treatment for additional 24hr.

Cells are pelleted (at 1500 rpm, 5 minutes) and lysed for 30 minutes on ice by vortexing at every 10 minutes. Lysis buffer components are 1% Nonidet P40 (NP-40), 1mM EDTA, 50 mM Tris- HCl (pH 7.8), 150 mM NaCl, 0.5 mM PMSF, 1 mM NaF, 1X phosphatase inhibitor cocktail (PhosSTOP, Roche, Switzerland) and 1X protease inhibitor cocktail (Complete Protease Inhibitor Cocktail Tablets, Roche, Germany). Lysates are centrifuged at 13.000 rpm for 10 mins at 4C and supernatants which contains protein extracts were collected. Quantification of protein concentration is done using with BCA Protein Assay kit (Life Technologies). Remaining protein extracts were stabilized by boiling at 95ºC for 15 minutes in 4x loading dye. Loading dye is prepared by mixing of 900 µl 4X Laemmli sample buffer (Biorad, USA) with 100 ul of beta-mercaptoethanol (Biorad, USA). Protein samples are loaded to gradient SDS polyacrylamide gels and run at 20 mA for 40 minutes. Proteins were transferred from gel to PVDF membrane by semidry Trans-Blot® Turbo™ RTA Mini PVDF Transfer Kit (#170-4272, Biorad, USA). To assess the transfer efficiency, membrane is stained with Ponceau Red (Biorad, USA) and washed several times with ddH_2O to remove excess staining. Membrane is cut into pieces considering the size of proteins of interest and blocked in 5% non-fat dry milk (Biorad, USA) in 1xTBS-T (20 mM Tris-HCl, pH 7.8, 150 mM NaCl, 0.1%, v/v Tween-20) at RT for 1 hour. Blocking buffer is discarded and membranes are incubated with primary antibody of interest at specific dilutions in primary antibody solution (2% BSA, 0.02%NaN_3 in TBST) overnight at 4ºC. Next day membrane is washed 3x15min with TBST and then incubated with HRP/IR conjugated secondary antibody in blocking buffer for 1 hour at RT. Membranes are washed 3 times 15 mins each with TBST and then proteins are visualized via chemiluminescence detection kit using Pierce ECL Western Blotting substrate (Life Technologies) . Emitted light is detected either at Licor Odyssey ® Fc Imaging System or captured in CL-XPosure Film (Thermo-Scientific, USA). All antibodies are listed in **Table 2.3**.

Table 2.3 Antibodies used for Western blot and immunostaining experiments

Primary Antibodies	Purchased from
Cleaved Caspase-3	Cell Signaling/9664
Caspase-3	Cell Signaling/9665

Caspase-7	Cell Signaling/12827
Caspase 8	Enzo / ALX-804-242
Caspase-9	Cell Signaling/9508
PARP	Cell Signaling/9542
cleaved PARP	Cell Signaling/9541
BIM	Cell Signaling/2933
BID (Human specific)	Cell Signaling/2002
Alpha tubulin	Abcam /ab15246
Alpha tubulin	Sigma/T9026
BCL-2 (human)	BD Biosciences/551098
BCL-XL (human)	BD Biosciences/610746
DR5	ProSci/2019
TP53	Santa Cruz/sc-126 L2217
H3K9me(3)	Abcam/ AB8898
H3	Cell Signaling / D1H2 4499S
H2AX(Ser139)	Sigma-Aldrich/ 05-636
Secondary Antibodies	Purchased from
Anti-rabbit	Santa Cruz/sc-2054
Anti-mouse	Santa Cruz/sc-2055

2.8 Annexin V/PI staining

Cells were seeded to 6-well plates (300.000 cells/well). After simultaneous treatment with Chaetocin and TRAIL (100 nM and 100 ng/ml respectively for 24h), all cells (both live cells attached to culture plate and dead cells free floating in medium) were harvested and pelleted. Pellets were washed in cold PBS, centrifuged and resuspended in 500 µl 1X Annexin binding buffer ($1x10^6$ cell/ml). 100 µl of cell suspension was transferred to BD flow tubes and 5 µl of Alexa Fluor 488 Annexin V (ThermoFisher, Waltham, MA, USA) and 1 µl of 100 µg/ml PI working solution (5ul of 1mg/ml PI stock diluted in 45 µl Annexin binding buffer) were added. Cell suspension was incubated at room temperature for 15 minutes. 400 µl Annexin V binding buffer was added. Stained cells were analyzed by BD Accuri C6 (BD Biosciences, USA) flow cytometer (excitation

488 nm, emission 530/575 nm) according to manufacturers'' instruction and 10.000 events were recorded for each sample.

2.9 Terminal deoxynucleotidyl transferase dUTP nick end labeling (TUNEL) Assay

Cells were seeded to 12-well plates (25.000 cells/well) on glass coverslips. Chaetocin and TRAIL simultaneous treatment (100 nM, 100ng/ml respectively) was performed for 24h. After washing with PBS, air dried cells were fixed by 300 µl fixation solution (4% PFA in PBS, pH 7.4, freshly prepared) at 4ºC for 1h. After rinsing 3 times with PBS, 300 µl Blocking solution (3% H_2O_2 in methanol) was added for 10 min at RT. Coverslips were rinsed with PBS 3 times and then incubated in 30µl Permeabilization solution (0.1% TritonX-100 in 0.1% sodium citrate, freshly prepared) at RT. After drying, 50 µl TUNEL reaction mixture (5µl enzyme solution + 45µl label solution) was added on top of each coverslips and samples were incubated 60 min at 37ºC. Coverslips were washed 3 times and with DAPI dye, sealed and visualized by Leica DMi8 inverted microscope (Leica Microsystems, Germany). Quantification of images was done with ImageJ software (NIH Image, NIH Bethesda, USA). TUNEL experiments were performed with help of Dr. İlknur Sur Erdem.

2.10 YO-PRO-1/PI staining

Cells were seeded to 12-well plates (30.000 cells/well). Chaetocin and TRAIL simultaneous treatments (100 nM, 100 ng/ml respectively) were performed for 6h. Wells are rinsed once with PBS followed by incubation in 300 µl staining solution (1µM YO-PRO-1 by Invitrogen Cat. No: Y3603, Thermo Fisher, USA and 1:1000 PI (1mg/ml) in PBS) for 15 min at 37^0C in dark. Each well was visualized, and representative images were taken by Nikon Eclipse TS100 Inverted Fluorescence Microscope (Nikon Instruments Inc., NY, USA). Quantification of images was done with ImageJ software (NIH Image, NIH, Bethesda, USA).

2.11 RNA sequencing (RNAseq)

2.11.1 Sample preparation

Cells were seeded (400.000 cells/well) to 6-well plates. Experimental group consisted of duplicates of untreated control cells and cells treated with Chaetocin (50 nM) for 24h. RNA extraction was performed by Qiagen RNAeasy Mini Kit. Samples were sent to Berkeley University Functional Genomics Laboratory (Berkeley, CA) for sequencing at Illumina Hiseq4000 system to generate 50 bp single-end reads.

2.11.2 Library preparation

Library preparation was performed by the Functional Genomics Laboratory (FGL), a QB3-Berkeley Core Research Facility at UC Berkeley. mRNA enrichment was performed on total RNA using polyA selection with the Invitrogen Dynabeads mRNA Direct kit. Subsequent library preparation steps of enzymatic fragmentation, adapter ligation and cDNA synthesis were done on the enriched RNA on an Apollo 324™ liquid handling system, with PrepX™ RNAseq Library Prep Kits (WaferGen/now TakaraBio). 15 cycles of PCR amplification was used for index addition and library fragment enrichment. Libraries were sequenced on an Illumina HiSeq4000 by the Vincent J. Coates Genomics Sequencing Laboratory at UC Berkeley, supported by NIH S10 OD018174 Instrumentation Grant.

2.11.3 Bioinformatical analysis

The reads were aligned to human genome assembly hg19 through HISAT[342], which utilizes Bowtie alignment. Read counts were obtained for each transcriptome and were assigned with Ensembl ID derived from UCSC Genome Browser. Bioinformatical analysis was done by Fırat Uyulur. Data have been deposited in NCBI's Gene Expression Omnibus, accessible with GEO# GSE126462. Differentially expressed genes were identified based on negative binomial distribution using DESeq2(v.1.18.1)[343]. Enrichment of gene sets were analyzed using Gene Set Enrichment Analysis (GSEA) software[344] to obtain enriched hallmark pathways related to drug treatment.

2.12 In Vitro ROS detection

U87MG cells were seeded (300.000 cells/well) in 6-well plates. NAC was applied 24h prior to and during Chaetocin treatment. Chaetocin treatment is started 3h before the induction with ROS detection reagent and endured during the loading process, whereas

pyocyanin is added right at the induction step. Cells were detached by trypsinization, collected, washed with wash buffer and centrifuged at RT. Cells were induced by loading with ROS/Superoxide detection mix (Abcam, ab139476 kit) supplemented with above mentioned treatments and incubated for 30 min in the cell culture incubator (37º C, 5% CO_2). Samples were kept on ice and analyzed with Flow Cytometry (BD Biosciences, USA) at FL1-A (green oxidative stress detection reagent) and FL2-A (orange, superoxide detection reagent) channels for 10.000 cells. Compensation correction was made to avoid overlap between green and orange fluorescent signals.

2.13 H2AX staining

U87MG cells were seeded (25.000 cells/well) on glass coverslips in 24-well plates. Upon completion of treatment (simultaneous combinatorial treatment with Chaetocin and TRAIL), wells were washed with PBS (3 times) and cells were fixed using 100% ice-cold methanol. Cells were washed with PBS (3 times) and then incubated in Blocking Solution (5 ml Triton-X, 7,5 ml FBS, 37.5 ml PBS) for 15 min at RT. Cells were washed with PBS (3 times) and then incubated in primary antibody (Anti-phospho-Histone H2AX Ser139 Antibody, Millipore, 05-636, 1:100 diluted) at RT for 2h (or overnight at 4ºC). Cells were washed with PBS (3 times) and incubated with secondary antibody (anti-Mouse IgG, Texas Red IR conjugated, 1:100 diluted) for 1h at RT. After washing, coverslips were mounted in DAPI on microscope slides and visualized with Leica DMi8 inverted microscope (Leica Microsystems, Germany). H2AX staining experiments were performed with help of Dr. İlknur Sur Erdem.

2.14 Cloning

2.14.1 gRNA

In order to deplete the expression of selected genes such as DR5, CASP8, BID, CASP3, CASP7 and HMOX1 with CRISPR/Cas9 method, gRNAs were either derived from Gecko v2 library[345] . gRNA for SUV39H1 gene was designed against proteins' functional domains using CCtop tool[346] following the procedure: Information on protein sequences of conserved functional domains was retrieved from NCBI Unigene software.

Protein sequences of the domains were traced back to coding exonic sequences by UCSC Blat software and then given as input to CCTop to yield candidate gRNA sequences[346]. Four-step criteria was followed to choose appropriate gRNA for efficient CRISPR /Cas9 targeting; 1) gRNAs with non-exonic targets were ignored, 2) Exonic off-targets of gRNA should have more than 3 mismatches, 3) Mismatches between gRNA and its' target gene sequence should be after 8 bp downstream from 5' end and finally 4) gRNA should not contain repetitive TTTTTT sequence.

All gRNA sequences are presented in **Table 2.4**. For cloning, top and bottom strands of gRNA against target genes were annealed. For annealing reaction 1ul from top and bottom gRNA (from 100 µM stock) is mixed with 6.5 µl nuclease-free water, 1 µL T4 ligase buffer with ATP (10X) and 0.5 µL T4 PNK. Mixture is run in PCR machine with conditions: 37ºC 30 mins, 95ºC 4 mins, ramp down to 25ºC (5º/min), infinite hold at 4ºC. Annealed gRNA is diluted 1/200 in nuclease free water and 1 µL of diluted gRNA is used for ligation reaction. Annealed gRNA sequences are used for ligation into pLenti-CRISPR-V2 vector (for HMOX1), pLenti-CRISPR-V1 vector (for SUV39H1) and pLenti-Guide vector (for DR5, BID, CASP8, CASP3 and CASP7). Vectors are digested with BsmB1 enzyme (in Buffer3.1) at 60 C for 3 h, run on 1% agarose gel, excised from gel and cleaned up from agarose and then treated with Antarctic phosphatase (AP) at 37C for 1 h followed by 15 min 65C enzyme inactivation step. AP treatment prevents self-ligation of vector, thus increase efficiency of gRNA cloning. For ligation reaction gRNA is mixed with 50 ng processed vector, 7.5 µL Quick Ligase buffer (2X), 1 µL Quick Ligase (Roche, Switzerland) and nuclease free water up to 20.5 µL reaction. No insert negative control which does not contain gRNA component is also set up. Ligation is performed at RT for 15 minutes. Ligated vector is transformed to competent bacteria Stbl3 step by step mixing 50 µL competent bacteria with ligation reaction, keeping on ice for 15 minutes, heat shocking bacteria at 42ºC for 30 seconds, adding 150 µL LB without antibiotic and growing bacteria at 37ºC 225 rpm for 1 hour. Transformed bacteria are spread on Ampicillin or Carbenicillin containing LB agar plates and colonies are grown overnight (16 hours). Grown colonies are picked and grown in Ampicillin containing LB Broth for 16 hours to proliferate. Plasmids are isolated by MN miniprep kit and after diagnostic digestion sent for sequencing by mixing with U6 forward sequencing primer (ACTATCATATGCTTACCGTAAC). Part of the clonings were performed with Fidan Şeker. The efficiency of gRNAs was then verified in cells transduced with each vector

using T7 Endonuclease Assay, as described in Supplemental Information. Efficient knockout with gRNA occurs within approximately 18 days since cas9 activity takes time.

Table 2.4 gRNA sequences for CRISPR experiments.

Gene		Sequence
DR5	F	CACCGATAGTCCTGTCCATATTTGC
	R	AAACGCAAATATGGACAGGACTATC
CASP8	F	CACCGTCCTTTGCGGAATGTAGTCC
	R	AAACGGACTACATTCCGCAAAGGAC
CASP3	F	CACCGAATGGACTCTGGAATATCCC
	R	AAACGGGATATTCCAGAGTCCATTC
CASP7	F	CACCGTTGATATTTAGGCTTGCCGA
	R	AAACTCGGCAAGCCTAAATATCAAC
BID	F	CACCGAGAACCTACGCACCTACGTG
	R	AAACCACGTAGGTGCGTAGGTTCTC
HMOX1	F	CACCGAAGGGCCAGGTGACCCGAGA
	R	AAACTCTCGGGTCACCTGGCCCTTC
SUV39H1_SET	F	CACCGAGCTTCGTCATGGAGTACGT
	R	AAACACGTACTCCATGACGAAGCTC
g-NT	F	CACCGACGGAGGCTAAGCGTCGCAA
	R	AAACTTGCGACGCTTAGCCTCCGTC
g-GFP-1	F	CACCGTGAACCGCATCGAGCTGAA
	R	AAACTTCAGCTCGATGCGGTTCAC
g-GFP-2	F	CACCGGAGCGCACCATCTTCTTCA
	R	AAACTGAAGAAGATGGTGCGCTCC

2.14.2 shRNA

shRNA sequences targeting BCL-2 and BCL-XL were designed using RNAi Codex program[347]. These oligos were PCR-amplified by using following primers having compatible restriction ends with backbone vector:

F: 5'GATGGCTGCTCGAGAAGGTATATTGCTGTTGACAGTGAGCG-3',

R: 5'-CCCTTGAACCTCCTCGTTCGACC-3'.

PCR reagents and conditions are listed in **Table 2.5**.

Table 2.5 PCR reagents and conditions

Reagent	Reaction volume
Phusion Buffer (HF)	10 ul
Betaine (1M)	10 ul
DMSO (5%)	2,5 ul
dNTPs (50 µM)	1 ul
Primer Mix (0,5 µM)	1 ul
Template Oligo (0,5 µM)	2,5 ul
Phusion Tag (1U)	0,5 ul
H_2O	22,5 ul

PCR protocol	Step
94ºC 5 min	Initial Denaturation
94ºC 30 sec	Cycle 25X
54ºC 30 sec (Adjusted depending on primers' Tm)	
75ºC 30 sec	
75ºC 2 min	Final Extension
4ºC ∞	Hold

PCR products were cloned into pSMP retro-viral backbone as described[348]. Briefly; samples are run on 2% agarose gel and extracted by MN Gel Extraction kit. Concentration of PCR product was measured by nanodrop. 250 ng PCR product as well as 10 µg backbone vector (MSCV) are digested with EcoRI- XhoI in 20 µl reaction for 1 h at 37ºC. 10x Antarctic phosphatase buffer and 1µl Antarctic phosphatase (NEB) is added to vector digestion mix and incubated at 37ºC for 15 min and 70 ºC for 30 min to eliminate self-ligation of vector. Digested PCR products (100 bp) and vector (6.5 kb) are run on 2% agarose gel and extracted by MN Gel Extraction kit. PCR product is ligated to vector at 1:3 molarity ratio by Quick Ligation Kit (Roche, Switzerland) together with negative control at RT for 15 minutes. Ligated vector is transformed to competent bacteria Stbl3 step by step mixing 50 µL competent bacteria with ligation reaction, keeping on ice

for 15 minutes, heat shocking bacteria at 42ºC for 30 seconds, adding 150 µL LB without antibiotic and growing bacteria at 37ºC 225 rpm for 1 hour. Transformed bacteria are spread on Ampicillin or Carbenicillin containing LB agar plates and colonies are grown overnight (16 hours). Grown colonies are picked and grown in Ampicillin containing LB Broth for 16 hours to proliferate. Plasmids are isolated by MN miniprep kit and after diagnostic digestion with EcoRI and XhoI, sent for sequencing. Sequences of cloned shRNAs from 5' to 3' are as follows:

sh BCL-XL:

TGCTGTTGACAGTGAGCGAGCTCACTCTTCAGTCGGAAATTAGTGAAGCCA
CAGATGTAATTTCCGACTGAAGAGTGAGCCTGCCTACTGCCTCGGA

sh *BCL-2*:

TGCTGTTGACAGTGAGCGAGGAGATAGTGATGAAGTACATTAGTGAAGCCA
CAGATGTAATGTACTTCATCACTATCTCCCTGCCTACTGCCTCGGA

2.14.3 Tet-*TRAIL* vector

Tet-TRAIL vector was cloned by Alişan Kayabölen. DNA sequence producing secreted TRAIL protein was amplified from LV-TRAIL plasmid via primers containing BamHI and XbaI cut sites and ligated into pENTR1A plasmid (Addgene plasmid #17398). Then, Gateway cloning was performed to take pLIX_402 Tet-inducible lentiviral expression vector (Addgene plasmid #41394). Vectors were verified by sequencing. The efficiency of the Tet-TRAIL was tested *in vitro* after transduction of U87MG cells with lentiviruses and treating with different concentrations of Dox (D9891 Sigma-Aldrich, MO, USA).

2.15 Viral packaging and transduction

All lentiviral or retroviral vectors used to transduce GBM cells throughout this study are listed in (**Table 2.1**) and all viral packaging was performed as described[349,348]. Briefly, on day 0, 2.5×10^6 HEK 293T cells were seeded to 10cm culture dish with DMEM supplemented with 10% FBS and 1% Pen/Strep. Viral plasmid DNA (2,5 µg), packaging plasmids Gag-Pol (2,250 µg of pUMVC or 8.2DeltaVPR for retroviruses and lentiviruses

respectively) and VSVG (250 ng) were transfected to cells using FugeneHD Transfection Reagent (Promega, USA) in serum-free DMEM or Opti-MEM. Next day (minimum 8 hours after transfection), media of plate was changed and 48 and 72 hours post transfection, media containing virus was collected and filtrated by 0.45 µm low protein binding filters. Viral media was aliquoted and stored at -80ºC.

Cells were seeded at desired density and were transduced with virus containing media supplemented with protamine sulfate (10µg/ml). 16 hours post-transduction, viral medium was replaced by fresh media. Transduced cells were selected by Puromycin at a final concentration of 1µg/ml for 3 days. For constructs in pLenti-Guide backbone, cells were transduced with lentiCas9-Blast vector and selected with Blasticidin for 6 days prior to transduction with gRNAs.

2.16 Virus concentration

PEG-8000 (Sigma) at the final concentration of 10% (w/v) was prepared by in PBS. Produced and securely filtered viruses were mixed with PEG solution at 1/5 ratio and kept overnight at 4ºC. Mixture was centrifuged at 1500 g at 4°C for 30 minutes and supernatant was discarded into bleach. Pellets were re-centrifuged at 1500 g for 5 minutes to completely remove the supernatant remnant by pipetting. Concentrated viral pellets were resuspended with cold 1X PBS at desired concentration. Concentrated viruses were aliquoted and stored at -80ºC.

2.17 Patient survival analysis

Patient survival analysis was performed by Dr. Mehmet Gönen. Gene expression profiles of GBM and "brain lower grade glioma" (LGG) tumors were preprocessed by the unified RNA-Seq pipeline of the Cancer Genome Atlas (TCGA) consortium (https://portal.gdc.cancer.gov). For both cancer types, HTSeq-FPKM files of all primary tumors from the most recent data freeze (i.e. Data Release 14–December 18, 2018) were downloaded, leading to 703 files in total. Metastatic tumors were not included since their underlying biology would be very different than primary tumors. Clinical annotation files of cancer patients were used to extract their survival characteristics (i.e. days to last

follow-up for alive patients and days to death for dead patients). For both cancer types, Clinical Supplement files of all patients from the most recent data freeze were downloaded, leading to 1114 files in total. To perform survival analysis using gene expression profiles, only patients with available survival information and gene expression profile were included, which led to a collection of 663 patients in total. The gene expression profiles of primary tumors were first $\log_2$-transformed and then *z*-normalized within each cohort before further analysis. The heat maps of gene expression values were based on these *z*-normalized gene expression values. For gene set analyses, 663 samples were grouped into two categories using *k*-means clustering ($k = 2$) on the *z*-normalized gene expression values of all genes included. Kaplan-Meier survival curves of these two groups were then compared. For single gene analyses, 663 samples were first grouped into two categories (i.e. low and high) by comparing each sample's gene expression value against the mean expression value of that particular gene. Kaplan-Meier survival curves of these two groups were then compared. *p*-value obtained from the log-rank test performed on these two survival curves were displayed.

2.18 In vivo experiment

All in vivo experiments were performed with help of Ahmet Cingöz. Non-obese diabetic/severe combined immunodeficient (NOD/SCID) mice, housed and cared in appropriate conditions at Koç University Animal Facility, were used and all protocols were approved by the Animal Experiment Local Ethics Committee. Firefly Luciferase (Fluc) and mCherry expressing stable U87MG cells were generated by viral transduction as described[349]. mCherry expression was validated by fluorescence microscopy and Fluc activity was validated by utilizing *in vitro* luminescence assay and Synergy Biotek Plate reader. Before implantation, Fluc-mCherry expressing U87MG cells were transduced with Tet-*TRAIL* lentiviruses. For subcutaneous tumor implantation, $2x10^6$ were injected in 100µl PBS per mouse (n=5/group) into the flanks of mice. For orthotopic model, $1x10^5$ cells were injected in 7µl PBS intracranially using stereotaxic injection [from bregma, AP: -2 mm, ML: 1.5 mm, V (from dura): 2 mm], as described[350]. Tumor development was monitored by repeated noninvasive bioluminescence imaging (IVIS Lumina III ,Perkin Elmer, USA) using 150 µg/g of D-Luciferin intraperitoneally under the isoflurane anesthesia. To test the effect of TRAIL and/or Chaetocin, mice with established tumors

were categorized into four experimental groups and Dox (10mg/ml) and Chaetocin (20mg/kg) treatments were performed simultaneously as intraperitoneal injections (twice/week). Two weeks after treatment, mice were sacrificed, and tumors were dissected. Statistical analysis was performed with GraphPad PRISM software (San Diego, CA, USA)

2.19 Sphere invasion assay

Spheroids were generated by culturing 20.000 U87MG cells per sphere in 20 µl medium as hanging droplets on tissue culture plate lid for 3 days. The plate was filled with culture media to prevent drying of droplets due to evaporation. Generated spheres were transferred to 6 well plates by pipetting and after attaching to surface of the plate, spheres were treated with Chaetocin (100 nM) for 2 days. Number of the cells invading out of the spheres were counted by ImageJ software (NIH Image, NIH Bethesda, USA).Sphere invasion assay was performed with help of Fidan Şeker.

2.20 Cell cycle assay

Cells were seeded to 6-well plates (300.000 cells/well). After treatment with Chaetocin (100 nM for 24h), all cells (both live cells attached to culture plate and dead cells free floating in medium) were harvested and pelleted. Harvested cells were washed with PBS and then fixed with ice cold 70% ethanol by adding 1 ml ethanol dropwise to the pellet while gently vortexing and then incubating at 4ºC for 30 minutes. Pellets were washed 2 times with PBS, spun at 850g, supernatant was carefully removed after each round. Pellets were treated with RNase (50 µl of 100 µg/ml stock) and incubated for 15 min. 200 µl PI (from 50 µg/ml stock) was added and cells were incubated at RT for 30 minutes. Tubes were stored at 4ºC, protected from light. Stained cells were analyzed by BD Accuri C6 (BD Biosciences, USA) flow cytometer (excitation 488 nm, emission 530/575 nm).

2.21 Xgal staining

Cells were seeded to 6-well plates (300.000 cells/well) and treated with Chaetocin (100 nM for 24h). NAC treatment (10 µM) was applied 24h prior to and during Chaetocin treatment. After treatment, cells were washed with PBS and fixed with 2% formaldehyde, 0.2% glutaraldehyde for 5 min at RT. Fixed cells were washed three times with PBS and stained with freshly prepared β-Gal staining solution (1 mg/ml X-Gal, 150 mM NaCl, 2 mM $MgCl_2$, 5 mM $K_3Fe(CN)_6$, 5 mM $K_4Fe(CN)_6$, 40 mM citric acid/sodium phosphate with pH 6.0) at 37 ˚C until blue color develops in positive control samples. X-gal solution was removed and cells were washed with PBS. Slides were covered with 50% Glycerol solution and stored at 4˚C. Images were taken by Nikon Eclipse TS100 Inverted Fluorescence Microscope (Nikon Instruments Inc., NY, USA). Xgal staining experiments were performed with help of Dr. İlknur Sur Erdem.

2.22 T7 Endonuclease assay

CRISPR edited cells were pelleted and their genomic DNA were isolated with MN Nucleospin Tissue kit (Macherey-Nagel, Germany). 30 cycle PCR was performed using specific surveyor primers (**Table 2.6**) for each gene with following steps: initial denaturation 95ºC for 3 min, denaturation 95 ºC for 30 sec, annealing at 60 ºC for 30 sec, extension 72 ºC for 1 min and final extension 72 ºC for 5 min. Amplified DNA were cleaned up with MN Gel and PCR extraction kit (Macherey-Nagel, Germany). T7 endonuclease digestion was performed as following steps: 95 ºC initial denaturation, (-2 ºC/sec) 95 ºC → 85 ºC, (-0.1 ºC /sec) 85 ºC →25 ºC. 1µl T7 endonuclease enzyme was added and samples were incubated at 37 ºC for 2 hours. Reaction was stopped by adding 1.5 µl 0.25 M EDTA to each sample. Samples were run on 1.5 % gel and visualized.

Table 2.6 Sequence information of primers used for T7 assay.

Gene		Sequence
SUV39H1	F	CTGGGACGCATCACTGTAGA
	R	GATCAGTCTCCCAGGCCTTTC
HMOX1	F	GAGAACGTGGCCTGAATGAG
	F	ACAAAATGCCCAACATGGAACC

2.23 Histone extraction

Cells were harvested and washed twice with ice-cold PBS. Cells were resuspended in Triton Extraction Buffer (TEB: PBS containing 0.5% Triton X 100 (v/v), 2 mM phenylmethylsulphonyl fluoride (PMSF), 0.02% (w/v) NaN3) at a cell density of 10^7 cells per ml. Cells were lysed on ice for 10 minutes with gentle stirring and then centrifuged at 6,500 x g for 10 minutes at 4°C to spin down the nuclei. Supernatant was discarded. Nuclei was washed in half the volume of TEB and centrifuged as before. The pellet was resuspended in 0.2 N HCl. Histones were acid extracted over night at 4°C. 1M NaOH was added as of 1/5 volume of the HCl solution. Samples were centrifuged at 6,500 x g for 10 minutes at 4°C to pellet debris. The supernatant which contains the histone proteins was stored. Protein content was quantified by Pierce BCA Protein Assay Kit (Cat.No:23227, Thermo Scientific, USA).

2.24 Luciferase reporter cell lines

Reporter construct was generated by Nazife Tolay and Melike Gezen from Sabancı University. A stable *TP53* reporter cell line was generated in HCT116 human colon cancer cells by inserting a single copy donor DNA into the hAAVS safe harbor site. The donor DNA plasmid was constructed by assembling DNA fragments containing 13 *TP53* binding sites and the Polyoma Virus promoter (from the PG13-luc plasmid), luciferase gene (from the pGL3 plasmid) into the AAVS1 SA-2A-puro-pA plasmid. This donor DNA was transfected into HCT116 cells along with two TALEN plasmids targeting a safe harbor site (hAAVS1 1L TALEN and hAAVS1 1R TALEN) using a 1:3 ratio (w/w) of plasmid: Polyethyleneimine (PEI - Polysciences 23966). Stably transfected colonies were selected with 1 µg/ml Puromycin (Sigma P9620) for 14 days and screened by PCR for correct integration. A highly TP53 responsive colony was selected by treatment with 1µM Doxorubicin (Sigma D1515) followed by luciferase assays.

2.25 Luciferin reporter assay

HCT116 cells stably expressing luciferase under the TP53 driven promoter were seeded to 96 well plate as 5.000 cells/well. NAC (10 µM) pretreatment started 24h before Chaetocin (100, 200, 400 nM for 24h) treatment. After treatment, 100 µg/ml D-Luciferin was added to each well and incubated for 10 min. Bioluminescence was measured by Synergy H1 plate reader (BioTek, VT, USA) and Gen5 data analysis software.

2.26 In vivo tumor growth with Dox-inducible TRAIL expression

NOD/SCID mice housed and cared in appropriate conditions of Koç University Animal Facility were used and all protocols were approved by the institution boards of Koç University. Fluc and mCherry expressing stable U87MG were transduced with Tet-TRAIL viruses. 1x 10^5 cells were injected in 7µl PBS intracranially using stereotaxic injection (Coordinates: 2 mm lateral, 2 mm caudal; 2 mm deep from bregma). Presence and progression of tumors was monitored by repeated noninvasive bioluminescence imaging (IVIS Lumina III). Accordingly, mice were injected with 150 µg/g body weight of D-Luciferin intraperitoneally and sum of the photon counts of tumor regions were obtained. To test the effect of Dox treatment induced TRAIL expression on tumor growth, mice with established tumors were treated with either saline or Dox (10 mg/ml) as intraperitoneal injections (once in every three-days starting from day 14). Quantification of tumor progression was performed with GraphPad PRISM software (San Diego, CA, USA)

Chapter 3

3. RESULTS

Despite recent developments in era of surgery chemo and radiotherapy, poor prognosis of GBM patients is still evident which points out the need for novel treatment strategies. TRAIL is a potent anti-cancer agent since it can induce both extrinsic and intrinsic apoptosis selectively in cancer cells. However, GBM cells possess intrinsic resistance to TRAIL which render clinical application of TRAIL inefficient. Epigenetic modulation of death receptor mediated pathway is evident in the literature therefore epigenetic mechanisms are proposed to be effective for TRAIL response of tumor cells. Our research mainly focused on breaking TRAIL resistance by combinatorial treatment with distinct epigenetic modifier agents and thus challenged one of the important limitations of clinical application of TRAIL.

In scope of this research, we aimed to identify epigenetic modifier chemical probes which can sensitize GBM cells to TRAIL mediated apoptosis. To this end, we conducted a chemical screen in U87MG cells in combination with TRAIL treatment, using the library composed of epigenetic drugs. Chemical probes that significantly sensitize GBM cells to TRAIL mediated apoptosis were identified and further characterized to understand underlying genetic mechanism.

3.1 Epigenetic compound screen identifies Chaetocin as novel TRAIL sensitizer

To identify compounds that can sensitize GBM cells to TRAIL, we conducted a chemical screen in U87MG cells using a library composed of compounds targeting different classes of chromatin modifiers; namely 12 Bromodomain inhibitor, 8 HDAC inhibitors, 9 HMT inhibitors, 8 HDM inhibitors, 2 DNMT inhibitors, 2 kinase inhibitors and 1 HAT inhibitor[341] (**Figure 3.1a**). Chemical probes in the library were generated by Structural Genomic Consortium, to which we had an access in collaboration with Prof. Udo Oppermann (University of Oxford, UK).

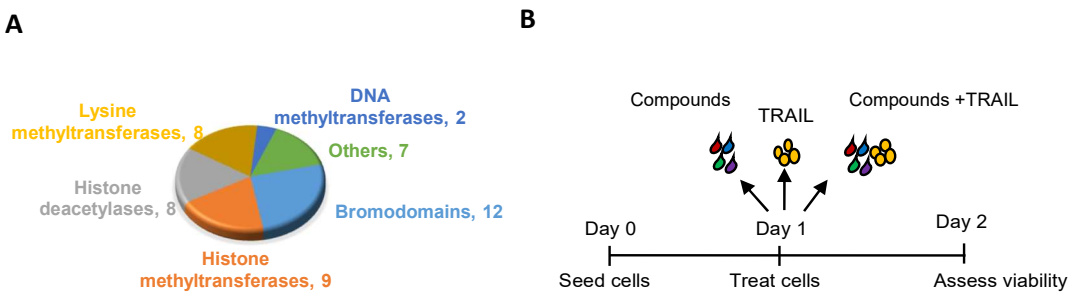

Figure 3.1 Epigenetic Compound Screen Components and Methodology (a) Chemical library consisted of inhibitors of chromatin modifier proteins (12 Bromodomain inhibitors, 8 HDAC inhibitors, 9 HMT inhibitors, 8 HDM inhibitors, 2 DNMT inhibitors, 2 kinase inhibitors and 1 HAT inhibitor). (b) Schematic diagram of the experimental setup.

The screen assessed the effects of the inhibitors alone or in combination with a fixed concentration of TRAIL through ATP based cell viability assays (**Figure 3.1b**). DMSO-only treated and untreated cells served as negative controls. On average, compounds alone had minimal effect on cell viability (98.8±9.9%). To determine which compounds to follow-up, we took into account total variability across all compounds and considered a compound a hit if it reduced cell viability 1 SD or lower (88.9% for compound alone and 42.1% for TRAIL combination). Accordingly, 9 compounds significantly decreased viability (namely; HDAC inhibitors Belinostat, CI-994 and TrichostatinA, HDM inhibitors GSK-J4, JIB-04 and Tranylcypromine; bromodomain inhibitor PFI-1, HMT inhibitor SGC0946 and methyl-lysine reader domain antagonist UNC1215) on their own. The response to TRAIL alone was 62±0.8% for control and 65±1% for DMSO groups (**Figure 3.2a**). When combined with TRAIL, compounds that decreased viability below 42.1% were SGC0946, GSK-J4, SAHA, 5-Azacytidine, PFI-1, HASPIN, Chaetocin, TrichostatinA and Belinostat (**Table 3.1**). After validating the hits from the screen (**Figure 3.2b**), we focused on those that did not reveal toxicity on their own but augmented the TRAIL-response of GBM cells. Those compounds were Chaetocin, HASPIN, and SAHA. While SAHA, a well-known HDAC inhibitor, has been previously reported to cooperate with TRAIL[351] and the antitumor role of protein kinase HASPIN has been established[352,353], Chaetocin has not been studied in relation to TRAIL in GBM. Therefore, we chose to further assess the effects of Chaetocin, a fungal metabolite produced by *Chaetomium* fungal species that has antimicrobial and cytostatic activity[305].

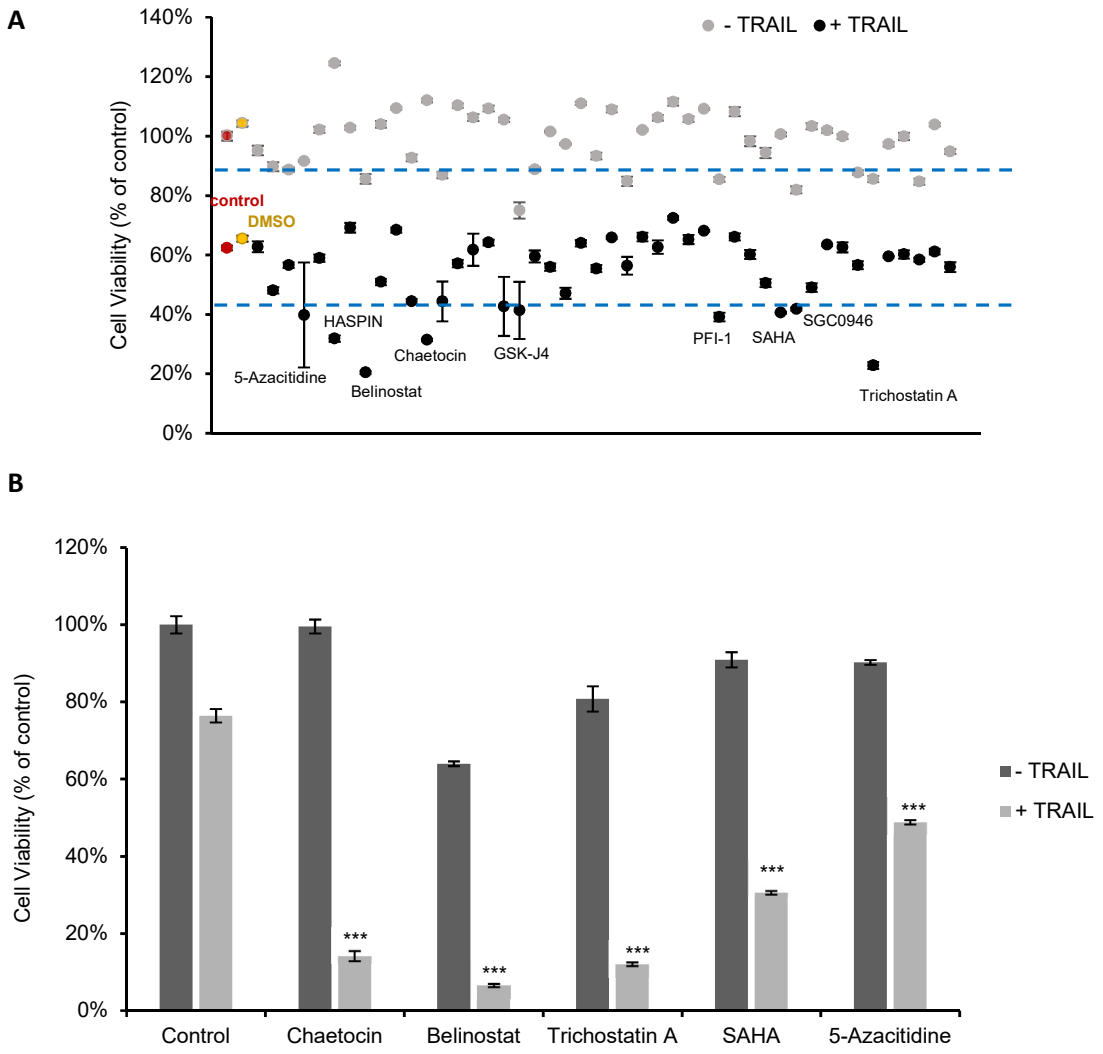

Figure 3.2 Epigenetic Compound Screen Identified Chaetocin as TRAIL Sensitizer (a) Plot of percent cell viability after treatment. Data were normalized to untreated control cells. Dotted lines denote 1 S.D. from % Mean cell viability upon treatment. Compounds lying below the lower threshold are TRAIL sensitizers. (b) Viability analysis of U87MG cells upon Chaetocin (50 nM), Belinostat (5 µM), Trichostatin A (500 nM), SAHA (1 µM) and 5-Azacitidine (10 µM) treatments for 24 h followed by TRAIL (100 ng/ml, 24h) treatment. Data were normalized to untreated control. (*** denotes P<0.001, two-tailed Student's t-test)

Table 3.1 List of compounds that augmented TRAIL response

Compound Name	**Compound Alone**	**Compound+ TRAIL**
SGC0946	82 ± 1,1	42 ± 0,5
GSK-J4	75 ± 2,8	41 ± 9,6
SAHA	101 ± 0,6	41 ± 0,3
5-Azacitidine	92 ± 0,3	40 ± 17,7
PFI-1	85 ± 0,8	39 ± 1,4
HASPIN	124 ± 0,6	32 ± 1,1
Chaetocin	112 ± 0,6	31 ± 0,4
Trichostatin A	86 ± 1,0	23 ± 1,2
Belinostat	86 ± 1,6	20 ± 0,5

Chaetocin is a nonspecific inhibitor of lysine-specific histone methyltransferases including SU(VAR)3-9[306] and also inhibits the oxidative stress mitigation enzyme thioredoxin reductase-1 (TrxR1 or TXNRD1)[308]. To assess the potential of Chaetocin as a TRAIL sensitizer, we performed viability assays. Accordingly, Chaetocin sensitized U87MG cells to TRAIL in a dose-dependent manner, even at low doses which did not exert toxicity alone (**Figure 3.3a**). Using CompuSyn software[354] based on Chou-Talalay model[355] for synergy quantification, we calculated combination index (CI) value for Chaetocin and TRAIL (**Table 3.2**). In Chou-Talalay model CI<1, =1, and >1 indicates synergistic, additive and antagonistic effect respectively. At effect level (Fa) >0.5; meaning more than 50% death of the drug treated cell population, Chaetocin and TRAIL combination yielded CI value smaller than 1 which indicates strong synergism between the two drugs. Synergism was most pronounced at 100 nM Chaetocin concentration (**Figure 3.3b**).

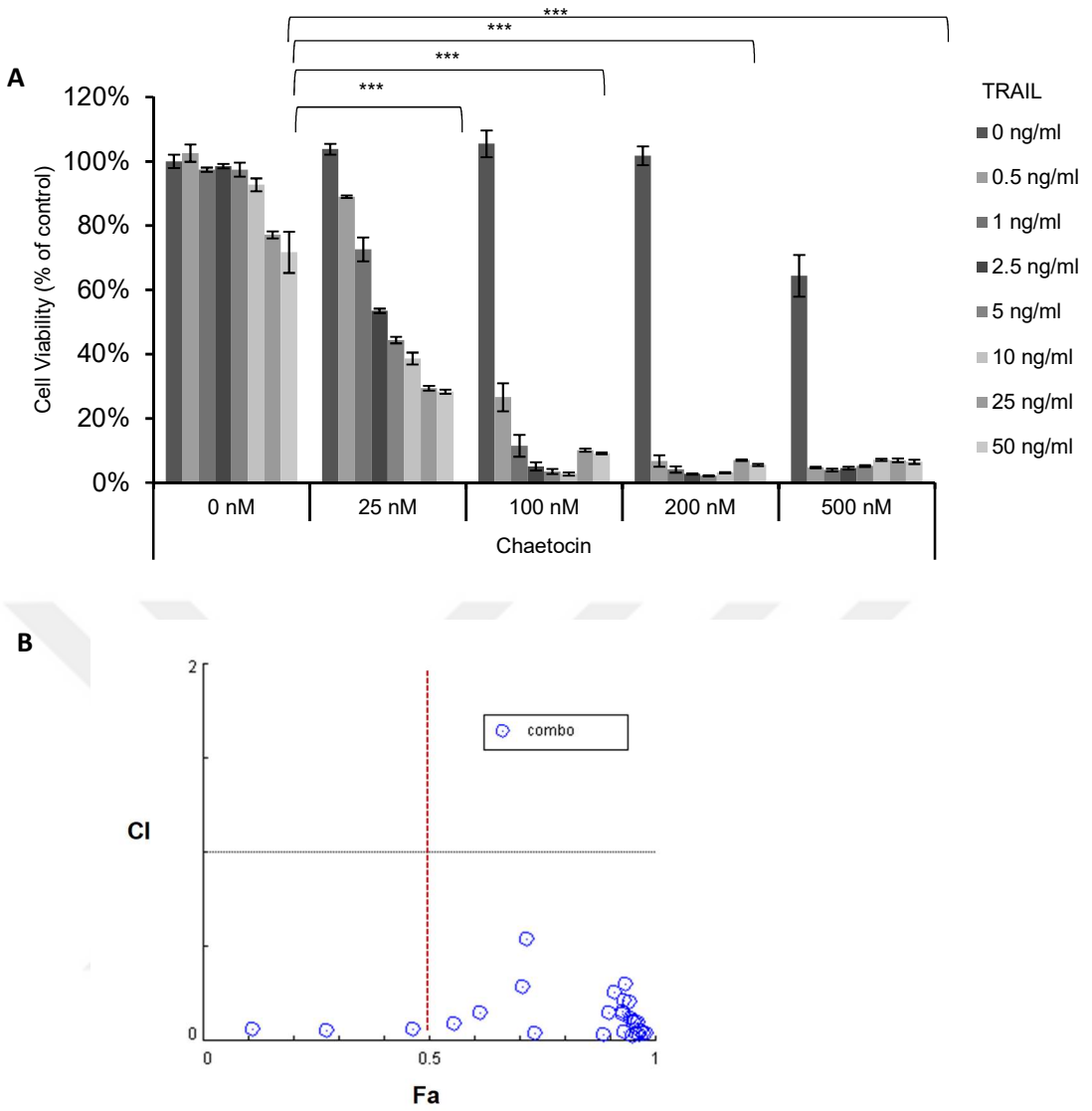

Figure 3.3 Chaetocin and TRAIL work synergistically to induce GBM cell death. (a) Viability analyses of U87MG cells showing markedly reduced viability upon Chaetocin and TRAIL combinatorial treatment at various dosages for 24h. Data were normalized to untreated control. (b) Combination index (CI) vs effect level (Fa) plot. (*** denotes P<0.001, two-tailed Student's t-test)

Table 3.2 Percent cell death and CI values for Chaetocin and TRAIL combinatorial treatment, calculated by CompuSyn software.

Dose Chae (nM)	Dose TRAIL (ng/ml)	Effect (% apoptotic cells)	CI Value
100.0	2.5	95	0.028
100.0	5.0	97	0.030
100.0	1.0	89	0.033
100.0	10.0	97	0.038
200.0	2.5	97	0.038
200.0	5.0	98	0.040
200.0	1.0	96	0.041
100.0	0.5	73	0.043
200.0	0.5	93	0.047
25.0	1.0	27	0.052
200.0	10.0	97	0.058
25.0	0.5	11	0.059
25.0	2.5	47	0.064
25.0	5.0	56	0.093
500.0	1.0	96	0.096
500.0	0.5	95	0.101
500.0	2.5	95	0.106
500.0	5.0	95	0.119
200.0	25.0	93	0.143
100.0	25.0	90	0.150
25.0	10.0	61	0.152
500.0	10.0	93	0.154
200.0	50.0	95	0.209
500.0	25.0	93	0.211
100.0	50.0	91	0.257
25.0	25.0	71	0.283
500.0	50.0	94	0.297
25.0	50.0	72	0.540

To visualize the timing and mode of cell death, we performed live cell imaging on GBM cells. Chaetocin and TRAIL, when applied as single agents were not potent death inducers, however when applied in combination, they induced cell death significantly (**Figure 3.4a**). The observed death involved membrane blebbing, cell shrinkage and formation of apoptotic bodies, as characteristic changes observed during apoptosis. Quantification of the number of cells that remain viable in response to treatment revealed significant cooperation of Chaetocin and TRAIL in reducing cell viability (**Figure 3.4b**).

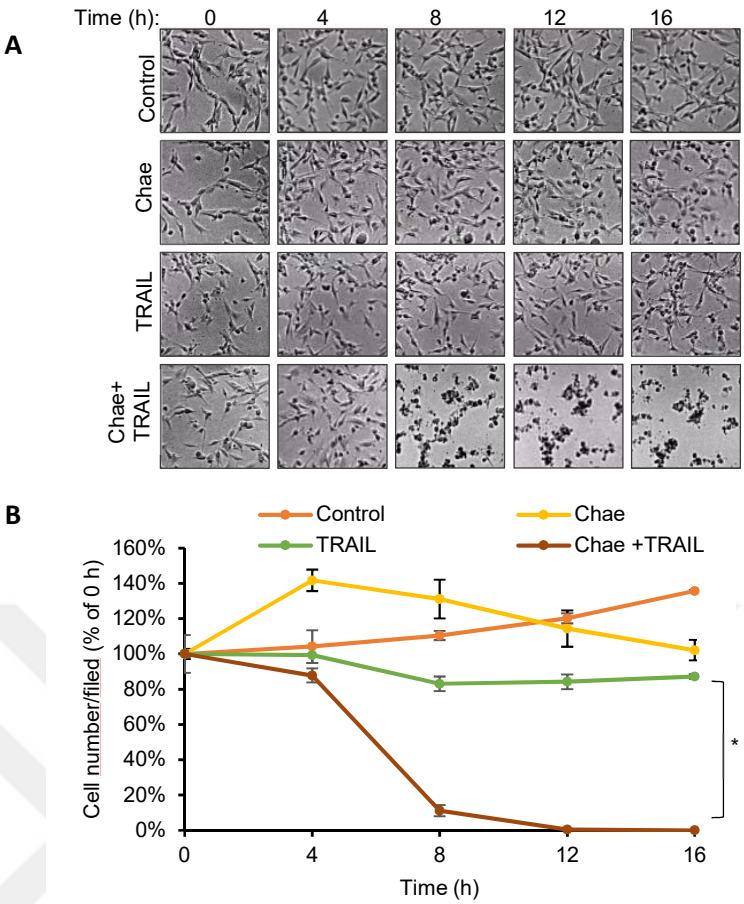

Figure 3.4 Chaetocin sensitize U87MG cells to TRAIL (a) Representative snapshot images from live cell imaging of U87MG cells upon Chaetocin (100 nM) and *TRAIL* (100 ng/ml) combinatorial treatment for 16h. Experiments were carried out by Olympus Xcellence Pro inverted microscope (Center Valley, PA, USA) with a 10x air objective. Time-lapse images were captured right after drug treatments in 6-minute time intervals. (b) Quantification of live cell imaging data by ImageJ program through counting live/death cell percentage at each time point. (* denotes P<0.05, two-tailed Student's t-test)

As U87MG exhibit only medium sensitivity to TRAIL[356], we examined the effects of Chaetocin in fully TRAIL-resistant cells lines as well. Using a resistant derivative of U87MG, U87MG-TR (*manuscript under review*) and innately resistant U373 cells, we showed that Chaetocin could also sensitize these cells to TRAIL (**Figure 3.5a-b**). This effect was observed in a sensitive primary GBM cell line GBM8 as well (**Figure 3.5c**). Together, these findings suggest that Chaetocin is a potent agent to overcome TRAIL resistance and augment TRAIL response of GBM cells.

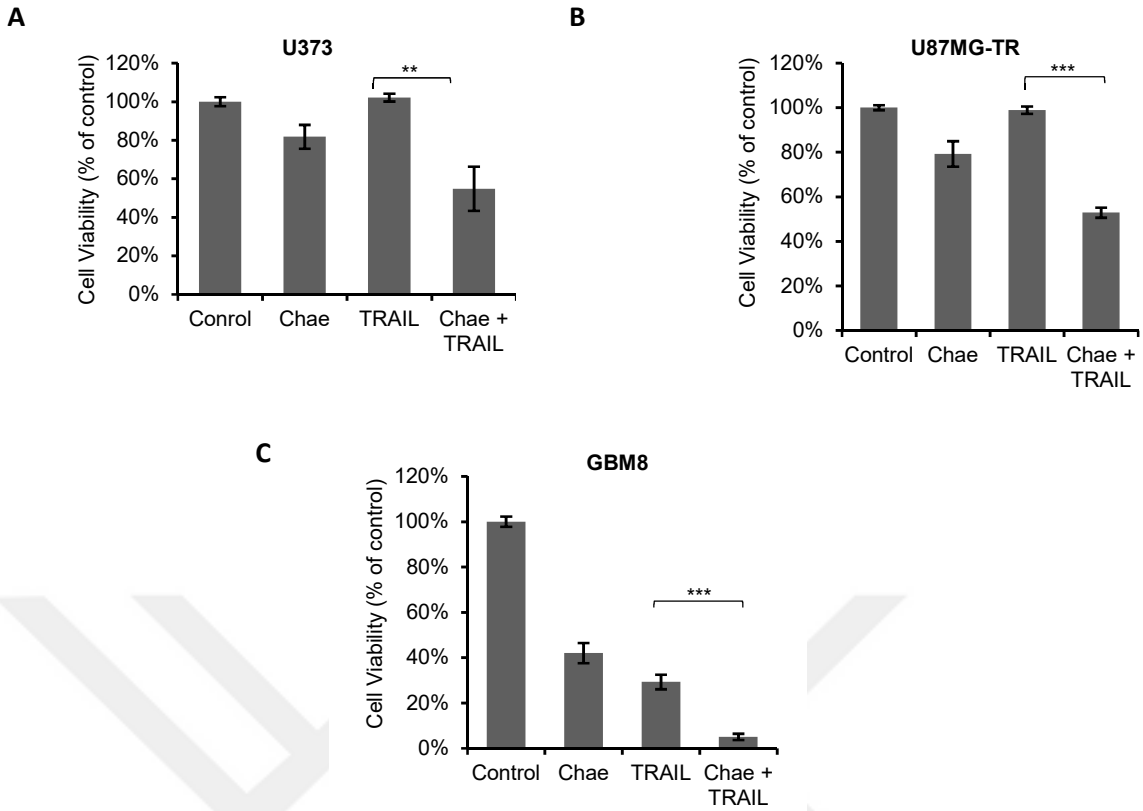

Figure 3.5 Chaetocin mediated TRAIL sensitization is applicable to U373, U87MG-TR and primary GBM cells. Viability analyses of (a) innately TRAIL resistant U373 cells, (b) U87MG-TR cells with acquired TRAIL resistance and (c) primary GBM cell line GBM8 upon Chaetocin and TRAIL combinatorial treatment Chaetocin (100nM) and TRAIL (100 ng/ml) for 24h. Data were normalized to untreated control cells (** and *** denote P<0.01 and P<0.001 respectively; two-tailed Student's t-test)

3.2 Combined Chaetocin and TRAIL treatment leads to efficient apoptosis of GBM cells

To address whether the observed death upon combinatorial treatment indeed involves apoptosis, we investigated caspase activity of GBM cells. While Chaetocin or TRAIL as single agents only moderately increased CASP3/7 activity, combinatorial treatment resulted in major elevation of CASP3/7 activity (**Figure 3.6**).

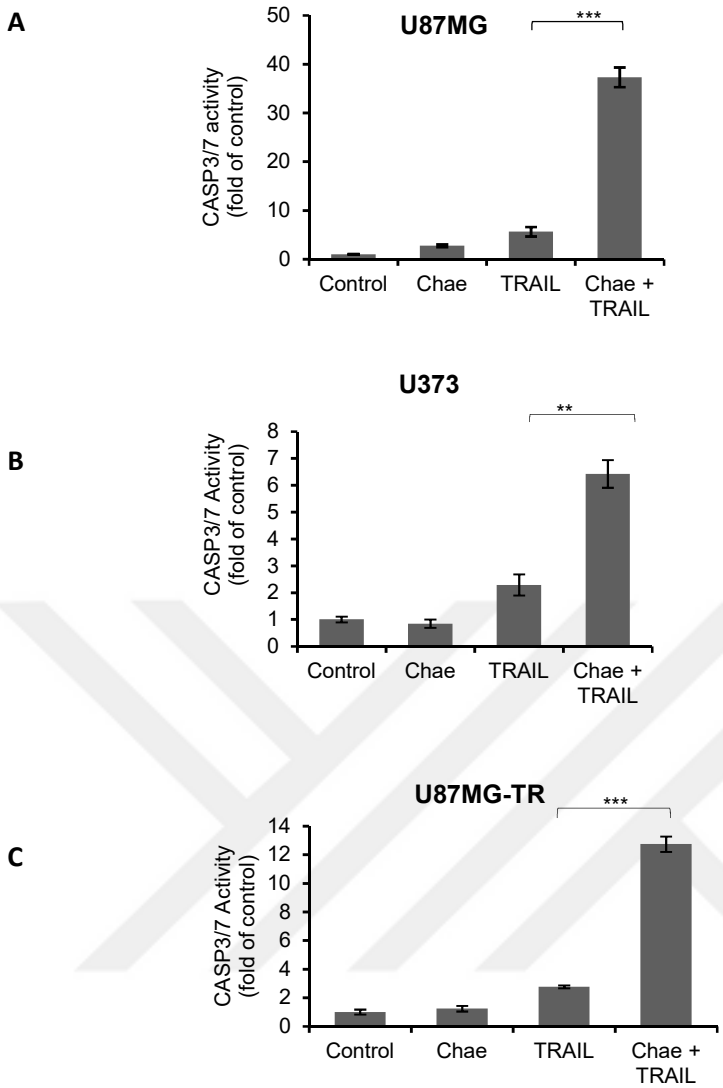

Figure 3.6 GBM cells display augmented caspase3/7 activity upon Chaetocin and TRAIL combinatorial treatment. Caspase-3/7 activity analyses of (a) U87MG cells, (b) innately TRAIL resistant U373 cells and (c) U87MG cells with acquired TRAIL resistance (U87MG-TR) upon Chaetocin (100 nM) and TRAIL (100 ng/ml) combinatorial treatment. Data were normalized to untreated control cells. (** and *** denote P<0.01 and P<0.001 respectively, two-tailed Student's t-test)

Similarly, enhanced cleavage of both initiator (CASP8) and effector (CASP9, CASP3) caspases were evident in combinatorial treatment, as revealed by western blotting. Furthermore, significant truncation and activation of BID, a link between extrinsic and intrinsic apoptosis, was detected when GBM cells were treated with both Chaetocin and TRAIL. Finally, as an important hallmark of apoptosis, cleavage of Poly (ADP-ribose) polymerase-1 (PARP-1) was also markedly enhanced upon combinatorial treatment (**Figure 3.7**).

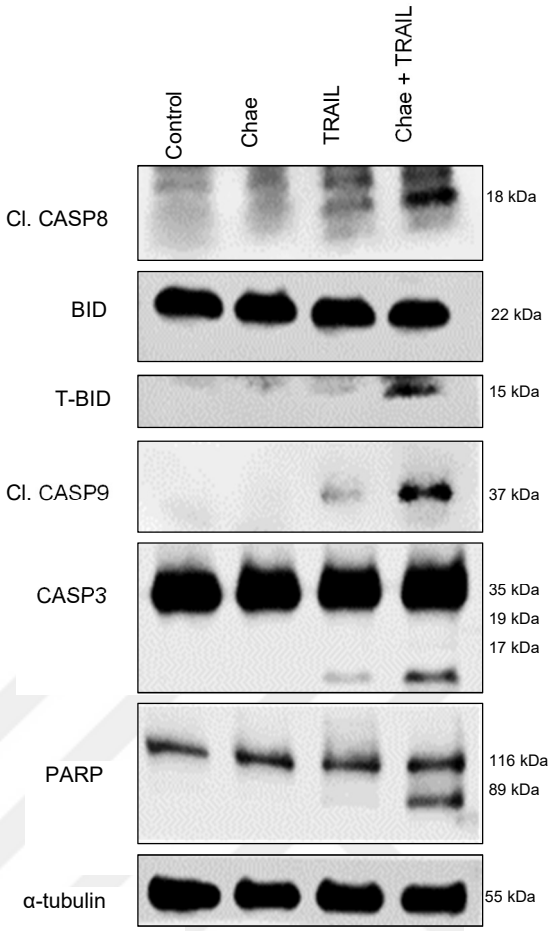

Figure 3.7 Apoptotic machinery is fully activated upon Chaetocin and TRAIL combinatorial treatment. Western blot analyses of U87MG cells for cleaved caspase-8, BID, tBID, caspase 3 and PARP after pretreatment with Chaetocin (100 nM for 24h) followed by 6 h TRAIL (100 ng/ml) treatment. α-tubulin was shown as protein loading control.

To further validate the involvement of caspases in the sensitization process, we investigated the functional effect of caspase activation using general caspase inhibitor Z-VAD-FMK. Accordingly, the inhibitor interfered with TRAIL sensitizing effect of Chaetocin and markedly reduced cell death (**Figure 3.8**).

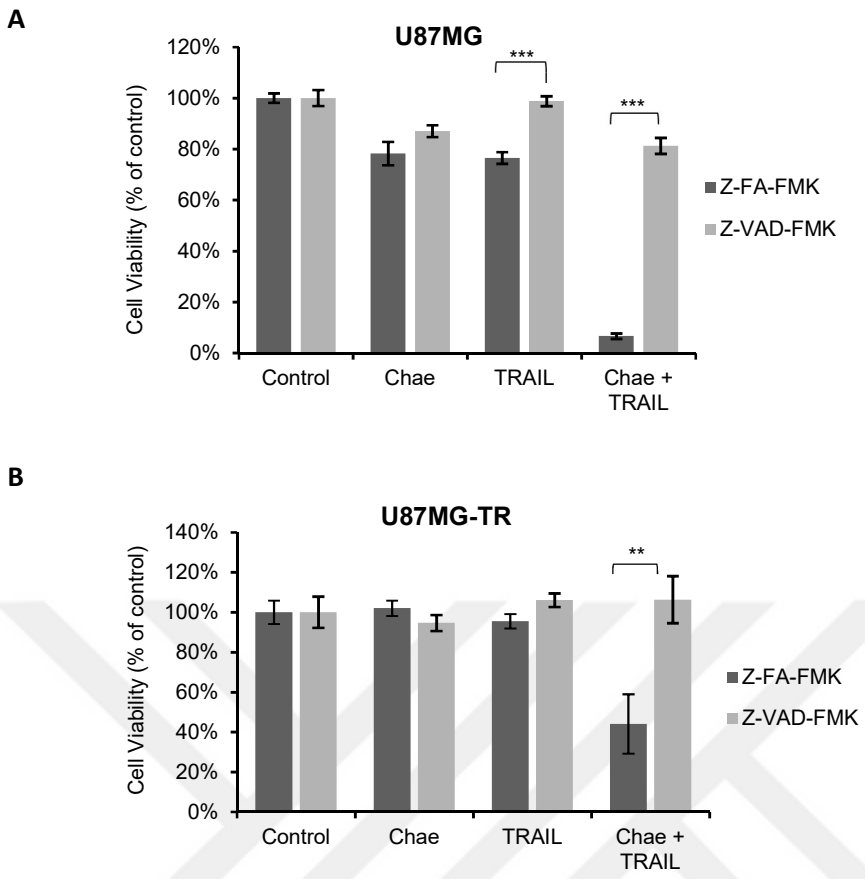

Figure 3.8 Caspases are indispensable for Chaetocin mediated TRAIL sensitization process. Cell viability analysis of (a) U87MG and (b) U87MG-TR cells pretreated with caspase inhibitors (20 µM for 24h) followed by Chaetocin (100 nM) and TRAIL (100 ng/ml) treatment for 24h in presence of inhibitors. Z-FA-FMK: negative control, Z-VAD-FMK: general caspase inhibitor. (** and *** denote P<0.01 and P<0.001 respectively, two-tailed Student's t-test)

To examine the apoptotic features of GBM cells, we performed TUNEL assay, which detects fragmented DNA generated during apoptosis[357] and showed TUNEL-positive cells were significantly more abundant in GBM cells sensitized to TRAIL through Chaetocin (**Figure 3.9**).

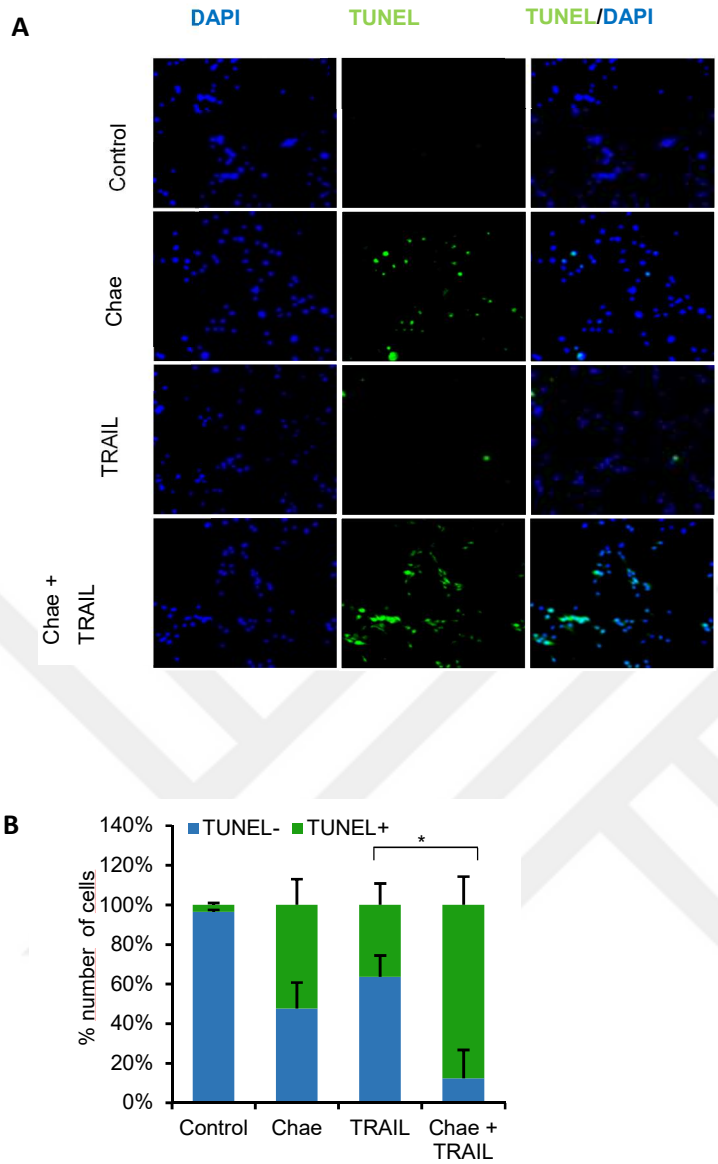

Figure 3.9 Chaetocin and TRAIL combinatorial treatment induce DNA fragmentation. (a) Terminal deoxynucleotidyl transferase dUTP nick end labeling (TUNEL) assay on U87MG cells showing increased DNA fragmentation upon Chaetocin (100 nM) and TRAIL (100 ng/ml) combinatorial treatment for 24h. Blue: DAPI staining nuclei, Green: TUNEL (+) cells. (b) Quantification of TUNEL staining by ImageJ program through counting TUNEL (+) cells with green fluorescence. (* denotes $P<0.05$, two-tailed Student's t-test)

Similarly, in a fluorescence dye-based "live/dead assay", we observed significant increases in the percentage of apoptotic cells upon combinatorial treatment (**Figure 3.10**).

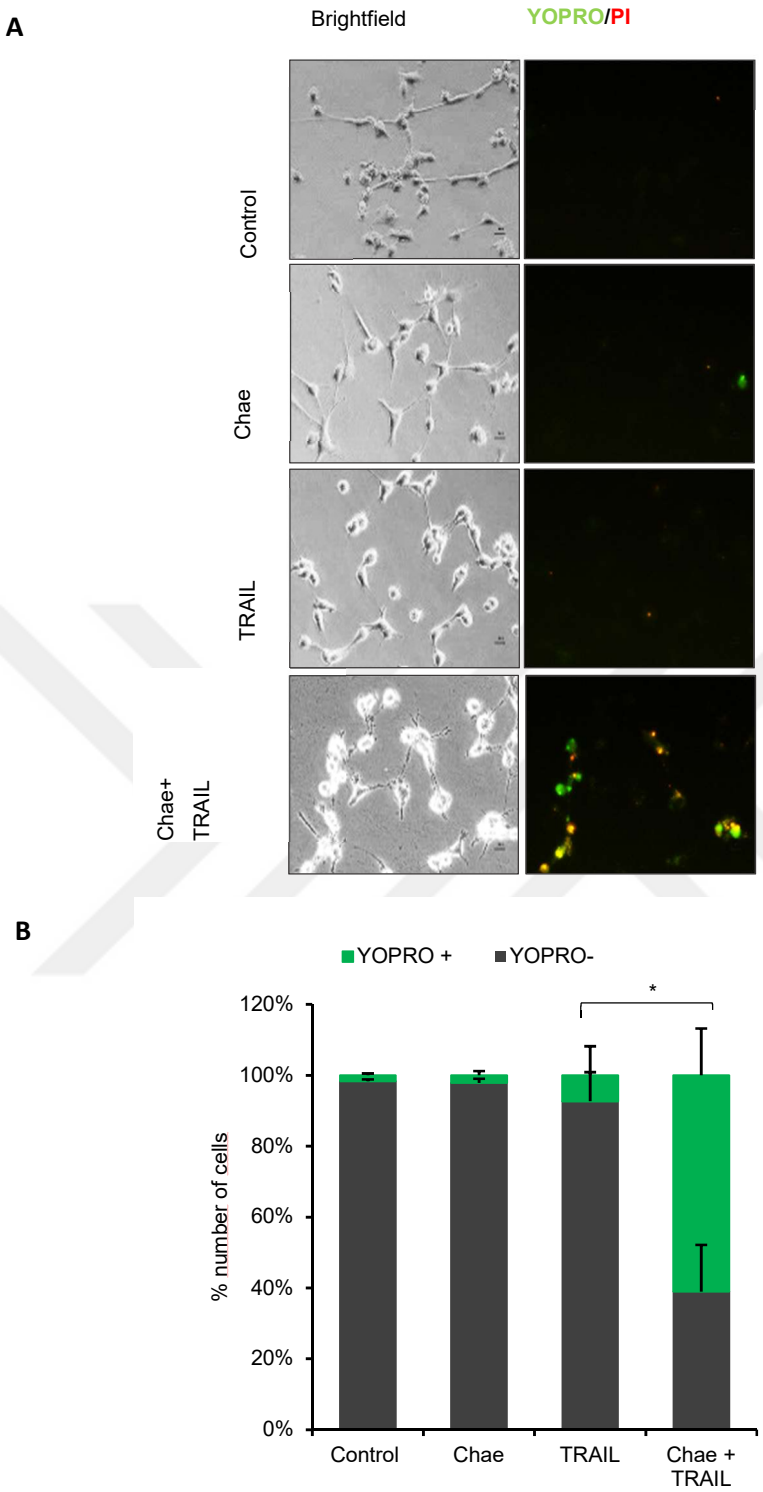

Figure 3.10 Number of YOPRO(+) apoptotic cells increase upon Chaetocin and TRAIL combinatorial treatment (a) YO-PRO-1 and PI staining upon Chaetocin (100 nM) and TRAIL (100 ng/ml) combinatorial treatment of U87MG cells for 24h. Green: YO-PRO-1 staining apoptotic cells, Red: PI staining dead/necrotic cells. (b) Quantification of YO-PRO-1/PI staining by ImageJ program through counting green and red fluorescence positive cells. (* denotes $P<0.05$, two-tailed Student's t-test)

These results were supported by flow cytometric analysis of Annexin V and PI-positive cells, where the presence of enhanced early and late apoptotic cells were evident with both Chaetocin and TRAIL treatment (**Figure 3.11**) indicating that Chaetocin and TRAIL cooperate to induce apoptosis in GBM cells.

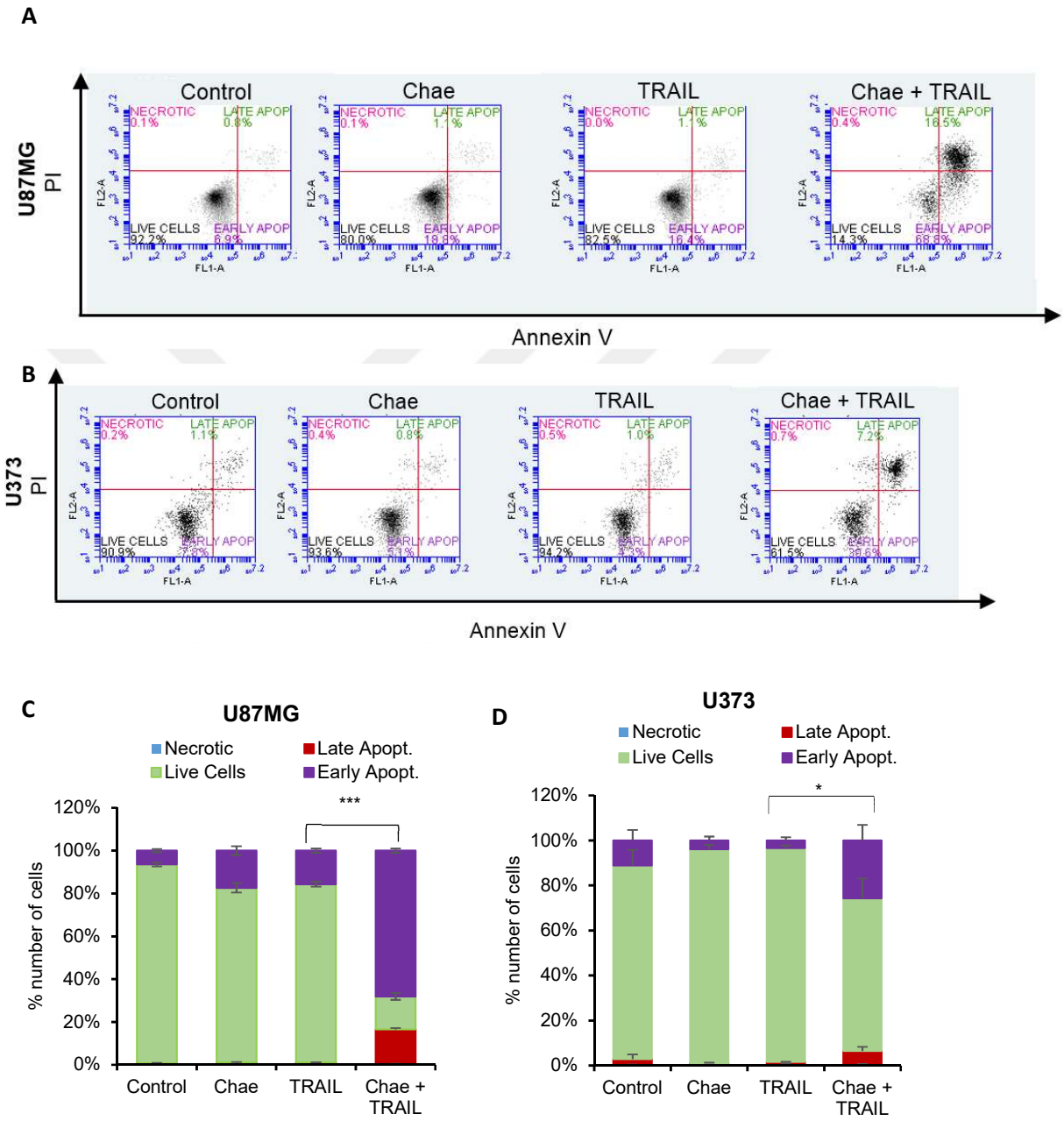

Figure 3.11 Number or Annexin V & PI (+) apoptotic cells increase upon Chaetocin and TRAIL combinatorial treatment. Flow cytometric analysis of Annexin V/PI stained (a) U87MG cells and (b) U373 cells upon Chaetocin (100 nM) and TRAIL (100 ng/ml) combinatorial treatment for 24h. Quantification of flow cytometry data for (c) U87MG and (d) U373 shows marked increase in apoptotic cell populations upon combinatorial

treatment. Data were normalized to total number of cells under each condition. (*, *** denote P<0.05 and P<0.001 respectively, two-tailed Student's t-test)

Next, we generated CRISPR/Cas9 mediated ablation of apoptosis-mediator proteins DR5, CASP8, BID, CASP7 and CASP3 in U87MG cells (**Figure 3.12a**). While individual knockout of the major components of extrinsic apoptosis pathway, DR5 and CASP8, recovered the cell death induced by Chaetocin and TRAIL, the knockout of either CASP3 or CASP7 alone were not sufficient to recover the Chaetocin induced TRAIL sensitization (data not shown). When both effector caspases were simultaneously ablated, there was a recovery in the response of GBM cells. Similarly, the reduction of BID levels led to effective recovery of cell viability upon combinatorial treatment (**Figure 3.12b**). Taken together, our data demonstrate that Chaetocin-induced TRAIL sensitization involves the activation of major apoptotic machinery in GBM cells.

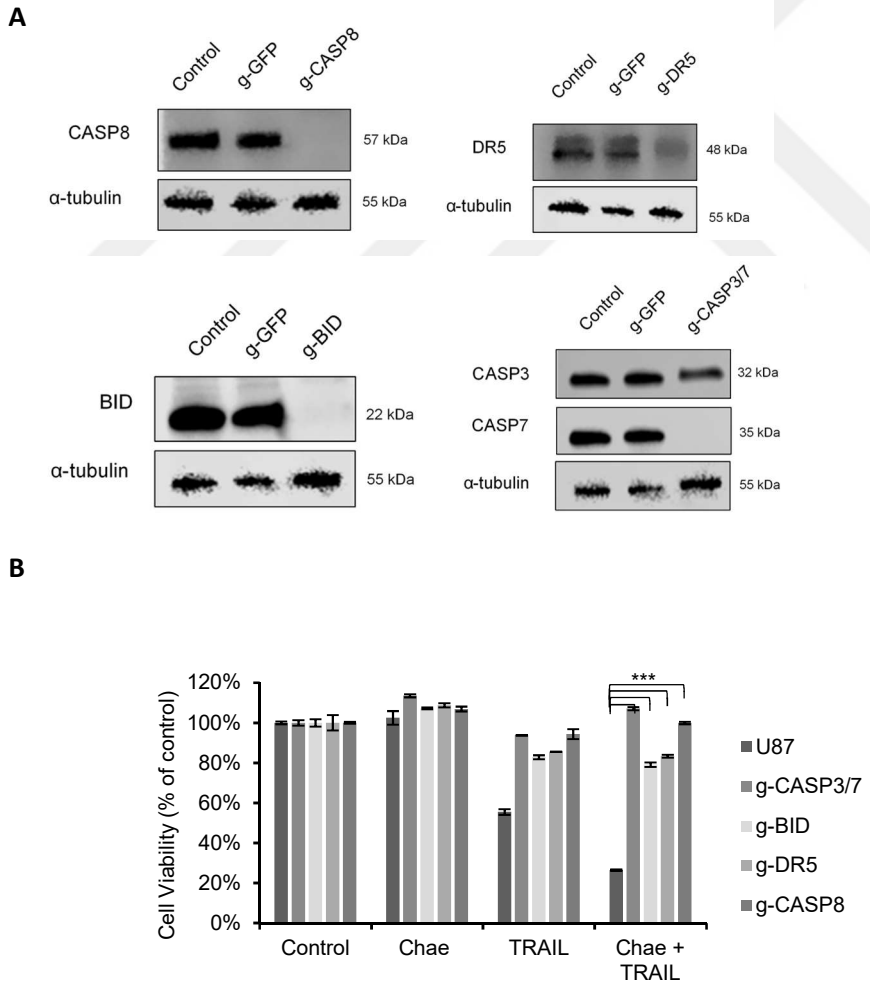

Figure 3.12 Major apoptotic pathway elements are crucial for Chaetocin mediated TRAIL sensitization to occur (a) Western blot analyses of U87MG cells showing individual stable CRISPR knockouts of DR5, BID and CASP8 as well as double knock

out CASP3/7 genes. GFP targeting gRNA (g-GFP) was used as negative control for CRISPR assay. α-tubulin was shown as protein loading control. (b) Viability analysis of CRISPR edited U87MG cells upon combinatorial treatment with Chaetocin (100 nM) and TRAIL (100 ng/ml) for 24h. Data were normalized to untreated control. (*** denotes P<0.001, two-tailed Student's t-test)

3.3 Chaetocin effectively sensitizes GBM cells to other pro-apoptotic agents, such as FasL and BH3 mimetics

To evaluate whether Chaetocin mediated apoptotic sensitization is exclusive to TRAIL or whether it can be a general sensitizer for apoptosis, we explored the effect of Chaetocin in combination with further pro-apoptotic agents. Chaetocin effectively sensitized GBM cells as well as U87MG-TR cells to FasL, another extrinsic apoptosis ligand as revealed by end-point cell viability assays (**Figure 3.13a-c**) and live cell imaging (**Figure 3.14a-b**).

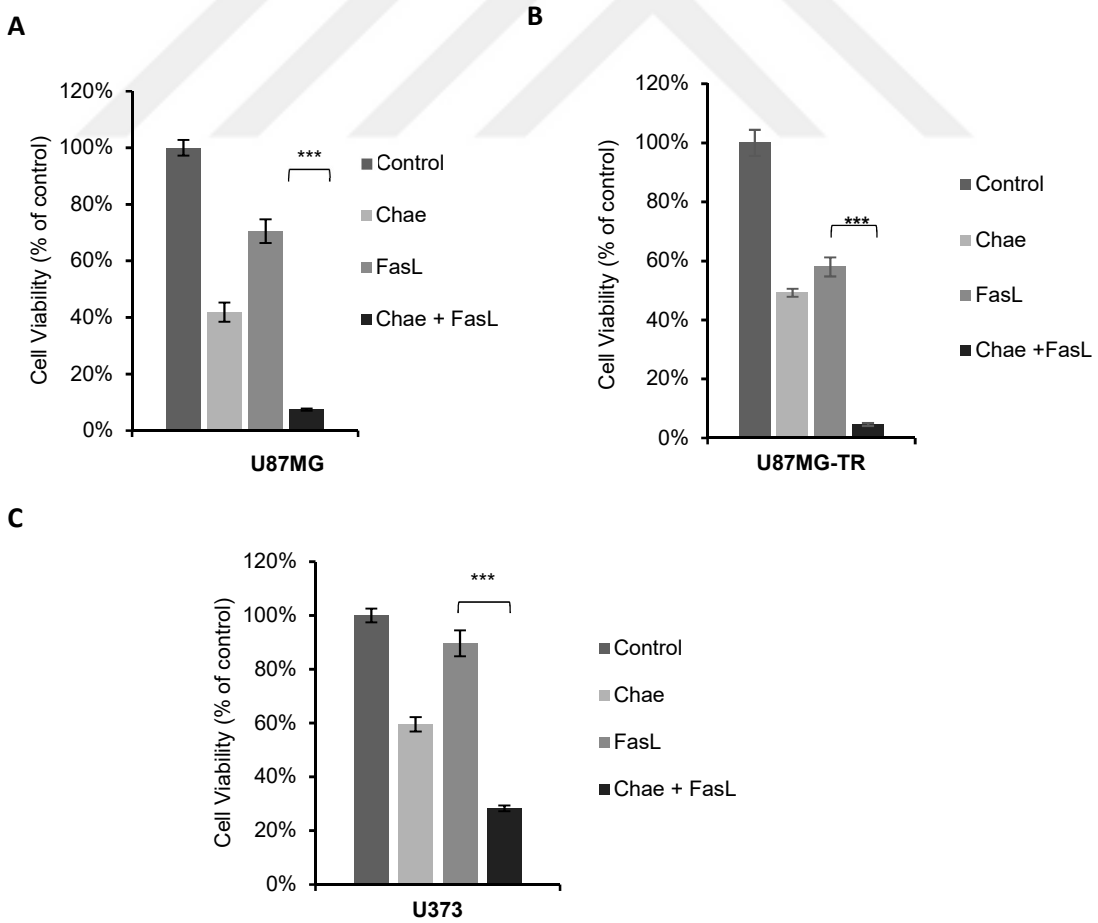

Figure 3.13 Chaetocin effectively sensitizes GBM cells to FasL. Viability analyses of (a) U87MG cells (b)U87MG-TR cells and (c) U373 cells showing markedly reduced viability upon combinatorial treatment with Chaetocin (100 nM) and FasL (100 ng/ml) for 24h

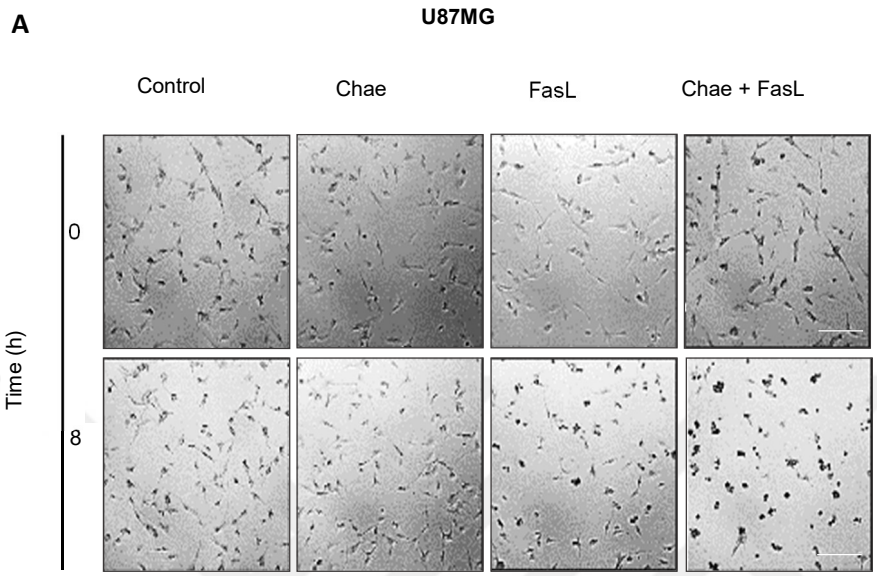

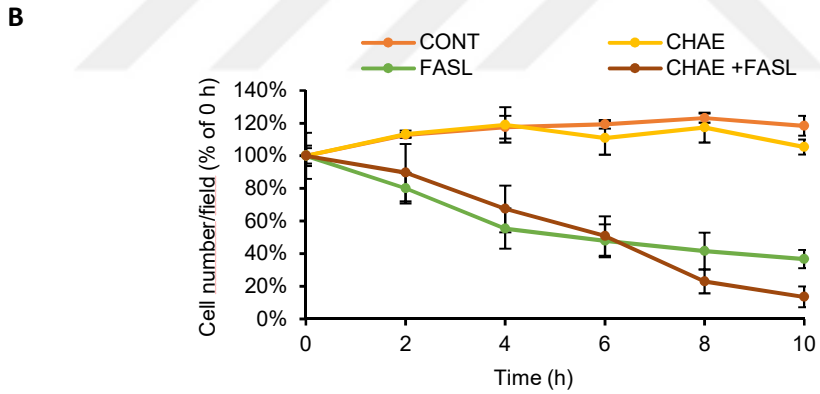

Figure 3.14 GBM cells treated with Chaetocin are more prone to FASL mediated apoptosis (a) Representative snapshot images from live cell imaging of U87MG cells upon Chaetocin (100 nM) and FASL (200 ng/ml) combinatorial treatment for 10h. Experiments were carried out by Olympus Xcellence Pro inverted microscope (Center Valley, PA, USA) with 10x air objective. Time-lapse images were captured right after drug treatments with 5-minute time intervals. (b) Quantification of live cell imaging by ImageJ program through counting live/dead cell percentage at each time point. Data was normalized to untreated control. (*** denotes P<0.001, two-tailed Student's t-test)

In addition, depletion of CASP8, but not DR5, recovered Chaetocin mediated sensitization to FASL (**Figure 3.15**).

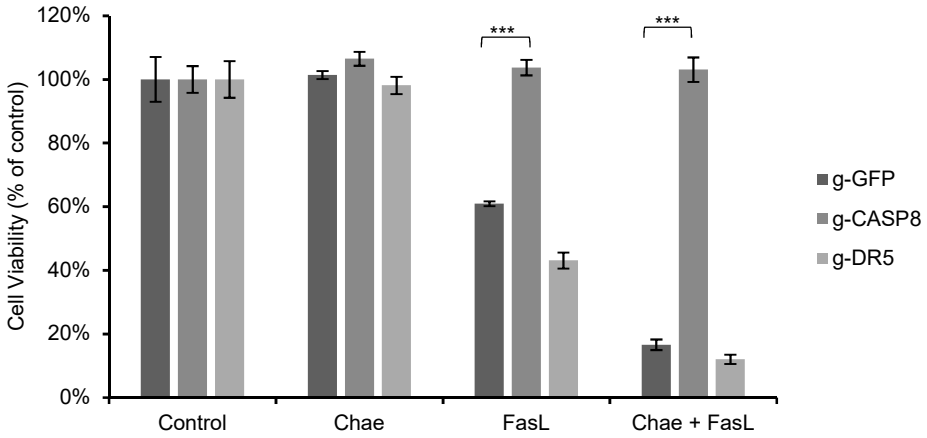

Figure 3.15 Viability analysis of CRISPR edited U87MG cells with Caspase 8 and DR5 knockouts upon combinatorial treatment with Chaetocin (100 nM) and FASL (200 ng/ml) for 24h. Data were normalized to untreated control. (*** denotes P<0.001, two-tailed Student's t-test)

The effect of Chaetocin was also tested in combination with are intrinsic apoptosis inducer BH3 mimetics; namely ABT263 (BCL-2 and BCL-XL dual inhibitor[358]) (**Figure 3.16**, **Figure 3.17**) and WEHI539 (BCL-XL inhibitor[359]) (**Figure 3.18**, **Figure 3.19**). Chaetocin was found to be strong sensitizer against these intrinsic apoptosis inducers Taken together, these results show that Chaetocin cooperated with several apoptotic agents to induce apoptosis in GBM cells.

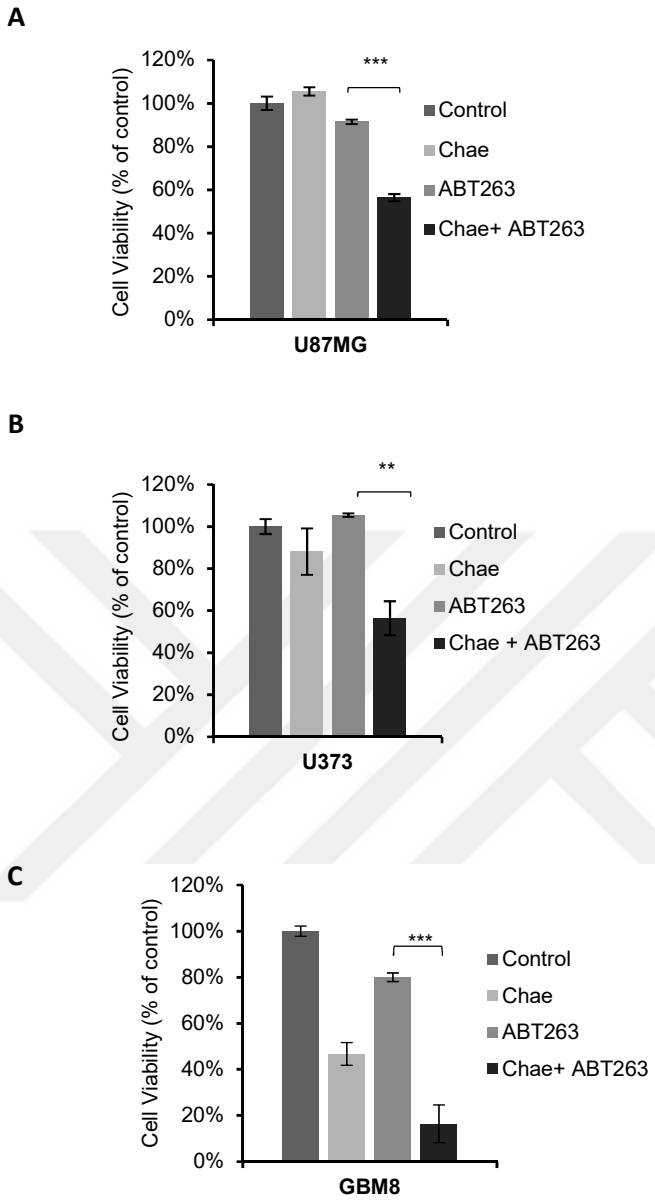

Figure 3.16 Chaetocin effectively sensitizes GBM cells to ABT263. Viability analyses of (a) U87MG and (b) U373 (c) GBM8 cells showing significantly reduced viability upon combinatorial treatment with Chaetocin (100 nM) and ABT263 (1 µM) for 24h.

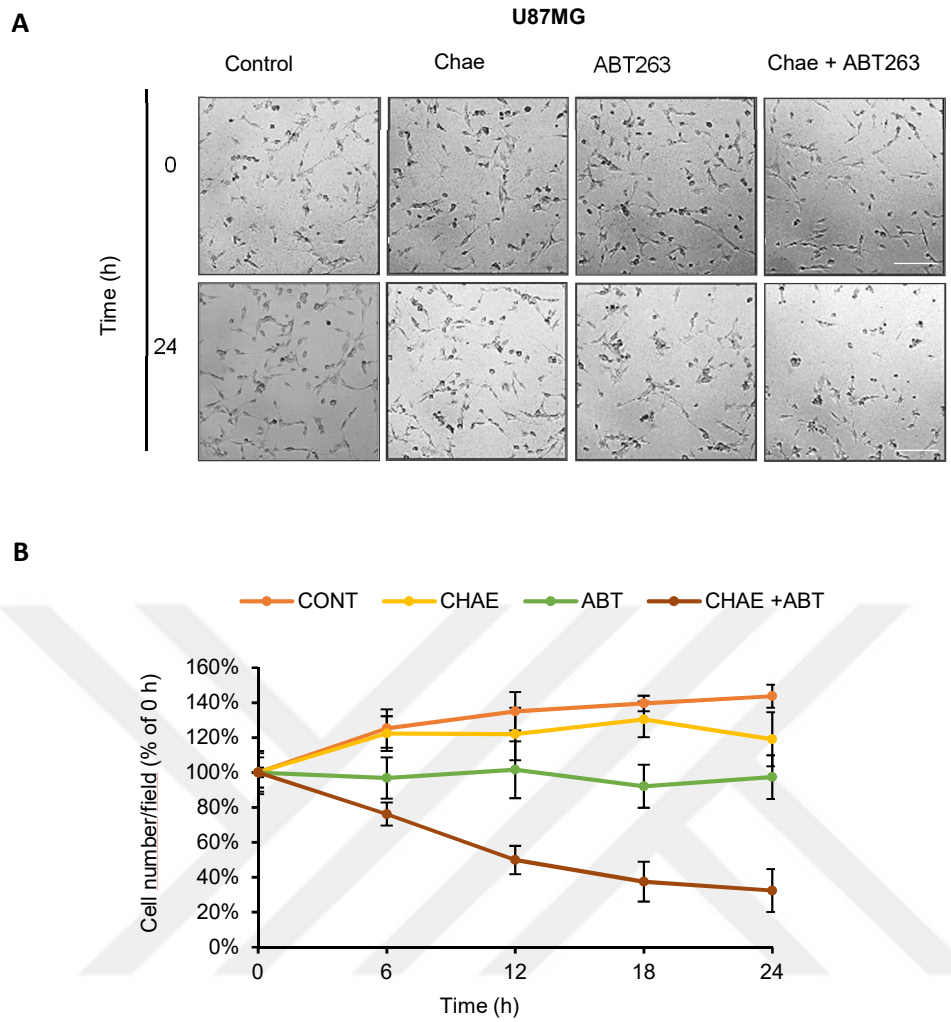

Figure 3.17 GBM cells treated with Chaetocin are more prone to ABT263 mediated apoptosis (a) Representative snapshot images from live cell imaging of U87MG cells upon Chaetocin (100 nM) and ABT263 (1 µM) combinatorial treatment for 24h. Experiments were carried out by Olympus Xcellence Pro inverted microscope (Center Valley, PA, USA) with 10x air objective. Time-lapse images were captured right after drug treatments with 5-minute time intervals. (b) Quantification of live cell imaging by ImageJ program through counting live/dead cell percentage at each time point. (** and *** denote P<0.01 and P<0.001 respectively, two-tailed Student's t-test)

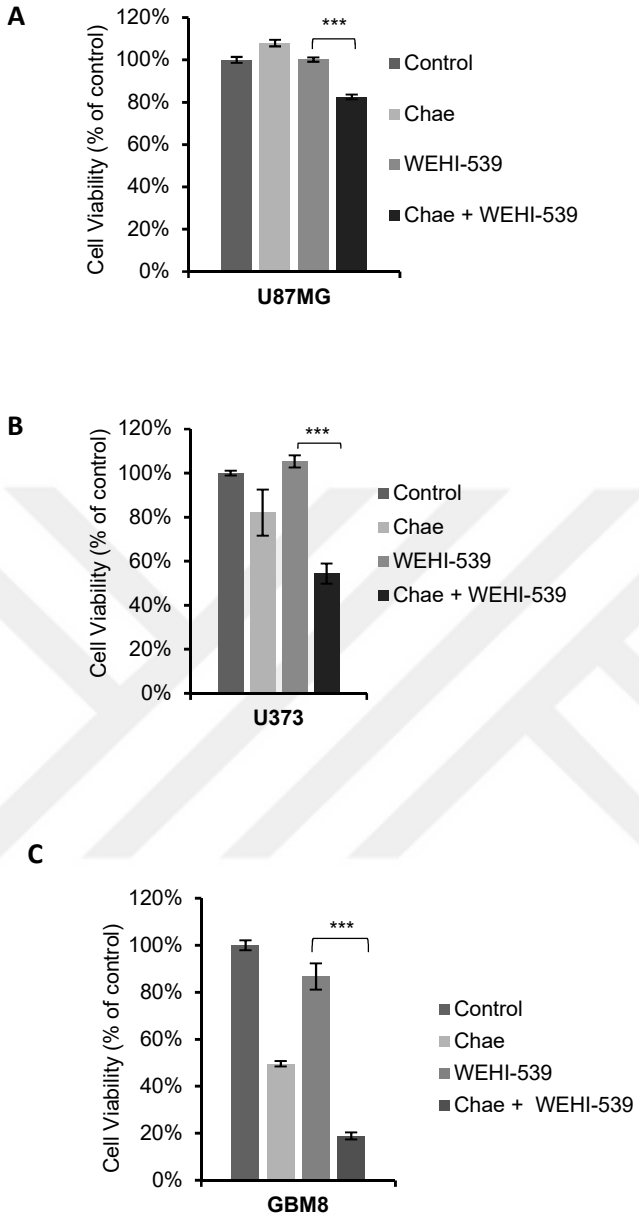

Figure 3.18 Chaetocin effectively sensitizes GBM cells to WEHI-539. Viability analyses of (a) U87MG and (b) U373 and (c) GBM8 cells showing significantly reduced viability upon combinatorial treatment with Chaetocin (100 nM) and WEHI-539 (1 µM) for 24h

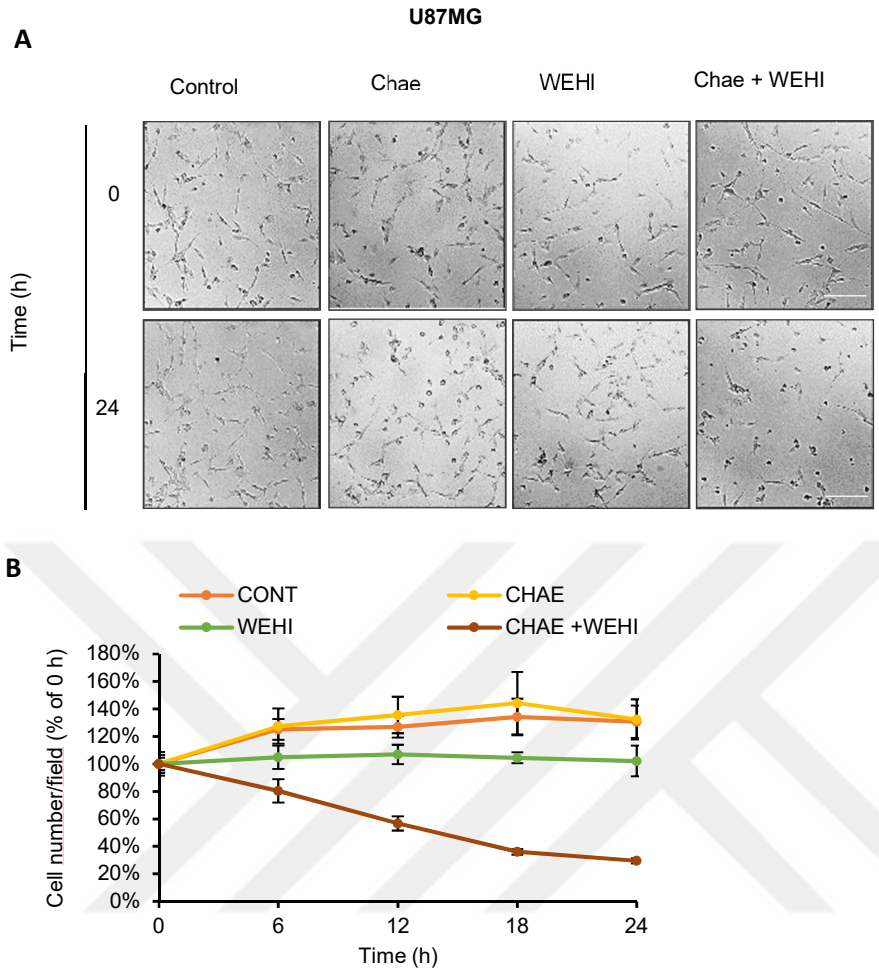

Figure 3.19 GBM cells treated with Chaetocin are more prone to WEHI-539 mediated apoptosis (a)Representative snapshot images from live cell imaging of U87MG cells upon Chaetocin (100 nM) and WEHI-539 (1 µM) combinatorial treatment for 24h. Experiments were carried out by Olympus Xcellence Pro inverted microscope (Center Valley, PA, USA) with 10x air objective. Time-lapse images were captured right after drug treatments with 5-minute time intervals. (b) Quantification of live cell imaging by ImageJ program through counting live/dead cell percentage at each time point. (*** denotes P<0.00, two-tailed Student's t-test)

3.4 Manipulation of the intrinsic apoptosis machinery regulates the Chaetocin-mediated *TRAIL* sensitization

Intrinsic apoptosis ultimately leads to reduction of mitochondrial integrity[360] where release of cytochrome C is regulated by the expression and activity of anti-apoptotic BCL-2 and BCL-XL proteins. Following up on our findings that Chaetocin cooperates with BCL-2/BCL-XL inhibitors, we further examined whether genetic manipulation of BCL-2 and/or BCL-XL could change the Chaetocin-mediated TRAIL

sensitization in GBM cells. Endogenous expression of *BCL-XL*, but not *BCL-2* levels were significantly affected by Chaetocin treatment (**Figure 3.20**).

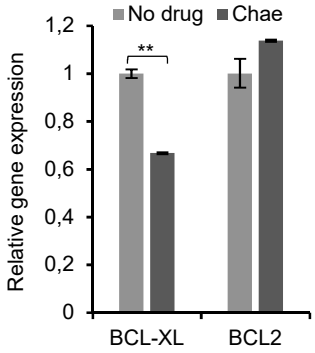

Figure 3.20 qPCR analysis showing *BCL-2* and *BCL-XL* mRNA levels in U87MG cells upon Chaetocin treatment (100 nm, 24h). Data were normalized to no drug conditions.

In a gain-of-function approach, we overexpressed *BCL-2* or *BCL-XL* using retroviral vectors that co-expressed GFP (or GFP alone as controls) (**Figure 3.21a-c**). BCL-2 or BCL-XL expression rendered U87MG cells more resistant to apoptosis induced both by TRAIL-only or combinatorial treatment (**Figure 3.21d**).

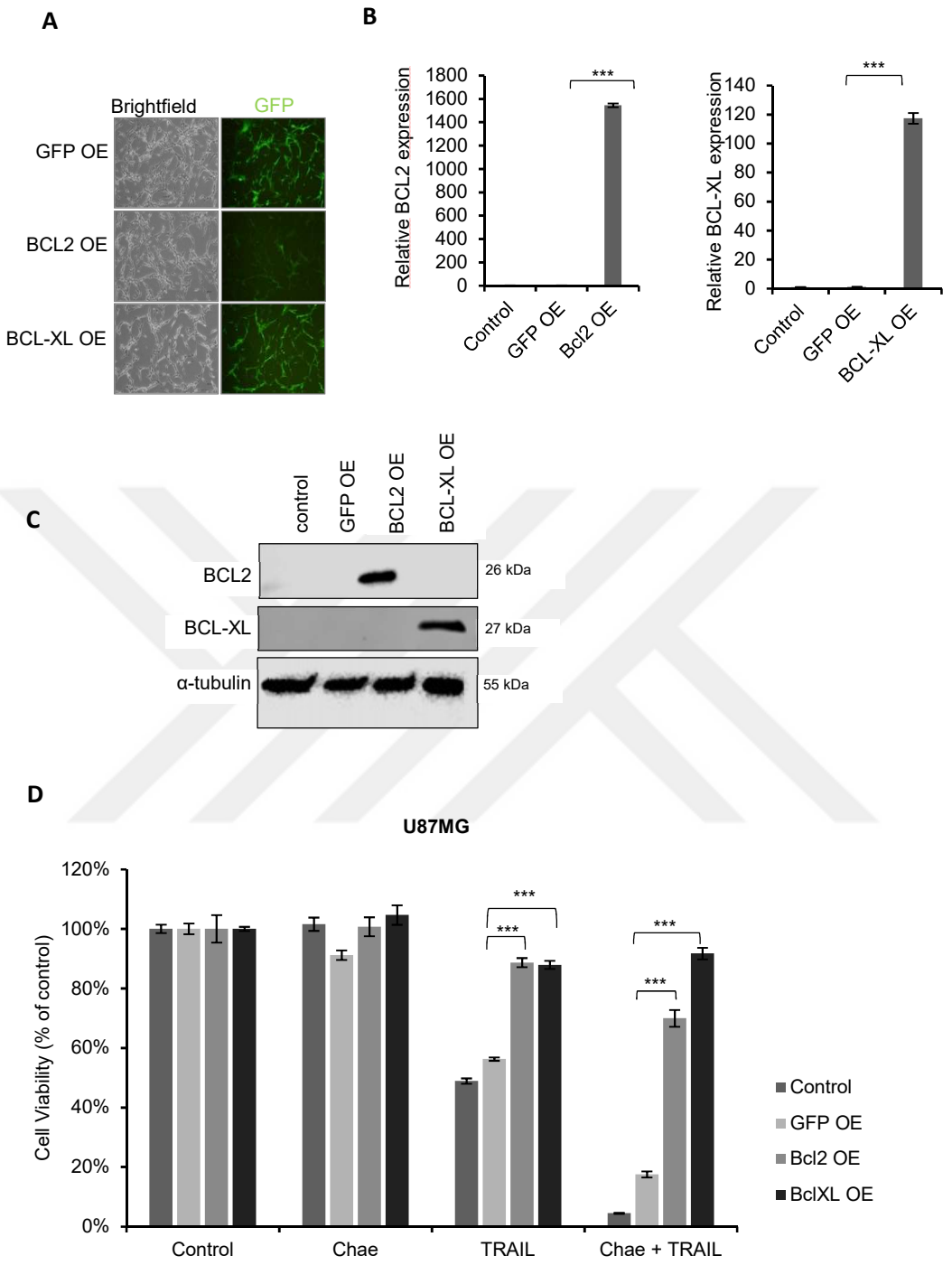

Figure 3.21 Overexpression of anti-apoptotic BCL-2 and BCL-XL renders GBM cells resistant to combinatorial therapy. (a) Manipulation of the intrinsic apoptosis machinery regulates Chaetocin-mediated TRAIL sensitization Representative images showing GFP signal of U87MG cells transduced with GFP, BCL-2 and BCL-XL overexpression constructs with an incorporated GFP. (b) qPCR analysis confirming elevated *BCL-2* and *BCL-XL* mRNA levels in transduced U87MG cells. (c) Western Blot showing overexpression of BCL-2 and BCL-XL proteins. α-tubulin was shown as protein equal loading control. (d) Viability analysis of U87MG cells overexpressing either BCL-2 and

BCL-XL proteins or negative control GFP upon Chaetocin (100 nM) and *TRAIL* (100 ng/ml) combinatorial treatment. (*** denotes P<0.001, two-tailed Student's t-test)

Conversely, in a loss-of-function approach using shRNA vectors, *BCL-XL* expression was efficiently downregulated at the mRNA and protein level (**Figure 3.22a-b**). Knockdown of *BCL-XL* led to further augmentation of TRAIL sensitization in U87MG cells (**Figure 3.22c**) as well as reducing TRAIL resistance in the fully resistant U373 cells (**Figure 3.22d**). Taken together, these results show that BCL-2/BCL-XL play critical roles in Chaetocin-mediated TRAIL sensitization in GBM cells which emphasized the active role of mitochondria in sensitization process.

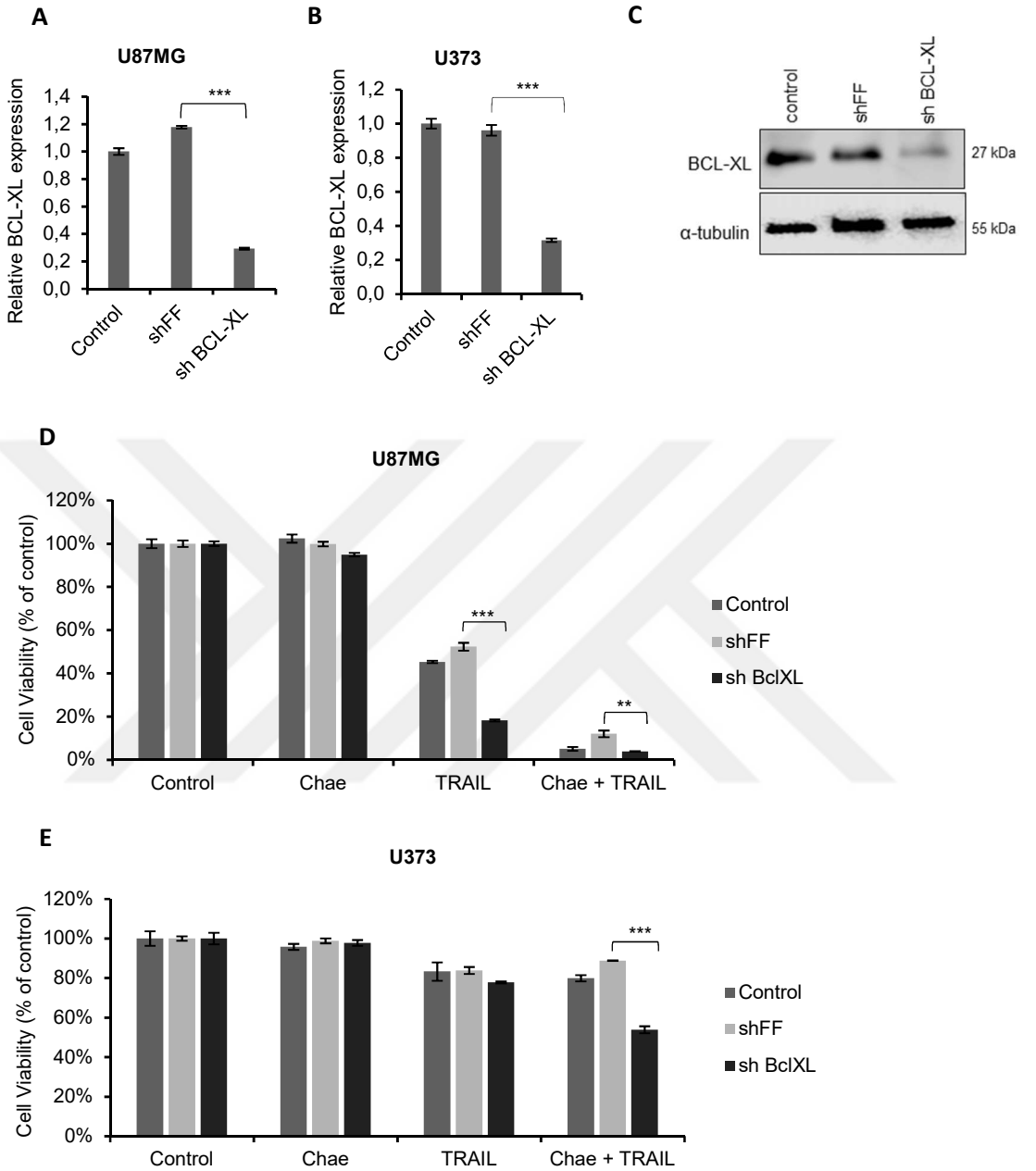

Figure 3.22 Knockdown of anti-apoptotic BCL-XL elevates apoptosis mediated both by *TRAIL* and the combinatorial treatment. qPCR illustrating shRNA mediated knockdown of BCL-XL protein in (a) U87MG and (b) U373 cells. shFF is negative control shRNA. (c) Western Blot showing the knockdown of BCL-XL protein levels. α-tubulin was shown as protein loading control. Cell viability assay of (d) U87MG and (e) U373 cells showing further sensitization of cells to Chaetocin+ TRAIL mediated apoptosis upon BCL-XL knockdown. (** and *** denote P<0.01 and P<0.001 respectively, two-tailed Student's t-test)

3.5 Chaetocin-mediated apoptosis sensitization in general is not mediated by SUV39H1 inhibition though the involvement of epigenetic regulations is still evident in the process

Chaetocin's potency as general apoptosis-sensitizer prompted us to check its effect on apoptosis related gene expression. In U87MG cells, Chaetocin positively modulated the expression of pro-apoptotic genes such as *PUMA, NOXA, HRK, BIM, BAD, DR4, CASP3* and *CASP7*, whereas downregulated anti-apoptotic genes such as *CIAP1, CIAP2* and *MCL1* (**Figure 3.23**).

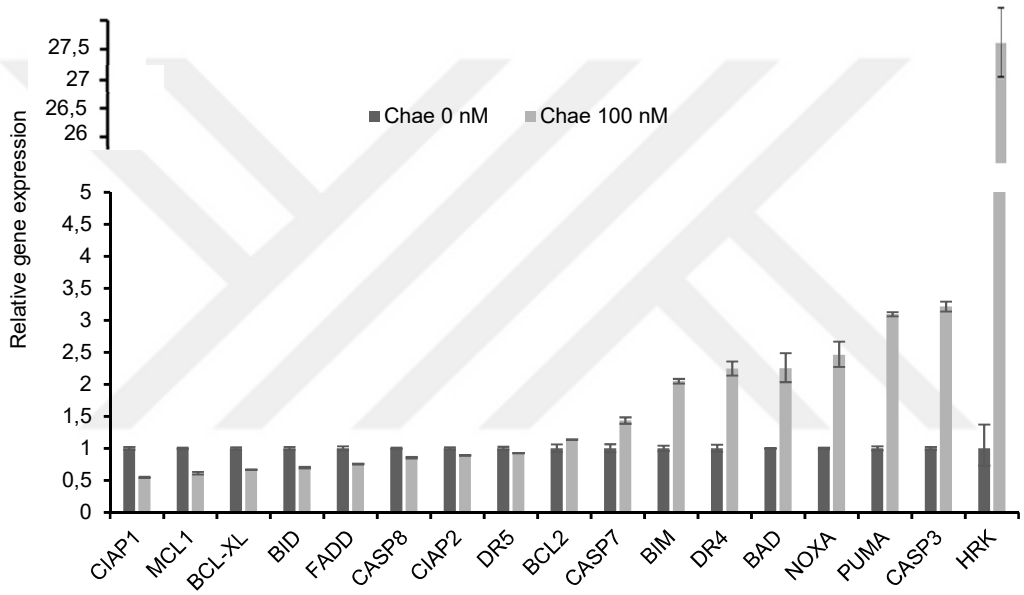

Figure 3.23 qPCR analysis of apoptosis related genes upon Chaetocin treatment (100 nM, 24h). Pro-apoptotic genes (*PUMA*, *NOXA*, *CASP3*, *HRK*, *BIM*, *BAD* and *DR4*) were upregulated by Chaetocin. Data were normalized to untreated control.

Since modulation of gene expression is attributed to epigenetic changes within the cell; we speculated that Chaetocin potency as general apoptosis sensitizer is linked to its' epigenetic modifier function. In accordance, since effects of epigenetic alterations are long term within cells, we investigated whether the apoptosis priming capacity of single day Chaetocin treatment is endured for long period of time. To this end, U87MG cells were treated with Chaetocin for 24h and then the drug was removed and cells were subjected to only TRAIL treatment in following days. We observed that Chaetocin

mediated apoptosis sensitization was sustained in long term (even 4 day after removal of the drug) suggesting the involvement of the epigenetic regulations in the process (**Figure 3.24**).

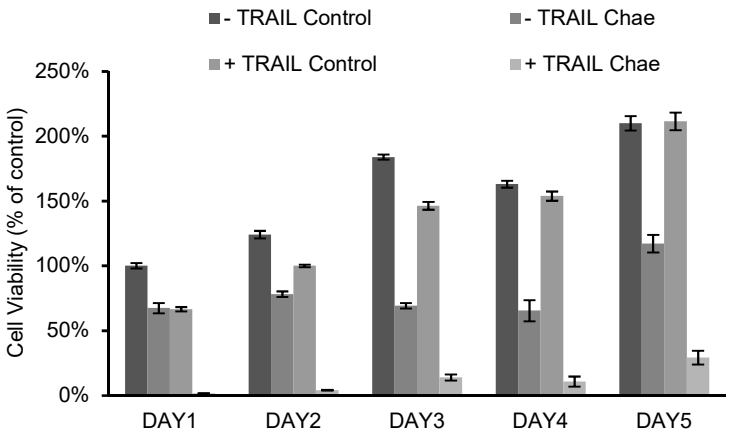

Figure 3.24 Chaetocin mediated apoptosis sensitization is sustained in long term. Viability analysis of U87MG cells treated with Chaetocin (100 nM) and TRAIL (100 ng/ml, 24h). Chaetocin treatment was performed at day0 and cells were kept under treatment only for 24h. After removal of Chaetocin and TRAIL was supplemented (at day1 or day2 or day3 or day4). Data were normalized to untreated control conditions.

Epigenetic role of Chaetocin is the inhibition of histone methyltransferases, including the H3K9 histone methyltransferase SUV39H1. In addition to its direct inhibition by Chaetocin, SUV39H1 was previously shown to be indirectly modulated by cellular ROS produced by Chaetocin[361]. We wondered whether the observed TRAIL sensitization is modulated through SUV39H1 inhibition. We generated SUV39H1 knockout U87MG cells (**Figure 3.25a**) and checked their TRAIL response. Depletion of SUV39H1 failed to sensitize cells further to apoptosis and rendered them slightly more resistant to TRAIL (**Figure 3.25b**). H3K9me(3) levels remained unchanged upon Chaetocin treatment clearly indicating that SUV39H1 inhibition is not the root cause for the pro-apoptotic effects of Chaetocin (**Figure 3.25c**).

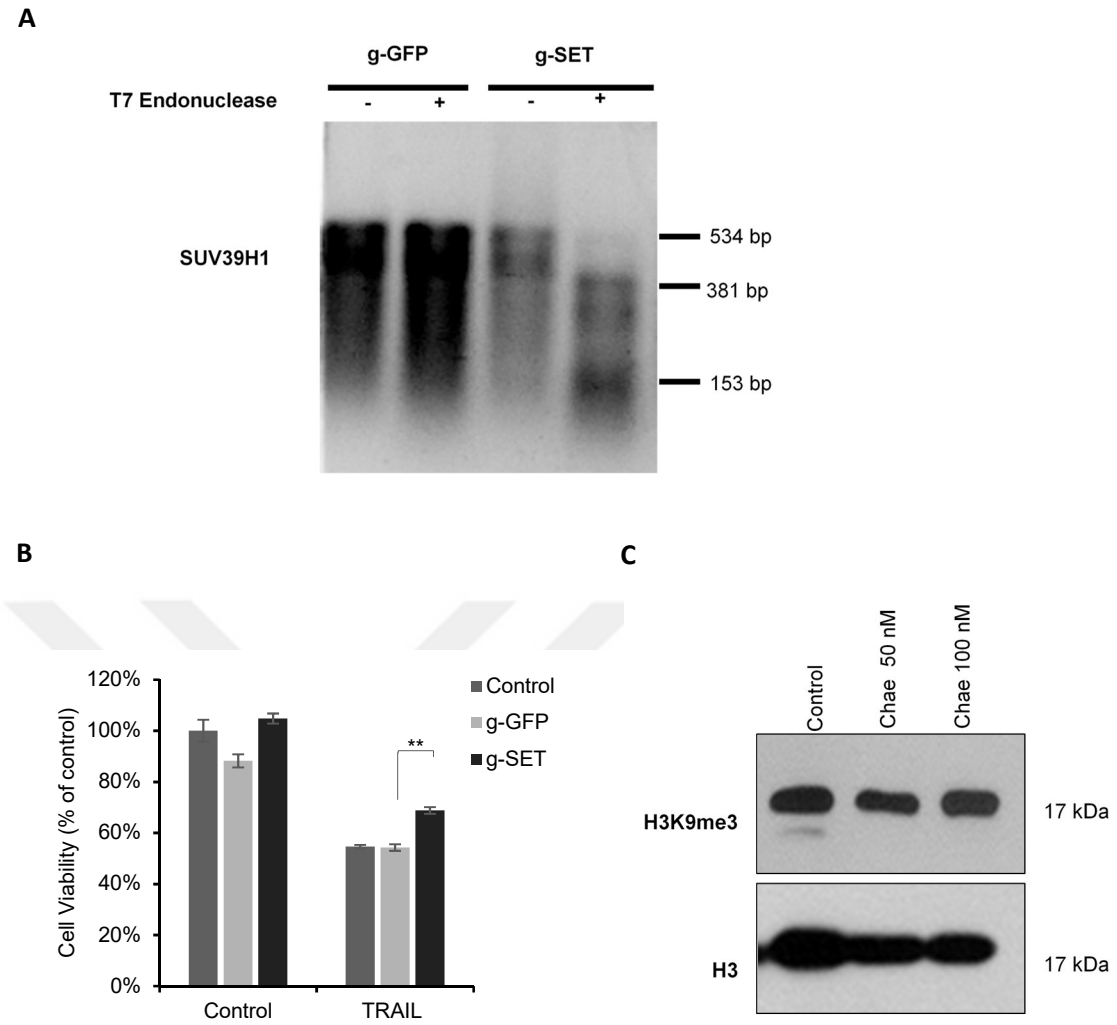

Figure 3.25 Chaetocin mediated apoptosis sensitization is not through SUV39H1 inhibition (a) T7 endonuclease assay showing CRISPR mediated SUV39H1 knockout in U87MG cells. T2 is negative control gRNA for CRISPR assay (b) Viability analysis of U87MG cells with SUV39H1 knockout. Data were normalized to untreated control conditions. Depletion of SUV39H1 protein did not sensitize cells any further to apoptosis and rather rendered them slightly more resistant to TRAIL. (** denotes P<0.01, two-tailed Student's t-test). (c) Western blot analysis showing H3K9me(3) levels in Chaetocin (50,100 nM for 24h) treated cells.H3 was shown as loading control.

3.6 Chaetocin-induced global transcriptome changes reveal the alteration of important hallmarks of cancer

We then performed global transcriptional profiling using RNAseq to analyze the Chaetocin-mediated changes at the whole transcriptome. Heatmap of differentially regulated genes upon Chaetocin treatment is illustrated below in **Figure 3.26**.

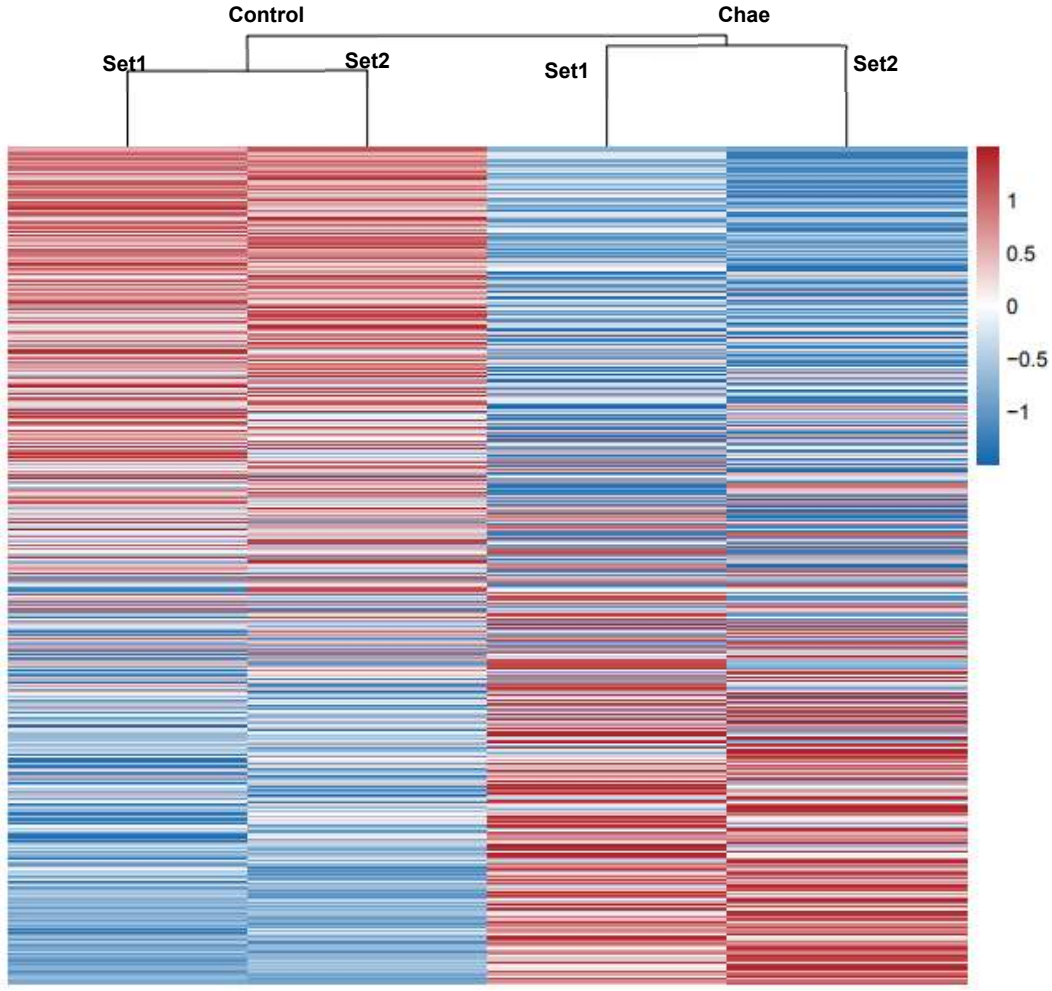

Figure 3.26 Heatmaps of all genes revealing significantly transcriptome modulation by Chaetocin treatment. Expression data were normalized to control condition and log 2 transformed ($p<0.05$).

A volcano plot for fold-changes in gene expression illustrated that 373 genes were up-regulated, 478 genes were down-regulated significantly (FDR<0.05) upon 24h treatment with a low dose (50nM) Chaetocin (**Figure 3.27a**). Changes in the expression

of top scoring genes (*HMOX1, MLC1, ARL14EPL, ANO8, ITGA2, ITGA11,* and *TENM2*) were validated by qPCR (**Figure 3.27b-c**).

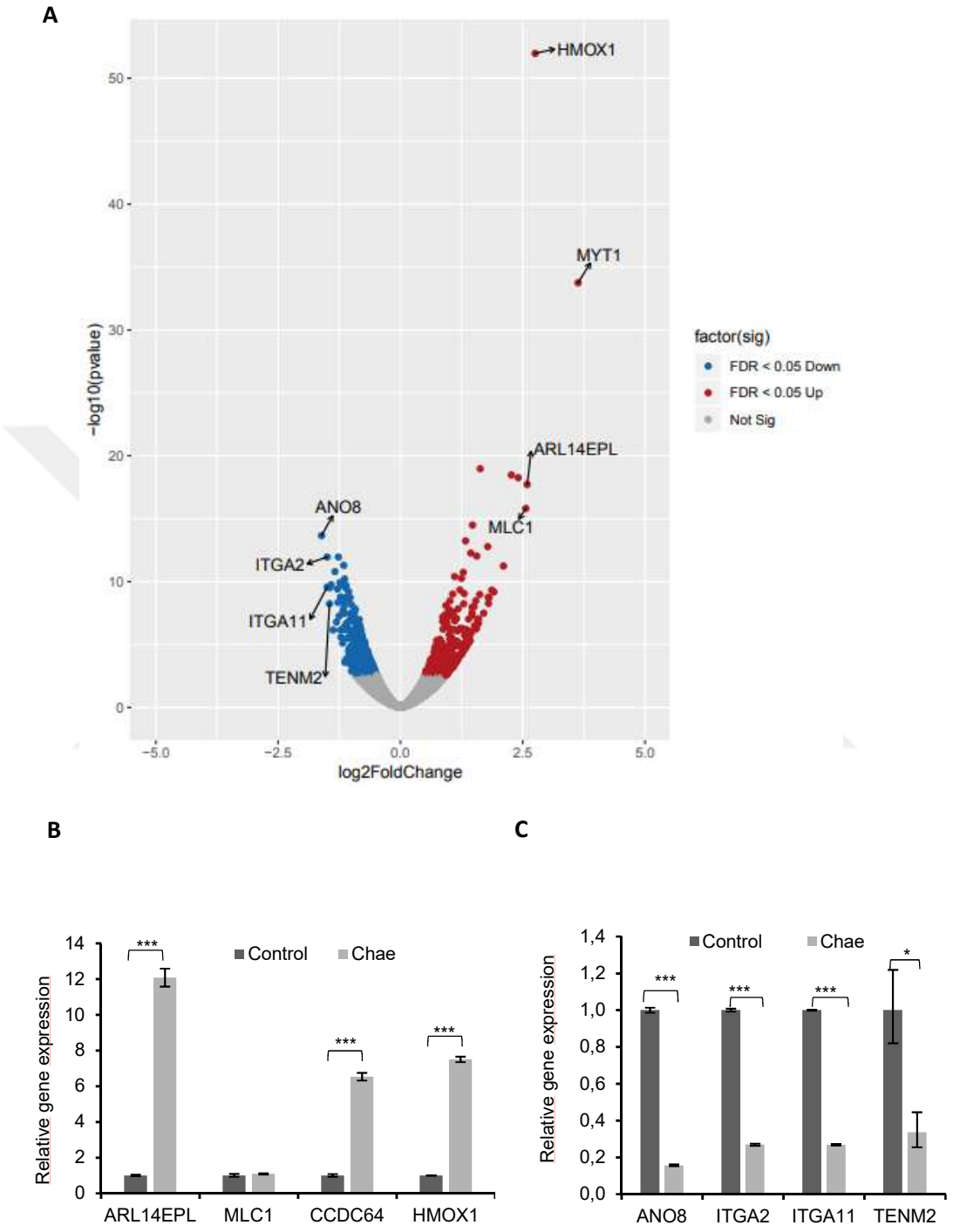

Figure 3.27 Chaetocin treatment modulates transcriptome of GBM cells. (a) Volcano plot of RNAseq data showing significantly ($p<0.05$) up and down regulated genes by Chaetocin (50 nM, 24h) based on their log2 transformed expression data with false discovery rate (FDR) threshold of 0.05. (b) qPCR validation of top 4 upregulated (*MLC1,*

ARL14EPL, HMOX1, CCDC64) and (c) downregulated (*ANO8, ITGA2, ITGA11, TENM2*) genes obtained from RNAseq analysis. Data were normalized to untreated control. (* and *** denote P<0.05 and P<0.001 respectively, two-tailed Student's t-test)

We performed GSEA[344] and observed that E2F targets, UV response up, G2M checkpoint, ROS and TP53 pathways were among top positively regulated, and EMT, UV response down, protein secretion and oxidative phosphorylation pathways were among top negatively regulated hallmark pathways (**Figure 3.28a**). Enrichment plots for enriched hallmark gene sets upon Chaetocin treatment are illustrated in **Figure 3.28b**.

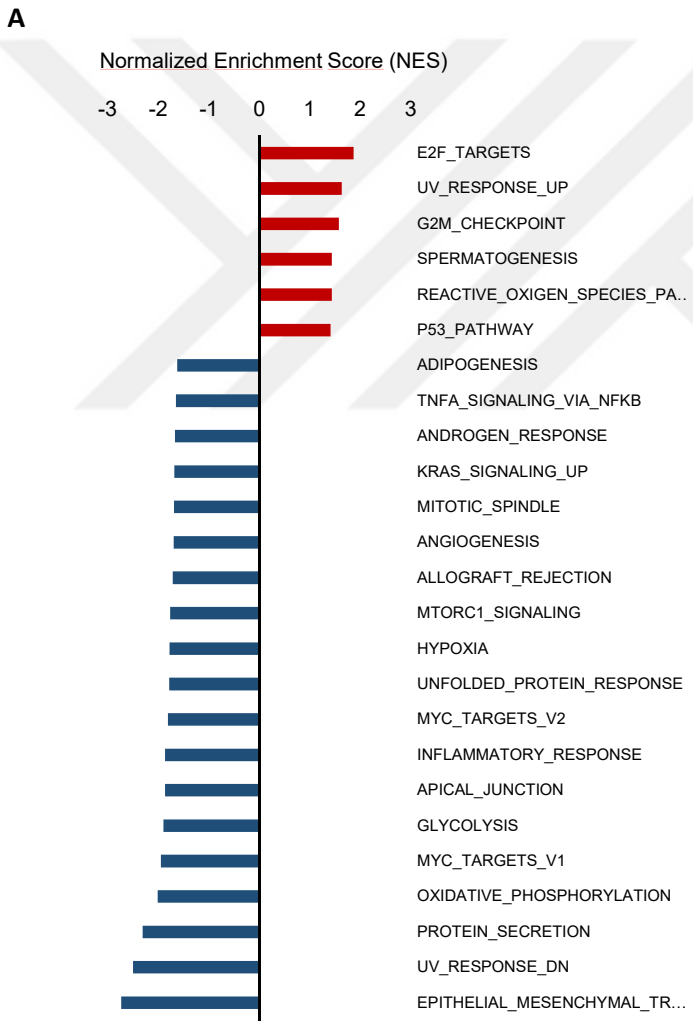

B

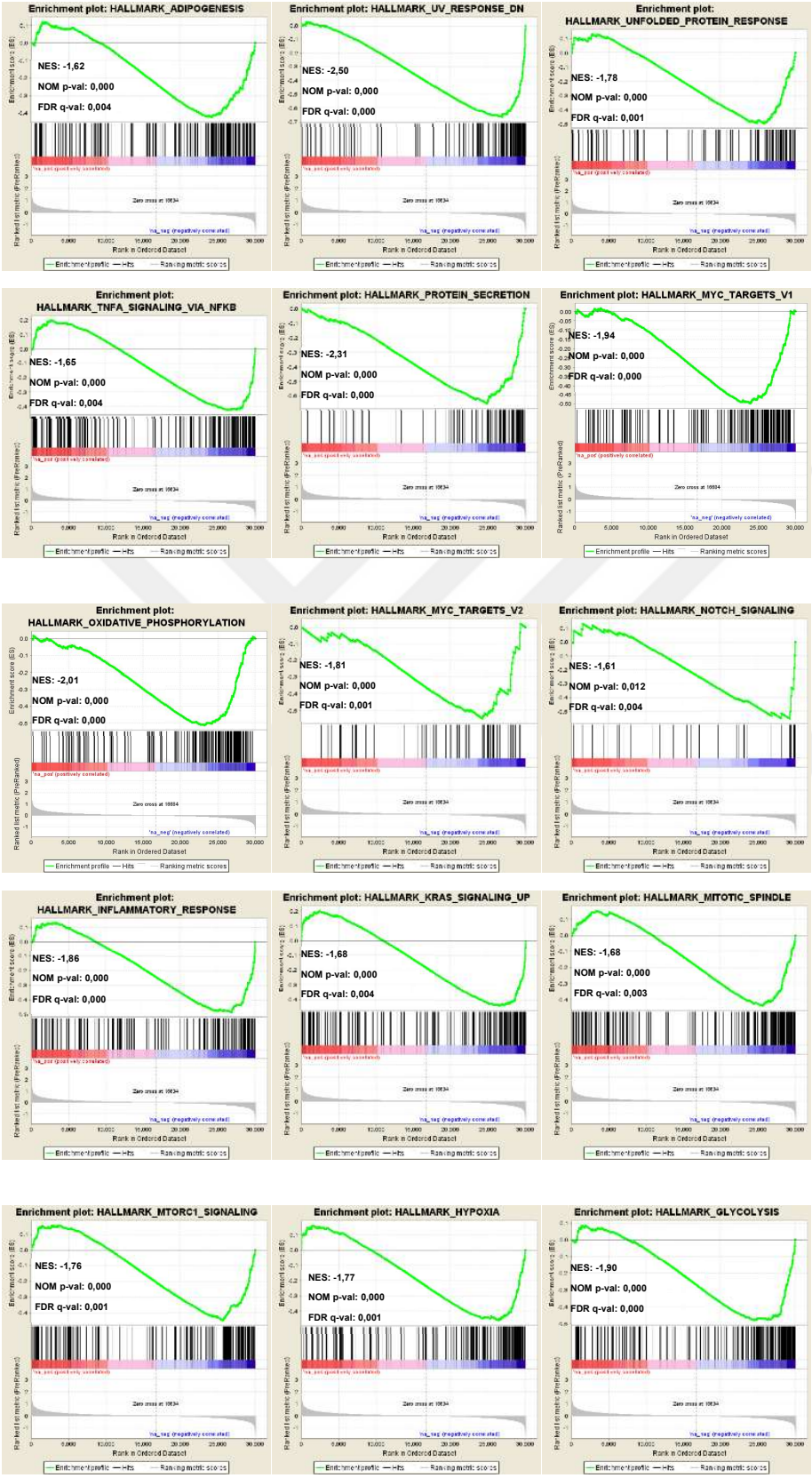
Enrichment plot: HALLMARK_ADIPOGENESIS
NES: -1,62
NOM p-val: 0,000
FDR q-val: 0,004
Enrichment plot: HALLMARK_UV_RESPONSE_DN
NES: -2,50
NOM p-val: 0,000
FDR q-val: 0,000
Enrichment plot: HALLMARK_UNFOLDED_PROTEIN_RESPONSE
NES: -1,78
NOM p-val: 0,000
FDR q-val: 0,001
Enrichment plot: HALLMARK_TNFA_SIGNALING_VIA_NFKB
NES: -1,65
NOM p-val: 0,000
FDR q-val: 0,004
Enrichment plot: HALLMARK_PROTEIN_SECRETION
NES: -2,31
NOM p-val: 0,000
FDR q-val: 0,000
Enrichment plot: HALLMARK_MYC_TARGETS_V1
NES: -1,94
NOM p-val: 0,000
FDR q-val: 0,000
Enrichment plot: HALLMARK_OXIDATIVE_PHOSPHORYLATION
NES: -2,01
NOM p-val: 0,000
FDR q-val: 0,000
Enrichment plot: HALLMARK_MYC_TARGETS_V2
NES: -1,81
NOM p-val: 0,000
FDR q-val: 0,001
Enrichment plot: HALLMARK_NOTCH_SIGNALING
NES: -1,61
NOM p-val: 0,012
FDR q-val: 0,004
Enrichment plot: HALLMARK_INFLAMMATORY_RESPONSE
NES: -1,86
NOM p-val: 0,000
FDR q-val: 0,000
Enrichment plot: HALLMARK_KRAS_SIGNALING_UP
NES: -1,68
NOM p-val: 0,000
FDR q-val: 0,004
Enrichment plot: HALLMARK_MITOTIC_SPINDLE
NES: -1,68
NOM p-val: 0,000
FDR q-val: 0,003
Enrichment plot: HALLMARK_MTORC1_SIGNALING
NES: -1,76
NOM p-val: 0,000
FDR q-val: 0,001
Enrichment plot: HALLMARK_HYPOXIA
NES: -1,77
NOM p-val: 0,000
FDR q-val: 0,001
Enrichment plot: HALLMARK_GLYCOLYSIS
NES: -1,90
NOM p-val: 0,000
FDR q-val: 0,000

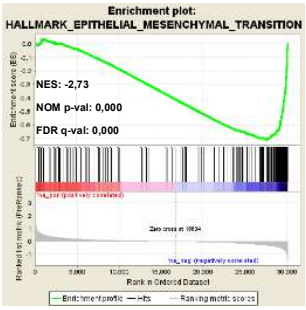
Enrichment plot:
HALLMARK_EPITHELIAL_MESENCHYMAL_TRANSITION
NES: -2,73
NOM p-val: 0,000
FDR q-val: 0,000

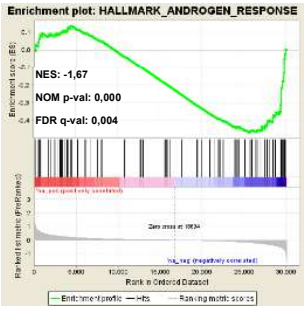
Enrichment plot: HALLMARK_ANDROGEN_RESPONSE
NES: -1,67
NOM p-val: 0,000
FDR q-val: 0,004

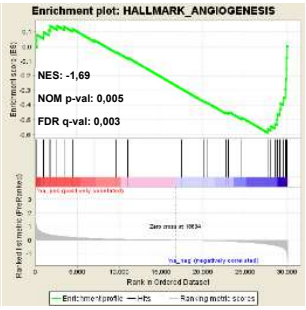
Enrichment plot: HALLMARK_ANGIOGENESIS
NES: -1,69
NOM p-val: 0,005
FDR q-val: 0,003

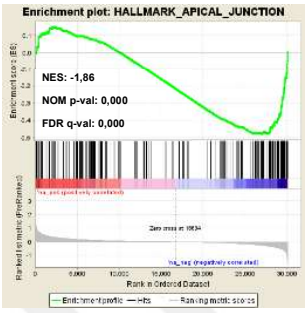
Enrichment plot: HALLMARK_APICAL_JUNCTION
NES: -1,86
NOM p-val: 0,000
FDR q-val: 0,000

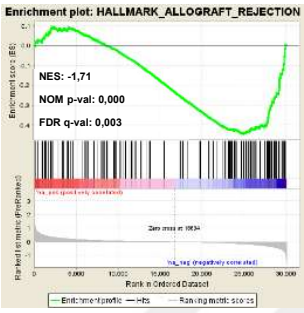
Enrichment plot: HALLMARK_ALLOGRAFT_REJECTION
NES: -1,71
NOM p-val: 0,000
FDR q-val: 0,003

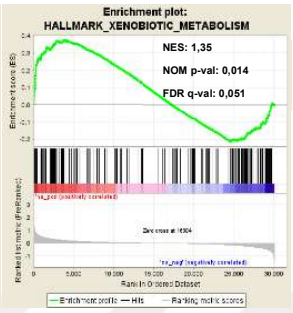
Enrichment plot:
HALLMARK_XENOBIOTIC_METABOLISM
NES: 1,35
NOM p-val: 0,014
FDR q-val: 0,051

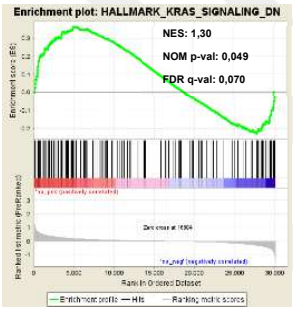
Enrichment plot: HALLMARK_KRAS_SIGNALING_DN
NES: 1,30
NOM p-val: 0,049
FDR q-val: 0,070

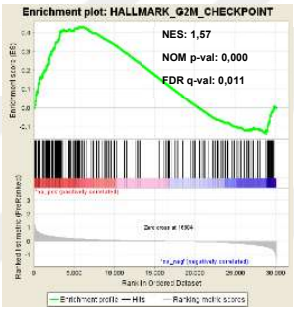
Enrichment plot: HALLMARK_G2M_CHECKPOINT
NES: 1,57
NOM p-val: 0,000
FDR q-val: 0,011

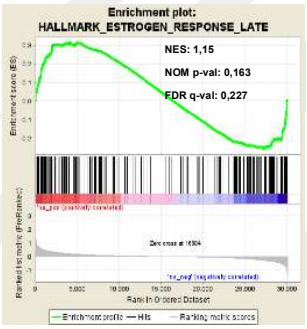
Enrichment plot:
HALLMARK_ESTROGEN_RESPONSE_LATE
NES: 1,15
NOM p-val: 0,163
FDR q-val: 0,227

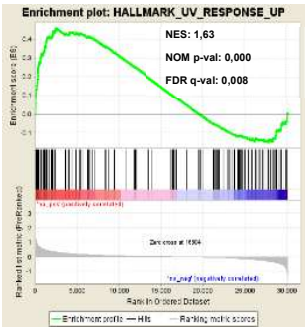
Enrichment plot: HALLMARK_UV_RESPONSE_UP
NES: 1,63
NOM p-val: 0,000
FDR q-val: 0,008

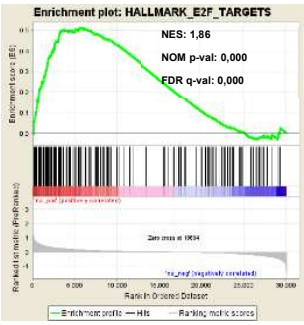
Enrichment plot: HALLMARK_E2F_TARGETS
NES: 1,86
NOM p-val: 0,000
FDR q-val: 0,000

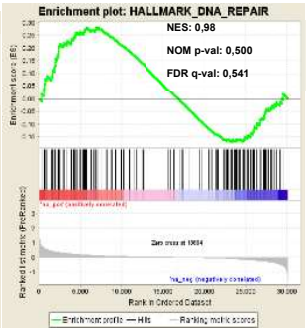
Enrichment plot: HALLMARK_DNA_REPAIR
NES: 0,98
NOM p-val: 0,500
FDR q-val: 0,541

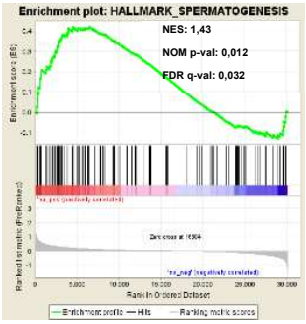
Enrichment plot: HALLMARK_SPERMATOGENESIS
NES: 1,43
NOM p-val: 0,012
FDR q-val: 0,032

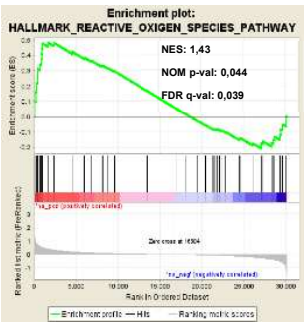
Enrichment plot:
HALLMARK_REACTIVE_OXIGEN_SPECIES_PATHWAY
NES: 1,43
NOM p-val: 0,044
FDR q-val: 0,039

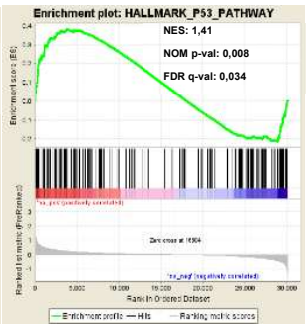
Enrichment plot: HALLMARK_P53_PATHWAY
NES: 1,41
NOM p-val: 0,008
FDR q-val: 0,034

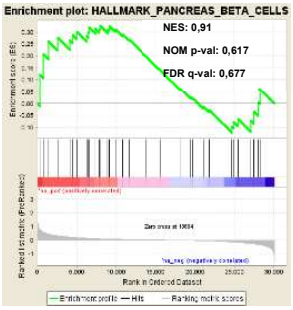

Figure 3.28 Hallmark of apoptosis pathways are enriched in GBM cells upon Chaetocin treatment (a) Graph represents GSEA results pointing out Chaetocin mediated positively and negatively enriched hallmark pathways based on their Normalized Enrichment Score (NES). (b) Enrichment plots for enriched hallmark gene sets upon Chaetocin treatment (50 nM, 24h), obtained from GSEA. Normalized enrichment scores (NES), NOM p values and FDR q values were depicted on each graph.

The heatmaps of genes positively contributing to each enrichment plot revealed significant differences in the expression patterns of UV-response up, TP53 and ROS pathway (**Figure 3.29**).

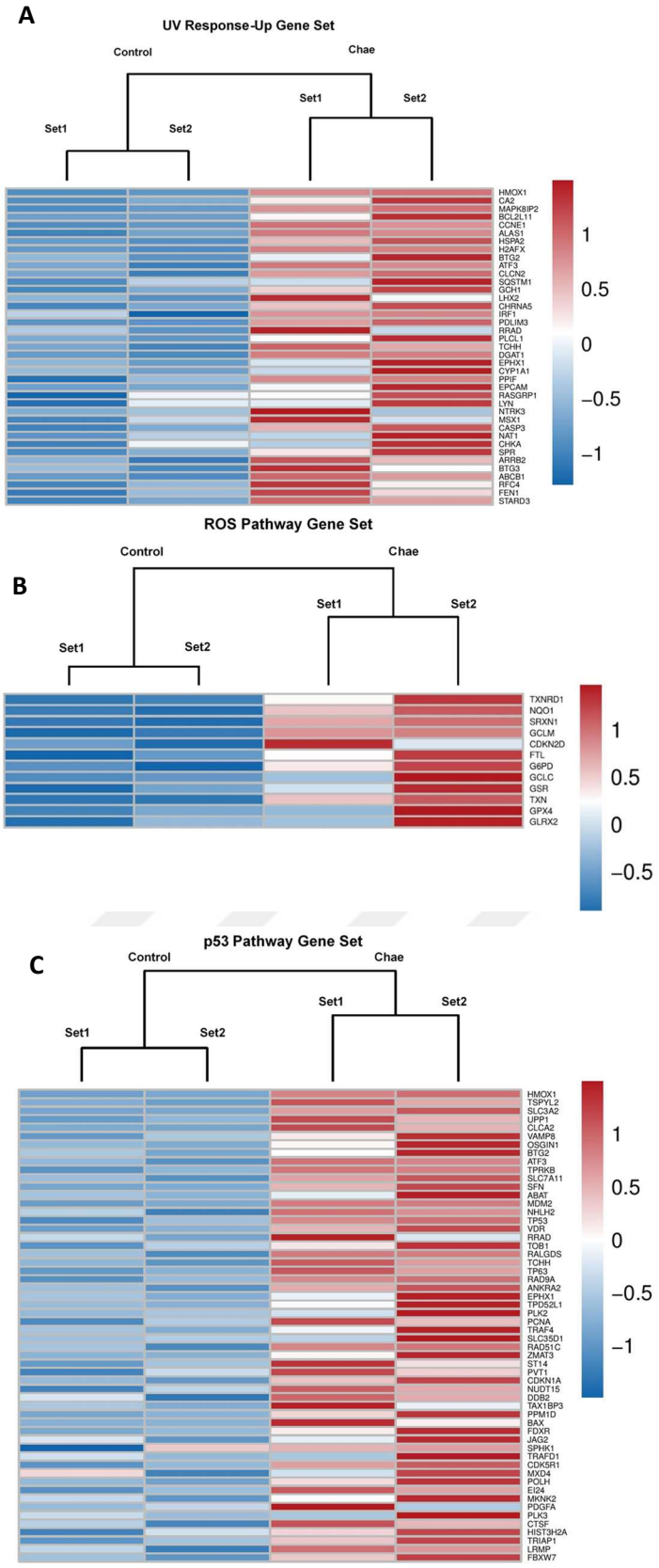

Figure 3.29 Heatmaps of genes listed under (a) UV response-up, (b) ROS and (c) TP53 pathways from GSEA revealing significantly upregulated genes upon Chaetocin

treatment. Expression data were normalized to control condition and log 2 transformed ($p<0.05$).

To validate the implications from the GSEA data, we tested the effect of Chaetocin on cell cycle distribution (as an output for G2-M checkpoint) and cellular invasion (as output for EMT deregulation). PI staining revealed cell cycle arrest induction with a significant decrease in the S phase and an increase in G2/M phase following Chaetocin treatment (**Figure 3.30**).

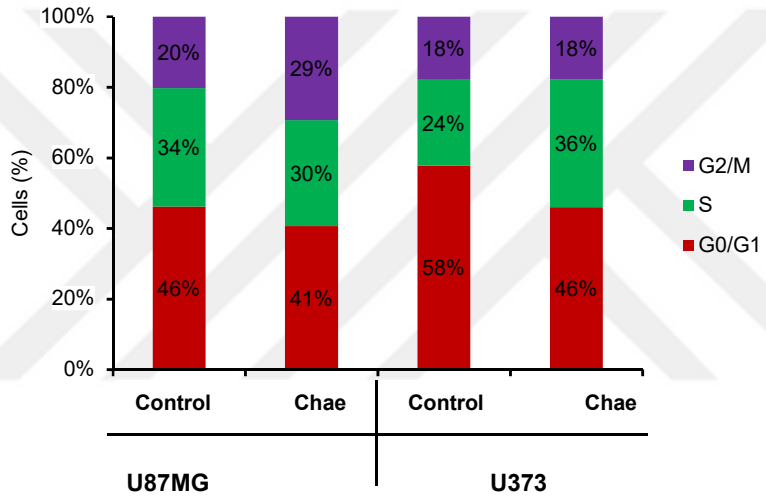

Figure 3.30 Flow cytometric analysis showing the effect of Chaetocin on cell cycle distribution of the U87MG and U373 cells. Percentage of cells in G2/M, S and G0/G1 phases was shown upon Chaetocin (100 nM) treatment for 24h.

Spheroid invasion assay to measure the invasive ability of GBM cells showed a reduction of dispersal upon Chaetocin treatment, supporting the negative effect of Chaetocin on EMT (**Figure 3.31**).

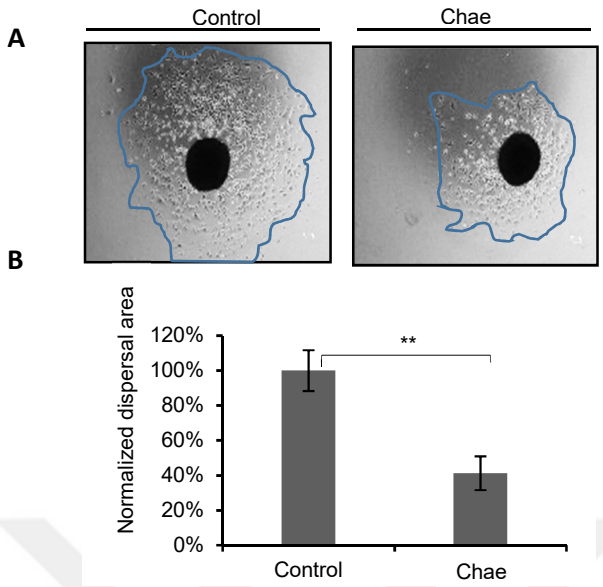

Figure 3.31 Chaetocin represses invasion of GBM cells. (a) Representative images from spheroid invasion assays to measure the migration ability of GBM cells upon Chaetocin treatment (50 nM, 24h). (b) Quantification of dispersal area of spheroids. Data were normalized to untreated control. Images were taken by inverted live-cell light microscope (4x magnification). (** denotes P<0.01, two-tailed Student's t-test)

ROS was higher upon Chaetocin treatment, supporting the earlier findings on Chaetocin mediated ROS induction [307]. As expected, the ROS scavenger N-acetyl-L-cysteine (NAC) reduced the level of ROS generated by Chaetocin (**Figure 3.32a**). Further evidence for Chaetocin-mediated induction of the ROS pathway and its role during apoptosis is elevated expression levels of antioxidant genes such as *TXNRD1, GCLM* and *NQO1* (**Figure 3.32b**) and pro-apoptotic mediators such as *FADD, CASP3* and *BIM*, which could be blocked with NAC treatment (**Figure 3.33a**). Chaetocin-induced changes in expression levels of other genes such as *ARL14EPL* and *ANO8* were also ROS-dependent (**Figure 3.33b**).

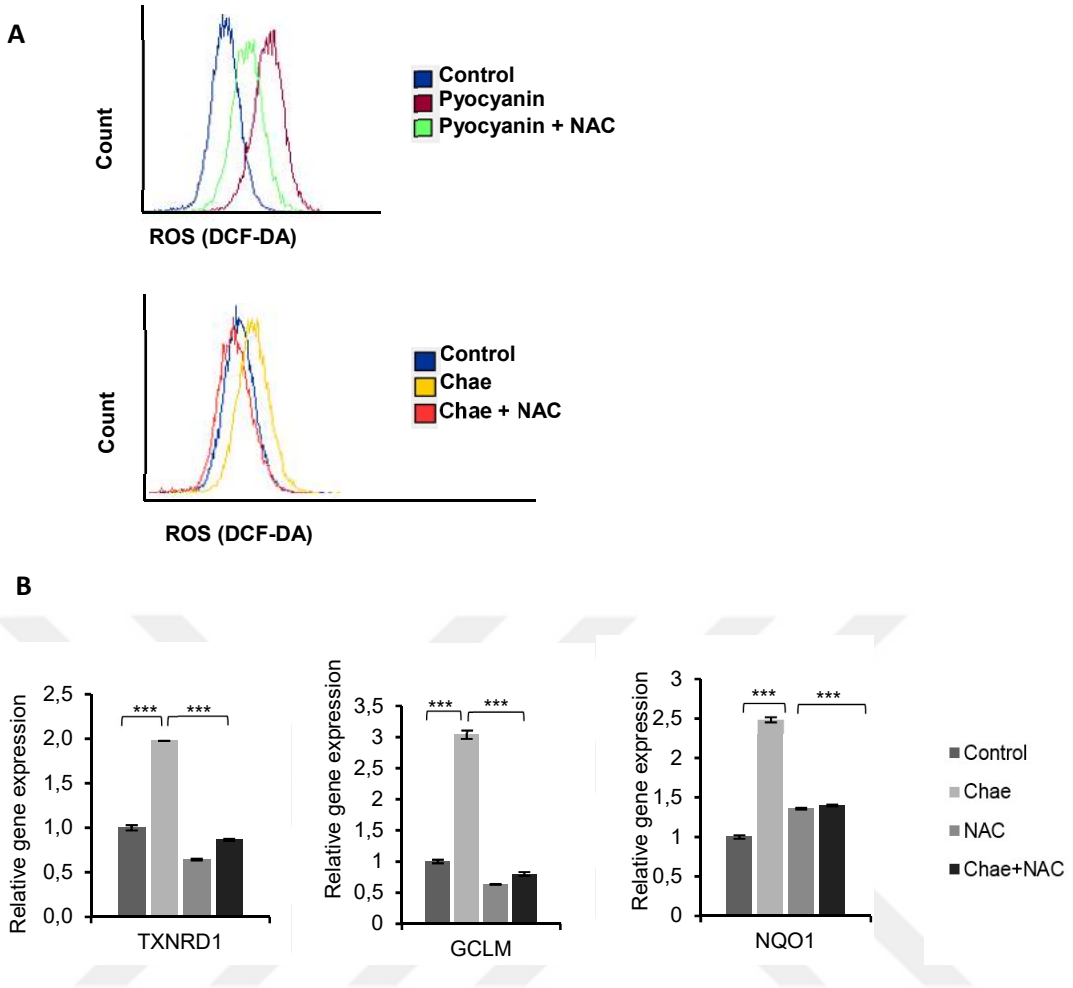

Figure 3.32 Chaetocin generates ROS (a) DCFDA flow cytometric analysis of ROS generation in U87MG cells treated with Chaetocin in the presence or absence of N-acetyl-cysteine (NAC). (b) qPCR analysis showing that Chaetocin treatment (100 nm, 24h) upregulated *TXNRD1, GCLM* and *NQO1* gene levels in ROS-dependent manner. Data were normalized to no drug conditions.

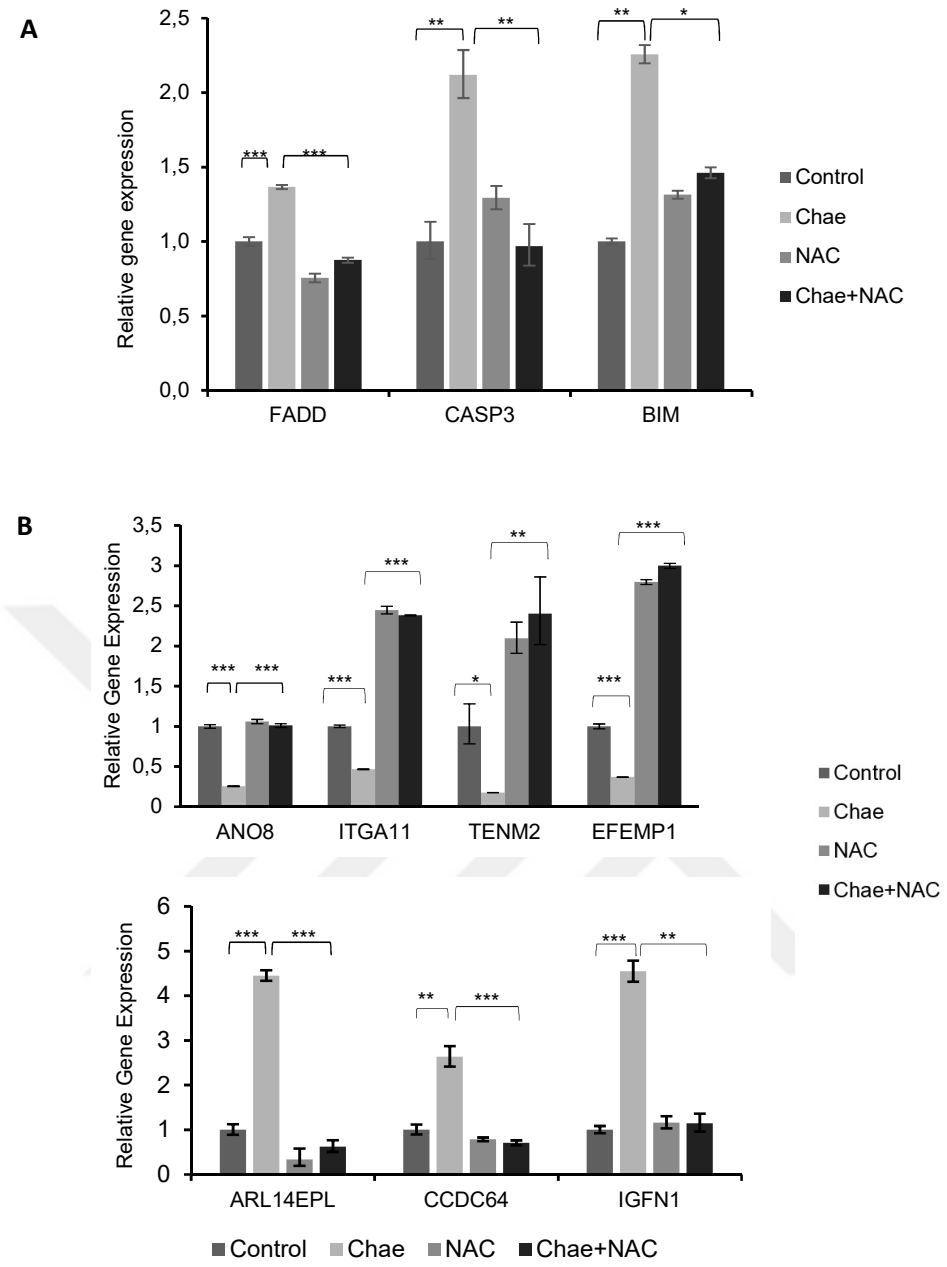

Figure 3.33 ROS generated by Chaetocin leads to transcriptomic changes in GBM cells (a) qPCR analysis demonstrating the effect of NAC on Chaetocin-induced changes in the expression of *FADD*, CASP3 and *BIM*. NAC and Chaetocin were applied as 10 µM and 100 nM, respectively, for 24h. (b) qPCR analysis showing modulation of selected RNA-seq hit upregulated (*CCDC64, IGFN1, ARL14EPL*) and downregulated (*ITGA11, TENM2 AND EFEMP1, ANO8*) gene levels by Chaetocin treatment (100 nm, 24h) in ROS-dependent manner. NAC and Chaetocin were used as 10 µM and 100 ng/ml, respectively, for 24h. Data were normalized to untreated control. (*, ** and *** denote P<0.05, P<0.01 and P<0.001, respectively, two-tailed Student's t-test).

3.7 Chaetocin mediated apoptosis sensitization of GBM cells is through ROS generation and consequent DNA damage induction

To assess the role of ROS in Chaetocin mediated apoptosis sensitization, we performed cell viability assays in the presence of NAC. Indeed, NAC treatment completely abolished Chaetocin-mediated sensitization to TRAIL (**Figure 3.34a**), to FASL (**Figure 3.34b**) and to BH3 mimetic (**Figure 3.34c**) in GBM and U87MG-TR cells.

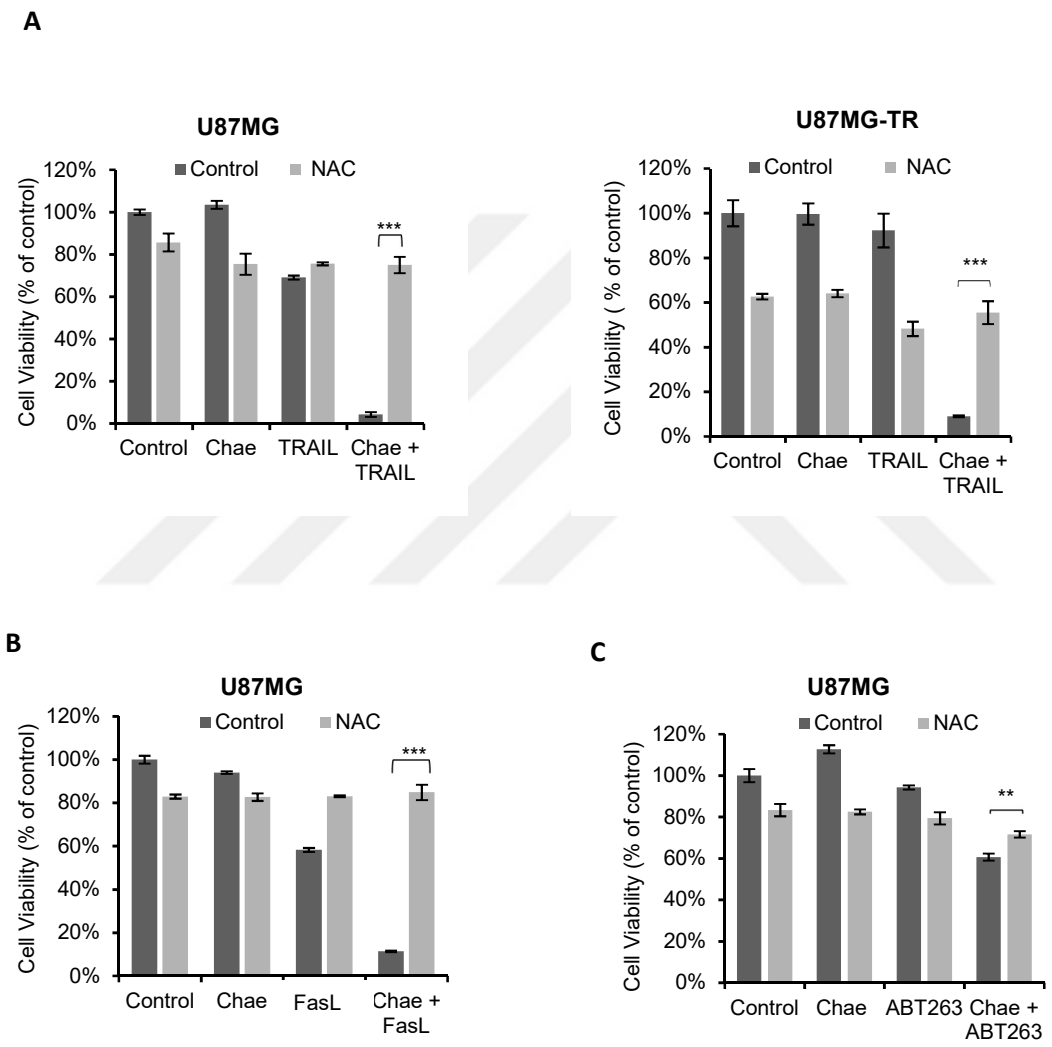

Figure 3.34 ROS scavenger interferes with Chaetocin mediated apoptosis sensitization. (a) Viability analysis of Chaetocin and TRAIL treated (100 nM, 100 ng/ml respectively for 24h) U87MG and U87MG-TR cells in presence and absence of NAC (10 µM). (b) Viability analysis of Chaetocin and FASL treated (100 nM, 100 ng/ml respectively for 24h) U87MG cells in presence and absence of NAC (10 µM). (c) Viability analysis of Chaetocin and ABT263 treated (100 nM, 1 µM respectively for 24h) U87MG cells in presence and absence of NAC (10 µM). (** and *** denote P<0.01 and P<0.001 respectively, two-tailed Student's t-test)

PARP and CASP3 cleavage induced by Chaetocin and TRAIL treatment was reduced in the presence of NAC (**Figure 3.35**).

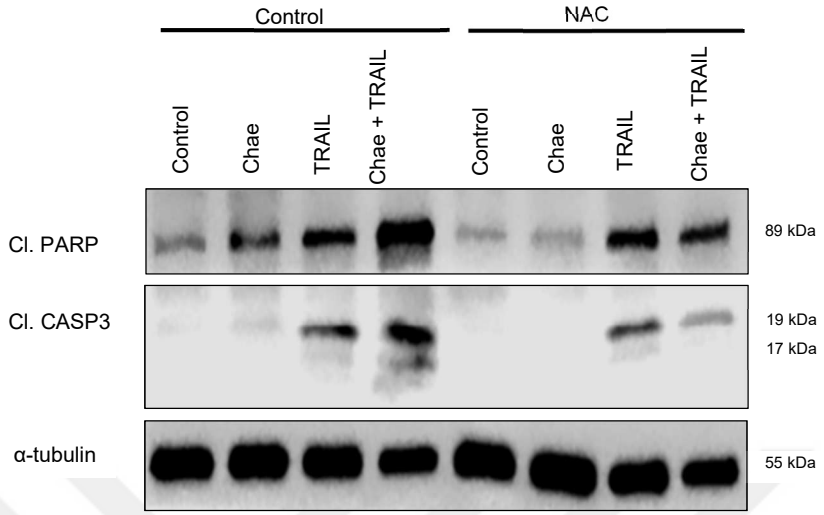

Figure 3.35 NAC blocks Chaetocin mediated TRAIL sensitization process. Western blot showing the effect of NAC (10 µM) on activation of main players of apoptosis by Chaetocin + TRAIL combinatorial treatment.

Since ROS is general DNA damage inducer, we examined the role of Chaetocin treatment on DNA damage. We analyzed canonical markers of DNA damage such as phospho-H2AX foci formation. Accordingly, ɣH2AX staining revealed increased DNA damage by prolonged exposure to Chaetocin, which could be blocked by NAC treatment (**Figure 3.36**).

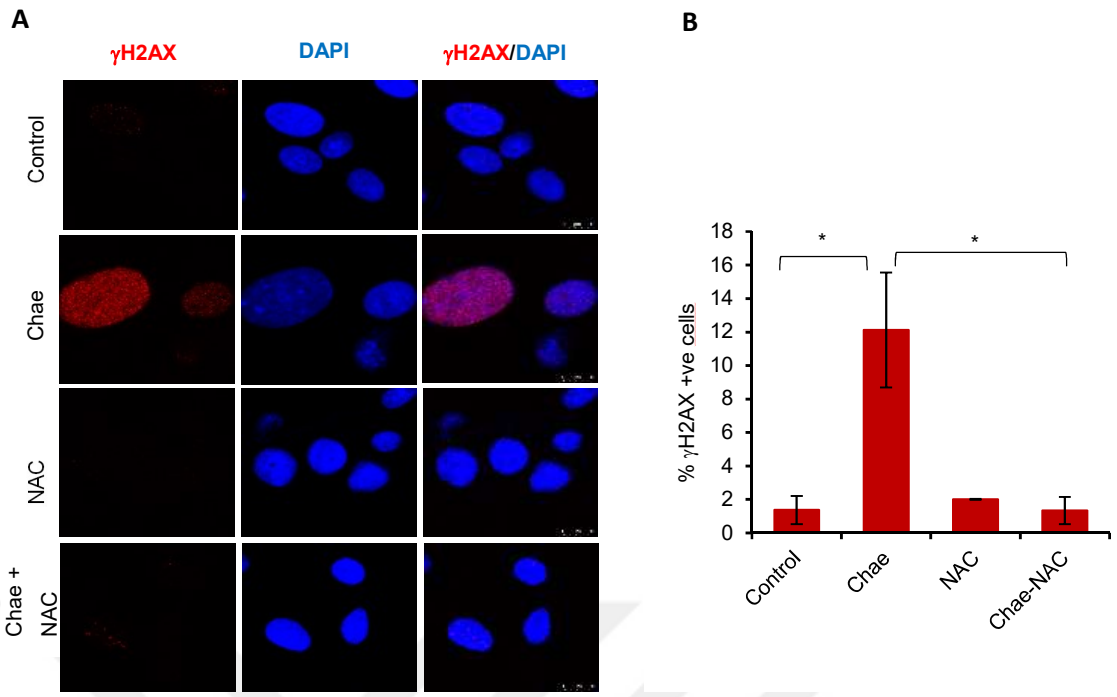

Figure 3.36 Chaetocin treatment induces DNA damage, marked with Phospho-H2AX (Ser139) (a) Representative fluorescent images from Phospho-H2AX (Ser139) staining showing DNA damage by prolonged exposure to Chaetocin (100 nM, 24h), which was blocked by pretreatment with NAC (10uM). Red: H2AX, Blue:DAPI. (b) Quantification of Phospho-H2AX (Ser139) staining. Number of % positive cells was plotted by counting the cells having more than 5 foci. Data were normalized to untreated control. (* denotes P<0.05, two-tailed Student's t-test)

We observed expression changes of DNA damage related genes; including mismatch repair (*MSH2, MSH6, KU70* and *EXO2)* and base excision repair (*BRCA1* and *BRCA2*) (**Figure 3.37**).

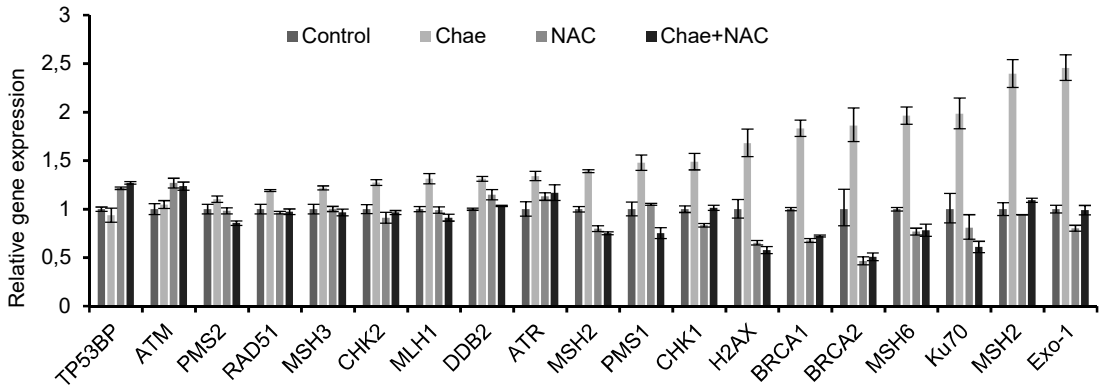

Figure 3.37 qPCR analysis revealing the modulation of DNA damage related gene expressions; specifically, those involved in mismatch repair pathway (*MSH2, MSH6, KU70* and *EXO2*) and base excision repair (*BRCA1* and *BRCA2*) by Chaetocin in ROS-dependent manner. NAC pretreatment (10 µM) was performed for 24 h prior to Chaetocin (100 nM, 24h).

As TP53 activation was one of the top enriched gene sets from GSEA, we measured TP53 protein levels and observed accumulation of TP53 protein in Chaetocin treated cells in a ROS-dependent manner (**Figure 3.38a**). NUTLIN, a well-studied MDM2 antagonist and TP53 activator[362] sensitized U87MG cells to TRAIL, providing further evidence for TP53 in the Chaetocin-induced apoptotic process (**Figure 3.38b**).

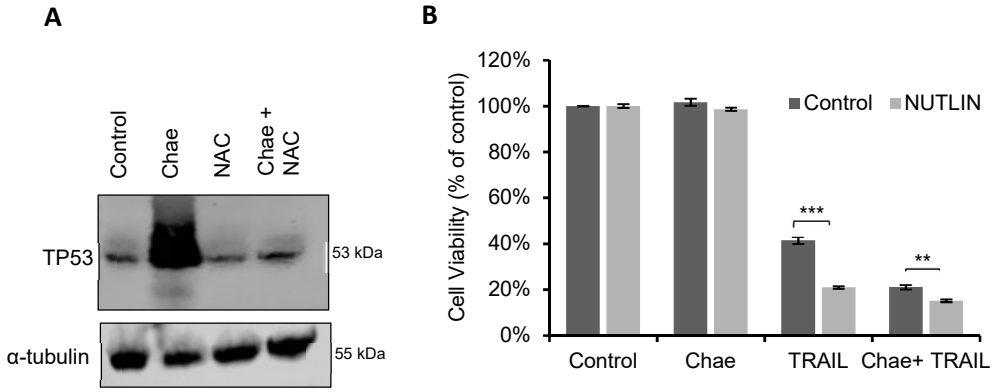

Figure 3.38 TP53 is involved in Chaetocin mediated apoptosis sensitization process. (a) Western blot analysis revealing accumulation of TP53 protein in Chaetocin (100 nM, 24h) treated cells in ROS-dependent manner. α-tubulin was shown as loading control. (b) Viability analysis showing that pretreatment with TP53 activator NUTLIN (10 mM, 24h) increased the response of U87MG cells to Chaetocin +TRAIL treatment (100 nM, 100 ng/ml respectively). Data were normalized to untreated control. (** and *** denote P<0.01 and P<0.001 respectively, two-tailed Student's t-test)

The relationship between Chaetocin treatment, TP53 and TRAIL sensitization was further evaluated using a TP53 reporter system in HCT116 colon cancer cells (**Figure 3.39a-b**). Also, TP53 knockout rendered HCT116 cells slightly resistant to Chaetocin-mediated TRAIL sensitization (**Figure 3.39c**).

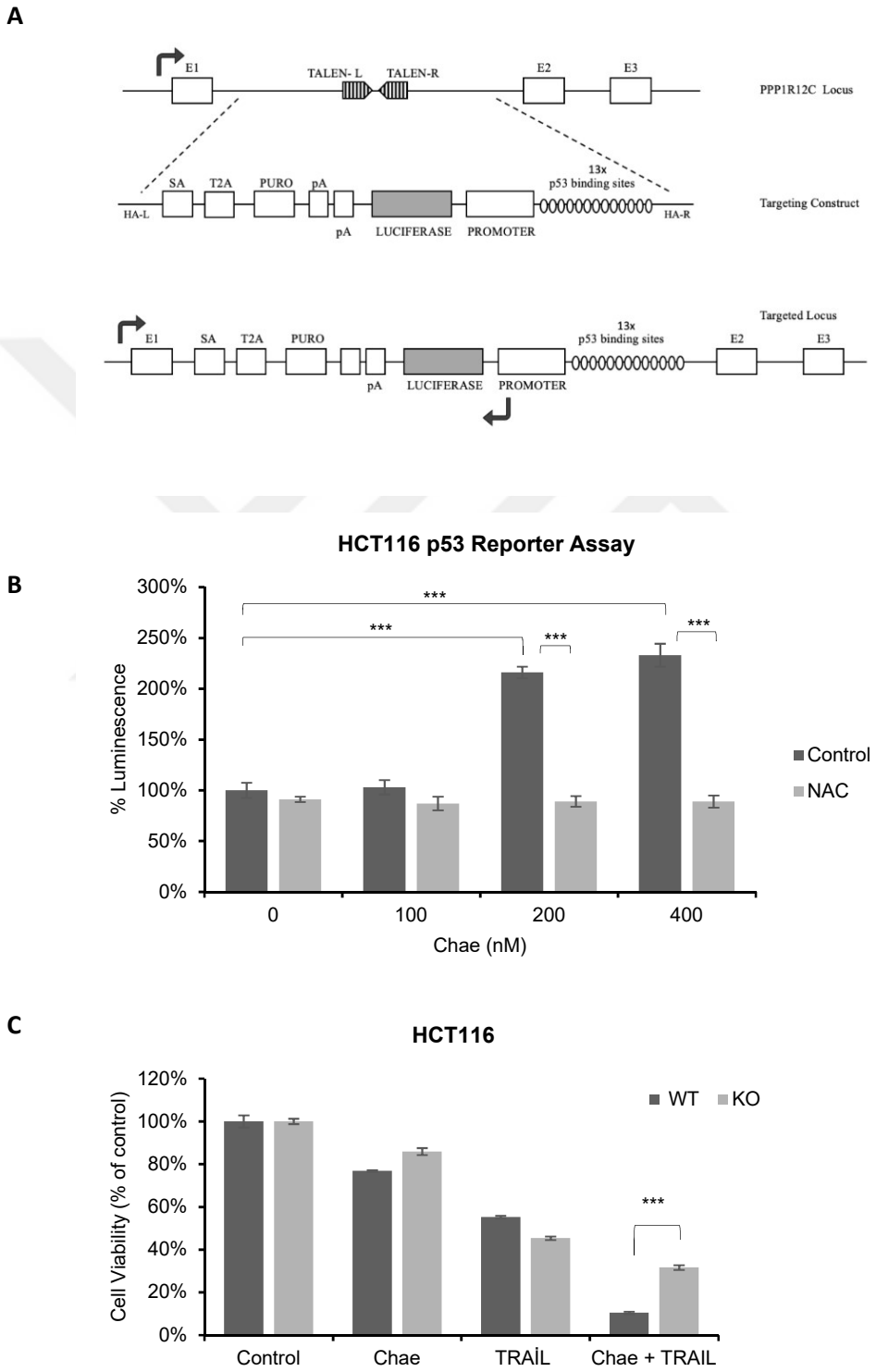

Figure 3.39 TP53 activity is required for apoptosis induction through combinatorial treatment (a) Schematic of the TP53 reporter system (b) TP53 transcriptional activity in

HCT116 colon cancer cells, stably expressing luciferase under the TP53 driven promoter, upon Chaetocin (100, 200, 400 nM for 24h) treatment. TP53 transcriptional activity was induced in dose-dependent manner. NAC (10 µM) pretreatment was started 24h before Chaetocin (100 nM for 24 h) addition (c) Viability analysis of wild type (WT) and TP53 knockout (KO) HCT116 cells upon Chaetocin and TRAIL treatment. Data were normalized to untreated control condition. (*** denotes P<0.001, two-tailed Student's t-test)

To rule out the changes in the senescence state due to high TP53 activity upon Chaetocin treatment, we performed X-gal staining revealing no changes in senescence (**Figure 3.40**).

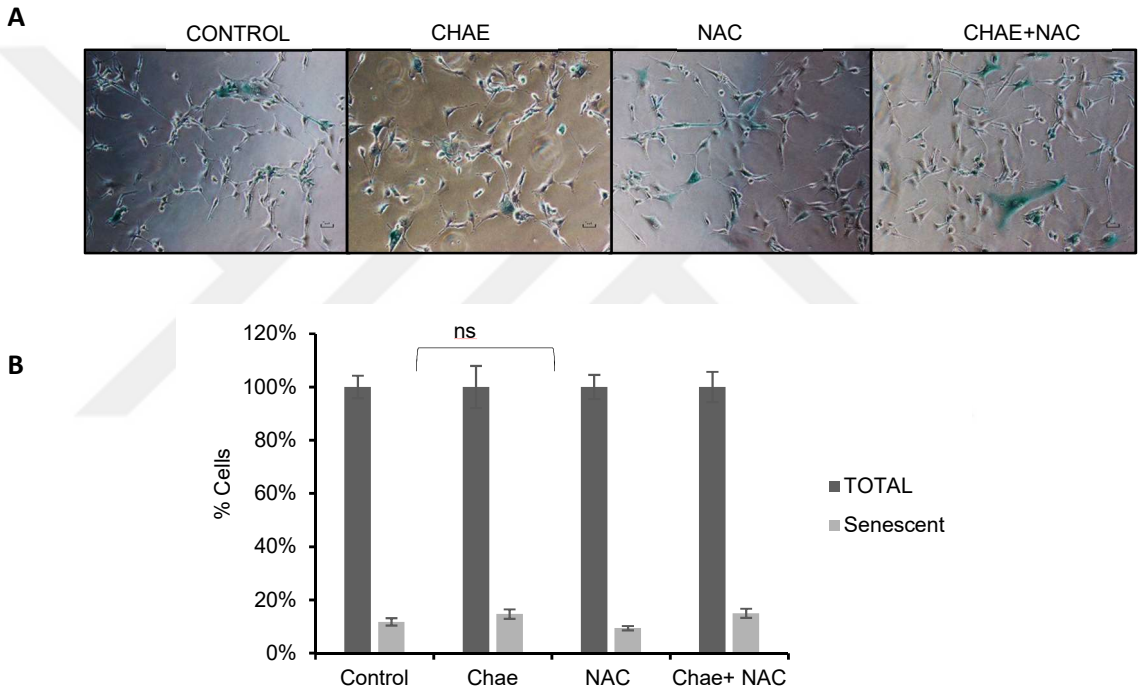

Figure 3.40 Chaetocin does not lead to senescence in GBM cells. (a) X-gal staining to show senescent cells upon Chaetocin treatment (100 nM, 24h) in ROS dependent manner (NAC pretreatment 10 µM, 24h). Images were taken by light microscope at 10x magnification. (b) Quantification of X-gal staining showing no significant elevation in senescent state upon Chaetocin treatment. (ns denotes P>0.05, two-tailed Student's t-test)

3.8 Heme Oxygenase 1 (HMOX1) regulates Chaetocin-induced apoptotic sensitization

Enrichment of UV response, ROS, and TP53 as hallmark pathways by GSEA led us to examine whether these Chaetocin-induced changes can be recognized in the context of clinical information. We curated a list of genes that were significantly altered within the UV response, ROS, and TP53 gene sets and correlated them with glioma patient survival using available TCGA data of GBM and lower grade glioma patient data. We first grouped a total of 663 patient samples into two categories using *k*-means clustering (k=2) on the *z*-normalized gene expression values. Comparing the Kaplan-Meier survival curves of these two groups, we observed a significant clustering and survival difference between the groups (**Figure 3.41**).

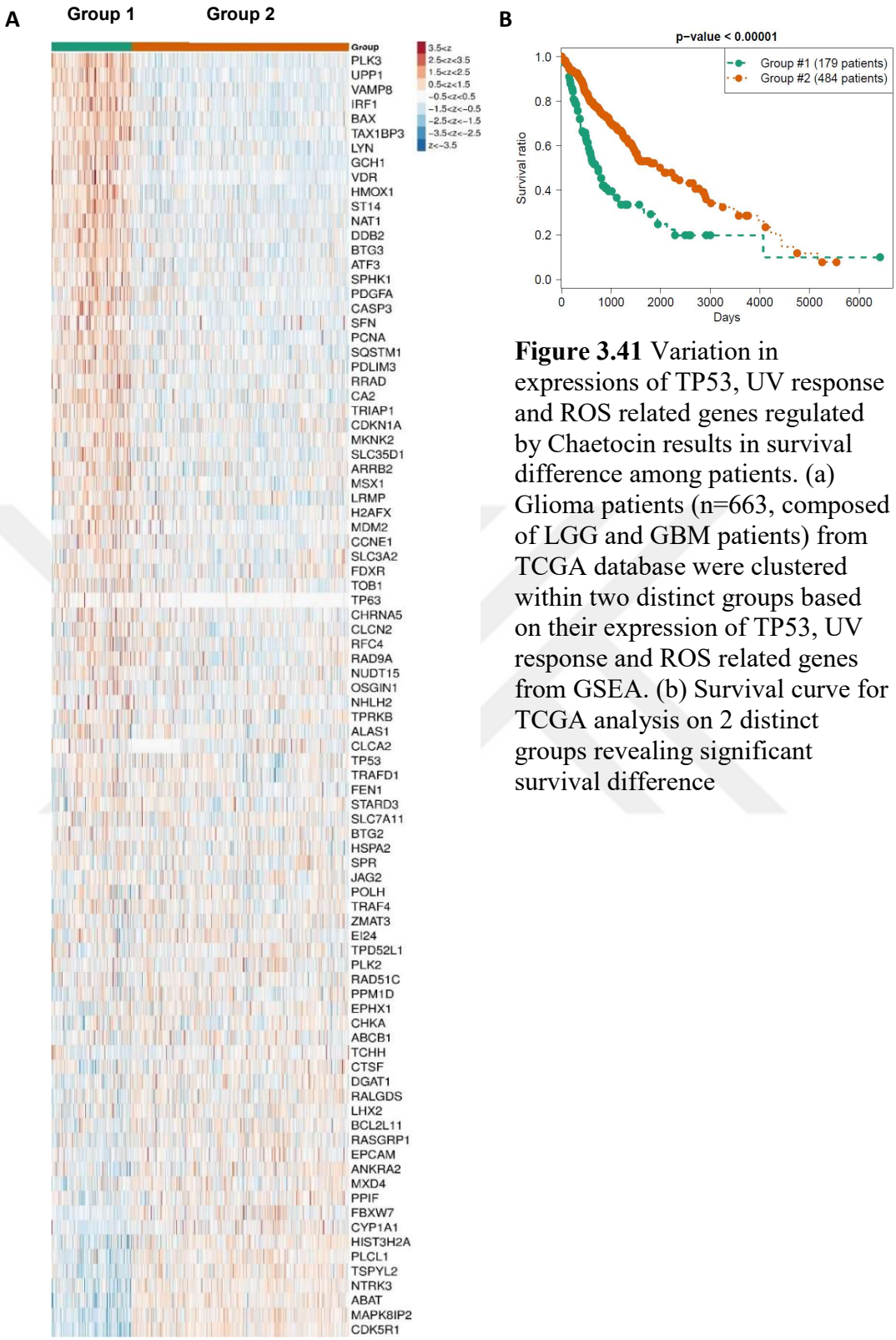

Figure 3.41 Variation in expressions of TP53, UV response and ROS related genes regulated by Chaetocin results in survival difference among patients. (a) Glioma patients (n=663, composed of LGG and GBM patients) from TCGA database were clustered within two distinct groups based on their expression of TP53, UV response and ROS related genes from GSEA. (b) Survival curve for TCGA analysis on 2 distinct groups revealing significant survival difference

HMOX1 was among the topmost upregulated gene both by TP53 and UV and RNAseq data. HMOX1 is an essential enzyme for heme catabolism[363]. HMOX1 cleaves heme to form biliverdin and carbon monoxide, which exhibit anti-oxidant and anti-inflammatory functions, respectively[363]. Targeting HMOX1 was previously shown to be

an effective approach to overcome therapy resistance of hormone-refractory prostate cancer[364], urothelial and pancreatic cancers[365,366]. *HMOX1* expression levels, when analyzed alone, is inversely correlated with glioma patient survival as well (**Figure 3.42**).

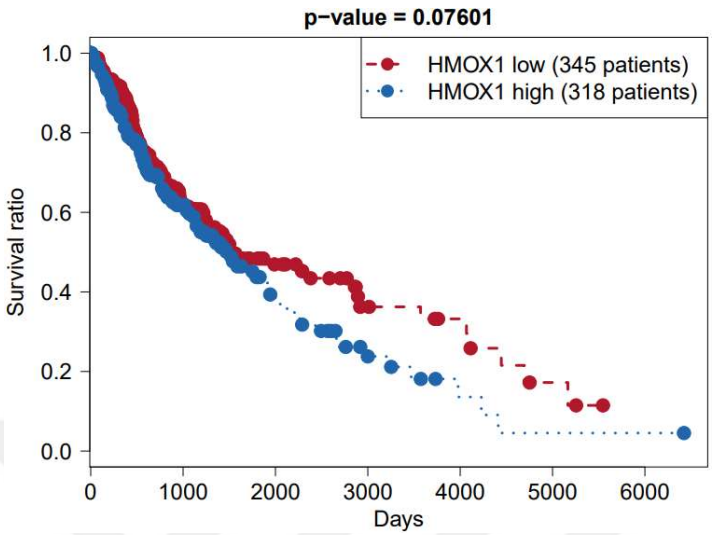

Figure 3.42 Survival curve of glioma patients (from TCGA database) showing inverse correlation between patient survival and *HMOX1* gene expression.

Since the expression of *HMOX1* was significantly modulated by Chaetocin (**Figure 3.43a**) we asked whether HMOX1 could be within the regulatory axis during sensitization of GBM cells to TRAIL. We ablated HMOX1 in U87MG cells by CRISPR/Cas9 (**Figure 3.43b**). Cells that lost HMOX1 expression were more sensitive to TRAIL and combinatorial treatments, again highlighting a critical role for ROS formation (**Figure 3.43c**).

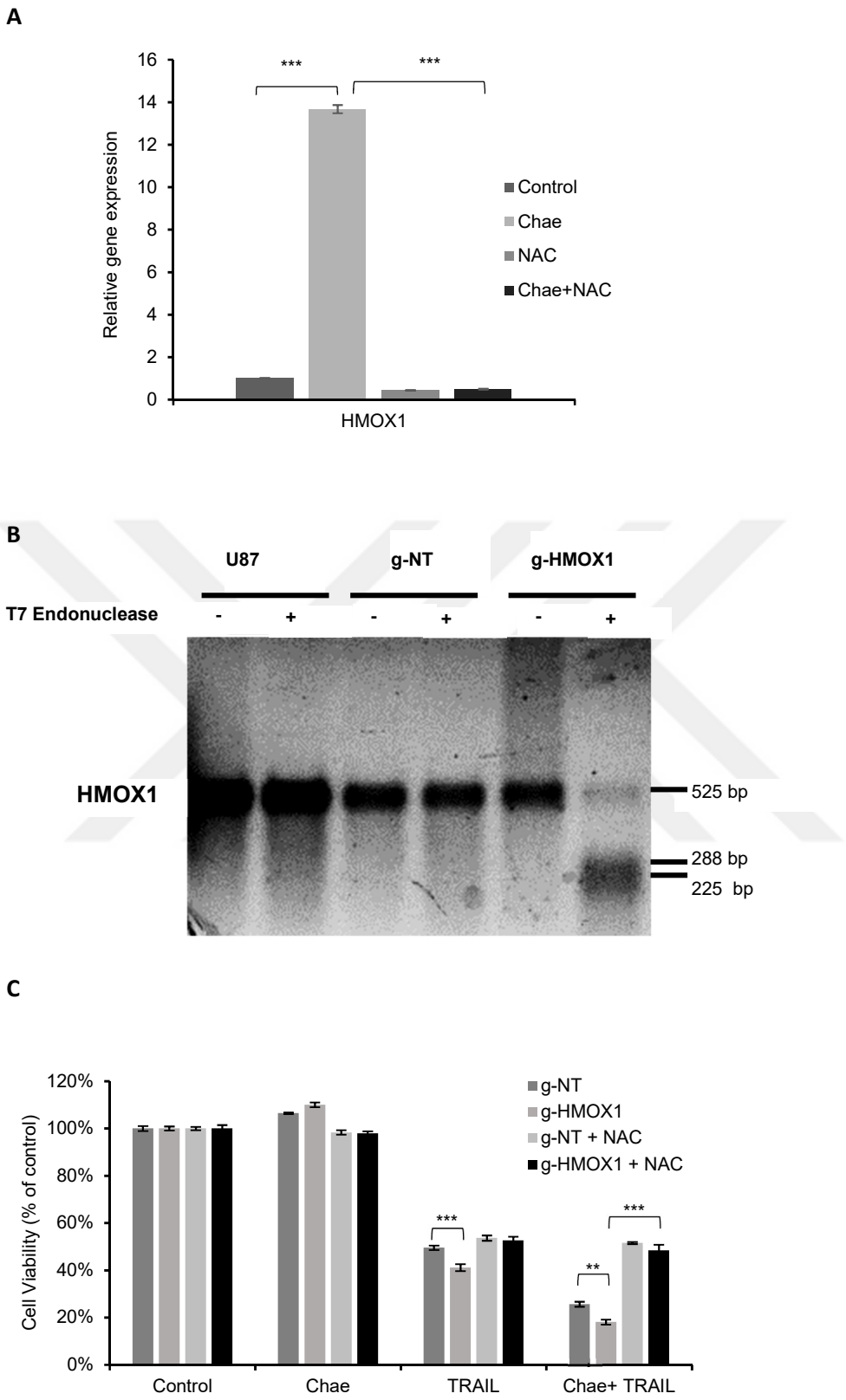

Figure 3.43 HMOX1 gene modulates Chaetocin mediated apoptosis sensitization (a) qPCR data showing upregulation of *HMOX1* upon Chaetocin treatment in ROS-dependent manner. Data were normalized to untreated control. (b) T7 Endonuclease assay showing CRISPR knock out of HMOX1 gene. g-NT is negative control gRNA for

CRISPR system. (c) Viability analysis showing that HMOX1 knock out sensitized U87MG cells further to TRAIL and Chaetocin + TRAIL in ROS-dependent manner. NAC pretreatment (10 µM) was performed for 24h. Data were normalized to untreated control. (** and *** denote P<0.01 and P<0.001 respectively, two-tailed Student's t-test)

3.9 Chaetocin and *TRAIL* treatments cooperate to reduce tumor growth in vivo

To explore the efficacy of TRAIL sensitization by Chaetocin *in vivo*, we examined subcutaneous (subQ) and orthotopic xenograft models of U87MG cells expressing Fluc and mCherry (**Figure 3.44**).

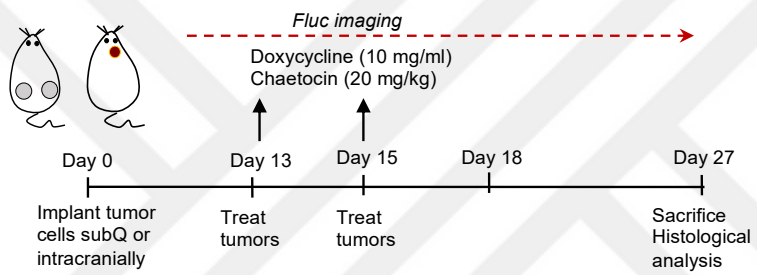

Figure 3.44 Schematic description of the in vivo experiments. U87MG cells expressing Fluc and mCherry together with an inducible TRAIL vector (Tet-TRAIL) were injected subcutaneously or intracranially to NOD/SCID mice. Tumor cell injection was confirmed with noninvasive bioluminescence imaging (BLI) on day 0. After tumors are established, Chaetocin + Dox administration was performed at Days 13 and 15. Tumor growth was monitored until Day 27 with BLI.

To supply tumors with TRAIL on-site, we developed tetracycline-inducible TRAIL vector, whose presence on its own was not toxic to U87MG cells. However, with Dox treatment, TRAIL secretion was sufficient to markedly reduce U87MG cell viability and tumor growth (**Figure 3.45**).

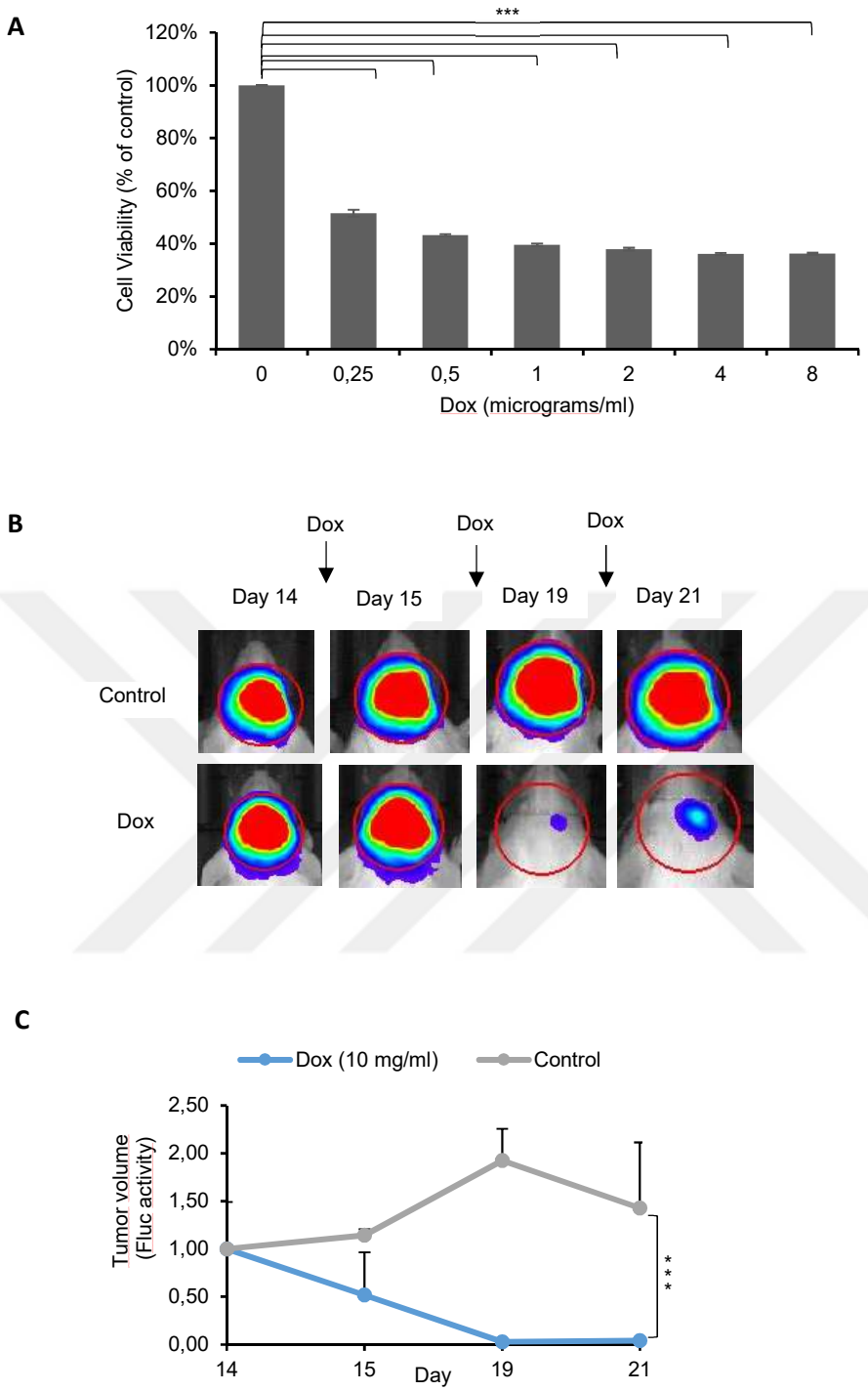

Figure 3.45 Dox inducible TRAIL potently decreases tumor mass in vivo (a) Viability analysis of Fluc-mCherry expressing and Tet-TRAIL transduced U87MG cells upon Dox treatment. Data were normalized to untreated control conditions. Increasing TRAIL secretion by elevating Dox concentration markedly reduced U87MG cell viability. (*** denotes P<0.001, two-tailed Student's t-test) (b) Representative images from intracranial tumors on day-14, day-15, day-16 and day-21 displaying normalized bioluminescent efficiencies acquired (blue to red indicates lower to higher radiance as photons/s/cm2/steradian). (c) Plots depicting tumor volumes of intracranial tumors under each condition (n=2/group). (*** denotes P<0.001, unpaired parametric t-test)

In the subcutaneous model, Dox and Chaetocin treatments were performed simultaneously and tumor growth was observed over 2 weeks (**Figure 3.46**).

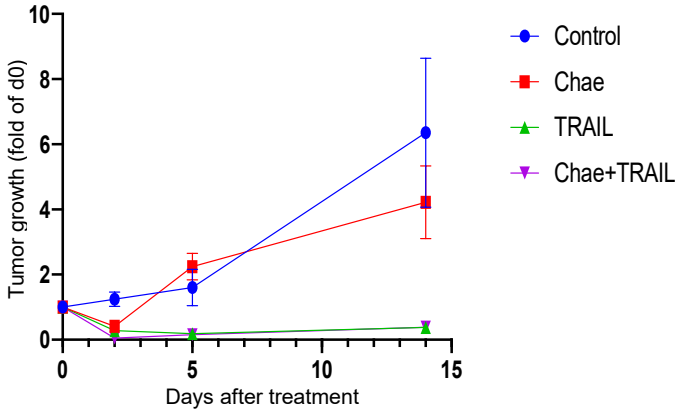

Figure 3.46 Chaetocin works synergistically with TRAIL in vivo. Graph depicting tumor growth as measured by bioluminescent radiance on 4 time points for 14 days (after treatment). Data were normalized to day 13 (day 0 of drug treatment) signal of each group (n= 8 tumors per group).

Chaetocin+TRAIL treatment attenuated subcutaneous tumor growth faster in comparison to the TRAIL only group which was most notable right after treatment (d15); but overall effects of the TRAIL and combinatorial treatments were similar at d27 (**Figure 3.47**).

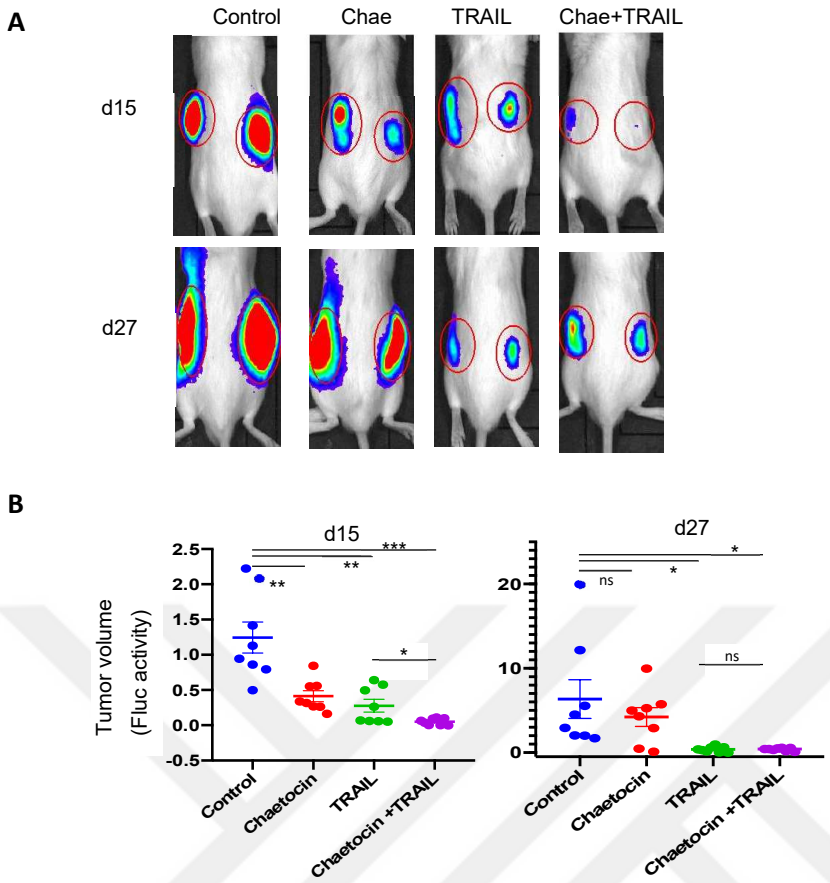

Figure 3.47 Chaetocin works with TRAIL in vivo subcutaneous GBM model (a) Representative images of bilateral tumors from days 15 and 27 displaying normalized bioluminescent efficiencies acquired (blue to red indicates lower to higher radiance as photons/s/cm2/steradian). (b) Plots depicting tumor volumes of each subQ tumor on d15 (left) and d27(right). (*, ** and *** denote P<0.05, P<0.01 and P<0.001 respectively, unpaired parametric t-test)

Similarly, intracranial tumor volumes decreased more rapidly in combination treatment group at d15 though the effects became similar at day 27 (**Figure 3.48**).

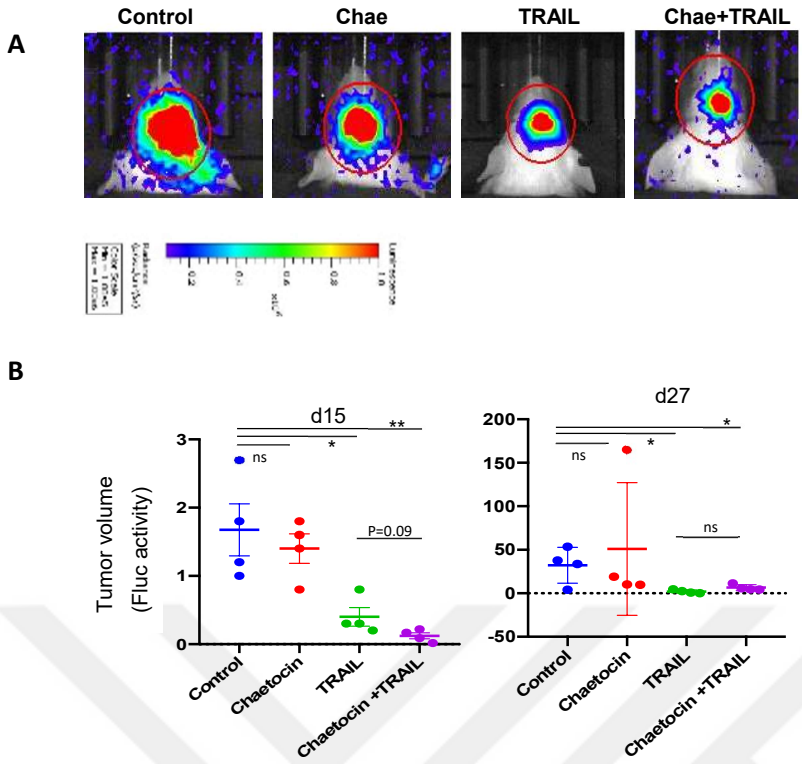

Figure 3.48 Chaetocin works with TRAIL in vivo intracranial GBM model(a) Representative images of intracranial tumors on d27. (b) Plots depicting tumor volumes of each intracranial tumor on d15 (left) and d27(right) (n=4/group). (* and ** denote P<0.05 and P<0.01 respectively, unpaired parametric t-test)

Representative subcutaneous tumors resected from sacrificed mice are illustrated (**Figure 3.49**). Together, these results suggest that Chaetocin and TRAIL combination might serve as efficient therapies for GBM models.

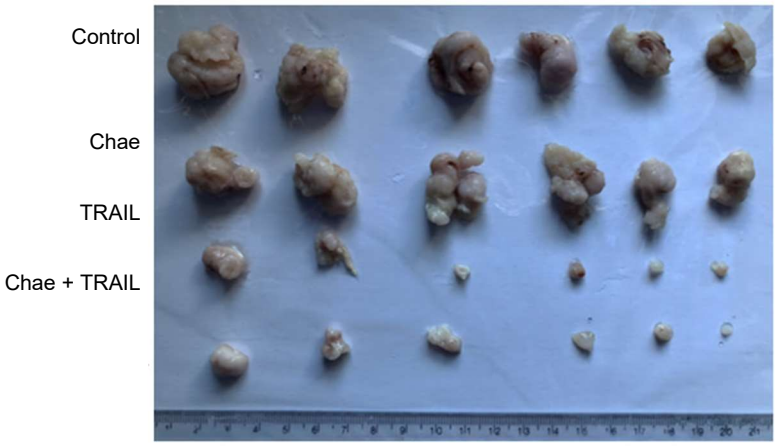

Figure 3.49 Representative subcutaneous tumors excised on day 30.

Chapter 4

4. DISCUSSION

4.1 Combinatorial approach is the key for elevating GBM apoptosis

TRAIL is a widely investigated preclinical agent for glioma since current treatment strategies for GBM fail to fulfill demands of patients and clinicians, and the need for the cancer-specific and potent death inducer agents is tremendous. Apoptosis induction ability of TRAIL is restricted to GBM tumor cells, setting aside nonmalignant astrocytes, a concept that supports the highly tumor-specific property of TRAIL[367].

Various approaches have been taken to increase apoptotic potential of TRAIL in GBM cells since resistance against TRAIL monotherapy is evident across various GBM cell lines. Constitutive activation of NF-κB pathway through ectopic expression of pathway activators was shown to facilitate DISC complex assembly and caspase activation, contributing to TRAIL mediated apoptosis of GBM cells[368]. SMAC mimetics have also been discovered to enhance anti-tumor effect of recombinant TRAIL as well as TRAIL receptor agonist Drozitumab in GBM primary cells, GSC as well as GBM intracranial xerographs[369,370]. Similarly BH3 mimetic such as specific BCL-2 inhibitor HA14-1 and the BCL-2/BCL-XL inhibitor BH3I-20 potentiated TRAIL mediated cell death in GBM cell lines[79]. Inhibitors of PI3K/ Akt/mTOR signaling such LY294002 also potentiates TRAIL mediated apoptosis in glioma cells[80]. Proteasome inhibitors such as Bortezomib were also revealed as potent TRAIL sensitizers for GBM in vitro and in vivo models. Synergy between Bortezomib and TRAIL was previously based on elevated tBID accumulation and stability which results in potent trigger of intrinsic apoptosis[371]. In addition, DNA damaging agents such as Mitoxantrone was revealed to augment TRAIL response of glioma cells through modulation of pro and anti-apoptotic gene expression[356]. Modulation of the tumor epigenome was another widely pursued approach to overcome TRAIL resistance of glioma cells. HDAC inhibitors such as MS275 and valproic acid was shown to sensitize GBM cells to TRAIL mediated apoptosis though reducing cFLIP expression[293].

4.2 Epigenetic-based clinical trials are encouraging for GBM therapy

Epigenomic alterations are among the main drivers of GBM progression. For instance, repression of RRP22, a candidate tumor suppressor by hypermethylation an H3 and H4 acetylation contribute to high grade glioma formation with low prognosis[372]. As another example, low level acetylation of H3K18 and high level of H4K20me3 is associated with better survival for GBM patients[373] .

Epigenetic based treatment strategies interfering with abnormal DNA methylation, acetylation and chromatin remodeling patterns of GBM are under deep investigation. In glioma patients, outcome of conventional treatment with TMZ is tightly dependent on DNA methylation status of the tumor. As previously mentioned, DNA damaging-based cytotoxicity of the alkylating agent TMZ is cancelled out by MGMT gene and therefore glioma patients with methylated MGMT have survival advantage over individuals with unmethylated, active MGMT gene[154]. Considering this information, several clinical trials have been launched to investigate the effect of synthetic inhibitors of MGMT, one of which were O6-Benzylguanine (NCT00613093). Yet, unfortunately this inhibitor failed to augment drug response of TMZ-resistant GBM patients[374].

Chromatin remodeling especially through enhanced HDAC expression is a clever and fast strategy of GBM cells to gain resistance against drugs and therefore modulation of epigenetic histone code through HDAC inhibitors holds promise for better clinical outcome of patients[288]. Vorinostat, Romidepsin, Belinostat, Panobinostat and Valproic acid are FDA approved HDAC inhibitors which are frequently involved in clinical trials. Vorinostat, both as single agent and as combined with standard of care chemo (e.g. TMZ and bevacizumab) and radiotherapy was subjected to 14 different Phase I/II clinical studies (e.g. NCT00238303, NCT00268385, NCT00731731, NCT00555399 and NCT01738646)[375]. So far, no significant survival advantage conferred by Vorinostatin combinatorial therapies with TMZ and radiation[376] though as single agent it stabilized the disease [377]. Clinical trial on Panobinostat in combination with bevacizumab and radiation for treatment of GBM (NCT00859222 and NCT01324635 respectively) was terminated due to ineffectiveness. On the other hand; Valproic acid, in Phase II trial with TMZ and radiotherapy (NCT00302159,) gave encouraging results[378,379]. Romidepsin was studies in Phase I/II trials (NCT00085540) yet turned out to be fruitless for GBM therapy[380]. Belinostat in combination with TMZ has ongoing clinical investigation (NCT02137759)

which reveals encouraging results in terms of GBM recurrence delay and decreased psychological symptoms of patients[381]. In addition, inhibitors of chromatin remodeling complex, namely Oliparib and Veliparib are FDA approved and clinically investigated for GBM alone or in combination with chemo/radio therapy (NCT01390571, NCT03212274, and NCT02152982, NCT03581292, NCT01514201 respectively) with promising results though not yet fully revealed[382,383].

4.3 Joint force against GBM: Epigenetic modulation & Apoptosis

Combinatorial therapies are under investigation widely and have clinical implications for GBM which is not surprising considering the heterogeneity of GBM as an obstacle for single agent treatments. Considering broad effect of epigenetics in cancer drug response and frequent epigenetic alterations in GBM; utility of epigenetic modifiers for *TRAIL* sensitization of GBM cells might provide a therapeutic benefit to patients.

In this study, we interrogated the effects of epigenetic modifying compounds on GBM cell apoptosis in a screening approach and identified Chaetocin as a novel sensitizer for apoptotic therapies in GBM cells. Our study explored the Chaetocin-induced global effects and sensitizing ability in GBM cells. We showed that the effects of Chaetocin on GBM cell apoptosis are unrelated to the alleged effect of Chaetocin as SUV9H1 inhibitor; but are through the generation of ROS and DNA damage induction leading to a TP53 induced pro-apoptotic program. Furthermore, we demonstrated that Chaetocin effectively cooperates with TRAIL, FASL, and BH3 mimetics ABT263 and WEHI539 to induce apoptosis in GBM cells. Finally, Chaetocin and TRAIL combinatorial treatment revealed efficacy in reducing tumor growth *in vivo*. Detailing of above-mentioned findings with reference to supportive literature follows:

4.4 Chaetocin is a general apoptosis sensitizer

In the screen that involved chemical probes against chromatin modifiers, we identified HDAC inhibitors (Belinostat, Trichostatin A and SAHA) in accordance with their established role in apoptosis sensitization[384]. We also identified Chaetocin as a novel apoptosis regulator in GBM cells. Whilst the relation of Chaetocin with death receptor-

dependent apoptosis was previously reported[385,386] and the synergistic cytotoxicity of Chaetocin with other epigenetic drugs such as SAHA, JQ-1[387], Trichostain A[388], Vorinostat and AraC[361] was previously explored in other cancers, no attempt was made to investigate effect of sub-toxic dose of Chaetocin in combination therapies with pro-apoptotic agents, eliminating the problem of single agent toxicity. We here demonstrate that low dose treatments of GBM cells are sufficient to induce cell death in combination with pro-apoptotic agents such as TRAIL, FASL and BH3 mimetics, suggesting that a brief treatment with Chaetocin might be sufficient to prime GBM cells for apoptotic agents. The cooperation between Chaetocin and TRAIL involved canonical apoptosis pathways, activation of effector caspases and regulation of DR5, CASP8, BID, BCL-2 and BCL-XL.

4.5 Chaetocin rewires the metabolism of GBM cells and attenuates their cell cycle and invasion

In glioma, Chaetocin was previously shown to induce apoptosis through the Atm–Yap1 axis and Jnk-dependent metabolic adaptation, where Chaetocin reduced lactate levels, ATP production and glucose uptake[307]. In concordance, our GSEA results revealed oxidative phosphorylation and glycolysis as negatively enriched upon Chaetocin treatment, implying metabolic rewiring of glioma cells by Chaetocin treatment.

Chaetocin was also shown to inhibit invasive ability and trigger cell cycle arrest of the human intrahepatic cholangiocarcinoma in ROS-dependent manner[389]. Our results showing the Chaetocin-induced cell cycle arrest are in accordance with these findings. As another literature-supported finding, hallmark EMT pathway was negatively enriched upon Chaetocin treatment in our GSEA results.

4.6 Chaetocin produces ROS and activates antioxidant defense mechanisms

GSEA data helped us to further dwell into Chaetocin mode of action and revealed that Chaetocin is a potent ROS producer. ROS is generated during regular oxygen metabolism and when at low and moderate levels, trigger various signaling pathways to endure proliferation and survival of cells under stress as well as cellular homeostasis[390]. However, at excessive amounts under environmental stress such as UV exposure, ROS

cause oxidative damage to DNA, protein and lipids, cause oxidative stress within the cell and render cells prone to apoptosis[391]. ROS levels are tightly balanced in cell via the transcription factors such as nuclear factor erythroid 2-related factor 2 (NRF2)[392] which drives the expression of antioxidant genes namely HMOX1, NQO1, GCLM and TXNRD1[393,394,395]. Among these antioxidant genes, Chaetocin inhibits TXNRD1[396,397] by competing with thioredoxin for binding. TXNRD1 enzyme activates thioredoxin, an oxidoreductase that reduces oxidized cysteine residues on cellular proteins and prevents oxidative damage to cells. Chaetocin was illustrated to inhibit the progression of various cancer types including chronic myelogenous leukemia[398] and non-small cell lung cancer[385] through ROS stress induction.

In this study, we showed that the antioxidant defense system is initiated in U87MG cells upon Chaetocin treatment. Chaetocin led to ROS generation and upregulation of NRF2[392] target antioxidant gene expression namely *HMOX1, NQO1, GCLM* and *TXNRD1*[393,394]. Indeed, our observation of the Chaetocin mediated increase in antioxidant gene expression by RNA-seq and qPCR might be a feedback response to activate ROS scavenging mechanisms, yet which fail to suppress ROS mediated TRAIL sensitization.

4.7 Apoptosis sensitization by Chaetocin is mediated by ROS production and is not dependent on Suv39H1 inhibition

Chaetocin was found to be a specific inhibitor of the lysine-specific histone methyltransferase SU(VAR)3-9 at a narrow concentration window (IC_{50}= 0.6 μM) and acts as a competitive inhibitor for S-adenosyl methionine[306]. Although modulation of SUV39H1 activity can induce ER stress and subsequent apoptosis in lung cancer[385], we showed that Chaetocin effects on GBM were independent of SUV39H1 regulation. Depletion of SUV39H1 failed to sensitize GBM cells further to apoptosis and in addition; H3K9me(3) levels remained unchanged upon Chaetocin treatment clearly indicating that SUV39H1 inhibition is not the root cause for the pro-apoptotic effects of Chaetocin.

We revealed that Chaetocin mediated GBM cell sensitization to TRAIL, FASL and BH3 mimetics was ROS dependent, since NAC interfered with all Chaetocin effects. In concordance Chaetocin elevated expression proapoptotic genes such as *FADD*, *CASP3* and *BIM* in ROS dependent manner. Supporting our findings, there have been studies

showing the interplay between TRAIL-mediated signaling and oxidative stress responses. For example, ROS production was previously shown to upregulate *DR5* expression in human carcinoma cell lines[399]. Baicalein[400] and Vitisin A[401] sensitized prostate cancer cells to TRAIL via ROS generation and DR5 upregulation. As another important modulator of oxidative stress response, Glutathione reductase inhibitors potentiated TRAIL toxicity in prostate carcinoma and melanoma[402].

Though ROS production was identified as the main driver of apoptosis sensitization process, involvement of epigenetic regulation in the process is undeniable since the apoptosis sensitization is sustained in long term; even 4 day after removal of the drug. Since Suv39h1 inhibition and regulation of H3K9 methylation levels were proven to be inefficient to explain apoptotic sensitization process, we speculated that ROS mediated modulation of epigenome might be explanatory for the current situation.

Besides directly damaging cellular genetic material and proteins, ROS can also induce epigenetic alterations within the cell. ROS was shown to downregulate tumor suppressor genes through excessive DNA methylation at promoter site. For instance, ROS-JNK-DNMT1 pathway was previously shown to silence tumor suppressor *P16* via promoter hypermethylation and consequently result in lung carcinogenesis[403]. Furthermore, DNMT1 and HDAC1 activity was shown to be elevated by ROS which results in silencing of tumor suppressor RUNX3 and the progression of colorectal cancer[404]. In HCC, ROS facilitates promoter methylation of E-cadherin through inducing Snail expression and subsequent DNMT1 and HDAC1 recruitment[405]. Besides modifications of DNA, ROS can also alter modifications of histones, particularly euchromatin related mark H3K4me2/3 and heterochromatin marks H3K9me2/3 and H3K27me3[406,407]. To exemplify, ROS significantly downmodulates H3K4 and H3K9 methylation[408]. ROS can enhance or inhibit histone acetylation based on the circumstances. ROS was shown to elevate H4 acetylation and H3K9 acetylation in alveolar epithelial cells[409] and in the primary rat hepatocytes[410] respectively; whereas in human hepatoma cells histone acetylation was decreased by ROS[411,412]. ROS mediated modulation of epigenome might be explanatory for potent and long term sensitization of tumor cells to any apoptotic stimuli by Chaetocin treatment.

4.8 Chaetocin induces DNA damage and activates downstream repair pathways involving *TP53* activity

Elevated γH2AX staining and upregulation of DNA repair genes' expression upon Chaetocin treatment prove DNA damaging ability of Chaetocin in ROS dependent manner. In accordance, protein level pf TP53; major sensor of DNA damage and the guardian or our genome, was highly elevated upon Chaetocin treatment. NUTLIN mediated over sensitization of U87MG cells to TRAIL was also a supportive finding for the role of TP53 in our cells. The undeniable role of TP53 during Chaetocin mediated TRAIL sensitization is not surprising as TP53 is the genome guardian ready to fight consequences of oxidative stress and is a well-established modulator of TRAIL response for various cancer types. In glioma, Chaetocin mediated activation of JNK resulted in apoptosis via inhibition of BCL-2[413] as well as activation of TP53[414], suggesting a similar mechanism as identified in our GBM work. TP53 mediated TRAIL sensitization is likely linked to increased expression of TP53 target genes such as *DR5*, *BAX*, *NOXA*, and *PUMA*[415].

4.9 Repression of antioxidant defense mechanism enhances Chaetocin mediated apoptosis sensitization

Interrogating ROS related and DNA damage response associated genes, we noted that HMOX1 was the top scoring gene subcategorized under hallmark UV response and TP53 pathways and was also highly enriched upon Chaetocin treatment. HMOX1 cleaves heme to form biliverdin and carbon monoxide, which exhibit anti oxidative and anti-inflammatory functions, respectively[363]. Various cellular stress agents, such as heavy metals, xenobiotics, cytokines, hypoxia, or UV irradiation promote HMOX1 expression through activation of transcriptional factors such as NRF2, NF-κB, AP2[416,417,418]. Carbon monoxide produced by HMOX1 contributes to cell survival by inhibiting ROS formation and triggering DNA repair which associates HMOX1 with therapeutic resistance[419,420,421]. HMOX1 downregulation leads to elevated ROS and subsequent DNA damage and consequent apoptosis in cells[422].

Targeting HMOX1 was previously shown to be an effective approach to overcome therapy resistance of hormone-refractory prostate cancer[364], urothelial and pancreatic

cancers[365,366]. Similarly, we revealed that in the absence of HMOX1, U87MG cells' response to Chaetocin and/or TRAIL was elevated, which was blocked by NAC. Therefore, our results show that HMOX1 is within the regulatory axis during apoptotic process initiated by Chaetocin in GBM cells.

4.10 Overall mode of action of Chaetocin

Taken together, we postulate a model in which ROS production by Chaetocin treatment increases the apoptotic priming of GBM cells and renders them more prone to apoptosis initiated by other intrinsic and extrinsic agents. Elevated cellular ROS levels cause DNA damage and TP53 activation. Active TP53 initiates DNA repair mechanisms and render mitochondria primed for cytochrome c release and consequent apoptosis in case damage is unrepairable. To eradicate the detrimental effect of cellular ROS accumulation, antioxidant defense mechanisms get activated in response to Chaetocin treatment. When Chaetocin is combined with extrinsic and intrinsic apoptosis inducers, ROS mediated primed state of mitochondria as well as elevated pro-apoptotic gene expression (*FADD, CASP3, CASP8, DR4, PUMA, NOXA, BAD, BIM, HRK)* render cells much more prone to apoptosis (**Figure 4.1**).

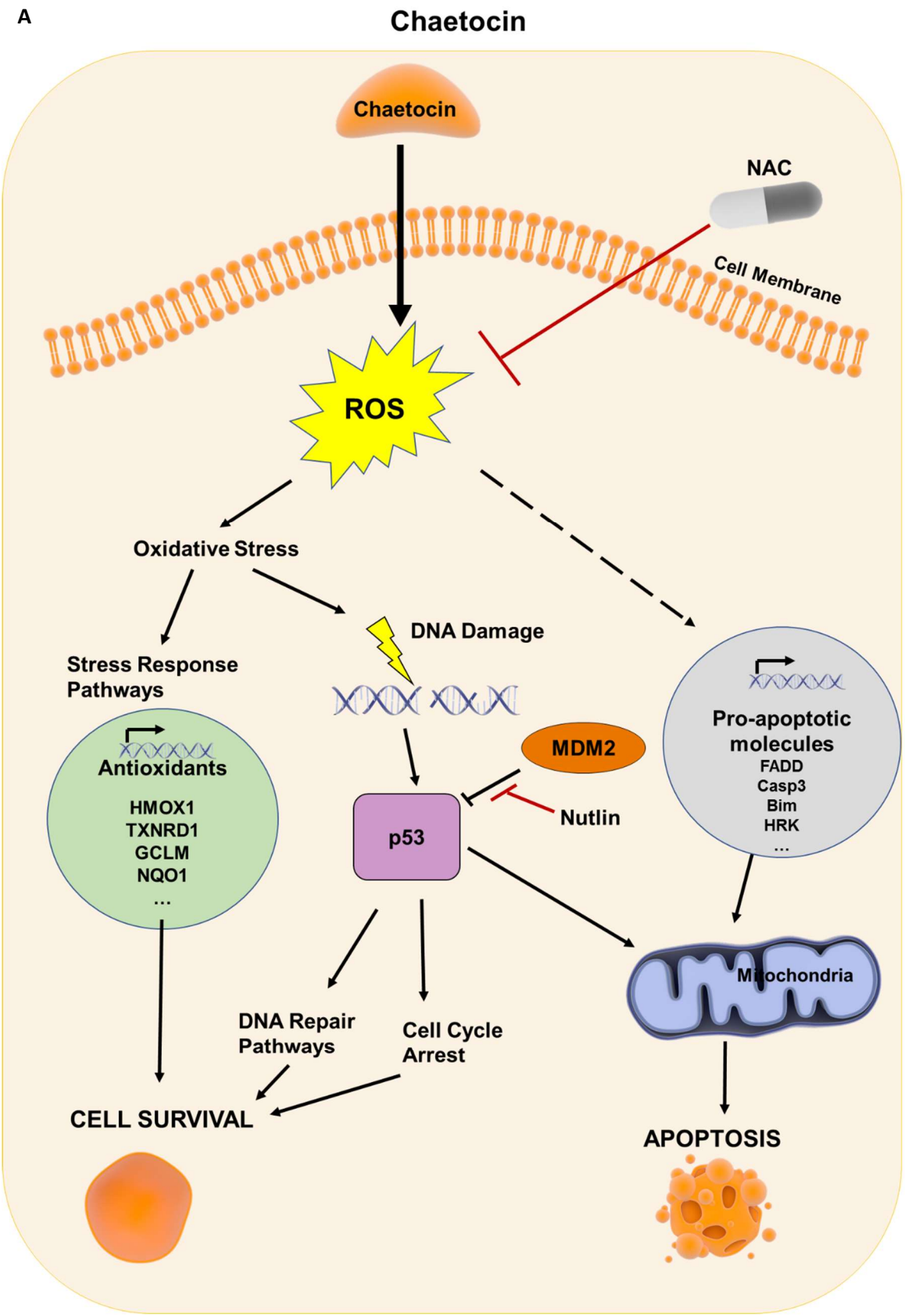
A
Chaetocin
Chaetocin
NAC
Cell Membrane
ROS
Oxidative Stress
DNA Damage
Stress Response Pathways
Antioxidants
HMOX1
TXNRD1
GCLM
NQO1
...
MDM2
Nutlin
p53
Pro-apoptotic molecules
FADD
Casp3
Bim
HRK
...
Mitochondria
DNA Repair Pathways
Cell Cycle Arrest
CELL SURVIVAL
APOPTOSIS

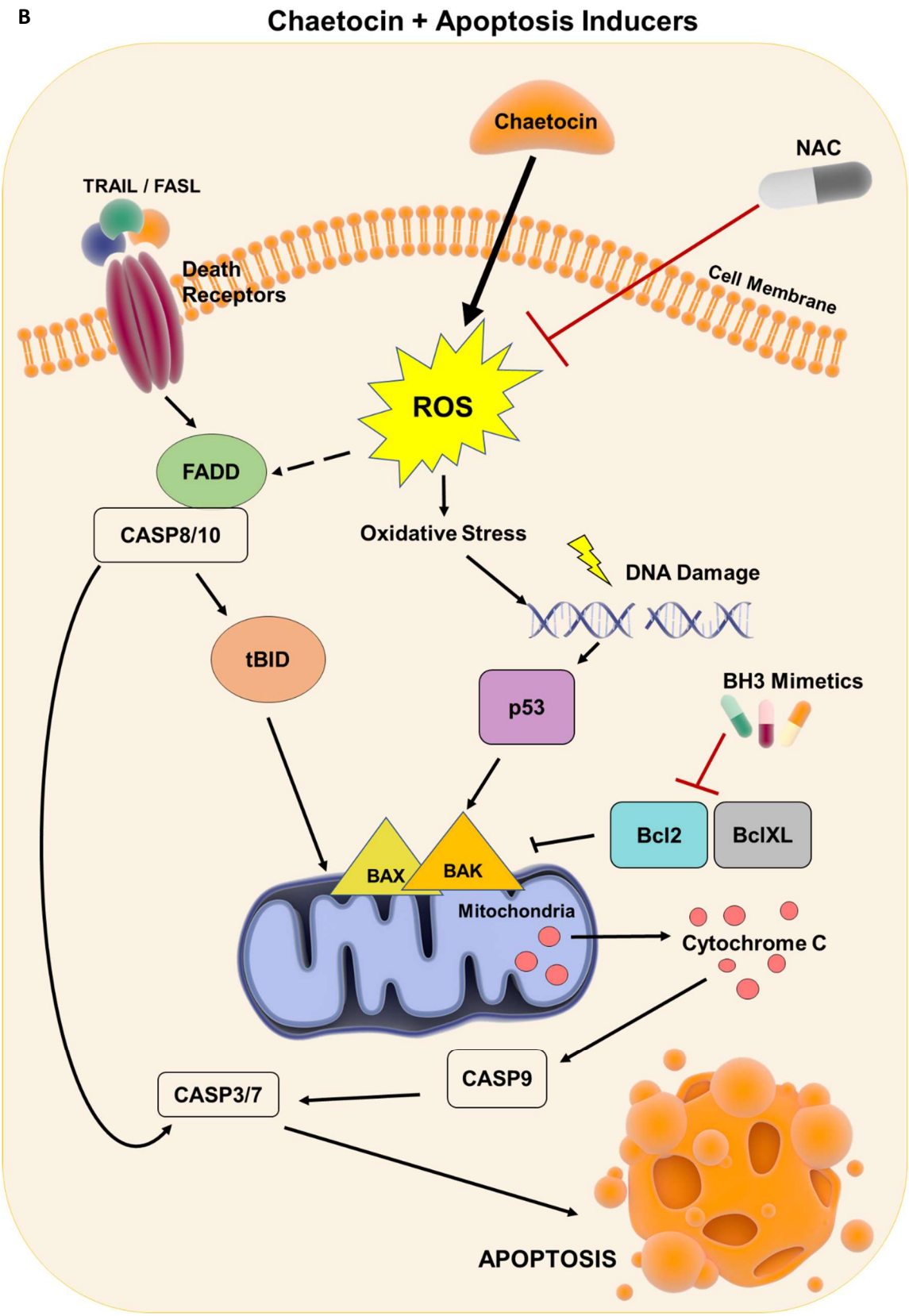

Figure 4.1 Representative model illustrating Chaetocin's mode of action. (a) Chaetocin elevates cellular ROS levels which cause DNA damage mediated TP53 activation. Active TP53 leads to cell cycle arrest and trigger DNA repair mechanism rendering mitochondria primed for apoptosis in case damage is unrepairable. ROS also elevates the expression of

pro-apoptotic genes such as *FADD* and *CASP*3 and contributes to initiation of apoptosis. Antioxidant defense mechanisms get activated in response to Chaetocin treatment to eradicate the detrimental effect of cellular ROS accumulation. (b) When Chaetocin is combined with apoptosis inducers, Chaetocin mediated primed state of mitochondria as well as elevated pro-apoptotic gene expression render cells much more prone to apoptosis induced by any extrinsic (TRAIL/ FASL) or intrinsic (BH3 mimetics) stimuli.

Our identification of Chaetocin as an apoptosis-sensitizer makes it a strong weapon against GBMs, and possibly a wide range of cancers. Importantly, previously revealed ability of Chaetocin to cross BBB[307] as well as our illustration on potency of Chaetocin and TRAIL combination in reducing tumor growth *in vivo* offers a potential therapeutic approach against GBM.

Chapter 5

5. CONCLUSIONS & FUTURE DIRECTIONS

Evasion of apoptosis plays a major role for emergence and progression of wide variety of tumors. Modulation of apoptosis related genes via epigenetic alterations obtained much more attention as our comprehension of cancer epigenome has rapidly grown with the discovery of novel epigenetic modifier enzymes and their target oncogenes/tumor suppressors. Global changes of epigenome via aberrant modifications of DNA and histones as well as altered miRNA expression modulate expression of genes critical to apoptosis and render malignant cells resistant to current chemo and radiotherapy mediated death. Increased understanding of tumor-specific epigenetic alteration of apoptosis will enable discovery of novel targeted therapies.

Our awareness on the importance of epigenetic mechanisms for tumor initiation, progression and apoptotic response led us to investigate epigenetic regulators of apoptosis resistance and survival in GBM through a chemical screen. Screen revealed candidate apoptosis sensitizer drugs including Chaetocin which will be subjects of our future investigations.

Despite the complexity and heterogeneous nature of cancer, epigenetic therapies hold great promise for improved survival of patients alone or in combinatorial approach with other therapeutic modalities due to their potential of resetting the cancer epigenome. Detection of epigenetic factors modulating tumor drug response and survival via high throughput, robust and affordable screens such as our screen detailed in this study, will ultimately lead to rapid discovery of novel cancer biomarkers and production of effective therapies. Reverting cancer therapy resistance and overcoming side effects of current therapy options are our ultimate aim to increase life span and dignity of cancer patients, particularly ones suffering from GBM

Chapter 6

6. APPENDIX

Relative fold changes of genes significantly ($p<0.05$) modulated by Chaetocin are listed in **Table 6.1**.

Table 6.1 Relative fold change of top 30 genes significantly ($p<0.05$) up and down regulated by Chaetocin.

Gene Name	Ensembl ID	Log2 Fold Change	p value	padj value
MYT1	ENSG00000196132	3.632583146	1.79E-34	1.41E-30
HMOX1	ENSG00000100292	2.752764052	1.05E-52	1.67E-48
ARL14EPL	ENSG00000268223	2.591746988	1.89E-18	4.98E-15
MLC1	ENSG00000100427	2.563845041	1.53E-16	3.03E-13
BICDL1	ENSG00000135127	2.406108283	5.59E-19	1.77E-15
RPLP0P2	ENSG00000243742	2.267782555	3.38E-19	1.34E-15
IGFN1	ENSG00000163395	2.105435428	5.80E-12	5.10E-09
HTRA3	ENSG00000170801	1.910562193	6.60E-10	2.99E-07
CYSRT1	ENSG00000197191	1.867239541	4.73E-10	2.27E-07
ENKUR	ENSG00000151023	1.805041416	1.66E-09	6.42E-07
NMRAL1P1	ENSG00000171658	1.801922247	1.99E-09	7.14E-07
RELN	ENSG00000189056	1.800889128	5.36E-09	1.70E-06
ENO3	ENSG00000108515	1.783809261	1.64E-13	2.17E-10
CTD-2292P10.4	ENSG00000253741	1.701510007	3.20E-08	7.57E-06
UNKL	ENSG00000059145	1.629754162	1.07E-19	5.65E-16
KB-1732A1.1	ENSG00000253669	1.621909162	1.05E-09	4.38E-07
MTTP	ENSG00000138823	1.596594188	9.02E-08	1.70E-05
LINC01054	ENSG00000229723	1.596013267	2.02E-07	3.18E-05
FLG	ENSG00000143631	1.578389634	1.29E-07	2.27E-05
HSPA1B	ENSG00000204388	1.561366059	9.40E-13	1.06E-09
ZNF469	ENSG00000225614	1.556834831	4.68E-07	6.74E-05
RP11-481E4.2	ENSG00000261285	1.547756765	5.73E-07	7.91E-05
EDNRB	ENSG00000136160	1.540894067	3.34E-09	1.15E-06
CD53	ENSG00000143119	1.516857684	3.16E-07	4.68E-05
GPR63	ENSG00000112218	1.504035322	9.68E-09	2.78E-06
SMIM13	ENSG00000224531	1.474361814	3.24E-15	5.70E-12
MYOM2	ENSG00000036448	1.468058381	4.99E-08	1.07E-05
RP11-874J12.4	ENSG00000266401	1.464846918	1.09E-08	3.02E-06
LBX2-AS1	ENSG00000257702	1.462342022	3.07E-08	7.36E-06
NCAN	ENSG00000130287	1.449047802	1.11E-06	0.00012813
MMP14	ENSG00000157227	-1.12222384	3.06E-10	1.65E-07
DLC1	ENSG00000164741	-1.135356883	3.56E-07	5.22E-05
NEK3	ENSG00000136098	-1.137025254	0.00025335	0.00911182

ADAM12	ENSG00000148848	-1.142575612	6.21E-11	4.27E-08
DCBLD2	ENSG00000057019	-1.147370523	3.38E-08	7.77E-06
SEMA5A	ENSG00000112902	-1.14758342	1.92E-09	7.07E-07
ANK2	ENSG00000145362	-1.149835942	4.06E-09	1.34E-06
COL6A3	ENSG00000163359	-1.153214108	1.00E-08	2.83E-06
SLC2A3	ENSG00000059804	-1.159416111	5.05E-12	4.70E-09
CHI3L1	ENSG00000133048	-1.169353286	1.90E-10	1.13E-07
SYNPO	ENSG00000171992	-1.174946595	6.19E-07	8.24E-05
OLFML2A	ENSG00000185585	-1.175731596	2.20E-08	5.61E-06
PLCB4	ENSG00000101333	-1.181099387	7.77E-06	0.00066807
CDH11	ENSG00000140937	-1.214748491	2.62E-06	0.0002767
ALPK2	ENSG00000198796	-1.223144111	7.04E-07	8.78E-05
NEGR1	ENSG00000172260	-1.227128391	1.64E-09	6.42E-07
RP4-555D20.2	ENSG00000261786	-1.237899137	1.18E-10	7.78E-08
PALMD	ENSG00000099260	-1.250213293	5.43E-08	1.13E-05
CRIM1	ENSG00000150938	-1.268142534	1.11E-12	1.10E-09
TUBA1A	ENSG00000167552	-1.275423114	4.53E-09	1.46E-06
KIAA1549L	ENSG00000110427	-1.286591364	3.89E-10	1.99E-07
PDCD1LG2	ENSG00000197646	-1.306424471	1.62E-07	2.64E-05
CEMIP	ENSG00000103888	-1.337289082	1.61E-11	1.34E-08
ITGA10	ENSG00000143127	-1.375963239	6.92E-07	8.69E-05
PDGFRB	ENSG00000113721	-1.4176069	1.77E-10	1.12E-07
PAPPA	ENSG00000182752	-1.447295805	3.13E-10	1.65E-07
TENM2	ENSG00000145934	-1.449560126	5.75E-09	1.78E-06
ITGA2	ENSG00000164171	-1.497434554	1.11E-12	1.10E-09
ITGA11	ENSG00000137809	-1.497629316	2.72E-10	1.54E-07
ANO8	ENSG00000074855	-1.613562732	2.23E-14	3.53E-11

Chapter 7

7. REFERENCES

1. Agnihotri, S. *et al.* Glioblastoma, a brief review of history, molecular genetics, animal models and novel therapeutic strategies. *Arch. Immunol. Ther. Exp.* **61**, 25–41 (2013).
2. Committee, C. C. S. S. Canadian Cancer Statistics 2010. *Statistics.***60**, 277-300. (2010).
3. Wen, P. Y. & Kesari, S. Malignant gliomas in . *N. Engl. J. Med.* **359**, 492–507 (2008).
4. ElAli, A. & Hermann, D. M. ATP-Binding Cassette Transporters and Their Roles in Protecting the Brain. *Neurosci.* **17**, 423–436 (2011).
5. Chen, J. *et al.* A restricted cell population propagates glioblastoma growth after chemotherapy. *Nature* **488**, 522–526 (2012).
6. Alcantara Llaguno, S. R. *et al.* Adult Lineage-Restricted CNS Progenitors Specify Distinct Glioblastoma Subtypes. *Cancer Cell* **28**, 429–440 (2015).
7. Liu, C. *et al.* Mosaic analysis with double markers reveals tumor cell of origin in glioma. *Cell* **146**, 209–221 (2011).
8. Louis, D. N. *et al.* The 2007 WHO classification of tumours of the central nervous system. *Acta Neuropathologica* **114**, 97–109 (2007).
9. Verhaak, R. G. W. *et al.* Integrated Genomic Analysis Identifies Clinically Relevant Subtypes of Glioblastoma Characterized by Abnormalities in PDGFRA, IDH1, EGFR, and NF1. *Cancer Cell* **17**, 98–110 (2010).
10. Maleszewska, M. & Kaminska, B. Is glioblastoma an epigenetic malignancy? *Cancers.* **5**, 1120–1139 (2013).
11. Louis, D. N., Holland, E. C. & Cairncross, J. G. Glioma classification: A molecular reappraisal. *Am. J. Pathol.* **159**, 779–786 (2001).
12. Ostrom, Q. T. *et al.* CBTRUS Statistical Report: Primary brain and other central nervous system tumors diagnosed in the United States in 2010–2014. *Neuro. Oncol.* **19**, v1-v88 (2017). doi:10.1093/neuonc/nox158
13. Hanif, F., Muzaffar, K., Perveen, K., Malhi, A. M. & Simjee, S. U. Glioblatoma

Multiforme: A Review of its Epidemiology and Pathogenesis through Clinical Presentation and Treatment. *Asian Pacific J. Cancer Prev.* **18**, 3-9 (2017).

14. Kleihues P, C. W. K. Pathology and Genetics. Tumours of the Nervous System. IARC Press: Lyon. **314** (2000).
15. Preusser, M. *et al.* Current concepts and management of glioblastoma. *Ann. Neurol.* **70**, 9–21 (2011).
16. Iacob, G. & Dinca, E. B. Current data and strategy in glioblastoma multiforme. *J. Med. Life* **2**, 386–93 (2009).
17. Zorzan, M., Giordan, E., Redaelli, M., Caretta, A. & Mucignat-Caretta, C. Molecular targets in glioblastoma. *Futur. Oncol.* **11**, 1407–1420 (2015).
18. Nørøxe, D. S., Poulsen, H. S. & Lassen, U. Hallmarks of glioblastoma: a systematic review. *ESMO open* **1**, e000144 (2016).
19. Brennan, C. W. *et al.* The somatic genomic landscape of glioblastoma. *Cell* **155**, (2013).
20. Aldape, K. D. *et al.* Immunohistochemical Detection of EGFRvIII in High Malignancy Grade Astrocytomas and Evaluation of Prognostic Significance. *J. Neuropathol. Exp. Neurol.* **63**, 700–707 (2004).
21. Krivtsov, A. V. & Armstrong, S. A. MLL translocations, histone modifications and leukaemia stem-cell development. *Nat. Rev. Cancer* **7**, 823–833 (2007).
22. Varambally, S. *et al.* The polycomb group protein EZH2 is involved in progression of prostate cancer. *Nature* **419**, 624–629 (2002).
23. Xu, W. *et al.* Oncometabolite 2-hydroxyglutarate is a competitive inhibitor of α-ketoglutarate-dependent dioxygenases. *Cancer Cell* **19**, 17–30 (2011).
24. Killian, J. K. *et al.* Succinate dehydrogenase mutation underlies global epigenomic divergence in gastrointestinal stromal tumor. *Cancer Discov.* **3**, 648–657 (2013).
25. Noushmehr, H. *et al.* Identification of a CpG Island Methylator Phenotype that Defines a Distinct Subgroup of Glioma. *Cancer Cell* **17**, 510–522 (2010).
26. Parsons, D. W. *et al.* An integrated genomic analysis of human glioblastoma multiforme. *Sci. (New York, NY)* **321**, 1807–1812 (2008).
27. Bamford, S. *et al.* The COSMIC (Catalogue of Somatic Mutations in Cancer) database and website. *Br. J. Cancer* **91**, 355–358 (2004).

28. Ohgaki, H. & Kleihues, P. The definition of primary and secondary glioblastoma. *Clin. Cancer Res.* **19**, 764–772 (2013).

29. Furnari, F. B. *et al.* Malignant astrocytic glioma: Genetics, biology, and paths to treatment. *Genes and Development* **21**, 2683–2710 (2007).

30. JOVČEVSKA, I., KOČEVAR, N. & KOMEL, R. Glioma and glioblastoma - how much do we (not) know? *Mol. Clin. Oncol.* **1**, 935–941 (2013).

31. Stupp, R. *et al.* Radiotherapy plus Concomitant\nand Adjuvant Temozolomide for Glioblastoma. *N. Engl. J. Med.* **352**, 987–96 (2005).

32. Adamson, C. *et al.* Glioblastoma multiforme: a review of where we have been and where we are going. *Expert Opin. Investig. Drugs* **18**, 1061–83 (2009).

33. Zhang, J., F.G. Stevens, M. & D. Bradshaw, T. Temozolomide: Mechanisms of Action, Repair and Resistance. *Curr. Mol. Pharmacol.* **5**, 102–114 (2012).

34. FUKAI, J. *et al.* Rapid regression of glioblastoma following carmustine wafer implantation: A case report. *Mol. Clin. Oncol.* **5**, 153–157 (2016).

35. Herrlinger, U. *et al.* Lomustine-temozolomide combination therapy versus standard temozolomide therapy in patients with newly diagnosed glioblastoma with methylated MGMT promoter (CeTeG/NOA–09): a randomised, open-label, phase 3 trial. *Lancet* **393**, 678-688 (2019).

36. Field, K. M. *et al.* Randomized phase 2 study of carboplatin and bevacizumab in recurrent glioblastoma. *Neuro. Oncol.* **11**, 1504-13 (2015).

37. Batchelor, T. T., Reardon, D. A., de Groot, J. F., Wick, W. & Weller, M. Antiangiogenic therapy for glioblastoma: current status and future prospects. *Clin. Cancer Res.* **20**, 5612–9 (2014).

38. Friedman, H. S. *et al.* Bevacizumab alone and in combination with irinotecan in recurrent glioblastoma. *J. Clin. Oncol.* **27**, 4733–4740 (2009).

39. Mehta, M., Wen, P., Nishikawa, R., Reardon, D. & Peters, K. Critical review of the addition of tumor treating fields (TTFields) to the existing standard of care for newly diagnosed glioblastoma patients. *Critical Reviews in Oncology/Hematology* **111**, 60–65 (2017).

40. Berens, M. E. & Giese, A. "…those left behind." Biology and oncology of invasive glioma cells. *Neoplasia* **1**, 208–19 (1999).

41. Mannino, M. & Chalmers, A. J. Radioresistance of glioma stem cells: Intrinsic characteristic or property of the 'microenvironment-stem cell unit'? *Molecular Oncology* **5**, 374–386 (2011).

42. Sheehan, J. P. *et al.* Improving the radiosensitivity of radioresistant and hypoxic glioblastoma. *Future Oncol.* **6**, 1591–1601 (2010).

43. Vries, H. E. de, Kuiper, J., Boer, A. G. de, Berkel, T. J. C. Van & Breimer, D. D. The Blood-Brain Barrier in Neuroinflammatory Diseases. *Pharmacol. Rev.* **49**, 143–156 (1997).

44. Tano, K., Shiota, S., Collier, J., Foote, R. S. & Mitra, S. Isolation and structural characterization of a cDNA clone encoding the human DNA repair protein for O6-alkylguanine. *Proc. Natl. Acad. Sci. U. S. A.* **87**, 686–690 (1990).

45. Green, D. R. Means to an End : Apoptosis and Other Cell Death Mechanisms. *Chicago Journals*.Cold Spring Harbor Laboratory Press (2010).

46. Wyllie, A. H., Kerr, J. F. R. & Currie, A. R. Cell Death: The Significance of Apoptosis. *Int. Rev. Cytol.* **68**, 251–306 (1980).

47. Fesik, S. W. Promoting apoptosis as a strategy for cancer drug discovery. *Nat. Rev. Cancer* **5**, 876–885 (2005).

48. Shi, Y. Caspase activation, inhibition, and reactivation: A mechanistic view. *Protein Sci.* **13**, 1979–1987 (2004).

49. Saelens, X. *et al.* Toxic proteins released from mitochondria in cell death. *Oncogene* **23**, 2861–2874 (2004).

50. Henry-Mowatt, J., Dive, C., Martinou, J. C. & James, D. Role of mitochondrial membrane permeabilization in apoptosis and cancer. *Oncogene* **23**, 2850-60 (2004).

51. Zou, H., Li, Y., Liu, X. & Wang, X. An APAf-1 · cytochrome C multimeric complex is a functional apoptosome that activates procaspase-9. *J. Biol. Chem.* **274**, 11549-56 (1999).

52. Breckenridge, D. G. & Xue, D. Regulation of mitochondrial membrane permeabilization by BCL-2 family proteins and caspases. *Current Opinion in Cell Biology* **16**, 647–652 (2004).

53. Martinou, J. C. & Green, D. R. Breaking the mitochondrial barrier. *Nat. Rev. Mol.*

Cell Biol. **2**, 63-7 (2001). doi:10.1038/35048069

54. Willis, S. N. & Adams, J. M. Life in the balance: How BH3-only proteins induce apoptosis. *Current Opinion in Cell Biology* **17**, 617–625 (2005).

55. Edlich, F. *et al.* Bcl-xL retrotranslocates Bax from the mitochondria into the cytosol. *Cell* **145**, 104-16 (2011).

56. Yee, K. S. & Vousden, K. H. Complicating the complexity of p53. *Carcinogenesis* **26**, 1317-22 (2005). doi:10.1093/carcin/bgi122

57. Wiley, S. R. *et al.* Identification and characterization of a new member of the TNF family that induces apoptosis. *Immunity* **3**, 673–82 (1995).

58. Johnstone, R. W., Frew, A. J. & Smyth, M. J. The TRAIL apoptotic pathway in cancer onset, progression and therapy. *Nat. Rev. Cancer* **8**, 782–798 (2008).

59. Debatin, K. M. & Krammer, P. H. Death receptors in chemotherapy and cancer. *Oncogene* **23**, 2950-66 (2004).

60. Falschlehner, C., Emmerich, C. H., Gerlach, B. & Walczak, H. TRAIL signalling: Decisions between life and death. *International Journal of Biochemistry and Cell Biology* **39**, 1462–1475 (2007).

61. Mérino, D. *et al.* Differential inhibition of TRAIL-mediated DR5-DISC formation by decoy receptors 1 and 2. *Mol. Cell. Biol.* **26**, 7046–55 (2006).

62. Ashkenazi, A. Directing cancer cells to self-destruct with pro-apoptotic receptor agonists. *Nat. Rev. Drug Discov.* **7**, 1001–1012 (2008).

63. Wang, X. *et al.* Akt-mediated eminent expression of c-FLIP and Mcl-1 confers acquired resistance to TRAIL-induced cytotoxicity to lung cancer cells. *Mol Cancer Ther* **7**, 1156–1163 (2008).

64. Li, H., Zhu, H., Xu, C. & Yuan, J. Cleavage of BID by Caspase 8 Mediates the Mitochondrial Damage in the Fas Pathway of Apoptosis. *Cell* **94**, 491–501 (1998).

65. Luo, X., Budihardjo, I., Zou, H., Slaughter, C. & Wang, X. Bid, a Bcl2 interacting protein, mediates cytochrome c release from mitochondria in response to activation of cell surface death receptors. *Cell* **94**, 481–490 (1998).

66. Du, C., Fang, M., Li, Y., Li, L. & Wang, X. Smac, a Mitochondrial Protein that Promotes Cytochrome c–Dependent Caspase Activation by Eliminating IAP Inhibition. *Cell* **102**, 33–42 (2000).

67. Barnhart, B. C., Alappat, E. C. & Peter, M. E. The CD95 Type I/Type II model. *Semin. Immunol.* **15**, 185-93 (2003).

68. Ozören, N. & El-Deiry, W. S. Defining characteristics of Types I and II apoptotic cells in response to TRAIL. *Neoplasia* **4**, 551–7 (2002).

69. Ashkenazi, A. *et al.* Safety and antitumor activity of recombinant soluble Apo2 ligand. *J. Clin. Invest.* **104**, 155–162 (1999).

70. Lim, B. *et al.* Targeting TRAIL in the treatment of cancer: new developments. *Expert Opin. Ther. Targets* **19**, 1171–1185 (2015).

71. Refaat, A., Abd-rabou, A. & Reda, A. TRAIL combinations: The new 'TRAIL' for cancer therapy (review). *Oncol. Lett.* **7**, 1327–1332 (2014).

72. Clancy, L. *et al.* Preligand assembly domain-mediated ligand-independent association between TRAIL receptor 4 (TR4) and TR2 regulates TRAIL-induced apoptosis. *Proc. Natl. Acad. Sci. U. S. A.* **102**, 18099–18104 (2005).

73. Kuijlen, J. M. A. *et al.* TRAIL-receptor expression is an independent prognostic factor for survival in patients with a primary glioblastoma multiforme. *J. Neurooncol.* **78**, 161-71 (2006).

74. Nagane, M., Shimizu, S., Mori, E., Kataoka, S. & Shiokawa, Y. Predominant antitumor effects by fully human anti-TRAIL-receptor 2 (DR5) monoclonal antibodies in human glioma cells in vitro and in vivo. *Neuro. Oncol.* **12**, 687–700 (2010).

75. Kuijlen, J. M. a *et al.* TRAIL-receptor expression is an independent prognostic factor for survival in patients with a primary glioblastoma multiforme. *J. Neurooncol.* **78**, 161–171 (2006).

76. Fernald, K. & Kurokawa, M. Evading apoptosis in cancer. *Trends in Cell Biology* **23**, 620-33 (2013).

77. Trivedi, R. & Mishra, D. P. TRAILing TRAIL Resistance: Novel Targets for TRAIL Sensitization in Cancer Cells. *Front. Oncol.* **5**, (2015).

78. Braeuer, S. J., Büneker, C., Mohr, A. & Zwacka, R. M. Constitutively activated nuclear factor-kappaB, but not induced NF-kappaB, leads to TRAIL resistance by up-regulation of X-linked inhibitor of apoptosis protein in human cancer cells. *Mol. Cancer Res.* **4**, 715–28 (2006).

79. Hetschko, H. *et al.* Pharmacological inhibition of Bcl-2 family members reactivates TRAIL-induced apoptosis in malignant glioma. *J. Neurooncol.* **86**, 265–272 (2008).

80. Opel, D. *et al.* Phosphatidylinositol 3-kinase inhibition broadly sensitizes glioblastoma cells to death receptor- and drug-induced apoptosis. *Cancer Res.* **68**, 6271–6280 (2008).

81. Roué, G. *et al.* Selective inhibition of IkappaB kinase sensitizes mantle cell lymphoma B cells to TRAIL by decreasing cellular FLIP level. *J. Immunol.* **178**, 1923–30 (2007).

82. Wang, P. *et al.* Inhibition of RIP and c-FLIP enhances TRAIL-induced apoptosis in pancreatic cancer cells. *Cell. Signal.* **19**, 2237–2246 (2007).

83. Nagane, M., Cavenee, W. K. & Shiokawa, Y. Synergistic cytotoxicity through the activation of multiple apoptosis pathways in human glioma cells induced by combined treatment with ionizing radiation and tumor necrosis factor-related apoptosis-inducing ligand. *J. Neurosurg.* **106**, 407–16 (2007).

84. Zou, W. *et al.* c-Jun NH2-terminal kinase-mediated up-regulation of death receptor 5 contributes to induction of apoptosis by the novel synthetic triterpenoid methyl-2-cyano-3,12-dioxooleana-1, 9-dien-28-oate in human lung cancer cells. *Cancer Res.* **64**, 7570-8 (2004).

85. Johnson, T. R. *et al.* The proteasome inhibitor PS-341 overcomes TRAIL resistance in Bax and caspase 9-negative or Bcl-xL overexpressing cells. *Oncogene* **22**, 4953-63 (2003). doi:10.1038/sj.onc.1206656

86. He, Q., Huang, Y. & Sheikh, M. S. Proteasome inhibitor MG132 upregulates death receptor 5 and cooperates with Apo2L/TRAIL to induce apoptosis in Bax-proficient and -deficient cells. *Oncogene* **23**, 2554-8 (2004).

87. Conticello, C. *et al.* Antitumor Activity of Bortezomib Alone and in Combination with TRAIL in Human Acute Myeloid Leukemia. *Acta Haematol.* **120**, 19-30 (2008).

88. Baritaki, S. *et al.* Inhibition of Yin Yang 1-Dependent Repressor Activity of DR5 Transcription and Expression by the Novel Proteasome Inhibitor NPI-0052 Contributes to its TRAIL-Enhanced Apoptosis in Cancer Cells. *J. Immunol.* **180**, 6199-210 (2008).

89. Kannappan, R. *et al.* Gamma-tocotrienol promotes TRAIL-induced apoptosis through reactive oxygen species/extracellular signal-regulated kinase/p53-mediated upregulation of death receptors. *Mol. Cancer Ther.* **9**, 2196–207 (2010).

90. Park, E. J., Choi, K. S., Yoo, Y. H. & Kwon, T. K. Nutlin-3, a small-molecule MDM2 inhibitor, sensitizes Caki cells to TRAIL-induced apoptosis through p53-mediated PUMA upregulation and ROS-mediated DR5 upregulation. *Anticancer. Drugs* **24**, 260–9 (2013).

91. Morimoto, R., Kline, M., Bimston, D. & Cotto, J. The heat-shock response: regulation and function of heat-shock proteins and molecular chaperones. *Essays Biochem* **32**, 17-29 (1997).

92. Panner, A., Murray, J. C., Berger, M. S. & Pieper, R. O. Heat shock protein 90α recruits FLIPS to the death-inducing signaling complex and contributes to TRAIL resistance in human glioma. *Cancer Res.* **67**, 9482–9 (2007).

93. Lu, X., Xiao, L., Wang, L. & Ruden, D. M. Hsp90 inhibitors and drug resistance in cancer: The potential benefits of combination therapies of Hsp90 inhibitors and other anti-cancer drugs. *Biochemical Pharmacology* **83**, 995-1004 (2012).

94. Williams, C. R., Tabios, R., Linehan, W. M. & Neckers, L. Intratumor Injection of the Hsp90 Inhibitor 17AAG Decreases Tumor Growth and Induces Apoptosis in a Prostate Cancer Xenograft Model. *J. Urol.* **178**, 1528-32 (2007).

95. Holliday, R. The inheritance of epigenetic defects. *Science* **238**, 163-70 (1987).

96. Saha, A., Wittmeyer, J. & Cairns, B. R. Chromatin remodelling: the industrial revolution of DNA around histones. *Nat. Rev. Mol. Cell Biol.* **7**, 437–447 (2006).

97. Cosgrove, M. S., Boeke, J. D. & Wolberger, C. Regulated nucleosome mobility and the histone code. *Nature Structural and Molecular Biology* **11**, 1037-43 (2004).

98. Khorasanizadeh, S. The Nucleosome: From Genomic Organization to Genomic Regulation. *Cell* **116**, 259-72 (2004).

99. Strahl, B. D. & Allis, C. D. The language of covalent histone modifications. *Nature* **403**, 41–45 (2000).

100. Yun, M., Wu, J., Workman, J. L. & Li, B. Readers of histone modifications. *Cell Research* **21**, 564-78 (2011).

101. Fan, H. Y., He, X., Kingston, R. E. & Narlikar, G. J. Distinct strategies to make nucleosomal DNA accessible. *Mol. Cell* **11**, 1311-22 (2003).

102. Fazzio, T. G. & Tsukiyama, T. Chromatin remodeling in vivo: Evidence for a nucleosome sliding mechanism. *Mol. Cell* **12**, 1333-40 (2003).

103. Kassabov, S. R., Zhang, B., Persinger, J. & Bartholomew, B. SWI/SNF unwraps, slides, and rewraps the nucleosome. *Mol. Cell* **11**, 391-403 (2003).

104. Mizuguchi, G. *et al.* ATP-Driven Exchange of Histone H2AZ Variant Catalyzed by SWR1 Chromatin Remodeling Complex. *Science* **303**, 343-8 (2004).

105. Ahmad, K. & Henikoff, S. The histone variant H3.3 marks active chromatin by replication-independent nucleosome assembly. *Mol. Cell* **9**, 1191-200 (2002).

106. Suto, R. K., Clarkson, M. J., Tremethick, D. J. & Luger, K. Crystal structure of a nucleosome core particle containing the variant histone H2A.Z. *Nat. Struct. Biol.* **7**, 1121-4 (2000).

107. Bolden, J. E., Peart, M. J. & Johnstone, R. W. Anticancer activities of histone deacetylase inhibitors. *Nat. Rev. Drug Discov.* **5**, 769–784 (2006).

108. Esteller, M. Epigenetics in cancer. - main article. *N. Engl. J. Med.* **358**, 1148–1159 (2008).

109. Fatemi, M. *et al.* Footprinting of mammalian promoters: Use of a CpG DNA methyltransferase revealing nucleosome positions at a single molecule level. *Nucleic Acids Res.* **33**, (2005).

110. Hermann, A., Goyal, R. & Jeltsch, A. The Dnmt1 DNA-(cytosine-C5)-methyltransferase methylates DNA processively with high preference for hemimethylated target sites. *J. Biol. Chem.* **279**, 48350-9 (2004).

111. Okano, M., Bell, D. W., Haber, D. A. & Li, E. DNA methyltransferases Dnmt3a and Dnmt3b are essential for de novo methylation and mammalian development. *Cell* **99**, 247-57 (1999).

112. Hajji, N. & Joseph, B. Epigenetic regulation of cell life and death decisions and deregulation in cancer. *Essays Biochem.* **48**, 121-46 (2010).

113. Roll, J. D., Rivenbark, A. G., Jones, W. D. & Coleman, W. B. DNMT3b overexpression contributes to a hypermethylator phenotype in human breast cancer cell lines. *Mol. Cancer* **7**, 15 (2008).

114. Turcan, S. *et al.* IDH1 mutation is sufficient to establish the glioma hypermethylator phenotype. *Nature* **483**, 479-83 (2012).

115. Letouzé, E. *et al.* SDH Mutations Establish a Hypermethylator Phenotype in Paraganglioma. *Cancer Cell* **23**, 739-52 (2013).

116. Yamazaki, J. *et al.* TET2 mutations affect Non-CpG island DNA methylation at enhancers and transcription factor-binding sites in chronic myelomonocytic Leukemia. *Cancer Res.* **75**, 2833-43 (2015).

117. Baylin, S. B. & Jones, P. A. A decade of exploring the cancer epigenome biological and translational implications. *Nat. Rev. Cancer* **11**, 726–734 (2011).

118. Wu, J. & Wood, G. S. Reduction of Fas/CD95 promoter methylation, upregulation of fas protein, and enhancement of sensitivity to apoptosis in cutaneous T-Cell lymphoma. *Arch. Dermatol.* 147, 443-9 (2011).

119. Petak, I. *et al.* Hypermethylation of the gene promoter and enhancer region can regulate Fas expression and sensitivity in colon carcinoma. *Cell Death Differ.* 10, 211-7 (2003).

120. Van Noesel, M. M. *et al.* Clustering of hypermethylated genes in neuroblastoma. *Genes Chromosom. Cancer* **38**, 226-33 (2003).

121. Bae, S. I., Cheriyath, V., Jacobs, B. S., Reu, F. J. & Borden, E. C. Reversal of methylation silencing of Apo2L/TRAIL receptor 1 (DR4) expression overcomes resistance of SK-MEL-3 and SK-MEL-28 melanoma cells to interferons (IFNs) or Apo2L/TRAIL. *Oncogene* **27**, 490-8 (2008).

122. Horak, P. Contribution of Epigenetic Silencing of Tumor Necrosis Factor-Related Apoptosis Inducing Ligand Receptor 1 (DR4) to TRAIL Resistance and Ovarian Cancer. *Mol. Cancer Res.* **3**, 335-43 (2005).

123. Cho, S. *et al.* Epigenetic methylation and expression of caspase 8 and survivin in hepatocellular carcinoma. *Pathol. Int.* **60**, 203-11 (2010).

124. Malekzadeh, K. *et al.* Methylation patterns of Rb1 and Casp-8 promoters and their impact on their expression in bladder cancer. *Cancer Invest.* **27**, 70-80 (2009).

125. Shivapurkar, N. *et al.* Differential inactivation of caspase-8 in lung cancers. *Cancer Biol. Ther.* **1**, 65-9 (2002).

126. Hervouet, E., Vallette, F. M. & Cartron, P. F. Impact of the DNA

methyltransferases expression on the methylation status of apoptosis-associated genes in glioblastoma multiforme. *Cell Death Dis.* **1**, e8 (2010).

127. Harada, K. *et al.* Deregulation of caspase 8 and 10 expression in pediatric tumors and cell lines. *Cancer Res.* **62**, 5897-901 (2002).

128. San José-Eneriz, E. *et al.* Epigenetic down-regulation of BIM expression is associated with reduced optimal responses to imatinib treatment in chronic myeloid leukaemia. *Eur. J. Cancer* **45**, 1877-89 (2009).

129. Furukawa, Y. Methylation Silencing of the Apaf-1 Gene in Acute Leukemia. *Mol. Cancer Res.* **3**, 325-34 (2005).

130. Soengas, M. S. *et al.* Inactivation of the apoptosis effector Apaf-1 in malignant melanoma. *Nature* **409**, 207-11 (2001).

131. Wang, H. L., Bai, H., Li, Y., Sun, J. & Wang, X. Q. Rationales for expression and altered expression of apoptotic protease activating factor-1 gene in gastric cancer. *World J. Gastroenterol.* **13**, 5060–5064 (2007).

132. Christoph, F. *et al.* Methylation of tumour suppressor genes APAF-1 and DAPK-1 and in vitro effects of demethylating agents in bladder and kidney cancer. *Br. J. Cancer* **95**, 1701–1707 (2006).

133. Byun, D. S. *et al.* Hypermethylation of XIAP-associated Factor 1, a Putative Tumor Suppressor Gene from the 17p13.2 Locus, in Human Gastric Adenocarcinomas. *Cancer Res.* **63**, 7068-75. (2003).

134. Shui, P. T. *et al.* Restoration of XAF1 expression induces apoptosis and inhibits tumor growth in gastric cancer. *Int. J. Cancer* **125**, 688-97 (2009).

135. Kempkensteffen, C. *et al.* Gene expression and promoter methylation of the XIAP-associated Factor 1 in renal cell carcinomas: Correlations with pathology and outcome. *Cancer Lett.* **254**, 227-35 (2007).

136. Wang, Y. *et al.* Survey of Differentially Methylated Promoters in Prostate Cancer Cell Lines. *Neoplasia* **7**, 748-60 (2005).

137. Pompeia, C. *et al.* Microarray analysis of epigenetic silencing of gene expression in the KAS-6/1 multiple myeloma cell line. *Cancer Res.* **64**, 3465-73 (2004). doi:10.1158/0008-5472.CAN-03-3970

138. Garrison, S. P. *et al.* Selection against PUMA Gene Expression in Myc-Driven B-

Cell Lymphomagenesis. *Mol. Cell. Biol.* **28**, 5391-402 (2008).

139. Xu, J. Da *et al.* BCL2L10 protein regulates apoptosis/proliferation through differential pathways in gastric cancer cells. *J. Pathol.* **223**, 400-9. (2011).

140. Fabiani, E. *et al.* Analysis of genome-wide methylation and gene expression induced by 5-aza-2′-deoxycytidine identifies BCL2L10 as a frequent methylation target in acute myeloid leukemia. *Leuk. Lymphoma* **51**, 2275-84 (2010).

141. Kim, T. Y., Zhong, S., Fields, C. R., Kim, J. H. & Robertson, K. D. Epigenomic profiling reveals novel and frequent targets of aberrant DNA methylation-mediated silencing in malignant glioma. *Cancer Res.* **66**, 7490-501 (2006).

142. Sturm, I. *et al.* Loss of the tissue-specific proapoptotic BH3-only protein Nbk/Bik is a unifying feature of renal cell carcinoma. *Cell Death Differ.* **13**, 619-27 (2006).

143. Murphy, T. M. *et al.* In silico analysis and DHPLC screening strategy identifies novel apoptotic gene targets of aberrant promoter hypermethylation in prostate cancer. *Prostate* **71**, 1-17 (2011).

144. Hatzimichael, E. *et al.* Bcl2-interacting killer CpG methylation in multiple myeloma: A potential predictor of relapsed/refractory disease with therapeutic implications. *Leuk. Lymphoma* **53**, 1709-13 (2012).

145. Sugita, H. *et al.* Methylation of BNIP3 and DAPK indicates lower response to chemotherapy and poor prognosis in gastric cancer. *Oncol. Rep.* **25**, 513-8 (2011).

146. Hiraki, M. *et al.* CpG island methylation of BNIP3 predicts resistance against S-1/CPT-11 combined therapy in colorectal cancer patients. *Oncol. Rep.* **23**, 191-7 (2010).

147. Pike, B. L. *et al.* DNA methylation profiles in diffuse large B-cell lymphoma and their relationship to gene expression status. *Leukemia* **22**, 1035-4 (2008).

148. Calvisi, D. F. *et al.* Mechanistic and prognostic significance of aberrant methylation in the molecular pathogenesis of human hepatocellular carcinoma. *J. Clin. Invest.* **117**, 2713-22 (2007).

149. Obata, T. *et al.* Identification of HRK as a Target of Epigenetic Inactivation in Colorectal and Gastric Cancer. *Clin. Cancer Res.* **9**, 6410-8 (2003).

150. Nakamura, M. *et al.* Frequent HRK inactivation associated with low apoptotic index in secondary glioblastomas. *Acta Neuropathol.* **110**, 402-10 (2005).

151. Nakamura, M. *et al.* Defective expression of HRK is associated with promoter methylation in primary central nervous system lymphomas. *Oncology* **70**, 212-21 (2006).

152. Higuchi, T. *et al.* HRK inactivation associated with promoter methylation and LOH in prostate cancer. *Prostate* **68**, 105-13 (2008).

153. Esteller, M. Cancer epigenomics: DNA methylomes and histone-modification maps. *Nat. Rev. Genet.* **8**, 286–298 (2007).

154. Esteller, M. *et al.* Inactivation of the DNA-Repair Gene *MGMT* and the Clinical Response of Gliomas to Alkylating Agents. *N. Engl. J. Med.* **343**, 1350–1354 (2000).

155. Mittag, F. *et al.* DAPK promotor methylation is an early event in colorectal carcinogenesis. *Cancer Lett.* **240**, 69-75 (2006).

156. Toyooka, S. *et al.* Epigenetic down-regulation of death-associated protein kinase in lung cancers. *Clin. Cancer Res.* **9**, 3034-41 (2003).

157. Kissil, J. L. *et al.* DAP-kinase loss of expression in various carcinoma and B-cell lymphoma cell lines: Possible implications for role as tumor suppressor gene. *Oncogene* **15**, 403-7 (1997).

158. Fujii, H. *et al.* Methylation of the HIC-1 candidate tumor suppressor gene in human breast cancer. *Oncogene* **16**, 2159-64 (1998).

159. Waha, A. *et al.* Epigenetic Silencing of the HIC-1 Gene in Human Medulloblastomas. *J. Neuropathol. Exp. Neurol.* **62**, 1192-201 (2003).

160. Agirre, X. *et al.* TP53 Is Frequently Altered by Methylation, Mutation, and/or Deletion in Acute Lymphoblastic Leukaemia. *Mol. Carcinog.* **38**, 201-8. (2003).

161. Juhlin, C. C. *et al.* Frequent promoter hypermethylation of the APC and RASSF1A tumour suppressors in parathyroid tumours. *PLoS One* **5**, e9472 (2010).

162. Wang, T. *et al.* Methylation associated inactivation of RASSF1A and its synergistic effect with activated K-Ras in nasopharyngeal carcinoma. *J. Exp. Clin. Cancer Res.* **28**, 160 (2009).

163. Niklinska, W. *et al.* Prognostic significance of DAPK and RASSF1A promoter hypermethylation in Non-Small Cell Lung Cancer (NSCLC). *Folia Histochemica et Cytobiologica* **47**, 275-80 (2009).

164. S., Honda *et al.* The methylation status of RASSF1A promoter predicts responsiveness to chemotherapy and eventual cure in hepatoblastoma patients. *Int. J. Cancer* **123**, 1117-25 (2008).

165. Cooper, D. N. & Youssoufian, H. The CpG dinucleotide and human genetic disease. *Hum. Genet.* **78**, 151-5 (1988).

166. Rideout, W. M., Coetzee, G. A., Olumi, A. F. & Jones, P. A. 5-Methylcytosine as an endogenous mutagen in the human LDL receptor and p53 genes. *Science* **249**, 1288-90 (1990).

167. Denissenko, M. F., Chen, J. X., Tang, M. -s. & Pfeifer, G. P. Cytosine methylation determines hot spots of DNA damage in the human P53 gene. *Proc. Natl. Acad. Sci.* **94**, 3893–3898 (1997).

168. Martinez-Fernandez, L., Banyasz, A., Esposito, L., Markovitsi, D. & Improta, R. UV-induced damage to DNA: effect of cytosine methylation on pyrimidine dimerization. *Signal Transduct. Target. Ther.* **2**, 17021. (2017).

169. Feinberg, A. P. & Vogelstein, B. Hypomethylation distinguishes genes of some human cancers from their normal counterparts. *Nature* **301**, 89–9 (1983).

170. Gama-sosa, M. A. *et al.* The 5-methylcytosin content of DNA from human tumors. *Nucleic Acids Res.* **11**, 6883–6894 (1983).

171. Bedford, M. T. & van Helden, P. D. Hypomethylation of dna in pathological conditions of the human prostate. *Cancer Res.* **47**, 5274-6 (1987).

172. Wahlfors, J. *et al.* Genomic hypomethylation in human chronic lymphocytic leukemia. *Blood* **80**, 2074-80. (1992).

173. Lin, C. H. *et al.* Genome-wide hypomethylation in hepatocellular carcinogenesis. *Cancer Res.* **61**, 4238-43 (2001).

174. Kim, Y. -I *et al.* Global DNA hypomethylation increases progressively in cervical dysplasia and carcinoma. *Cancer* **74**, 893-9 (1994).

175. Gaudet, F. Induction of Tumors in Mice by Genomic Hypomethylation. *Science (80-.).* **300**, 489–492 (2003).

176. Dante, R., Dante-Paire, J., Rigal, D. & Roizes, G. Methylation patterns of long interspersed repeated DNA and alphoid repetitive DNA from human cell lines and tumors. *Anticancer Res.* **12**, 559-63 (1992).

177. B., J., BJ., S.-D. & WA., S. Hypomethylation of L1 LINE sequences prevailing in human urothelial carcinoma. *Cancer Res.* **56**, 5698-703 (1996).

178. Takai, D. Hypomethylation of LINE1 Retrotransposon in Human Hepatocellular Carcinomas, but Not in Surrounding Liver Cirrhosis. *Jpn. J. Clin. Oncol.* **30**, 306-9 (2000).

179. Santourlidis, S., Florl, A., Ackermann, R., Wirtz, H. C. & Schulz, W. A. High frequency of alterations in DNA methylation in adenocarcinoma of the prostate. *Prostate* **39**, 166-74 (1999).

180. Ehrlich, M. DNA methylation in cancer: Too much, but also too little. *Oncogene* **21**, 5400-13 (2002).

181. Martin, V. *et al.* Involvement of DNA methylation in the control of the expression of an estrogen-induced breast-cancer-associated protein (pS2) in human breast cancers. *J. Cell. Biochem.* **65**, 95-106 (1997).

182. Watt, P. M., Kumar, R. & Kees, U. R. Promoter demethylation accompanies reactivation of the HOX11 proto-oncogene in leukemia. *Genes Chromosom. Cancer* **29**, 371-7 (2000).

183. Sharrard, R. M., Royds, J. A., Rogers, S. & Shorthouse, A. J. Patterns of methylation of the c-myc gene in human colorectal cancer progression. *Br. J. Cancer* **65**, 667–672 (1992)

184. Shen, L. *et al.* Correlation between DNA methylation and pathological changes in human hepatocellular carcinoma. *Hepatogastroenterology.* **45**, 1753-9 (1998).

185. Rose, N. R. & Klose, R. J. Understanding the relationship between DNA methylation and histone lysine methylation. *Biochimica et Biophysica Acta - Gene Regulatory Mechanisms* **1839**, 1362-72 (2014).

186. Fuks, F. *et al.* The methyl-CpG-binding protein MeCP2 links DNA methylation to histone methylation. *J. Biol. Chem.* **278**, 4035-40 (2003).

187. Okitsu, C. Y. & Hsieh, C.-L. DNA Methylation Dictates Histone H3K4 Methylation. *Mol. Cell. Biol.* **27**, 2746-57 (2007). doi:10.1128/mcb.02291-06

188. Nan, X. *et al.* Transcriptional repression by the methyl-CpG-binding protein MeCP2 involves a histone deacetylase complex. *Nature* **393**, 386-9 (1998).

189. Feldman, N. *et al.* G9a-mediated irreversible epigenetic inactivation of Oct-3/4

during early embryogenesis. *Nat. Cell Biol.* **8**, 188-94 (2006).

190. Fraga, M. F. *et al.* Loss of acetylation at Lys16 and trimethylation at Lys20 of histone H4 is a common hallmark of human cancer. *Nat. Genet.* **37**, 391-400 (2005).

191. Th'ng, J. P. Histone modifications and apoptosis: Cause or consequence? *Biochem. Cell Biol.* **79**, 305-311 (2011).

192. Trivedi, R. & Mishra, D. P. TRAILing TRAIL Resistance: Novel Targets for TRAIL Sensitization in Cancer Cells. *Front. Oncol.* **5**, (2015).

193. Lu, Y., Chu, A., Wajapeyee, N., Turker, M. S. & Glazer, P. M. Abstract 2887: Epigenetic silencing of the DNA repair genes, BRCA1 and MLH1, induced by hypoxic stress in a pathway dependent on the histone demethylase, LSD1. *Cancer Res.* **8**, 501–513 (2014).

194. Lu, J. *et al.* The transcription factor ZBP-89 suppresses p16 expression through a histone modification mechanism to affect cell senescence. *FEBS J.* **276**, 4197-206 (2009).

195. Yang, X. *et al.* CDKN1C (p57KIP2) is a direct target of EZH2 and suppressed by multiple epigenetic mechanisms in breast cancer cells. *PLoS One* **4**, e5011 (2009).

196. Richon, V. M., Sandhoff, T. W., Rifkind, R. A. & Marks, P. A. Histone deacetylase inhibitor selectively induces p21WAF1 expression and gene-associated histone acetylation. *Proc. Natl. Acad. Sci.* **97**, 10014-10019 (2000).

197. Stucki, M. Histone H2A.X Tyr142 phosphorylation: A novel sWItCH for apoptosis? *DNA Repair* **8**, 873-6 (2009).

198. Stucki, M. *et al.* MDC1 directly binds phosphorylated histone H2AX to regulate cellular responses to DNA double-strand breaks. *Cell* **123**, 1213-26 (2005).

199. Cheung, W. L. *et al.* Apoptotic phosphorylation of histone H2B is mediated by mammalian sterile twenty kinase. *Cell* **113**, 507-17 (2003).

200. Ajiro, K., Scoltock, A. B., Smith, L. K., Ashasima, M. & Cidlowski, J. A. Reciprocal epigenetic modification of histone H2B occurs in chromatin during apoptosis in vitro and in vivo. *Cell Death Differ.* **17**, 984–993 (2010).

201. Wong, C. H. *et al.* Apoptotic histone modification inhibits nuclear transport by regulating RCC1. *Nat. Cell Biol.* **11**, 36-45 (2009).

202. Hurd, P. J. *et al.* Phosporylation of histone H3 Thr-45 is linked to apoptosis. *J. Biol. Chem.* **284**, 16575-83 (2009). doi:10.1074/jbc.M109.005421

203. Aguilera, D. G. *et al.* Reactivation of death receptor 4 (DR4) expression sensitizes medulloblastoma cell lines to TRAIL. *J. Neurooncol.* **93**, 303–318 (2009).

204. Myzak, M. C., Dashwood, W. M., Orner, G. A., Ho, E. & Dashwood, R. H. Sulforaphane inhibits histone deacetylase in vivo and suppresses tumorigenesis in Apc min mice. *FASEB J.* **20**, 506-8 (2006).

205. Paschos, K. *et al.* Epstein-Barr virus latency in B cells leads to epigenetic repression and CpG methylation of the tumour suppressor gene Bim. *PLoS Pathog.* **5**, e1000492 (2009).

206. Glozak, M. A., Sengupta, N., Zhang, X. & Seto, E. Acetylation and deacetylation of non-histone proteins. *Gene* **363**, 15-23 (2005).

207. Ianari, A., Gallo, R., Palma, M., Alesse, E. & Gulino, A. Specific role for p300/CREB-binding protein-associated factor activity in E2F1 stabilization in response to DNA damage. *J. Biol. Chem.* **279**, 30830-5 (2004).

208. Cohen, H. Y. *et al.* Acetylation of the C terminus of Ku70 by CBP and PCAF controls Bax-mediated apoptosis. *Mol. Cell* **13**, 627-38 (2004).

209. Kim, K. *et al.* Gene dysregulation by histone variant H2A.Z in bladder cancer. *Epigenetics Chromatin* **6**, 34 (2013).

210. Yang, B. *et al.* H2A.Z regulates tumorigenesis, metastasis and sensitivity to cisplatin in intrahepatic cholangiocarcinoma. *Int. J. Oncol.* **52**, 1235-1245 (2018).

211. Friedman, R. C., Farh, K. K. H., Burge, C. B. & Bartel, D. P. Most mammalian mRNAs are conserved targets of microRNAs. *Genome Res.* **19**, 92–105 (2009).

212. Cimmino, A. *et al.* miR-15 and miR-16 induce apoptosis by targeting BCL2. *Proc. Natl. Acad. Sci.* **102**, 13944-9 (2005).

213. Bonci, D. *et al.* The miR-15a-miR-16-1 cluster controls prostate cancer by targeting multiple oncogenic activities. *Nat. Med.* **14**, 1271-7 (2008).

214. Bottoni, A. *et al.* miR-15a and miR-16-1 down-regulation in pituitary adenomas. *J. Cell. Physiol.* **204**, 280-5 (2005).

215. Sampath, D. *et al.* Histone deacetylases mediate the silencing of miR-15a, miR-16, and miR-29b in chronic lymphocytic leukemia. *Blood* **119**, 1162-72 (2012).

216. Zhang, X. *et al.* Myc represses miR-15a/miR-16-1 expression through recruitment of HDAC3 in mantle cell and other non-Hodgkin B-cell lymphomas. *Oncogene* **31**, 3002-3008 (2012).

217. Ji, Q. *et al.* Restoration of tumor suppressor miR-34 inhibits human p53-mutant gastric cancer tumorspheres. *BMC Cancer* **8**, 266 (2008).

218. Malumbres, M. MiRNAs and cancer: An epigenetics view. *Molecular Aspects of Medicine* **34**, 863-74 (2013).

219. Lodygin, D. *et al.* Inactivation of miR-34a by aberrant CpG methylation in multiple types of cancer. *Cell Cycle* **7**, 2591-600 (2008).

220. Garzon, R. *et al.* MicroRNA-29b induces global DNA hypomethylation and tumor suppressor gene reexpression in acute myeloid leukemia by targeting directly DNMT3A and 3B and indirectly DNMT1. *Blood* **113**, 6411-8 (2009).

221. Yanaihara, N. *et al.* Unique microRNA molecular profiles in lung cancer diagnosis and prognosis. *Cancer Cell* **9**, 189-98 (2006).

222. Wang, L. H. *et al.* Downregulation of miR-29b targets DNMT3b to suppress cellular apoptosis and enhance proliferation in pancreatic cancer. *Mol. Med. Rep.* **17**, 2113-2120 (2018).

223. Ratert, N. *et al.* Reference miRNAs for miRNAome analysis of urothelial carcinomas. *PLoS One* **7**, e39309 (2012).

224. Flavin, R. *et al.* MiR-29b expression is associated with disease-free survival in patients with ovarian serous carcinoma. *Int. J. Gynecol. Cancer* **19**, 641-7 (2009).

225. Cortez, M. A. *et al.* miR-29b and miR-125a regulate podoplanin and suppress invasion in glioblastoma. *Genes Chromosom. Cancer* **49**, 981-90 (2010).

226. Li, Y. *et al.* Epigenetic silencing of microRNA-193a contributes to leukemogenesis in t(8;21) acute myeloid leukemia by activating the PTEN/PI3K signal pathway. *Blood* **121**, 499-509 (2013).

227. Saito, Y. *et al.* Chromatin remodeling at Alu repeats by epigenetic treatment activates silenced microRNA-512-5p with downregulation of Mcl-1 in human gastric cancer cells. *Oncogene* **28**, 2738-44 (2009).

228. Ghasemi, A., Fallah, S. & Ansari, M. MIR-153 as a tumor suppressor in glioblastoma multiforme is downregulated by DNA methylation. *Clin. Lab.* **62**,

573-80 (2016).

229. Crawford, M. *et al.* MicroRNA 133B targets pro-survival molecules MCL-1 and BCL2L2 in lung cancer. *Biochem. Biophys. Res. Commun.* **388**, 483-9 (2009).

230. Chen, J., Wang, M., Guo, M., Xie, Y. & Cong, Y. S. miR-127 regulates cell proliferation and senescence by targeting BCL6. *PLoS One* **8**, e80266. (2013).

231. Saito, Y. *et al.* Specific activation of microRNA-127 with downregulation of the proto-oncogene BCL6 by chromatin-modifying drugs in human cancer cells. *Cancer Cell* **9**, 435-43 (2006).

232. Petrocca, F. *et al.* E2F1-Regulated MicroRNAs Impair TGFβ-Dependent Cell-Cycle Arrest and Apoptosis in Gastric Cancer. *Cancer Cell* **13**, 272-86 (2008).

233. Yang, H. *et al.* Histone deacetylase inhibitor SAHA epigenetically regulates miR-17-92 cluster and MCM7 to upregulate MICA expression in hepatoma. *Br. J. Cancer* **112**, 112-21 (2015).

234. Garofalo, M. *et al.* miR-221&222 Regulate TRAIL Resistance and Enhance Tumorigenicity through PTEN and TIMP3 Downregulation. *Cancer Cell* **16**, 498-509. (2009).

235. Zhang, C. Z. *et al.* MiR-221 and miR-222 target PUMA to induce cell survival in glioblastoma. *Mol. Cancer* **9**, 229 (2010).

236. Jin, X. *et al.* CASC2/miR-24/miR-221 modulates the TRAIL resistance of hepatocellular carcinoma cell through caspase-8/caspase-3. *Cell Death Dis.* **9**, 318 (2018).

237. Lu, Q. *et al.* MicroRNA-221 silencing predisposed human bladder cancer cells to undergo apoptosis induced by TRAIL. *Urol. Oncol. Semin. Orig. Investig.* **28**, 635-41 (2010).

238. Quintavalle, C. *et al.* MiR-221/222 overexpression in human glioblastoma increases invasiveness by targeting the protein phosphate PTP. *Oncogene* **31**, 858-68 (2012).

239. Zhao, Z. N. *et al.* TSA Suppresses miR-106b-93-25 Cluster Expression through Downregulation of MYC and Inhibits Proliferation and Induces Apoptosis in Human EMC. *PLoS One* **7**, e45133 (2012).

240. Hayashita, Y. *et al.* A polycistronic MicroRNA cluster, miR-17-92, is

overexpressed in human lung cancers and enhances cell proliferation. *Cancer Res.* **65**, 9628-32. (2005).

241. He, L. *et al.* A microRNA polycistron as a potential human oncogene. *Nature* **435**, 828-33 (2005).

242. Navarro, A. *et al.* Regulation of JAK2 by miR-135a: Prognostic impact in classic Hodgkin lymphoma. *Blood* **114**, 2945-51 (2009).

243. Wu, H. *et al.* MiR-135a targets JAK2 and inhibits gastric cancer cell proliferation. *Cancer Biol. Ther.* **13**, 281-8 (2012).

244. Xu, H. & Wen, Q. Downregulation of miR-135a predicts poor prognosis in acute myeloid leukemia and regulates leukemia progression via modulating HOXA10 expression. *Mol. Med. Rep.* **18**, 1134-1140 (2018).

245. Duan, S. *et al.* MicroRNA-135a-3p is downregulated and serves as a tumour suppressor in ovarian cancer by targeting CCR2. *Biomed. Pharmacother.* **107**, 712-720 (2018).

246. Nakano, H., Miyazawa, T., Kinoshita, K., Yamada, Y. & Yoshida, T. Functional screening identifies a microRNA, miR-491 that induces apoptosis by targeting Bcl-XLin colorectal cancer cells. *Int. J. Cancer* **127**, 1072-80 (2010).

247. Unoki, M. & Nakamura, Y. EGR2 induces apoptosis in various cancer cell lines by direct transactivation of BNIP3L and BAK. *Oncogene* **22**, 2172–2185 (2003).

248. Wu, Q. *et al.* MiR-150 promotes gastric cancer proliferation by negatively regulating the pro-apoptotic gene EGR2. *Biochem. Biophys. Res. Commun.* **392**, 340-5. (2010).

249. Beswick, E. J., Pinchuk, I. V., Suarez, G., Sierra, J. C. & Reyes, V. E. Helicobacter pylori CagA-Dependent Macrophage Migration Inhibitory Factor Produced by Gastric Epithelial Cells Binds to CD74 and Stimulates Procarcinogenic Events. *J. Immunol.* **176**, 6794-801 (2006).

250. Shen, Y., Gong, J.-M., Zhou, L.-L. & Sheng, J.-H. MiR-451 as a new tumor marker for gastric cancer. *Oncotarget* **8**, 56542–56545 (2017).

251. Pfeffer, S. *et al.* Identification of Virus-Encoded MicroRNAs. *Science* **304**, 734-6 (2004). doi:10.1126/science.1096781

252. Shah, K. M. & Young, L. S. Epstein-Barr virus and carcinogenesis: Beyond

Burkitt's lymphoma. *Clinical Microbiology and Infection* **15**, 982-8 (2009).

253. Choy, E. Y.-W. *et al.* An Epstein-Barr virus–encoded microRNA targets PUMA to promote host cell survival. *J. Exp. Med.* **205**, 2551-60 (2008).

254. Diaz-Meco, M. T. & Abu-Baker, S. The Par-4/PTEN connection in tumor suppression. *Cell Cycle* **8**, 2518-22. (2009).

255. Meng, F. *et al.* MicroRNA-21 Regulates Expression of the PTEN Tumor Suppressor Gene in Human Hepatocellular Cancer. *Gastroenterology* **133**, 647-58 (2007).

256. Tsukamoto, Y. *et al.* MicroRNA-375 is downregulated in gastric carcinomas and regulates cell survival by targeting PDK1 and 14-3-3ζ. *Cancer Res.* **70**, 2339-49 (2010).

257. Shen, H. M. & Tergaonkar, V. NFκB signaling in carcinogenesis and as a potential molecular target for cancer therapy. *Apoptosis* **14**, 348-63 (2009).

258. Thottassery, J. V. *et al.* Novel DNA methyltransferase-1 (DNMT1) depleting anticancer nucleosides, 4′-thio-2′-deoxycytidine and 5-aza-4′-thio-2′-deoxycytidine. *Cancer Chemother. Pharmacol.* **74**, 291-302 (2014).

259. Christman, J. K. 5-Azacytidine and 5-aza-2′-deoxycytidine as inhibitors of DNA methylation: Mechanistic studies and their implications for cancer therapy. *Oncogene* **21**, 5483–5495 (2002).

260. Fenaux, P. *et al.* Efficacy of azacitidine compared with that of conventional care regimens in the treatment of higher-risk myelodysplastic syndromes: a randomised, open-label, phase III study. *Lancet Oncol.* **10**, 223–232 (2009).

261. Lübbert, M. *et al.* Decitabine improves progression-free survival in older high-risk MDS patients with multiple autosomal monosomies: results of a subgroup analysis of the randomized phase III study 06011 of the EORTC Leukemia Cooperative Group and German MDS Study Group. *Ann. Hematol.* **95**, 191-9 (2016).

262. Issa, J. P. J. *et al.* Safety and tolerability of guadecitabine (SGI-110) in patients with myelodysplastic syndrome and acute myeloid leukaemia: A multicentre, randomised, dose-escalation phase 1 study. *Lancet Oncol.* **16**, 1099-1110 (2015).

263. Golub, D. *et al.* Mutant Isocitrate Dehydrogenase Inhibitors as Targeted Cancer Therapeutics. *Front. Oncol.* **9**, 417 (2019).

264. Duvic, M. *et al.* Phase 2 trial of oral vorinostat (suberoylanilide hydroxamic acid, SAHA) for refractory cutaneous T-cell lymphoma (CTCL). *Blood* **109**, 31-9 (2007).

265. Olsen, E. A. *et al.* Phase IIB multicenter trial of vorinostat in patients with persistent, progressive, or treatment refractory cutaneous t-cell lymphoma. *J. Clin. Oncol.* **25**, 3109-15 (2007).

266. Lee, H. Z. *et al.* FDA approval: Belinostat for the treatment of patients with relapsed or refractory peripheral T-cell lymphoma. *Clin. Cancer Res.* **21**, 2666-70 (2015).

267. Whittaker, S. J. *et al.* Final results from a multicenter, international, pivotal study of romidepsin in refractory cutaneous T-cell lymphoma. *J. Clin. Oncol.* **28**, 4485-91 (2010).

268. Piekarz, R. L. *et al.* Phase II multi-institutional trial of the histone deacetylase inhibitor romidepsin as monotherapy for patients with cutaneous T-cell lymphoma. *J. Clin. Oncol.* **27**, 5410-7 (2009).

269. San-Miguel, J. F. *et al.* Panobinostat plus bortezomib and dexamethasone versus placebo plus bortezomib and dexamethasone in patients with relapsed or relapsed and refractory multiple myeloma: A multicentre, randomised, double-blind phase 3 trial. *Lancet Oncol.* **15**, 1195-206 (2014).

270. Stathis, A. *et al.* Clinical response of carcinomas harboring the BRD4–NUT oncoprotein to the targeted bromodomain inhibitor OTX015/MK-8628. *Cancer Discov.* **6**, 492-500 (2016).

271. Cao, R. *et al.* Role of histone H3 lysine 27 methylation in polycomb-group silencing. *Science* **298**, 1039-43 (2002).

272. Li, H., Cai, Q., Godwin, A. K. & Zhang, R. Enhancer of zeste homolog 2 promotes the proliferation and invasion of epithelial ovarian cancer cells. *Mol. Cancer Res.* **8**, 1610–1618 (2010).

273. Shi, Y. *et al.* Histone demethylation mediated by the nuclear amine oxidase homolog LSD1. *Cell* **119**, 941-53 (2004).

274. Schenk, T. *et al.* Inhibition of the LSD1 (KDM1A) demethylase reactivates the all-trans-retinoic acid differentiation pathway in acute myeloid leukemia. *Nat. Med.* **18**, 605-11 (2012).

275. Theisen, E. R. *et al.* Reversible inhibition of lysine specific demethylase 1 is a novel anti-tumor strategy for poorly differentiated endometrial carcinoma. *BMC Cancer* **14**, 752 (2014).

276. Humphreys, K. J., Cobiac, L., Le Leu, R. K., Van der Hoek, M. B. & Michael, M. Z. Histone deacetylase inhibition in colorectal cancer cells reveals competing roles for members of the oncogenic miR-17-92 cluster. *Mol. Carcinog.* **52**, 459-74 (2013).

277. Cameron, E. E., Bachman, K. E., Myöhänen, S., Herman, J. G. & Baylin, S. B. Synergy of demethylation and histone deacetylase inhibition in the re- expression of genes silenced in cancer. *Nat. Genet.* **21**, 103-7 (1999).

278. Yang, X. *et al.* Synergistic activation of functional estrogen receptor (ER)-α by DNA methyltransferase and histone deacetylase inhibition in human ER-α-negative breast cancer cells. *Cancer Res.* **61**, 7025-9 (2001).

279. Belinsky, S. A. *et al.* Inhibition of DNA Methylation and Histone Deacetylation Prevents Murine Lung Cancer. *Cancer Res.* **63**, 7089-93 (2003).

280. Ecke, I. *et al.* Antitumor effects of a combined 5-aza-2′deoxycytidine and valproic acid treatment on rhabdomyosarcoma and medulloblastoma in Ptch mutant mice. *Cancer Res.* **69**, 887-95 (2009).

281. Steele, N., Finn, P., Brown, R. & Plumb, J. A. Combined inhibition of DNA methylation and histone acetylation enhances gene re-expression and drug sensitivity in vivo. *Br. J. Cancer* **100**, 758-63 (2009).

282. Dowdy, S. C. *et al.* Histone deacetylase inhibitors and paclitaxel cause synergistic effects on apoptosis and microtubule stabilization in papillary serous endometrial cancer cells. *Mol. Cancer Ther.* **5**, 2767-76 (2006).

283. Arnold, N. B., Arkus, N., Gunn, J. & Korc, M. The histone deacetylase inhibitor suberoylanilide hydroxamic acid induces growth inhibition and enhances gemcitabine-induced cell death in pancreatic cancer. *Clin. Cancer Res.* **13**, 18-26 (2007).

284. Rikiishi, H. *et al.* Chemosensitization of oral squamous cell carcinoma cells to cisplatin by histone deacetylase inhibitor, suberoylanilide hydroxamic acid. *Int. J. Oncol.* **30**, 1181-8 (2007).

285. Kim, M. S. *et al.* Inhibition of Histone Deacetylase Increases Cytotoxicity to

Anticancer Drugs Targeting DNA. *Cancer Res.* **63**, 7291-300 (2003).

286. Gomyo, Y., Sasaki, J. I., Branch, C., Roth, J. A. & Mukhopadhyay, T. 5-Aza-2′-deoxycytidine upregulates caspase-9 expression cooperating with p53-induced apoptosis in human lung cancer cells. *Oncogene* **23**, 6779-87 (2004).

287. Shang, D. *et al.* Synergy of 5-aza-2′-deoxycytidine (DAC) and paclitaxel in both androgen-dependent and -independent prostate cancer cell lines. *Cancer Lett.* **278**, 82-7 (2009).

288. Sharma, S. V. *et al.* A Chromatin-Mediated Reversible Drug-Tolerant State in Cancer Cell Subpopulations. *Cell* **141**, 69–80 (2010).

289. Knoechel, B. *et al.* An epigenetic mechanism of resistance to targeted therapy in T cell acute lymphoblastic leukemia. *Nat. Genet.* **46**, 364–370 (2014).

290. Arundel, C. M., Glicksman, A. S. & Leith, J. T. Enhancement of Radiation Injury in Human Colon Tumor Cells by the Maturational Agent Sodium Butyrate (NaB). *Radiat. Res.* **104**, 443-8 (1985).

291. Karagiannis, T. C. & El-Osta, A. Modulation of cellular radiation responses by histone deacetylase inhibitors. *Oncogene* **25**, 3885-93 (2006).

292. Karagiannis, T. C. & El-Osta, A. The paradox of histone deacetylase inhibitor-mediated modulation of cellular responses to radiation. *Cell Cycle* **5**, 288-95 (2006).

293. Bangert, A. *et al.* Histone deacetylase inhibitors sensitize glioblastoma cells to TRAIL-induced apoptosis by c-myc-mediated downregulation of cFLIP. *Oncogene* **31**, 4677-88 (2012).

294. Butler, L. M. *et al.* The histone deacetylase inhibitor, suberoylanilide hydroxamic acid, overcomes resistance of human breast cancer cells to Apo2L/TRAIL. *Int. J. Cancer* **119**, 944-54 (2006).

295. Lagneaux, L. *et al.* Valproic acid induces apoptosis in chronic lymphocytic leukemia cells through activation of the death receptor pathway and potentiates TRAIL response. *Exp. Hematol.* **35**, 1527-37 (2007).

296. Vanoosten, R. L., Moore, J. M., Ludwig, A. T. & Griffith, T. S. Depsipeptide (FR901228) enhances the cytotoxic activity of TRAIL by redistributing TRAIL receptor to membrane lipid rafts. *Mol. Ther.* **11**, 542-52 (2005).

297. Zhang, X. D., Gillespie, S. K., Borrow, J. M. & Hersey, P. The histone deacetylase inhibitor suberic bishydroxamate: A potential sensitizer of melanoma to TNF-related apoptosis-inducing ligand (TRAIL) induced apoptosis. *Biochemical Pharmacology* **66**, 1537-45 (2003).

298. Guo, F. *et al.* Cotreatment with Histone Deacetylase Inhibitor LAQ824 Enhances Apo-2L/ Tumor Necrosis Factor-Related Apoptosis Inducing Ligand-Induced Death Inducing Signaling Complex Activity and Apoptosis of Human Acute Leukemia Cells. *Cancer Res.* **64**, 2580-9 (2004).

299. Fulda, S. *et al.* Sensitization for death receptor- or drug-induced apoptosis by re-expression of caspase-8 through demethylation or gene transfer. *Oncogene* **20**, 5865-77 (2001).

300. Fulda, S. & Debatin, K. M. 5-Aza-2′-deoxycytidine and IFN-γ cooperate to sensitize for TRAIL-induced apoptosis by upregulating caspase-8. *Oncogene* **25**, 5125-33 (2006).

301. Grotzer, M. *et al.* Resistance to TRAIL-induced apoptosis in primitive neuroectodermal brain tumor cells correlates with a loss of caspase-8 expression. *Oncogene* **19**, 4604–4610 (2000).

302. Kaminskyyy, V. O., Surovay, O. V., Vaculova, A. & Zhivotovsky, B. Combined inhibition of DNA methyltransferase and histone deacetylase restores caspase-8 expression and sensitizes SCLC cells to TRAIL. *Carcinogenesis* **32**, 1450-8 (2011).

303. Kurita, S. *et al.* DNMT1 and DNMT3b silencing sensitizes human hepatoma cells to TRAIL-mediated apoptosis via up-regulation of TRAIL-R2/DR5 and caspase-8. *Cancer Sci.* **101**, 1431-9 (2010).

304. Florean, C. *et al.* Discovery and characterization of Isofistularin-3, a marine brominated alkaloid, as a new DNA demethylating agent inducing cell cycle arrest and sensitization to TRAIL in cancer cells. *Oncotarget* **7**, 24027-49 (2016).

305. Udagawa, S. *et al.* The production of chaetoglobosins, sterigmatocystin, O -methylsterigmatocystin, and chaetocin by Chaetomium spp. and related fungi. *Can. J. Microbiol.* **25**, 170–177 (1979).

306. Greiner, D., Bonaldi, T., Eskeland, R., Roemer, E. & Imhof, A. Identification of a specific inhibitor of the histone methyltransferase SU(VAR)3-9. *Nat. Chem. Biol.*

1, 143–145 (2005).

307. Dixit, D., Ghildiyal, R., Anto, N. P. & Sen, E. Chaetocin-induced ROS-mediated apoptosis involves ATM-YAP1 axis and JNK-dependent inhibition of glucose metabolism. *Cell Death Dis.* **5**, e1212 (2014).

308. Tibodeau, J. D., Benson, L. M., Isham, C. R., Owen, W. G. & Bible, K. C. The anticancer agent chaetocin is a competitive substrate and inhibitor of thioredoxin reductase. *Antioxid. Redox Signal.* **11**, 1097–106 (2009).

309. Holmström, K. M. & Finkel, T. Cellular mechanisms and physiological consequences of redox-dependent signalling. *Nat. Rev. Mol. Cell Biol.* **15**, 411–421 (2014).

310. Meitzler, J. L. *et al.* NADPH Oxidases: A Perspective on Reactive Oxygen Species Production in Tumor Biology. *Antioxid. Redox Signal.* **20**, 2873-89 (2014).

311. Speed, N. & Blair, I. A. Cyclooxygenase- and lipoxygenase-mediated DNA damage. *Cancer Metastasis Rev.* **30**, 437-47 (2011).

312. Gào, X. & Schöttker, B. Reduction-oxidation pathways involved in cancer development: a systematic review of literature reviews. *Oncotarget* **8**, 51888-51906 (2017).

313. Verschoor, M. L., Wilson, L. A. & Singh, G. Mechanisms associated with mitochondrial-generated reactive oxygen species in cancer. *Can J Physiol Pharmacol* **88**, 204-19 (2010).

314. Sosa, V. *et al.* Oxidative stress and cancer : An overview. *Ageing Res. Rev.* **12**, 376-90 (2013).

315. Valko, M. *et al.* Free radicals and antioxidants in normal physiological functions and human disease. *International Journal of Biochemistry and Cell Biology* **39**, 44-84 (2007).

316. Reuter, S., Gupta, S. C., Chaturvedi, M. M. & Aggarwal, B. B. Oxidative stress, inflammation, and cancer: How are they linked? *Free Radical Biology and Medicine* **49**, 1603-16 (2010).

317. McCubrey, J. A., LaHair, M. M. & Franklin, R. A. Reactive Oxygen Species-Induced Activation of the MAP Kinase Signaling Pathways. *Antioxid. Redox Signal.* **8**, 1775-89 (2006).

318. Koundouros, N. & Poulogiannis, G. Phosphoinositide 3-Kinase/Akt Signaling and Redox Metabolism in Cancer. *Front. Oncol.* **8**,160 (2018).

319. Giorgi, C. *et al.* Redox Control of Protein Kinase C: Cell- and Disease-Specific Aspects. *Antioxid. Redox Signal.* **13**, 1051-85 (2010).

320. Brigelius-Flohé, R. & Flohé, L. Basic Principles and Emerging Concepts in the Redox Control of Transcription Factors. *Antioxid. Redox Signal.* **15**, 2335-81 (2011).

321. Jinek, M. *et al.* A Programmable Dual-RNA-Guided DNA Endonuclease in Adaptive Bacterial Immunity. *Science* **337**, 816–821 (2012).

322. Mojica, F. J. M., Díez-Villaseñor, C., García-Martínez, J. & Almendros, C. Short motif sequences determine the targets of the prokaryotic CRISPR defence system. *Microbiology* **155**, 733–740 (2009).

323. Gong, C. *et al.* Mechanism of nonhomologous end-joining in mycobacteria: a low-fidelity repair system driven by Ku, ligase D and ligase C. *Nat. Struct. Mol. Biol.* **12**, 304–312 (2005).

324. Evers, B. *et al.* CRISPR knockout screening outperforms shRNA and CRISPRi in identifying essential genes. *Nat. Biotechnol.* **34**, 631-3 (2016).

325. Hart, T. *et al.* High-Resolution CRISPR Screens Reveal Fitness Genes and Genotype-Specific Cancer Liabilities. *Cell* **163**, 1515-26 (2015).

326. Steinhart, Z. *et al.* Genome-wide CRISPR screens reveal a Wnt-FZD5 signaling circuit as a druggable vulnerability of RNF43-mutant pancreatic tumors. *Nat. Med.* **23**, 60-68 (2017).

327. Florian, H. *et al.* CRISPR library designer (CLD): Software for multispecies design of single guide RNA libraries. *Genome Biol.* **17**, 55 (2016).

328. Ruiz, S. *et al.* A Genome-wide CRISPR Screen Identifies CDC25A as a Determinant of Sensitivity to ATR Inhibitors. *Mol. Cell* **62**, 307-313 (2016).

329. Krall, E. B. *et al.* KEAP1 loss modulates sensitivity to kinase targeted therapy in lung cancer. *Elife* **6**, e18970 (2017).

330. Korkmaz, G. *et al.* Functional genetic screens for enhancer elements in the human genome using CRISPR-Cas9. *Nat. Biotechnol.* 34, 192-8 (2016).

331. Sanjana, N. E. *et al.* High-resolution interrogation of functional elements in the

noncoding genome. *Science* **353**, 1545-1549 (2016).

332. Schwank, G. *et al.* Functional repair of CFTR by CRISPR/Cas9 in intestinal stem cell organoids of cystic fibrosis patients. *Cell Stem Cell* **13**, 653-8 (2013).

333. Drost, J. *et al.* Sequential cancer mutations in cultured human intestinal stem cells. *Nature* **521**, 43-7 (2015).

334. Matano, M. *et al.* Modeling colorectal cancer using CRISPR-Cas9-mediated engineering of human intestinal organoids. *Nat. Med.* **21**, 256-62 (2015).

335. Chen, S. *et al.* Genome-wide CRISPR screen in a mouse model of tumor growth and metastasis. *Cell* **160**, 1246-60 (2015).

336. Weber, J. *et al.* CRISPR/Cas9 somatic multiplex-mutagenesis for high-throughput functional cancer genomics in mice. *Proc. Natl. Acad. Sci.* **112**, 13982-7 (2015).

337. Platt, R. J. *et al.* CRISPR-Cas9 knockin mice for genome editing and cancer modeling. *Cell* **159**, 440-55 (2014).

338. Cyranoski, D. CRISPR gene-editing tested in a person for the first time. *Nature* **539**, 479 (2016).

339. Zhan, T., Rindtorff, N., Betge, J., Ebert, M. P. & Boutros, M. CRISPR/Cas9 for cancer research and therapy. *Seminars in Cancer Biology* **55**, 106-119 (2019).

340. Kurt, I. C. *et al.* KDM2B, an H3K36-specific demethylase, regulates apoptotic response of GBM cells to TRAIL. *Cell Death Dis.* **8**, e2897 (2017).

341. Cribbs, A. *et al.* Inhibition of histone H3K27 demethylases selectively modulates inflammatory phenotypes of natural killer cells. *J. Biol. Chem.* **293**, 2422-2437 (2018).

342. Kim, D., Langmead, B. & Salzberg, S. L. HISAT: A fast spliced aligner with low memory requirements. *Nat. Methods* **12**, 357-60 (2015).

343. Love, M. I., Huber, W. & Anders, S. Moderated estimation of fold change and dispersion for RNA-seq data with DESeq2. *Genome Biol.* **15**, 550 (2014).

344. Mootha, V. K. *et al.* PGC-1α-responsive genes involved in oxidative phosphorylation are coordinately downregulated in human diabetes. *Nat. Genet.* **34**, 267-73 (2003).

345. Sanjana, N. E., Shalem, O. & Zhang, F. Improved vectors and genome-wide libraries for CRISPR screening. *Nat. Methods* **11**, 783–784 (2014).

346. Stemmer, M., Thumberger, T., Del Sol Keyer, M., Wittbrodt, J. & Mateo, J. L. CCTop: An intuitive, flexible and reliable CRISPR/Cas9 target prediction tool. *PLoS One* **10**, e0124633 (2015).

347. Olson, a, Sheth, N., Lee, J. S., Hannon, G. & Sachidanandam, R. RNAi Codex: a portal/database for short-hairpin RNA (shRNA) gene-silencing constructs. *Nucleic Acids Res.* **34**, D153–D157 (2006).

348. Onder, T. T. *et al.* Chromatin-modifying enzymes as modulators of reprogramming. *Nature* **483**, 598–602 (2012).

349. Bagci-Onder, T. *et al.* Real-time imaging of the dynamics of death receptors and therapeutics that overcome TRAIL resistance in tumors. *Oncogene* **32**, 2818–2827 (2012).

350. Bagci-Onder, T., Wakimoto, H., Anderegg, M., Cameron, C. & Shah, K. A dual PI3K/mTOR inhibitor, PI-103, cooperates with stem cell-delivered TRAIL in experimental glioma models. *Cancer Res.* **71**, 154–163 (2011).

351. Lauricella, M., Ciraolo, A., Carlisi, D., Vento, R. & Tesoriere, G. SAHA/TRAIL combination induces detachment and anoikis of MDA-MB231 and MCF-7 breast cancer cells. *Biochimie* **94**, 287-99 (2012).

352. Huertas, D. *et al.* Antitumor activity of a small-molecule inhibitor of the histone kinase Haspin. *Oncogene* **31**, 1408-18 (2012).

353. Zhang, X. *et al.* Identification of 5-Iodotubercidin as a Genotoxic Drug with Anti-Cancer Potential. *PLoS One* **8**, e62527 (2013).

354. Chou, T. C. Drug combination studies and their synergy quantification using the chou-talalay method. *Cancer Research* **70**, 440-6 (2010).

355. Chou, T. C. & Talalay, P. Quantitative analysis of dose-effect relationships: the combined effects of multiple drugs or enzyme inhibitors. *Adv. Enzyme Regul.* **22**, 27-55 (1984). doi:10.1016/0065-2571(84)90007-4

356. Senbabaoglu, F. *et al.* Identification of Mitoxantrone as a TRAIL-sensitizing agent for Glioblastoma Multiforme. *Cancer Biol. Ther.* **17**, 546-57 (2016).

357. Kyrylkova, K., Kyryachenko, S., Leid, M. & Kioussi, C. Detection of apoptosis by TUNEL assay. *Methods Mol. Biol.* **887**, 41–47 (2012).

358. Tse, C. *et al.* ABT-263: A potent and orally bioavailable Bcl-2 family inhibitor.

Cancer Res. **68**, 3421-8 (2008).

359. Lessene, G. *et al.* Structure-guided design of a selective BCL-XLinhibitor. *Nat. Chem. Biol.* **9**, 390-7 (2013).

360. Chipuk, J. E., Moldoveanu, T., Llambi, F., Parsons, M. J. & Green, D. R. The BCL-2 Family Reunion. *Molecular Cell* **37**, 299-310 (2010).

361. Chaib, H. *et al.* Anti-leukemia activity of chaetocin via death receptor-dependent apoptosis and dual modulation of the histone methyl-transferase SUV39H1. *Leukemia* **26**, 662–674 (2012).

362. Vassilev, L. T. *et al.* In Vivo Activation of the p53 Pathway by Small-Molecule Antagonists of MDM2. *Science* **303**, 844-8 (2004).

363. Stocker, R., Yamamoto, Y., McDonagh, A. F., Glazer, A. N. & Ames, B. N. Bilirubin is an antioxidant of possible physiological importance. *Science* **235**, 1043-6 (1987).

364. Alaoui-Jamali, M. A. *et al.* A novel experimental heme oxygenase-1-targeted therapy for hormone-refractory prostate cancer. *Cancer Res.* **69**, 8017-24 (2009).

365. Sass, G. *et al.* Inhibition of heme oxygenase 1 expression by small interfering RNA decreases orthotopic tumor growth in livers of mice. *Int. J. Cancer* **123**, 1269-77 (2008).

366. Miyake, M. *et al.* Inhibition of heme oxygenase-1 enhances the cytotoxic effect of gemcitabine in urothelial cancer cells. *Anticancer Res.* **30**, 2145-52 (2010).

367. Hao, C. *et al.* Induction and intracellular regulation of tumor necrosis factor-related apoptosis-inducing ligand (TRAIL) mediated apotosis in human malignant glioma cells. *Cancer Res.* **61**, 1162-70 (2001).

368. Jennewein, C. *et al.* Identification of a novel pro-apoptotic role of NF-κB in the regulation of TRAIL- and CD95-mediated apoptosis of glioblastoma cells. *Oncogene* **31**, 1468-74 (2012).

369. Cristofanon, S. *et al.* Identification of RIP1 as a critical mediator of Smac mimetic-mediated sensitization of glioblastoma cells for Drozitumab-induced apoptosis. *Cell Death Dis.* **6**, e1724 (2015).

370. Li, L. *et al.* A small molecule smac mimic potentiates TRAIL- and TNFα-mediated cell death. *Science* **305**, 1471-4 (2004).

371. Unterkircher, T. *et al.* Bortezomib primes glioblastoma, including glioblastoma stem cells, for TRAIL by increasing tBid stability and mitochondrial apoptosis. *Clin. Cancer Res.* **17**, 4019-30 (2011).

372. Schmidt, N., Windmann, S., Reifenberger, G. & Riemenschneider, M. J. DNA hypermethylation and histone modifications downregulate the candidate tumor suppressor gene RRP22 on 22q12 in human gliomas. *Brain Pathol.* **22**, 17–25 (2012).

373. Liu, B. L. *et al.* Global histone modification patterns as prognostic markers to classify glioma patients. *Cancer Epidemiol. Biomarkers Prev.* **19**, 2888–2896 (2010).

374. Quinn, J. A. *et al.* Phase II Trial of Temozolomide Plus O6-Benzylguanine in Adults with Recurrent, Temozolomide-Resistant Malignant Glioma. *J. Clin. Oncol.* **27**, 1262-7 (2009).

375. Romani, M., Pistillo, M. P. & Banelli, B. Epigenetic Targeting of Glioblastoma. *Front. Oncol.* **8**, 448 (2018). doi:10.3389/fonc.2018.00448

376. Galanis, E. *et al.* Phase I/II trial of vorinostat combined with temozolomide and radiation therapy for newly diagnosed glioblastoma: Results of Alliance N0874/ABTC 02. *Neuro. Oncol.* **20**, 546-556 (2018).

377. Galanis, E. *et al.* Phase II trial of Vorinostat in recurrent glioblastoma multiforme: A north central cancer treatment group study. *J. Clin. Oncol.* **27**, 2052-8 (2009).

378. Krauze, A. V. *et al.* A Phase 2 Study of Concurrent Radiation Therapy, Temozolomide, and the Histone Deacetylase Inhibitor Valproic Acid for Patients with Glioblastoma. *Int. J. Radiat. Oncol. Biol. Phys.* **92**, 986-992 (2015).

379. Ochiai, S. *et al.* Roles of Valproic Acid in Improving Radiation Therapy for Glioblastoma: a Review of Literature Focusing on Clinical Evidence. *Asian Pac. J. Cancer Prev.* **17**, 463-6 (2016).

380. Iwamoto, F. M. *et al.* A phase I/II trial of the histone deacetylase inhibitor romidepsin for adults with recurrent malignant glioma: North American brain tumor consortium study 03-03. *Neuro. Oncol.* **13**, 509-16 (2011).

381. S., G. *et al.* Nimg-30. Assessing treatment response of glioblastoma to an HDAC inhibitor, belinostat (PXD101). *Neuro. Oncol.* **19**, vi148 (2017).

382. Halford, S. E. R. *et al.* Results of the OPARATIC trial: A phase I dose escalation

study of olaparib in combination with temozolomide (TMZ) in patients with relapsed glioblastoma (GBM). *J. Clin. Oncol.* **35**, 2022-2022 (2018).

383. JM., S. *et al.* A phase I trial of veliparib (ABT-888) and temozolomide in children with recurrent CNS tumors: a pediatric brain tumor consortium report. *Neuro. Oncol.* **16**, 1661-8 (2014).

384. Zhang, J. & Zhong, Q. Histone deacetylase inhibitors and cell death. *Cellular and Molecular Life Sciences* **71**, 3885-90 (2014).

385. Liu, X., Guo, S., Liu, X. & Su, L. Chaetocin induces endoplasmic reticulum stress response and leads to death receptor 5-dependent apoptosis in human non-small cell lung cancer cells. *Apoptosis* **20**, 1499–1507 (2015).

386. Chaib, H. *et al.* Anti-leukemia activity of chaetocin via death receptor-dependent apoptosis and dual modulation of the histone methyl-transferase SUV39H1. *Leukemia* **26**, 662–674 (2012).

387. Lai, Y.-S., Chen, J.-Y., Tsai, H.-J., Chen, T.-Y. & Hung, W.-C. The SUV39H1 inhibitor chaetocin induces differentiation and shows synergistic cytotoxicity with other epigenetic drugs in acute myeloid leukemia cells. *Blood Cancer J.* **5**, e313 (2015).

388. Tran, H. T. T. *et al.* Improved therapeutic effect against leukemia by a combination of the histone methyltransferase inhibitor chaetocin and the histone deacetylase inhibitor trichostatin A. *J. Korean Med. Sci.* **28**, 237–246 (2013).

389. He, J. *et al.* Chaetocin induces cell cycle arrest and apoptosis by regulating the ROS-mediated ASK-1/JNK signaling pathways. *Oncol. Rep.* **38**, 2489-2497 (2017).

390. Janssen-Heininger, Y. M. W. *et al.* Redox-based regulation of signal transduction: Principles, pitfalls, and promises. *Free Radical Biology and Medicine* **45**, 1-17 (2008).

391. Zhang, Y. *et al.* Exposure to HT-2 toxin causes oxidative stress induced apoptosis/autophagy in porcine oocytes. *Sci. Rep.* **6**, 33904 (2016).

392. Sporn, M. B. & Liby, K. T. NRF2 and cancer: The Good, the bad and the importance of context. *Nature Reviews Cancer* **12**, 564-71 (2012).

393. Frezza, C. *et al.* Haem oxygenase is synthetically lethal with the tumour suppressor fumarate hydratase. *Nature* **477**, 225-8 (2011).

394. Mandal, P. K. *et al.* Loss of thioredoxin reductase 1 renders tumors highly susceptible to pharmacologic glutathione deprivation. *Cancer Res.* **70**, 9505-14 (2010).

395. Harris, I. S. *et al.* Glutathione and Thioredoxin Antioxidant Pathways Synergize to Drive Cancer Initiation and Progression. *Cancer Cell* **27**, 211-22 (2015).

396. Isham, C. R., Tibodeau, J. D., Bossou, A. R., Merchan, J. R. & Bible, K. C. The anticancer effects of chaetocin are independent of programmed cell death and hypoxia, and are associated with inhibition of endothelial cell proliferation. *Br. J. Cancer* **106**, 314–323 (2012).

397. Isham, C. R. *et al.* Chaetocin: A promising new antimyeloma agent with in vitro and in vivo activity mediated via imposition of oxidative stress. *Blood* **109**, 2579-88 (2007).

398. Truitt, L., Hutchinson, C., DeCoteau, J. F. & Geyer, C. R. Chaetocin antileukemia activity against chronic myelogenous leukemia cells is potentiated by bone marrow stromal factors and overcomes innate imatinib resistance. *Oncogenesis* **3**, e122 (2014).

399. Yamaguchi, H. & Wang, H. G. CHOP is involved in endoplasmic reticulum stress-induced apoptosis by enhancing DR5 expression in human carcinoma cells. *J. Biol. Chem.* **279**, 45495-502 (2004).

400. Taniguchi, H. *et al.* Baicalein overcomes tumor necrosis factor-related apoptosis-inducing ligand resistance via two different cell-specific pathways in cancer cells but not in normal cells. *Cancer Res.* **68**, 8918-27 (2008).

401. Shin, D. *et al.* Upregulation of Death Receptor 5 and Production of Reactive Oxygen Species Mediate Sensitization of PC-3 Prostate Cancer Cells to TRAIL Induced Apoptosis by Vitisin A. *Cell. Physiol. Biochem.* **36**, 1151–1162 (2015).

402. Rozanov, D. *et al.* TRAIL-based high throughput screening reveals a link between TRAIL-mediated apoptosis and glutathione reductase, a key component of oxidative stress response. *PLoS One* **10**, e0129566 (2015).

403. Soberanes, S. *et al.* Particulate matter air pollution induces hypermethylation of the p16 promoter Via a mitochondrial ROS-JNK-DNMT1 pathway. *Sci. Rep.* **2**, 275 (2012).

404. Kang, K. A., Zhang, R., Kim, G. Y., Bae, S. C. & Hyun, J. W. Epigenetic changes

induced by oxidative stress in colorectalcancer cells: Methylation of tumor suppressor RUNX3. *Tumor Biol.* **33**, 403-12 (2012).

405. Lim, S. O. *et al.* Epigenetic Changes Induced by Reactive Oxygen Species in Hepatocellular Carcinoma: Methylation of the E-cadherin Promoter. *Gastroenterology* **135**, 2128-40 (2008).

406. Chervona, Y. & Costa, M. The control of histone methylation and gene expression by oxidative stress, hypoxia, and metals. *Free Radical Biology and Medicine* **53**, 1041-7 (2012).

407. Niu, Y., Desmarais, T. L., Tong, Z., Yao, Y. & Costa, M. Oxidative stress alters global histone modification and DNA methylation. *Free Radic. Biol. Med.* **82**, 22-8 (2015).

408. Gupta, J. & Tikoo, K. Involvement of insulin-induced reversible chromatin remodeling in altering the expression of oxidative stress-responsive genes under hyperglycemia in 3T3-L1 preadipocytes. *Gene* **504**, 181-91 (2012).

409. Rahman, I., Gilmour, P. S., Jimenez, L. A. & MacNee, W. Oxidative stress an TNF-α induce histone acetylation and NF-κB/AP-1 activation in alveolar epithelial cells: Potential mechanism in gene transcription in lung inflammation. *Mol. Cell. Biochem.* **234-235**, 239-48 (2002).

410. Choudhury, M., Park, P. H., Jackson, D. & Shukla, S. D. Evidence for the role of oxidative stress in the acetylation of histone H3 by ethanol in rat hepatocytes. *Alcohol* **44**, 531-40 (2010).

411. Kang, J. *et al.* Nickel-induced histone hypoacetylation: The role of reactive oxygen species. *Toxicol. Sci.* **74**, 279-86 (2003).

412. Kang, J., Chen, J., Shi, Y., Jia, J. & Zhang, Y. Curcumin-induced histone hypoacetylation: The role of reactive oxygen species. *Biochem. Pharmacol.* **69**, 1205-13 (2005).

413. Kelkel, M. *et al.* ROS-independent JNK activation and multisite phosphorylation of Bcl-2 link diallyl tetrasulfide-induced mitotic arrest to apoptosis. *Carcinogenesis* **33**, 2162-71 (2012).

414. Shi, Y. *et al.* ROS-dependent activation of JNK converts p53 into an efficient inhibitor of oncogenes leading to robust apoptosis. *Cell Death Differ.* **21**, 612-23 (2014).

415. Vousden, K. H. & Prives, C. Blinded by the Light: The Growing Complexity of p53. *Cell* **137**, 413-31 (2009).

416. Lavrovsky, Y., Schwartzman, M. L., Levere, R. D., Kappas, A. & Abraham, N. G. Identification of binding sites for transcription factors NF-kappa B and AP-2 in the promoter region of the human heme oxygenase 1 gene. *Proc. Natl. Acad. Sci. U. S. A.* **91**, 5987-91 (1994).

417. Keyse, S. M., Applegate, L. A., Tromvoukis, Y. & Tyrrell, R. M. Oxidant stress leads to transcriptional activation of the human heme oxygenase gene in cultured skin fibroblasts. *Mol. Cell. Biol.* **10**, 4967-9 (1990).

418. Lee, P. J. *et al.* Hypoxia-inducible factor-1 mediates transcriptional activation of the heme oxygenase-1 gene in response to hypoxia. *J. Biol. Chem.* **272**, 5375-81 (1997).

419. Wang, X. *et al.* Carbon monoxide protects against hyperoxia-induced endothelial cell apoptosis by inhibiting reactive oxygen species formation. *J. Biol. Chem.* **282**, 1718-26 (2007).

420. Liu, Z. M. *et al.* Upregulation of heme oxygenase-1 and p21 confers resistance to apoptosis in human gastric cancer cells. *Oncogene* **23**, 503-13 (2004).

421. Kweon, M. H., Adhami, V. M., Lee, J. S. & Mukhtar, H. Constitutive overexpression of Nrf2-dependent heme oxygenase-1 in A549 cells contributes to resistance to apoptosis induced by epigallocatechin 3-gallate. *J. Biol. Chem.* **281**, 33761-72 (2006).

422. Lin, P. H., Lan, W. M. & Chau, L. Y. TRC8 suppresses tumorigenesis through targeting heme oxygenase-1 for ubiquitination and degradation. *Oncogene* **32**, 2325-34 (2013).